Integrated Energy System with Beneficial Carbon Dioxide (CO_2) Use

FINAL SCIENTIFIC/TECHNICAL REPORT

REPORTING PERIOD START DATE: SEPTEMBER 9, 2009
REPORTING PERIOD END DATE: APRIL 30, 2011

PRINCIPAL AUTHORS: XIAOLEI SUN AND NANCY TURLEY RINK
REPORT ISSUE DATE: APRIL 30, 2011

THE PROJECT IS BEING FUNDED BY DOE NETL COOPERATIVE AGREEMENT NO: DE-FE0001099

BY
ARIZONA PUBLIC SERVICE
400 NORTH 5TH STREET
PHOENIX, ARIZONA, 85004

DISCLAIMER

This report was prepared as an account of work sponsored by an agency of the United States Government. Neither the United States Government nor any agency thereof, nor any of their employees, makes any warranty, express or implied, or assumes any legal liability or responsibility for the accuracy, completeness, or usefulness of any information, apparatus, product, or process disclosed, or represents that its use would not infringe privately owned rights. Reference herein to any specific commercial product, process, or service by trade name, trademark, manufacturer, or otherwise does not necessarily constitute or imply its endorsement, recommendation, or favoring by the United States Government or any agency thereof. The views and opinions of authors expressed herein do not necessarily state or reflect those of the United States Government or any agency thereof.

ABSTRACT

This report presents an integrated energy system that combines the production of substitute natural gas through coal hydrogasification with an algae process for beneficial carbon dioxide (CO_2) use and biofuel production (funded under Department of Energy (DOE) contract DE-FE0001099). The project planned to develop, test, operate and evaluate a 2 ton-per-day coal hydrogasification plant and 25-acre algae farm at the Arizona Public Service (APS) 1000 Megawatt (MW) Cholla coal-fired power plant in Joseph City, Arizona.

Conceptual design of the integrated system was undertaken with APS partners Air Liquide (AL) and Parsons. The process engineering was separated into five major areas: flue gas preparation and CO_2 delivery, algae farming, water management, hydrogasification, and biofuel production. The process flow diagrams, energy and material balances, and preliminary major equipment needs for each major area were prepared to reflect integrated process considerations and site infrastructure design basis.

The total project also included research and development on a bench-scale hydrogasifier, one-dimensional (1-D) kinetic-model simulation, extensive algae stressing, oil extraction, lipid analysis and a half acre algae farm demonstration at APS's Redhawk testing facility.

The bench-scale hydrogasification tests were conducted using a free-flow double-wall reactor designed, built and commissioned under DOE contract DE-FC26-06NT42759. The tests were conducted under a pressure of 1000 pounds per square inch (psi), temperature range of 1500 degrees Fahrenheit (°F) to 1750°F, hydrogen to coal mass ratio (H_2:coal) ranging from 0.3 to 0.5, and a residence time ranging from 5.3 to 21.4 seconds. The test results show that by increasing the temperature from 1500°F to 1750°F, the total carbon conversion increased from 42% to 52%. The carbon conversion into methane (CH_4) reached an upper limit of 46% at 1750°F. At a lower reaction temperature of 1500°F, the carbon conversion to Benzene, Toluene, Xylene (BTX) and oil reached 8%, then dropped to essentially zero when reaction temperature reached 1750°F. The carbon conversion to C_2+ hydrocarbons (mainly ethane (C_2H_6)) reached 10% at lower reaction temperatures and dropped to essentially 0% at the higher temperature. Increasing the residence time appeared to increase both total carbon conversion and carbon conversion to lighter products. Carbon conversion to carbon monoxide (CO) was less than 5% and to CO_2 was less than 0.5% for all experimental runs. The effect from changing the H_2:coal ratio, however, was not understood.

Experimental data also indicated that essentially all oxygen and 70% to 80% of the sulfur were gasified out of the coal regardless of the experimental conditions. Large percentages of nitrogen (50% to 75%) and hydrogen (75% to 90%) in coal were gasified when the reaction temperature was increased from 1500°F to 1750°F. The major liquid by-products were water, benzene, naphthalene, fluorene, anthracene and pyrene along with their derivatives. An Advanced Rapid Carbon Hydrogasification (ARCH) 1-D model was developed and fine-tuned to be able to fit overall carbon conversion, carbon conversion to CH_4, and carbon conversion to BTX within ±5% of the experimental value. Over the course of the project, the hydrogasifier demonstrated generally stable operation. Two major challenges were smooth coal feeding and reaching a high enough hydrogen injection temperature.

In the second research area of the project, a specific freshwater algae strain - *Scenedesmus* - was selected for the study. APS conducted extensive studies of algae stressing by manipulating the nitrate level in cultures to increase extractable non-polar lipid content. Indoor experimental cultures under nitrogen deprivation were found to accumulate lipids from less than 10 weight percentage (wt%) to 40+ wt%. The lipid level of outdoor stressed-cultivator samples increased less than 10 wt% to 25+ wt%. When under stress, it took anywhere from 7 to 22 days for the culture to greatly increase neutral lipid content. The lipid accumulation process also coincided with the loss of chlorophyll (2% under normal conditions to 0.03% when stressed), causing the green culture to become yellow.

During the project, a two-acre algae testing facility with a half-acre algae cultivation area was built at the APS Redhawk 1000 MW natural gas combined cycle power plant located 55 miles west of Phoenix. The test site integrated flue gas delivery, CO_2 capture and distribution, algae cultivation, algae nursery, algae harvesting, dewatering and onsite storage as well as water treatment. The site environmental, engineering, and biological parameters for the cultivators were monitored remotely. Parameters monitored on the cultivators included CO_2 in/CO_2 out, potential of hydrogen (pH) in/pH out, conductivity, temperature, and cultivation primary pump flow. Alarms were sent via e-mail and phone to the appropriate personnel in the event of a parameter perturbation.

A combined total of 332 days of culture growth within three 6-meter-radius cultivators at Redhawk was demonstrated. When optimal conditions and plentiful nutrients were provided, algae productivity reached 28 grams per square meters per (g/m^2/day). When under stress, lipid productivity during the course of these experiments reached 24.9 milligrams (mg) of lipids

per liter (L) of culture per day. During the course of the study, the 6-Meter Radius Cultivator (6M) cultivator demonstrated robust operation, remained free of contamination and exhibited good CO_2 capture. Consistent and good mixing of CO_2 and algae in the cultivator is critical for this design.

Urea and monopotassium phosphate were determined to be good replacement nutrients for the more expensive sodium nitrate and dipotassium phosphate. *Scenedesmus* maintained a reasonable growth rate and health in fresh Cholla water as well as five times (5X) concentrated Cholla aquifer water. *Scenedesmus* also demonstrated very attractive self-settling characteristics.

Direct biodiesel production from biomass through an acid-catalyzed transesterification reaction and a supercritical methanol transesterification reaction were evaluated. The highest oil-to-biodiesel conversion of 79.9% was achieved with a stressed algae sample containing 40% algae oil. The effort concluded that producing biodiesel directly from the algae biomass could be an efficient, cost-effective and readily scalable way to produce biodiesel by eliminating the oil extraction process.

TABLE OF CONTENTS

TABLES

FIGURES

APPENDIXES

EXECUTIVE SUMMARY

The objective of the project described in this report was to develop and demonstrate an integrated energy system for producing SNG through coal hydrogasification and to evaluate algae processes for beneficial CO_2 use and biofuel production. The project planned to develop, test, operate and evaluate a 2 tons-per-day (tpd) coal hydrogasification plant and 25-acre algae farm at the APS 1000 MW Cholla coal-fired power plant, in Joseph City, Arizona. The project was performed under a grant from the DOE.

APS teamed with AL and Parsons to prepare the preliminary conceptual design of the fully integrated process, which included five major areas: flue gas preparation and CO_2 delivery, algae farming, water management, hydrogasification and biofuel production. The process flow diagrams, energy and material balances, and preliminary major equipment needs for each major area were prepared to reflect integrated process considerations and site infrastructure design.

Flue gas from the Cholla Power Plant was to be processed to separate CO_2, which would be compressed and piped from the power plant to the algae farm CO_2 storage vessel. The CO_2 separation process would remove moisture, acid gases, and metals from the flue gas and return the CO_2-depleted flue gas back into the plant's ductwork to exit the stack in compliance with the plant's operating permits.

The algae farm would consist of multiple subsystems to perform (1) inoculation, (2) cultivation, (3) harvesting and dewatering, (4) gas management, and (5) instrumentation and control functions. The inoculation system would grow seed cultures for the farm. The algae farm would consist of 25-acres of enclosed cultivator area. The algae cultivators would be a semi-closed raceway system. The harvester would be in continuous operation, harvesting algae from the cultivators. The harvested algae would be supplied to slurry pumps, which would supply the biofuel production process. CO_2 monitors would track accumulation in the cultivators. The algae farm would be fully automated, with operational data analysis and instrumentation to provide required biological and chemical data. The algae farm would be operated from a control room which would provide information for facility monitoring and control.

The water management system of the algae farm would use saline water as its makeup source and would accept recycled water from the harvester. The Cholla power plant waste water

"hot" stream and cold saline-aquifer well water would also be used for algae farm thermal management to control cultivator temperature.

The hydrogasification process would encompass a two-tpd hydrogasifier with its coal feed and char removal systems. A hydrogasifier designer would be selected based upon competency and the ability to design commercial-scale equipment. Coal would be stored in an enclosed area and supplied directly to the feed system. An inert gas would be selected - either CO_2 or nitrogen as coal carrier gas. Compressors for hydrogen, oxygen, and the inert gas would deliver gas into American Society of Mechanical Engineers (ASME) storage vessels. Resulting product gas from the 2 tpd hydrogasifier would be flared, unless operating permits at Cholla would allow its use in the existing coal-fired units. Char from the hydrogasifier would be supplied to the existing coal-fired units, where it would be mixed with coal and consumed during operation. The system would be fully automated with data recording and analysis. The entire system would be operated from the control room.

The biofuel production area would receive slurry from the algae farm harvester. Crude algae oil would be extracted and processed into biofuel. Biodiesel or green diesel may be produced at the biofuel facility. The design process would consider biofuel process alternatives. De-lipidated algae mass would be processed.

The conceptual design effort also included the site infrastructure design. The site infrastructure scope included grading, drainage, roadways, vehicle parking, fire protection, potable water, electric service, and facility buildings including administration, laboratory, control room and restrooms.

Integrating a scaled-up facility with an operating coal-fired power plant would create the opportunity to more fully understand both the potential challenges and benefits of such system, as well as effectively "closing the loop" of an integrated process by recycling CO_2 produced onsite by the plant for the production of fuel. The saline aquifers that would be used for algae production are of no use for agriculture in the region, but can provide the water needed for large-scale farming of the microalgae used in this project for CO_2 recycling.

The research work of the project included two major areas: bench scale hydrogasification study and algae cultivation systems development. These two areas covered bench-scale hydrogasifier testing, 1D kinetics model simulation, algae stressing, oil extraction, lipid analysis and a half-acre algae farm demonstration at the APS Redhawk plant. The research work followed the previous project supported by DOE project DE-FC26-06NT42759, "Development of

a Hydrogasification Process for Coproduction of SNG and Electrical Power from Western Coals" (Coal to SNG).

During the Coal to SNG project, a double-wall free-flow hydrogasification reactor was designed, engineered, constructed, commissioned and operated. The reactor was ASME-certified under Section VIII with a rating of 1150 pounds per square inch gage (psig) at 1950°F. The reaction zone had a 1.75 inch inner diameter and was 13 feet (ft) long. During the course of the project, 12 successful hydrogasification tests were conducted. The experimental tests were conducted under the pressure of 1000 psi, temperature range of 1500°F to 1750°F, H_2:coal mass ratio ranging from 0.3 to 0.5, and residence time ranging from 5.3 to 21.4 seconds. Due to termination of the project, only preliminary analysis was performed on the obtained experimental data.

Results show that by increasing the temperature from 1500°F to 1750°F, the total carbon conversion was increased from 42% to 52%. The carbon conversion into CH_4 seemed to reach an upper limit of 46% at 1750°F. Methane production was primarily related to the yield of BTX/oil. The hydrocracking of BTX/oil contributed to the methane formation. At a lower reaction temperature of 1500°F, the carbon conversion to BTX/oil reached 8%. This conversion dropped to essentially zero when the reaction temperature reached 1750°F. The carbon conversion to C_2+ hydrocarbons (mainly C_2H_6) followed the same trend as the carbon conversion to BTX/oil. It reached 10% at lower reaction temperatures and dropped to essentially 0% at higher temperatures as these conditions caused more BTX/oil cracking. Increasing the residence time appeared to increase carbon conversion and carbon conversion to lighter products. Carbon conversion to carbon monoxide (CO) was within 5% for all experimental runs. Carbon conversion to CO_2 was minute, less than 0.5% for all runs. At this time, the effect from the H_2:coal ratio was not clear.

Experimental data also indicated that essentially all oxygen was gasified out of the coal regardless of the experimental conditions. The amount of sulfur that gasified out of the coal appeared to be independent of the experimental conditions. About 70 to 80% of the sulfur was gasified, mainly into hydrogen sulfide (H_2S). About 50% to 75% of the nitrogen in coal was gasified when the reaction temperature was increased from 1500°F to 1750°F and 75 to 90% of the hydrogen in coal was gasified within this temperature range. The major liquid by-products were water, benzene, naphthalene, fluorene, anthracene and pyrene with their derivatives.

Over the course of the project, the hydrogasifier demonstrated generally stable operation. After the modification of the preheater and reactor heating design during the Coal to SNG project, the biggest challenge encountered with this reactor was the screw-conveyor coal-feeding system. This coal feeding system was found to be sensitive to the coal moisture content, carrier-gas flow rate and transient pressure differences between the coal feeder and reactor. Coal clogging around the reactor injection neck occurred during testing and became more severe when the moisture content of the coal increased. Another challenge was to provide a suitably high enough hydrogen-injection temperature. With the current hydrogen preheater design, the hydrogen injection temperature was able to reach only 1350°F. This limited the study of lower-range H_2:coal ratio tests.

Refinement of the ARCH 1-D model progressed from the Coal to SNG project. The model parameters from the ARCH 1-D model were fine-tuned to define parameters that adjusted overall carbon conversion, carbon conversion to CH_4, and carbon conversion to BTX within ±5% of the experimental value. With those results, the model with the fitted parameters could be integrated into a comprehensive Computational Fluid Dynamic (CFD) model of the reactor, which could be used as an excellent tool for developing a commercial-scale hydrogasification reactor.

In the second research area of the project, a specific freshwater algae strain - *Scenedesmus* - was selected for the study. APS conducted extensive studies of algae stressing by manipulating the nitrate level in cultures to increase extractable non-polar lipid content. Indoor experimental cultures under nitrogen deprivation were found to accumulate lipids from less than 10 wt% to 40+ wt%. The lipid level of outdoor stressed-cultivator samples increased less than 10 wt% to 25+ wt%. When under stress, it took anywhere from 7 to 22 days for the culture to greatly increase neutral lipid content. The lipid accumulation process also coincided with the loss of chlorophyll (2% under normal conditions to 0.03% when stressed), causing the green culture to become yellow.

During the project, great progress was also made in the construction, commissioning and integration of multiple systems into a functional algae farm with clear implications for large-scale development. An integrated system was built at APS Redhawk 1000 MW natural gas combined cycle power plant located 55 miles west of Phoenix. The site has an independent 12.5 kV feeder, a half acre concrete thermal pond, two green houses (30 ft x 150 ft), and utility water. A 300-foot stack slip stream was installed to introduce the flue gas into the cultivation area. It integrated flue gas capture, algae inoculation, cultivation, harvesting, dewatering and storage of

an operation scale. Water treatment and gas distribution systems were established. The site environmental, engineering, and biological parameters for the cultivators were monitored remotely. Parameters monitored on the cultivators included CO_2 in/CO_2 out, pH in/pH out, conductivity, temperature, and primary pump flow for the cultivators. Alarms were sent via e-mail and phone to the appropriate personnel in the event of a plant perturbation.

The Redhawk algae facility was developed to test new technologies or utilize existing technologies in a new application. These new or innovative technologies include a unique algae cultivator design; enhanced method of harvesting; unique method for large-scale algae dewatering; enhanced design for gas separation, concentration and distribution; enhanced method of thermal management for cultivators; enhanced methods for controlling environmental and physical parameters of cultivators remotely; and new protocols and methods for managing day-to-day operations of the farm.

A combined total of 332 days of culture growth within three 6M radius cultivators at Redhawk was demonstrated. For cultivator 1 (C1), a total of 38,900 L was harvested, of which 14,900 L was used as inoculum and 24,000 L was harvested directly or used to test the dewatering unit. For cultivator 2 (C2), a total of 42,000 L was harvested, of which 9000 L was used as inoculum, 12,000 L of stressed algae was harvested and processed, and 21,000 L of non-stressed algae was harvested and processed or used to test the dewatering unit. For cultivator 3 (C3), a total of 43,500 L was harvested, of which 6000 L was used as inoculum, 10,500 L of stressed algae was harvested and processed, and 27,000 L of non-stressed algae was harvested and processed. When optimal conditions and plentiful nutrients were provided, algae productivity in C1, C2, and C3 reached 28, 17, and 18 g/m^2/day respectively. When under stress, lipid productivity during the course of these experiments ranged from 2.7 to 24.9 mg of lipid/L of culture/day.

During the course of the study, the 6M cultivator demonstrated robust operation, remained free of contamination and exhibited good CO_2 capture. Consistent and homogenous mixing of CO_2 and algae in the cultivator is critical for this design. Any malfunction of the control system and cavitation of the recirculation pumps would affect mixing and further optimal growth of algae. Further work on algae cultivation is needed to investigate ways to reduce the amount of time required to induce lipid accumulation and examine methods for increasing lipid-content cultures in a continuous method rather than the batch method employed during this period. The optimal fat level in the biomass to generate the best quality of crude algae oil for biodiesel production

still needs to be determined so that the biomass could be harvested at the right time once it was under stress. Longer stressing does not always produce higher fat levels and better quality oil.

An advanced CO_2 separation membrane system received from Membrane Technology & Research was tested at the site, which increased CO_2 in the flue gas from 3.6% at the stack to ~20%. An algae dewatering system received from Dynasep demonstrated a 12 gallons per minute (gpm) algae processing capacity and delivered ~20% solid content algae paste.

Other research on algae growth found inexpensive sources of nitrogen and phosphorous to reduce the nutrient cost. Urea and monopotassium phosphate were determined to be good replacements for more expensive sodium nitrate and dipotassium phosphate.

Effort also was spent investigating the adaptability of *Scenedesmus* on the Cholla aquifer water (which has 20% of the salinity of sea water). Significantly, *Scenedesmus* maintained a reasonable growth rate and healthiness in fresh Cholla water as well as the 5X concentrated Cholla aquifer water. *Scenedesmus* also demonstrated very attractive self-settling characteristics. Left in a settling tank, the biomass mostly settled out after 5 hours. The settled biomass was found to have a density of 47.7 grams per liter (g/L) and the non-settled portion was 0.04 g/L. With no energy expenditure for dewatering, this 5 hour settling period resulted in a nearly 32-fold increased concentration of the biomass.

Oil extractions from algae biomass were also tested during the project. Dichloromethane and methanol (2:1 volume concentration (v/v)) or acetone was used as a solvent. Direct biodiesel production from biomass through an acid-catalyzed transesterification reaction and a supercritical methanol transesterification reaction were evaluated. The highest oil to biodiesel conversion of 79.9% was achieved with a stressed algae sample containing 40 wt% algae oil using the acid-catalyzed transesterification method. Producing biodiesel directly from the algae biomass is an efficient, cost-effective and readily scalable way to produce biodiesel and eliminates the oil extraction process. The optimal reaction conditions and catalysts to apply, however, need further investigation.

Both the Coal to SNG and the Integrated Energy System with Beneficial CO_2 Use Project (IES) projects were terminated by APS on March 31, 2010. The Coal to SNG Final Scientific/Technical Report should be reviewed in conjunction with this report for a more comprehensive narrative.

THIS PAGE INTENTIONALLY LEFT BLANK.

1. INTRODUCTION

1.1 STATEMENT OF THE SIGNIFICANCE OF THE PROJECT

America is faced with well-known energy and economic challenges. As carried out by APS, the energy project described in this report builds upon America's existing fossil fuel infrastructure and prior research and development (R&D) by the DOE. Coal is a vast natural United States resource and is the fuel for approximately 50% of the nation's electricity generation; however, concerns about coal's impacts on the environment, including global warming, have put the future of coal at serious risk.

Climate change concerns have focused on the contribution that the global use of coal makes to increasing levels of the greenhouse gas CO_2. America has relied upon coal as the primary fuel to produce a significant percentage of its electricity. The impact on the nation's economy from developing and providing an economical means of capturing and sequestering CO_2 for the existing coal fleet would be significant. The earth's natural carbon cycle has been at work for hundreds of millions of years creating our fossil fuels. The earth's natural processes of capturing and recycling CO_2 are unable to keep up with current rate at which CO_2 is released into the atmosphere. An innovative approach - combining natural biological capture of CO_2, via algae cultivation which is then metabolized into lipids (fat), starch, and proteins to create fuel - may provide a viable economic solution and potentially create a value stream to relieve electric operations of CO_2 remediation costs.

The biological capture and reuse of CO_2 through algae cultivation is gaining attention as a possible means to reduce CO_2 emissions from fossil-fuel processes. Algae can double their size in a few hours while consuming CO_2. Because algae can be grown in non-arable regions such as deserts, they do not compete for space with farmland and forests, and they do not require potable or even agricultural-quality water to grow. Algae yields an amount of oil per acre that is approximately two orders of magnitude higher than that of traditional plant materials used to produce biofuel. Because the oils in algae can be extracted and converted into liquid transportation fuel, this CO_2 reuse technology is highly desirable economically as well as environmentally.

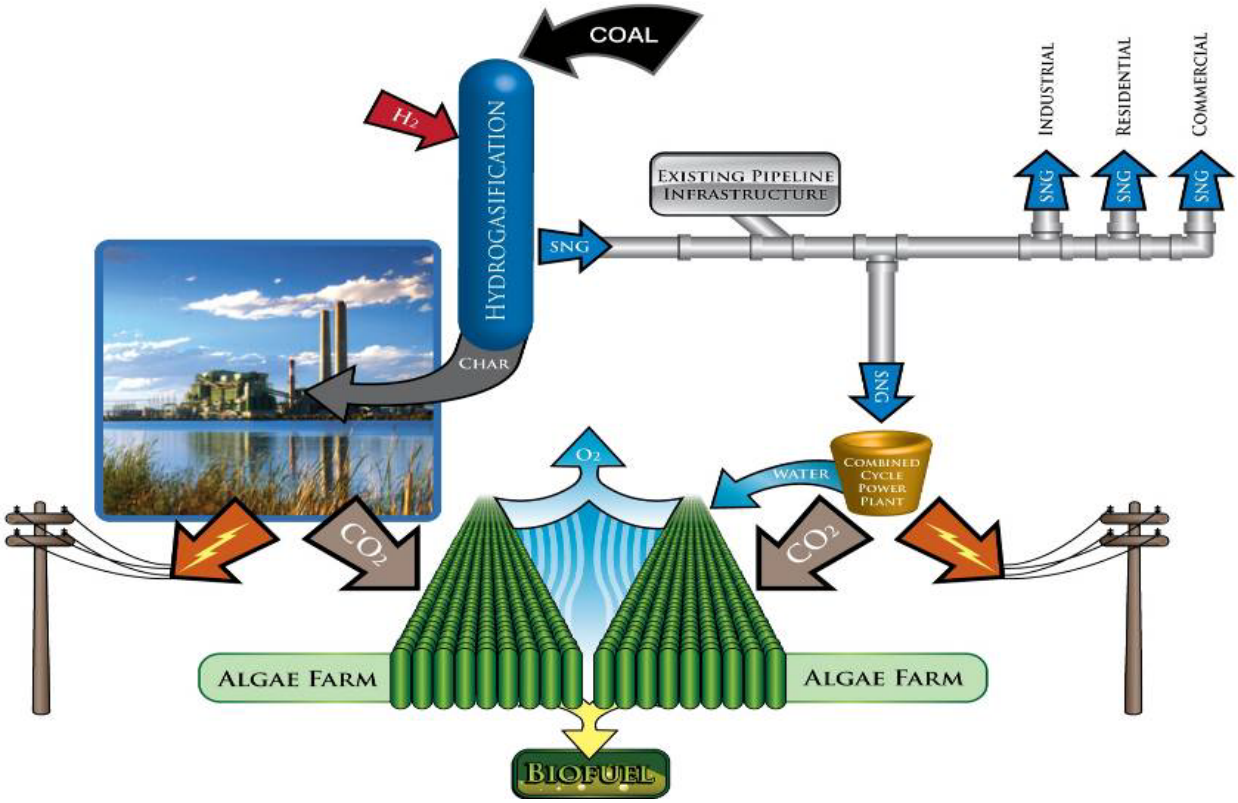

Figure 1-1. Conceptual Diagram of Integrated Energy System

Figure 1-1 illustrates the integrated energy system proposed by the project. In this system, hydrogen produced through electrolysis by using wind or off-peak grid electricity reacts with coal to produce substitute natural gas. Unreacted char is burned further to generate electricity. Although the hydrogasification process doesn't produce CO_2 emissions, the CO_2 generated from char or natural gas combustion would be captured by the algae farm to produce biofuel. This integrated process is intended to deliver energy and fuel in a long-term sustainable way.

1.2 SCOPE OF THE PROJECT

1.2.1 PROJECT OBJECTIVES

The objective of the project was to develop, test, operate, and evaluate at an engineering-scale, fully integrated energy system including: (1) an algae farm producing biofuel from algae cultivation using recycled CO_2 emissions, (2) a hydrogasification facility producing SNG using western coal, and (3) hydrogen production from electrolysis. The site of the project was to be adjacent to the APS 1000-MW Cholla coal-fired power plant, in Joseph City, Arizona

(Figure 1-2). The project intended to grow algae in water supplied from a saline aquifer adjacent to the Cholla plant. The planned cultivators were to be closed systems to facilitate water recycling, thereby minimizing water use. Continued R&D findings from the engineering-scale project would be utilized to develop a process design for commercial-scale co-production of SNG for pipeline injection and biofuel production.

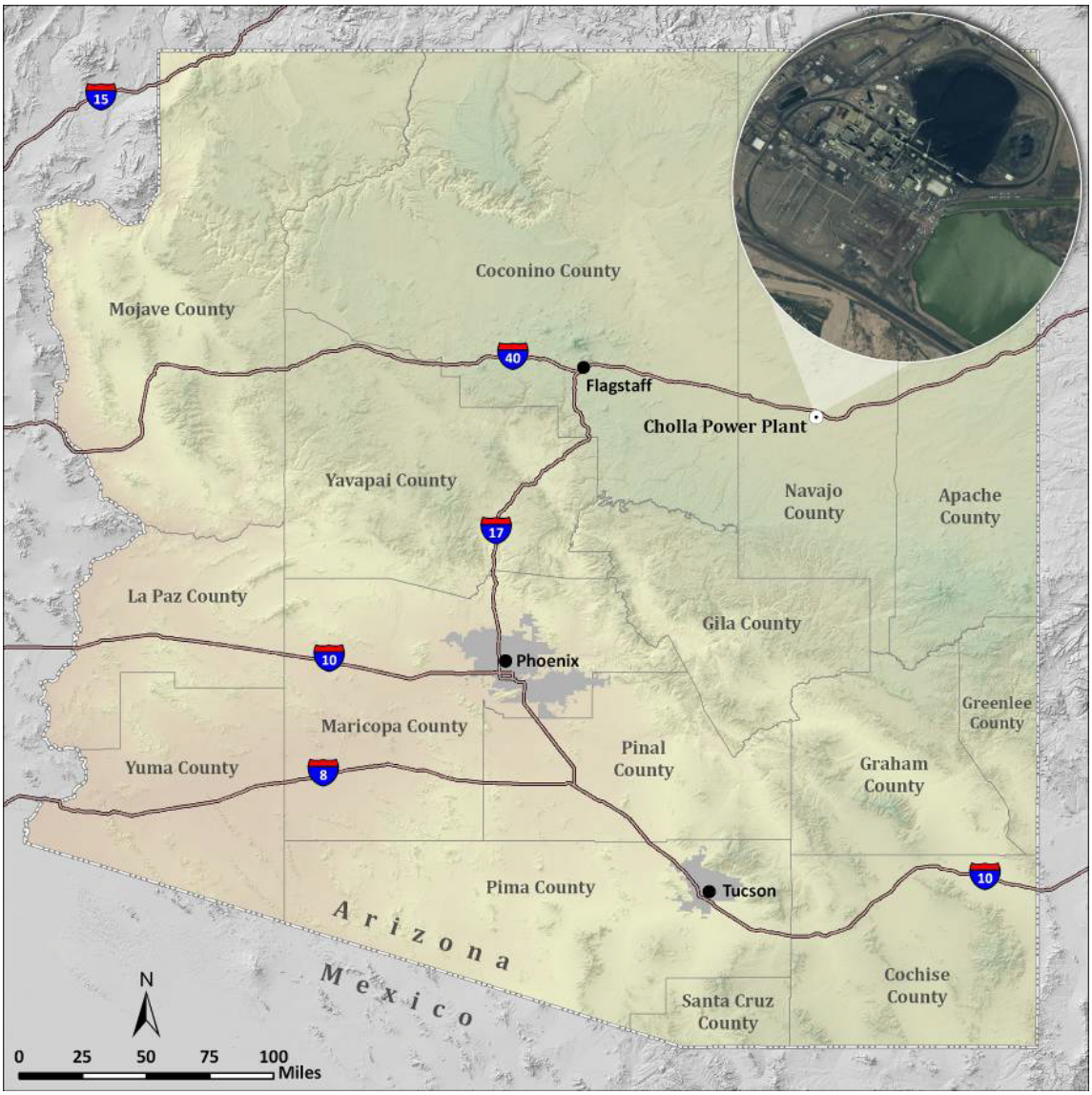

Figure 1-2. IES Project Location

Project objectives included the following performance targets: (1) an algae growth area of at least 25-acres, (2) an average annual CO_2 recycle rate of 70 metric tons per acre-year at a 75% capture rate, (3) an average annual biomass growth rate of 37 metric tons per acre-year, (4) an

average annual biofuel derived from algae lipids of 6 metric tons per acre-year, (5) an algae grown in saline water on non-arable land, and (6) SNG production from a continuous two tpd coal feed rate using western coal.

1.2.2 PROJECT TASK 1: CONCEPTUAL DESIGN

Task 1 of the project was to prepare a fully integrated process design. The process flow diagrams, energy and material balances, preliminary major equipment and other process considerations were proposed to reflect the fully integrated design. The process design was to be updated periodically using data from the project's R&D operations. The initial process design included: (1) CO_2 capture from the coal power plant flue gas, (2) CO_2 transport and control to and within the cultivator, (3) water delivery and water recycling, (4) nutrient injection and harvesting, (5) cultivator thermal management, (6) biomass processing with lipid extraction, (7) biofuel production from lipids, (8) hydrogen and oxygen production from electrolysis with ASME pressure vessel storage, (9) coal handling and processing, (10) char handling and processing, and (11) hydrogasification.

The conceptual design was implemented through the collaboration of APS, AL and Parsons. Engineering was broken down into the following areas as shown in Figure 1-3:

- CO_2 Delivery and Capture System: Flue gas from the Cholla Power Plant would be processed to separate CO_2, which would be compressed and piped from the power plant to the algae farm CO_2 storage vessel. The CO_2 process would remove moisture, acid gases, and metals from the flue gas, and return the CO_2-depleted flue gas back into the plant's ductwork to exit the stack in compliance with the plant's operating permits. The engineering design of this area was mainly prepared by Air Liquide although Parsons contributed as well.

- Algae Farm: The algae farm would be comprised of multiple subsystems to support (1) inoculation, (2) cultivation, (3) harvesting, (4) gas management, and (5) instrumentation and control. The algae farm would consist of 25-acres of enclosed cultivator surface area. The inoculation system would grow seed cultures for the farm. The algae cultivators would be semi-closed raceway systems. The harvester would be in continuous operation, harvesting algae from the cultivators. The harvester product would be supplied to the slurry pumps, which would supply the biofuel product process. CO_2 would be injected into the cultivators based upon results from the Redhawk pilot

project. Purge air would flow into the cultivators to remove excess oxygen. CO_2 monitors would track accumulation in the cultivators. The algae farm would be fully automated with operational data analysis and a field lab to provide supporting biological and chemical analysis. The algae farm would be operated from a control room. This engineering area received contributions from all team partners as well as Dynasep, Newark, Delaware, especially for algae farm design.

- Water Management: The water management system would use saline water as its makeup source, and would accept recycled water from the harvester growth surface. The Cholla power plant waste water "hot" stream and cold saline aquifer well water would also be used for the algae farm thermal management to control cultivator temperature. This process area was mainly designed by Parsons.

- Hydrogasification: The hydrogasification process would encompass a 2-tpd hydrogasifier with coal feed and char removal systems. A hydrogasifier designer would be selected based upon competency and the ability to design commercial-scale equipment. Coal would be stored in an enclosed area and supplied to the feed system. An inert gas would be selected - either CO_2 or nitrogen for system purging and coal carrying. Compressors for hydrogen, oxygen, and the inert gas would deliver gas into ASME storage vessels. Hydrogen in the product gas would be removed and recycled back into the hydrogasifier using a membrane technology. Resulting product gas from the 2 tpd hydrogasifier would be flared, unless operating permits at Cholla would allow its use in the existing coal-fired units. Char from the hydrogasifier would be supplied to the existing coal-fired units, where it would be mixed with coal and consumed during operations. The system would be fully automated with data recording and analysis. The entire system would be operated from the control room. The 2 tpd hydrogasifier with its coal feed and char removal systems was mainly designed by the APS technical team. AL focused on the engineering design of supporting processes.

- Biofuel Production: The biofuel production area would receive slurry from the algae farm harvester. Crude algae oil would be extracted and processed into biofuel. Biodiesel or green diesel may be produced at the biofuel facility. The design process would consider biofuel process alternatives. De-lipidated algae mass would be processed. AL was responsible for this area's engineering design with data input from APS.

The conceptual design also included the design of site infrastructure. The site infrastructure scope included grading, drainage, roadways, vehicle parking, fire protection, potable water, electric service, and facility buildings including administration, laboratory, control room, and rest rooms. This area was under the scope of Parsons.

This project would scale-up the algae system to 25 acres and hydrogasification to a 2 tpd coal feed rate, illuminating the barriers to successful development of a commercial-scale process. Integrating this scale-up with an operating coal-fired power plant would create the opportunity to more fully understand both the potential challenges and benefits of this system, as well as effectively closing the loop of this integrated process by recycling CO_2 produced onsite by the plant for the production of fuel. The saline aquifers that would be used for the algae production are of no use for the agriculture in the region with established methods, but can provide the water needed for large-scale farming of the microalgae used in this project for CO_2 recycling.

Integrated Energy Systems with Beneficial CO2 Use
DE-FE00001099

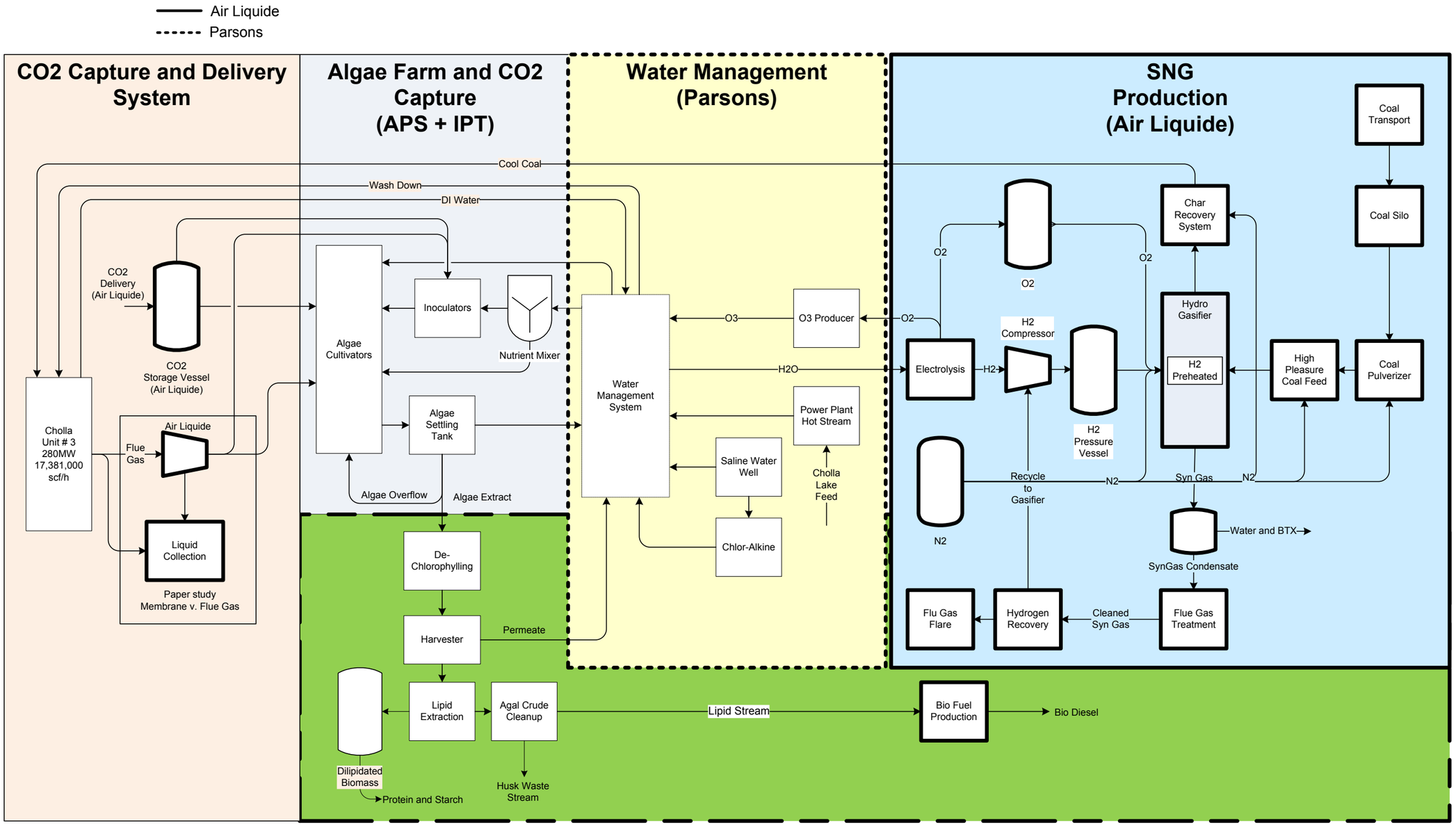

Figure 1-3. Block Diagram of Integrated Energy Systems with Beneficial CO_2 Use

THIS PAGE INTENTIONALLY LEFT BLANK.

1.2.3 PROJECT TASK 2: RESEARCH AND DEVELOPMENT TESTING

Task 2 of the project focused on two key elements of a carbon management strategy - hydrogasification and CO_2 recycling. The project continued the R&D performed under the Coal to SNG project.

In the Coal to SNG project, APS proposed an advanced hydrogasification process (AHP), where western coal is gasified under conditions that favor the production of methane; when processed, the coal produces SNG that meets specifications for direct injection into the nation's existing natural gas pipelines, thus providing an alternative to imported liquefied natural gas (LNG). The project included engineering, fabrication, construction, commissioning and initial testing of a bench-scale hydrogasifier at APS's South 2nd Avenue site in Phoenix. During the Budget Period One (BP1) of the IES project, the research focused on completing the product analysis protocols (including gas, liquid and solid), continuing bench scale testing and continuing the 1-D modeling to derive the kinetics of the hydrogasification of western coal to assist hydrogasifier scale-up.

The project also continued the algae testing initiated during the Coal to SNG project. In the Coal to SNG project an algae lab was built and a 6M cultivator testing system was designed, constructed and tested at APS' 3rd Avenue testing facility. During the course of IES, the research focused on the algae stressing to increase algae lipid content and reduce chlorophyll biologically, the development of methods for lipid analysis, oil extraction and biodiesel production from algae oil and algae biomass, and the demonstration of large-scale algae cultivation at APS Redhawk algae testing facility. At Redhawk, the project grew algae in cultivators on a two acre site. The cultivators were tested using power plant stack emissions to demonstrate sustainable algae growth. The use of algae for carbon management and recycling is an integral part of the project. This pilot effort at Redhawk substantially reduced the risks associated with an expansion of the algae portion of the IES project for its future implementation at the Cholla coal-fired generating station at a larger scale with larger cultivators.

A cost-effective, large-scale production system for growing algae using CO_2 from a power plant has not yet been demonstrated. The IES project could have lead to a commercial application in which a fully integrated energy system with beneficial CO_2 use could be implemented.

The project was officially terminated by APS on March 31, 2010. The remainder of this report summarizes the activities and research results covered by the project's BP1 from September 11, 2009 to March 31, 2010.

THIS PAGE INTENTIONALLY LEFT BLANK.

2. CONCEPTUAL DESIGN

The conceptual design was prepared through the collaboration of APS, AL and Parsons. The following incorporates the contributions of the three partners on the conceptual design, which was incomplete due to the termination of the project.

The contributions from AL covered the process design and the development of the preliminary major equipment list for the following processes: power plant flue gas preparation and CO_2 capture; CO_2 supply to algae farm; lipid extraction; crude algae cleanup; biodiesel production; de-lipidated biomass handling; and SNG fuel production from coal using hydrogasification. Parsons' contributions focused on process design and the development of the preliminary major equipment list for the water management system, including both the cold water and hot water management systems. Parsons also delivered the pre-conceptual design of the flue gas recovery and delivery, as well as the site infrastructure.

APS's efforts mainly focused on algae farm design, especially the 50 meter radius (50M) and 100 meter radius (100M) raceway design and hydrogasifier design, including coal feeding and char removal subsystems. Additionally, APS was the key to provide specifications, supporting documents, and knowhow to assist AL's and Parsons' design work.

Appendix A and B contain the design criteria prepared by APS for the hydrogasification process and algae farm, respectively.

2.1 FLUE GAS PREPARATION, CO_2 CAPTURE AND DELIVERY SYSTEM

2.1.1 PROCESS DESCRIPTION

The APS Cholla Unit 3 was the planned source of CO_2 for the project. The main flue gas supply would be conditioned (pressure, temperature, and/or composition) for direct introduction into the algae farm. The delivery line from the power plant would be designed to match the CO_2 on-demand requirement of the algae farm. A firm quote to engineer the delivery from the generating station to the farm was provided by Burns & McDonnell. The CO_2 transport included the following considerations:

- An eight-inch extraction tap installed in the discharge of the existing Sulfur Dioxide (SO_2) scrubber to withdraw the flue gas.
- An eight-inch injection tap installed in the existing bag house supply to return unutilized flue gas or farm exhaust back to the stack.

- The flue gas would travel about 4000 ft to the algae farm.
- Purchased CO_2 would be stored as backup during any power plant outages.

2.1.1.1 Flue Gas Conditioning

Several options were evaluated regarding how the flue gas would be conditioned before it was fed to the algae farm. In addition to pressure, temperature, and composition considerations at the point of injecting the CO_2 stream into the farm, the flue gas contains water as well as oxides of nitrogen. Therefore, when cooling and compressing this stream, care must be taken to handle the flue gas carefully to avoid the formation of a nitric acid condensate, which could be very corrosive to the equipment in some concentrations and conditions. More than one option is available for conditioning the flue gas, and A's pre-conceptual design proposed three process alternatives:

1. **Flue Gas Preparation Alternative 1: No additional flue gas preparation.**

   The process would purposely not cool the gas, remove moisture, treat for any metal contaminants, nor enrich the composition of CO_2. If the system can be designed to work in this manner, no gas conditioning provision would be required at Cholla. The flue gas pressure would be increased accordingly to satisfy line pressure losses in the system.

2. **Flue Gas Preparation Alternative 2: Dehydration of the entire flue gas stream prior to compression**.

   To protect the compressor by avoiding the formation of a nitric acid solution, a desiccation system was proposed this alternative for the entire flue gas stream. This alternative utilized the strong hygroscopic properties of concentrated sulfuric acid (as one desiccant choice) to selectively remove the water from the flue gas stream. This is a well-known pretreatment step used to desiccate air prior to use in a sulfuric acid plant.

   As the flue gas passes upwards through an absorption tower, it contacts the sulfuric acid and the water is absorbed by the acid. The acid is then sent to an evaporator where the water is evaporated, reconcentrating the sulfuric acid for reuse. A vacuum system is used to reduce the boiling point of the acid solution. The reconcentrated acid is cooled to assist in cooling the air as well as to prepare the acid for the exothermic reaction that results from mass transfer of the water from the flue gas stream to the acid stream. Once discharged from the desiccation unit, further cooling may be required by the compressor prior to compression.

Collected moisture from the evaporator would be processed in the power plant waste treatment system. While the baseline was drawn using sulfuric acid as our desiccant, a full list of desiccant technologies was reviewed for the optimal solution.

3. **Flue Gas Preparation Alternative 3: Cooling as required by compressor manufacturer for inlet temperature.**

As an alternative to dehydrating the entire flue gas stream, AL proposed an initial cooling step to reduce the inlet temperature to meet the compressor's specification while keeping the flue gas stream above the dew point. After compression, the gas stream must be cooled again to be below the maximum desired inlet temperature for the algae farm. A sensor at the entrance to the algae farm can adjust cooling water flow to provide a consistent temperature throughout the year.

2.1.1.2 Flue Gas Compression and CO_2 Concentration

- **Flue Gas Compression**

In order for the flue gas to be distributed to the algae farm, a flue gas pressure specification must be met. The flue gas stream requires a residual pressure of 18.0 pounds per square inch absolute (psia) at the algae farm inlet. Based on an average atmospheric pressure at 5300 ft elevation of 12.08 psia, a downstream residual pressure of 5.92 pounds per square inch gauge (psig) would be required, adding the pressure drop for the 4000 ft of 8 inch pipe of approximately 5.3 psia resulting in a gauge pressure of 11.22 psig or 23.3 psia at the discharge of the flue gas conditioning unit. These pressures are too high for a centrifugal fan. Compressor options would be reviewed including:

- Centrifugal Compressor - Lamson or Hoffman Style
- Liquid Ring Compressor - SIHI, NASH, others with flue gas experience
- Positive Displacement (PD) Blower

Each type of gas compression device would be reviewed based on experience with handling flue gas, the ability to mitigate the threat of nitric acid corrosion, the reliability of the unit, and the ancillary cost associated with each choice. The question of equipment redundancy (reliability concerns) would also be addressed. If the compression of the flue gas leads to gas temperature increase above the desired input temperature limit to the algae farm, a

post-compression cooling step would be included. If cross exchange with other existing streams could improve energy efficiency, this option would be reviewed as well.

The flue gas, once compressed and temperature adjusted, would be piped from the stack area to the algae farm.

- **CO_2 Concentration Subsystem**

The CO_2 content in the power plant stack is at a concentration of approximately 10 mole%. Concentration of this dilute stream minimizes over-all flue gas compression costs and degassing rates of inert gases at the algae farm "head space." AL and its subsidiary, Lurgi, have multiple options available for the recovery of CO_2 from streams of weak CO_2 content. If flue gas preparation alternative 1 or 3 above were chosen for the main flue gas stream, then the dehydration step outlined in alternative 2 could be used on the portion of the flue gas stream used as feed for a CO_2 concentration subsystem. After passing through this system the stream would be sufficiently dry to eliminate the concern of nitric acid formation.

- **Membrane Systems for the Physical Separation of Gas Molecules**

AL and its division Membrane Systems DuPont Air Liquide (MEDAL) have years of experience using membranes to separate gases. AL would use its experience and developmental capabilities to explore two opportunities for separation of CO_2 with membranes. Those two options are:

- **A Low-Pressure Membrane System:** The low-pressure system would utilize the pressure provided by the main flue gas compressor to a membrane separator so that an enriched CO_2 stream (up to 50%) could be produced. The flue gas stream would first be cooled to 77°F. The stream would pass through a knockout drum to separate liquid from the gas, and the feed would be sent to the membrane separation unit. A vacuum system would aid the permeation of the CO_2 enriched stream and would discharge to a storage/supply system, which would feed the algae farm.

- **A High-Pressure Membrane System:** A high-pressure membrane system adds an additional compressor to boost the pressure up to 50 psig to produce a 50% to 90% enriched CO_2 stream. The flue gas stream would first be cooled to 77°F. After passing through a knockout drum, the flue gas stream would be further compressed to near 50 psig. This would heat the flue gas stream, and an additional cooler followed by a knockout drum would return the stream to 77°F. The feed would enter the membrane

separation unit. A vacuum system would aid the permeation of the CO_2 enriched stream and would discharge to a storage/supply system.

- **Additional CO_2 Concentration Options**

AL and its subsidiary Lurgi would review additional options available for the recovery of CO_2 in more depth during later phases of engineering. The options would be evaluated for technical risk of implementation, initial capital cost and on-going operating cost.

The following diagram (Figure 2-1) provides a useful summary of the additional options available based on the flue gas CO_2 content and the final purity of the product.

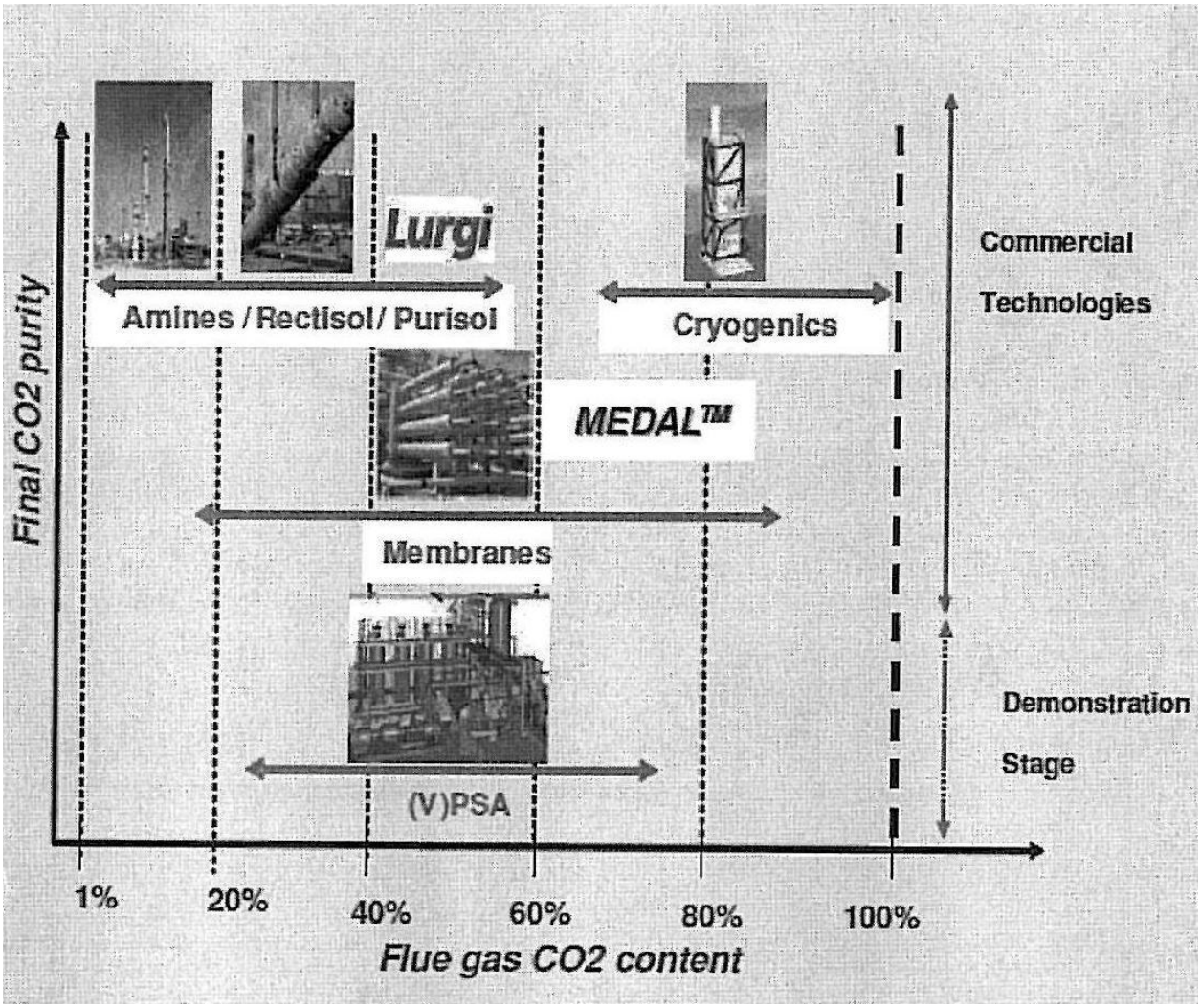

Figure 2-1. Summary of CO_2 Capture Techniques

AL can draw upon these Lurgi technologies:

1. The aMDEA® Process for the use of amines for chemical absorption and recovery of CO_2.
2. The Rectisol © process for the physical absorption and recovery of CO_2 from flue gas.
3. Pressure Swing Adsorption (PSA) process.

Under a separate opportunity a comparison test bed could be developed to compare these and additional technologies.

2.1.2 Process Flow Diagram and Material Balance

The basis of the flue gas heat and material balance was the data received from AL's Delaware Research & Technology Center (DRTC). It matched and expanded the preliminary process developed by APS. As the APS proposal requested a mass and energy balance, the balance provided was shown on both a molar and mass basis. In addition, the gas components were configured to include CO, which was outlined, and argon, which exists in the air and contributes to the bulk density (though not characterized in the original APS flow data).

The process mass balance (Table 2-1) was built to recover 70 metric ton/acre-year CO_2 (unit ratio) as input to the algae farm, to cover the CO_2 requirement for a 40-acre farm utilizing 365 days per year and 24 hours per day (note the project finalized the algae farm at 25-acres instead of 40 acres).

Table 2-1. CO_2 Recovery from Flue Gas Material Balance Prepared by Air Liquide Based on 40-Acre Farm Feed

APS C02 RECOVERY FROM FLUE GAS												
		1	2	3	4	5	6	9	10	11	12	13
Phase:		Vapor	Vapor	Vapor	Vapor	Vapor	Vapor	Vapor	Vapor	Mixed	Liquid	Liquid
Component Mole Flow												
N2	LBMOUHR	4.2E+07	126.43	4.2Et07	126.43	126.43	126.43	77.42	49.02	49.02	0	49.02
H2O	LBMOUHR	1.2E+07	36.27	1.2E...07	36.27	36.27	36.27	22.21	14.06	14.06	14.03	0.03
CO2	LBMOUHR	6400507	19.46	6400487	19.46	19.46	19.46	11.91	7.54	7.54	0	7.54
02	LBMOUHR	3189835	9.7	3189825	9.7	9.7	9.7	5.94	3.76	3.76	0	3.76
N02	LBMOUHR	8206.23	0.02	8206.2	0.02	0.02	0,02	0.02	0.01	0,01	0.01	0
CO	LBMOUHR	7703.01	0.02	7702.98	0.02	0.02	0.02	0.01	0.01	0.01	0	0.01
502	LBMOUHR	2764.88	0.01	2764.87	0.01	0,01	0.01	0.D1	0	0	0	0
H2SO4	LBMOUHR	0	0	0	0	0	0	0	0	0	0	0
AR	LBMOUHR	6313.94	0.02	6313.92	0.02	0.02	0.02	0.01	0.01	0.01	0	0.01
Component Mole Fraction												
N2		0.65872	0.65872	0.65872	0.65872	0.65872	0.65872	0.65872	0.65872	0.65872	1.SE-OS	0.81192
H2O		0.18899	0.18899	0.18899	0.18899	0.18899	0.18899	0.18899	0.18899	0.18899	0.99939	0.00051
CO2		0.10137	0.10137	0.101 37	0.10137	0.10137	0.10137	0.10137	0.10137	0.10137	0.00016	0.12491
02		0.05052	0.05052	0.05052	0.05052	0.05052	0.05052	0.05052	0.05052	0.05052	2.7E-05	0.06226
N02		0.00013	0.00013	0.00013	0.00013	0.00013	0.00013	0.0001 3	0.00013	0.00013	0.0004	B.7E-OS
CO		0.0001 2	0.0001 2	0.00012	0.00012	0.00012	0.00012	0.00012	0.00012	0.00012	a	0.00015
S02		4.4E-05	4.4E-05	4.4E-OS	4.4E-05	4.4E-05	4.4E-OS	4.4E-05	4.4E-OS	4.4E-05	6E-06	5.3E-05
H2SO4		0	0	0	0	0	0	0	0	0	0	0
AR		0.0001	0.0001	0.0001	0.0001	0.0001	0.0001	0.0001	0.0001	0.0001	0	0.00012
Component Mass Row												
N2	LBIHR	1.2E+09	3541.62	1.2E+09	3541.82	3541.82	*3541.B2*	2168.66	1373.16	1373.16	0.01	1373.1 5
H2O	LBIHR	2.1E+08	653.5	2.1E+08	653.5	653.5	653.5	400.14	253.36	253.36	252.6	0.56
CO2	LB/HR	2.BE+08	856.29	2.BE+08	856.29	856.29	856.29	524.31	331 .98	331 .98	0.1	331.88
02	LS/HR	1E+08	310.28	1E+OB	310.28	310.28	310.28	189.99	120.3	120.3	0.01	120.28
N02	L8/HR	377532	1.15	377531	1.15	1.15	1.15	0.7	0.44	0.44	0.26	0.19
CO	LBIHR	215764	0.66	215764	0.66	0.66	0.66	0.4	0.25	0.25	0	0.25
S02	LBIHR	177131	0.54	177131	0.54	0.54	0.54	0.33	0.21	0.21	0.01	0.2
H2SO4	LB/HR	0	0	0	0	0	0	0	0	0	0	0
AR	LBIHR	252229	0.77	252229	0.77	0.77	0.77	0.47	0.3	0.3	a	0.3
Component Mass Fraction												
N2		0.66017	0.66017	0.66017	0.66017	0.66017	0.66017	0.66017	0.66017	0.66017	2.3E-OS	0.75166
H2O		0.12181	0.12181	0.12181	0.12181	0.12181	0.12181	0.12181	0.12181	0.12181	0.9985	0.0003
CO2		0.15961	0.15961	0.15961	0.15961	0.15961	0.15961	0.15961	0. 15961	0.15961	0.00039	0.18167
02		0.05784	0.05784	0.05784	0.05784	0.05784	0.05784	0.05784	0.05784	0.05784	4.8E-05	0.06584
N02		0.00021	0.00021	0.00021	0.00021	0.00021	0.00021	0.00021	0.00021	0.00021	0.00102	0.0001
CO		0.00012	0.00012	0.00012	0.00012	0.00012	0.00012	0.00012	0.00012	0.00012	0	0.00014
S02		0.0001	0.0001	0.0001	0.0001	0.0001	0.0001	0.0001	0.0001	0.0001	2. 1 E-05	0.00011
H2SO4		0	0	0	0	0	0	0	0	0	0	0
AR		0.00014	0.00014	0.00014	0.00014	0.00014	0.00014	0.00014	0.00014	0.00014	0	0.00016
Mole Flow	LBMOUHR	6.3E+07	191.94	6.3E+07	191 .94	191 .94	191 .94	117.52	74.41	74.41	14.04	60.37
Mass Flow	LB/H R	1.8E+09	5365	1.8E+09	5365	5365	5365	3285	2080	2080	253.18	1826.82
Volume Flow	CUFT/HR	4.3E+l0	129589	4.3E+10	102105	66967.9	59055.8	36160	22895.8	15345.2	4.08	86.11
Temperature	F	302	302	302	140	298.65	201	201	201	77	77	77
Pressure	PSI	12. 1	12.1	12.1	12.08	23.3	23	23	23	23	23	23
Vapor Fraction		1	1	1	1	1	1	1	1	0.82	0	0
Liquid Fraction		0	0	0	0	0	0	0	0	0.18	1	1
Solid Fraction		0	0	0	0	0	0	0	0	0	0	0
Molar Enthalpy	BTUILBMOL	35133.1	35133.1	35133.1	36348.1	35162. 1	35897.9	35897.9	35897.9	40275.3	-123656	21863.9
Mass Enthalov	BTUILB	1256.91	1256.91	1258.91	1300.38	1257.95	1284.27	1284.27	1284.27	1440.88	6857.84	-722.55
Enthalpy Flow	BTU/HR	2.2E+1 2	6743330	2.2E+1 2	6976532	6748902	6890131	4218841	2671290	2997028	1736285	1319971
Molar Entroov	BTUILBMOL- R	3	3	3	1.21	1.66	0.65	0.65	0.65	-6.73	-40.09	-10.18
Mass Entropy	BTUILB-R	0.11	0.11	0.11	0.04	0.06	0.02	0.02	0.02	-0.24	-2.22	-0.34
Molar Density	L8MOUCUFT	0	0	0	0	0	0	0	0	0	3.44	0.7
Mass Density	La/CUFT	0.04	0.04	0.04	0.05	0.08	0.09	0.09	0.09	0.14	62.08	21.21
Average Molecular Weight		27.95	27.95	27.95	27.95	27.95	27.95	27.95	27.95	27.95	18.03	30.26

2.1.3 Process Chemistry

There was little process chemistry involved in the three options proposed by AL for CO_2 capture and delivery except for the possible reaction of nitric oxide with water to form nitric acid and its potential to corrode equipment. The use of sulfuric acid (or other desiccant) to selectively remove water from the flue gas, while not a chemical reaction as such, used the hydroscopic nature of the acid. If highly concentrated sulfuric acid is used to dehydrate the flue gas so as to prevent the condensation of water, it might lead to the formation of nitric acid in solution. Because of the possibility of some acid carrying over with the water vapor from the sulfuric acid concentration step, sodium hydroxide was added to neutralize the condensing stream. Waste water streams also had to be accommodated.

The effects of heavy metal content in the flue gas and its impact on algae growth would be reviewed in more detail during the initial work in later phases of engineering.

2.1.4 Process Flow Diagram

The following figures (Figure 2-2 to Figure 2-6) contain flow diagrams and material balances of the three options identified by AL for flue gas preparation and CO_2 capture.

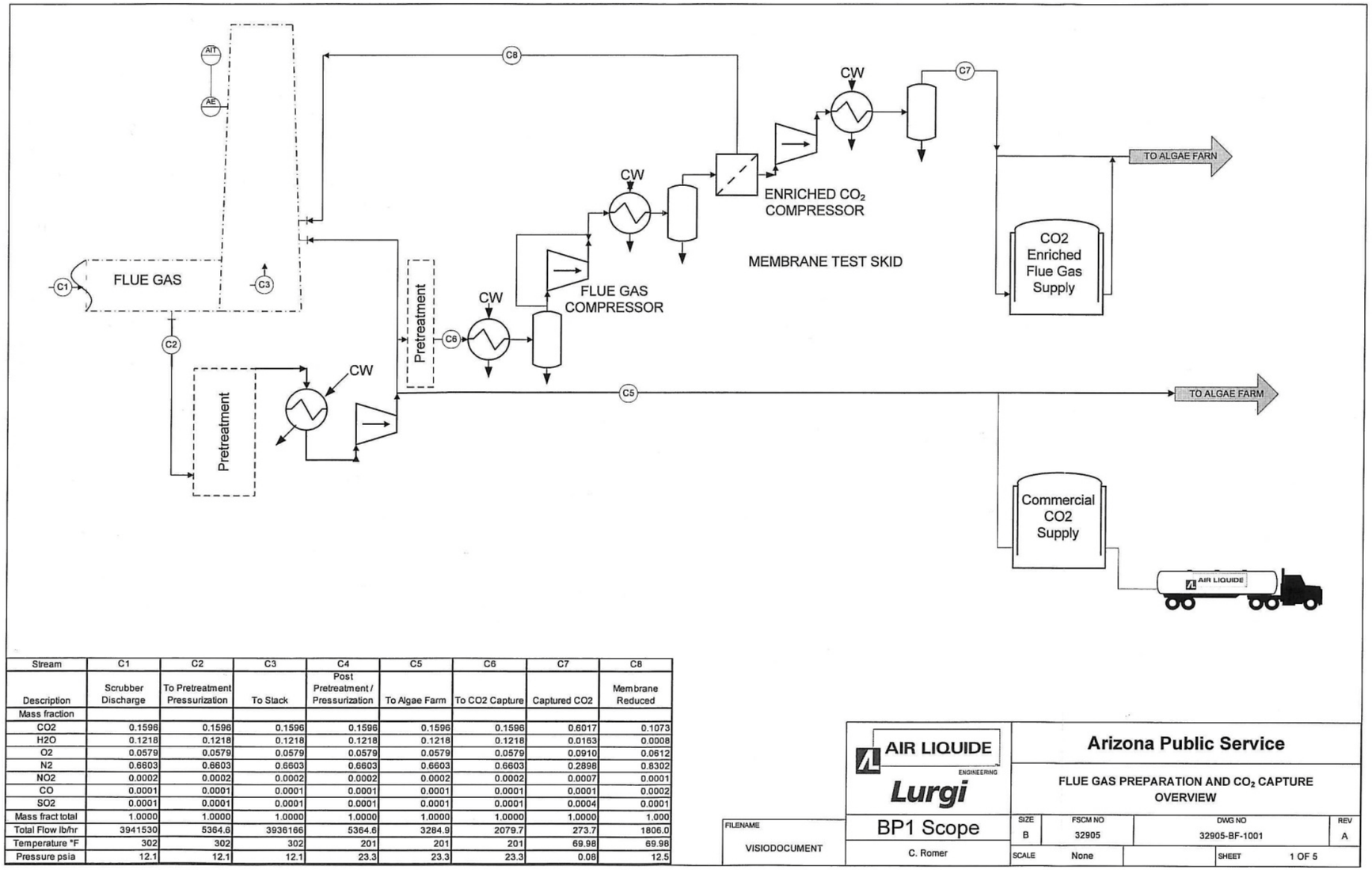

Stream	C1	C2	C3	C4	C5	C6	C7	C8
Description	Scrubber Discharge	To Pretreatment Pressurization	To Stack	Post Pretreatment / Pressurization	To Algae Farm	To CO2 Capture	Captured CO2	Membrane Reduced
Mass fraction								
CO2	0.1596	0.1596	0.1596	0.1596	0.1596	0.1596	0.6017	0.1073
H2O	0.1218	0.1218	0.1218	0.1218	0.1218	0.1218	0.0163	0.0008
O2	0.0579	0.0579	0.0579	0.0579	0.0579	0.0579	0.0910	0.0612
N2	0.6603	0.6603	0.6603	0.6603	0.6603	0.6603	0.2898	0.8302
NO2	0.0002	0.0002	0.0002	0.0002	0.0002	0.0002	0.0007	0.0001
CO	0.0001	0.0001	0.0001	0.0001	0.0001	0.0001	0.0001	0.0002
SO2	0.0001	0.0001	0.0001	0.0001	0.0001	0.0001	0.0004	0.0001
Mass fract total	1.0000	1.0000	1.0000	1.0000	1.0000	1.0000	1.0000	1.000
Total Flow lb/hr	3941530	5364.6	3936166	5364.6	3284.9	2079.7	273.7	1806.0
Temperature *F	302	302	302	201	201	201	69.98	69.98
Pressure psia	12.1	12.1	12.1	23.3	23.3	23.3	0.08	12.5

AIR LIQUIDE ENGINEERING Lurgi

Arizona Public Service

FLUE GAS PREPARATION AND CO_2 CAPTURE OVERVIEW

FILENAME	SIZE	FSCM NO	DWG NO	REV
VISIODOCUMENT	B	32905	32905-BF-1001	A
BP1 Scope	SCALE None		SHEET 1 OF 5	
C. Romer				

Figure 2-2. Process Flow Diagram and Material Balance of Air Liquide Flue Gas Preparation and CO_2 Capture

THIS PAGE INTENTIONALLY LEFT BLANK.

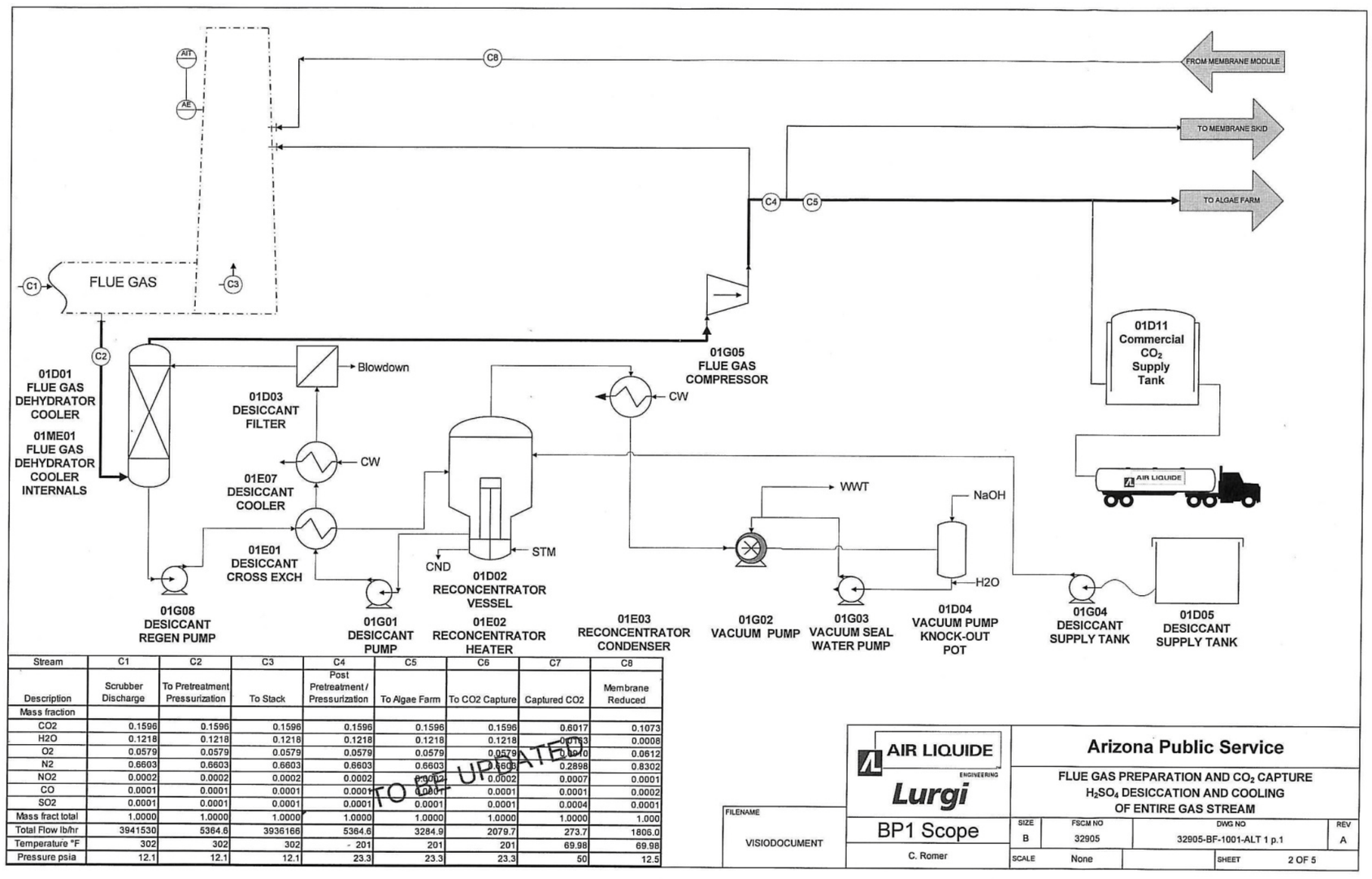

Stream	C1	C2	C3	C4	C5	C6	C7	C8
Description	Scrubber Discharge	To Pretreatment Pressurization	To Stack	Post Pretreatment / Pressurization	To Algae Farm	To CO2 Capture	Captured CO2	Membrane Reduced
Mass fraction								
CO2	0.1596	0.1596	0.1596	0.1596	0.1596	0.1596	0.6017	0.1073
H2O	0.1218	0.1218	0.1218	0.1218	0.1218	0.1218	0.0163	0.0008
O2	0.0579	0.0579	0.0579	0.0579	0.0579	0.0579	0.0320	0.0612
N2	0.6603	0.6603	0.6603	0.6603	0.6603	0.6603	0.2898	0.8302
NO2	0.0002	0.0002	0.0002	0.0002	0.0002	0.0002	0.0007	0.0001
CO	0.0001	0.0001	0.0001	0.0001	0.0001	0.0001	0.0001	0.0002
SO2	0.0001	0.0001	0.0001	0.0001	0.0001	0.0001	0.0004	0.0001
Mass fract total	1.0000	1.0000	1.0000	1.0000	1.0000	1.0000	1.0000	1.000
Total Flow lb/hr	3941530	5364.6	3936166	5364.6	3284.9	2079.7	273.7	1806.0
Temperature °F	302	302	302	201	201	201	69.98	69.98
Pressure psia	12.1	12.1	12.1	23.3	23.3	23.3	50	12.5

Figure 2-3. Process Flow Diagram and Material Balance of Air Liquide Alternative 1 for Flue Gas Preparation and CO_2 Capture

THIS PAGE INTENTIONALLY LEFT BLANK.

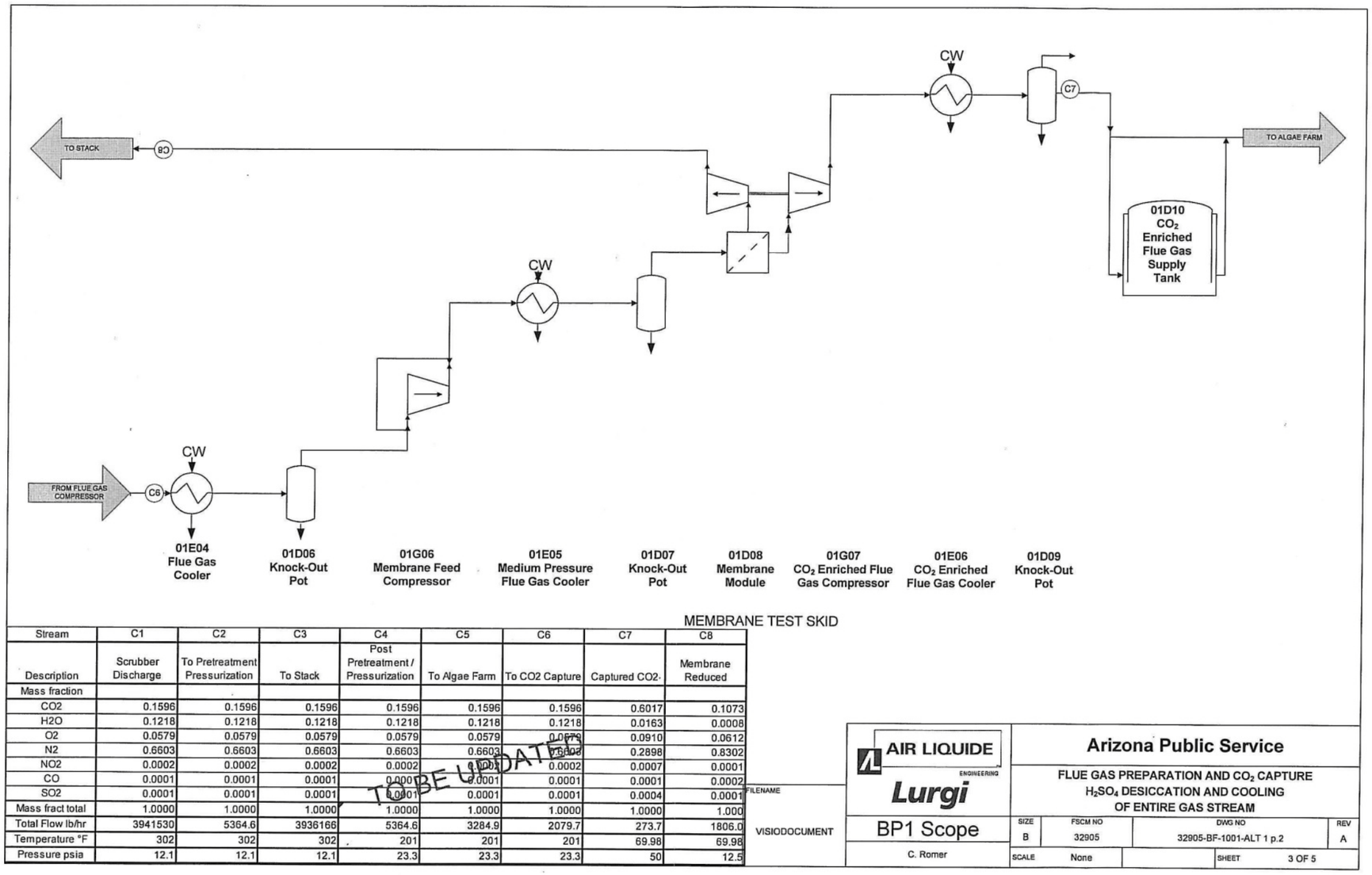

MEMBRANE TEST SKID

Stream	C1	C2	C3	C4	C5	C6	C7	C8
Description	Scrubber Discharge	To Pretreatment Pressurization	To Stack	Post Pretreatment / Pressurization	To Algae Farm	To CO2 Capture	Captured CO2	Membrane Reduced
Mass fraction								
CO2	0.1596	0.1596	0.1596	0.1596	0.1596	0.1596	0.6017	0.1073
H2O	0.1218	0.1218	0.1218	0.1218	0.1218	0.1218	0.0163	0.0008
O2	0.0579	0.0579	0.0579	0.0579	0.0579	0.0579	0.0910	0.0612
N2	0.6603	0.6603	0.6603	0.6603	0.6603	0.6603	0.2898	0.8302
NO2	0.0002	0.0002	0.0002	0.0002	0.0002	0.0002	0.0007	0.0001
CO	0.0001	0.0001	0.0001	0.0001	0.0001	0.0001	0.0001	0.0002
SO2	0.0001	0.0001	0.0001	0.0001	0.0001	0.0001	0.0004	0.0001
Mass fract total	1.0000	1.0000	1.0000	1.0000	1.0000	1.0000	1.0000	1.000
Total Flow lb/hr	3941530	5364.6	3936166	5364.6	3284.9	2079.7	273.7	1806.0
Temperature °F	302	302	302	201	201	201	69.98	69.98
Pressure psia	12.1	12.1	12.1	23.3	23.3	23.3	50	12.5

TO BE UPDATED

FILENAME
VISIODOCUMENT

AIR LIQUIDE ENGINEERING Lurgi

BP1 Scope

C. Romer

Arizona Public Service

FLUE GAS PREPARATION AND CO_2 CAPTURE
H_2SO_4 DESICCATION AND COOLING
OF ENTIRE GAS STREAM

SIZE	FSCM NO	DWG NO	REV
B	32905	32905-BF-1001-ALT 1 p.2	A
SCALE	None	SHEET	3 OF 5

Figure 2-4. Process Flow Diagram and Material Balance of Air Liquide Alternative 1 for CO_2 Membrane Capture

THIS PAGE INTENTIONALLY LEFT BLANK.

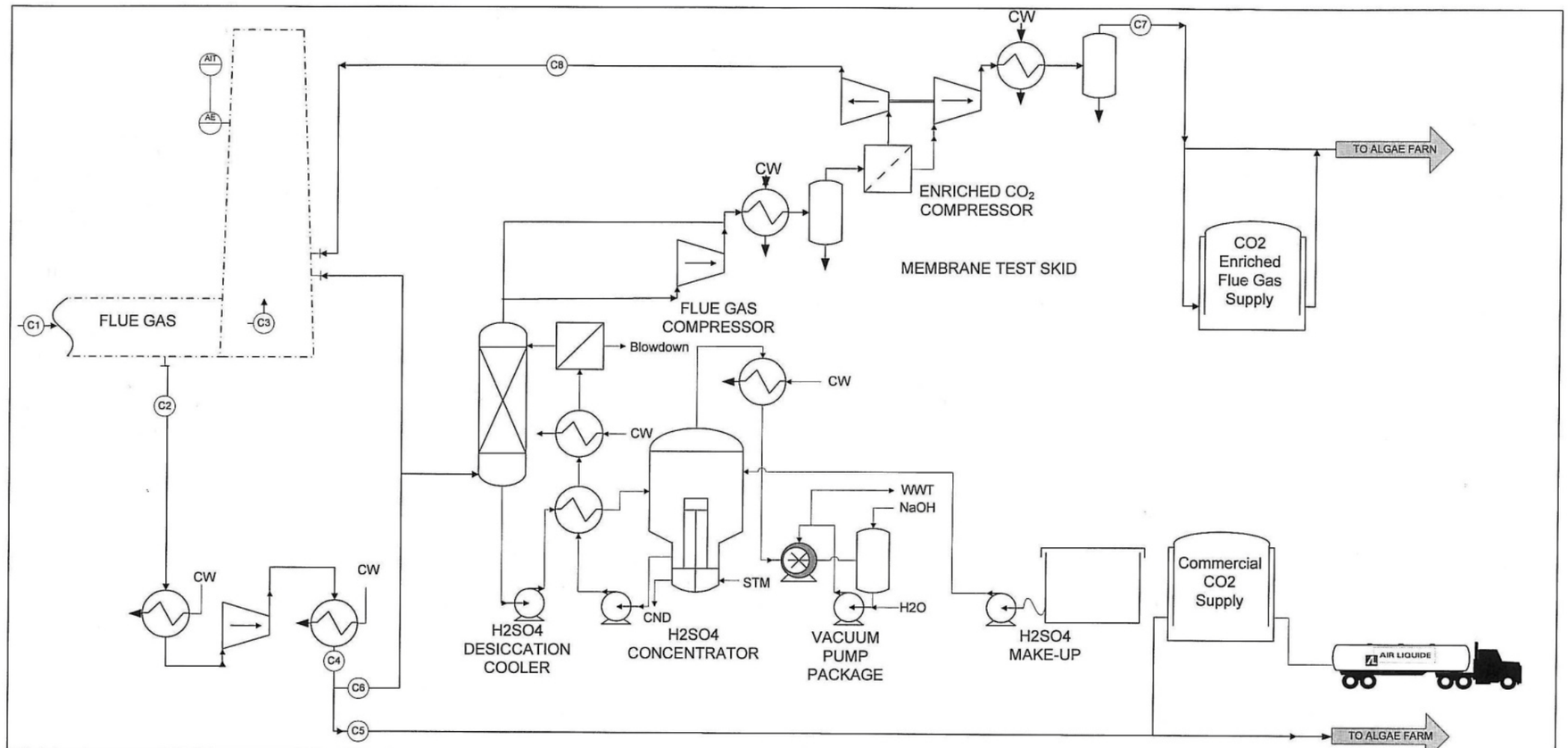

Stream	C1	C2	C3	C4	C5	C6	C7	C8
Description	Scrubber Discharge	To Pretreatment Pressurization	To Stack	Post Pretreatment / Pressurization	To Algae Farm	To CO2 Capture	Captured CO2	Membrane Reduced
Mass fraction								
CO2	0.1596	0.1596	0.1596	0.1596	0.1596	0.1596	0.6017	0.1073
H2O	0.1218	0.1218	0.1218	0.1218	0.1218	0.1218	0.0163	0.0008
O2	0.0579	0.0579	0.0579	0.0579	0.0579	0.0579	0.0910	0.0612
N2	0.6603	0.6603	0.6603	0.6603	0.6603	0.6603	0.2898	0.8302
NO2	0.0002	0.0002	0.0002	0.0002	0.0002	0.0002	0.0007	0.0001
CO	0.0001	0.0001	0.0001	0.0001	0.0001	0.0001	0.0001	0.0002
SO2	0.0001	0.0001	0.0001	0.0001	0.0001	0.0001	0.0004	0.0001
Mass fract total	1.0000	1.0000	1.0000	1.0000	1.0000	1.0000	1.0000	1.000
Total Flow lb/hr	3941530	5364.6	3936166	5364.6	3284.9	2079.7	273.7	1806.0
Temperature °F	302	302	302	201	201	201	69.98	69.98
Pressure psia	12.1	12.1	12.1	23.3	23.3	23.3	50	12.5

FILENAME: VISIODOCUMENT	AIR LIQUIDE ENGINEERING Lurgi	Arizona Public Service	
	BP1 Scope	FLUE GAS PREPARATION AND CO_2 CAPTURE H_2SO_4 DESICCATION AND COOLING OF MEMBRANE FEED	
	C. Romer	SIZE: B; FSCM NO: 32905; DWG NO: 32905-BF-10X01-ALT2; REV: A	
		SCALE: None; SHEET: 4 OF 5	

Figure 2-5. Process Flow Diagram and Material Balance of Air Liquide Alternative 2 for Flue Gas Preparation and CO_2 Capture

THIS PAGE INTENTIONALLY LEFT BLANK.

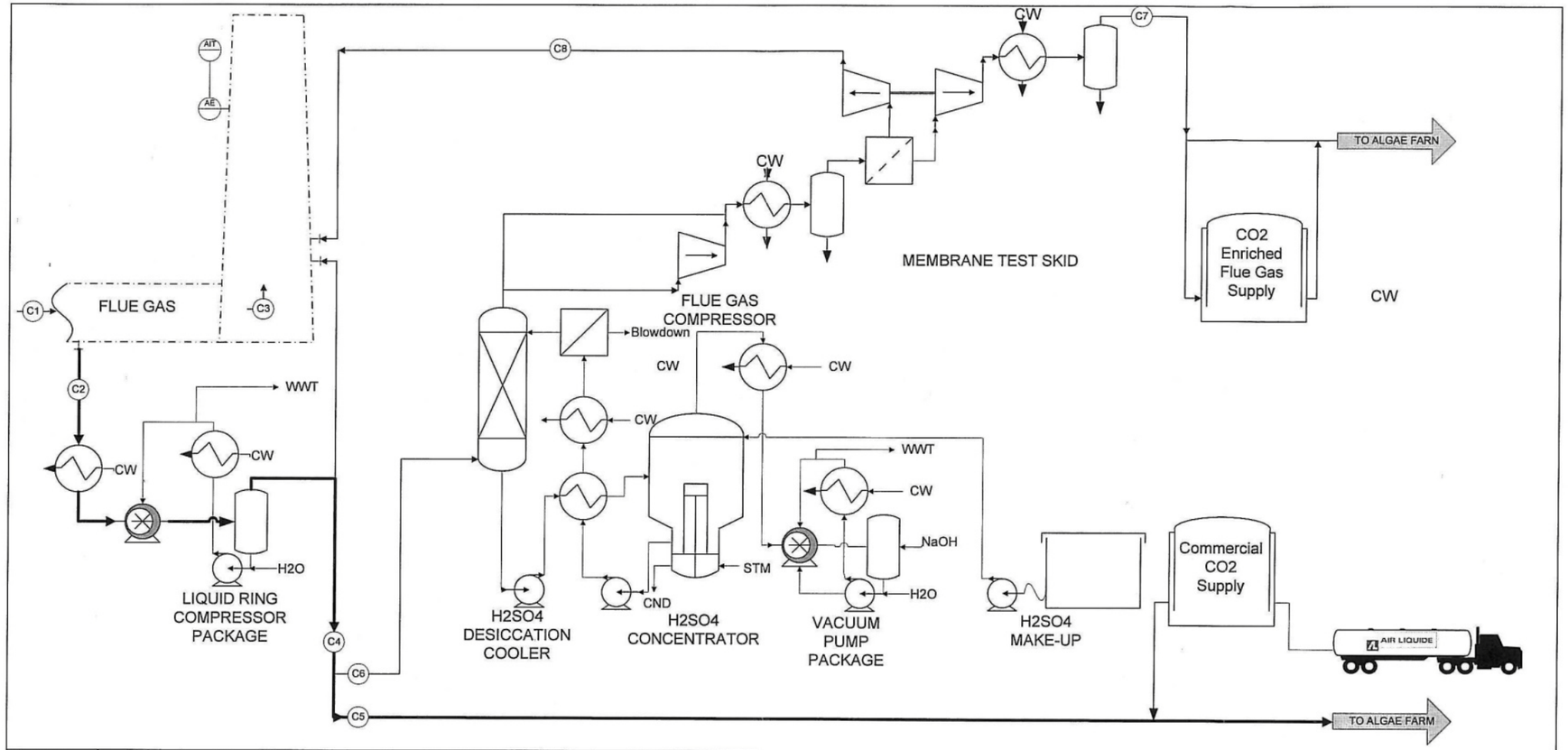

Stream	C1	C2	C3	C4	C5	C6	C7	C8
Description	Scrubber Discharge	To Pretreatment Pressurization	To Stack	Post Pretreatment / Pressurization	To Algae Farm	To CO2 Capture	Captured CO2	Membrane Reduced
Mass fraction								
CO2	0.1596	0.1596	0.1596	0.1596	0.1596	0.1596	0.6017	0.1073
H2O	0.1218	0.1218	0.1218	0.1218	0.1218	0.1218	0.0163	0.0008
O2	0.0579	0.0579	0.0579	0.0579	0.0579	0.0579	0.0910	0.0612
N2	0.6603	0.6603	0.6603	0.6603	0.6603	0.6603	0.2898	0.8302
NO2	0.0002	0.0002	0.0002	0.0002	0.0002	0.0002	0.0007	0.0001
CO	0.0001	0.0001	0.0001	0.0001	0.0001	0.0001	0.0001	0.0002
SO2	0.0001	0.0001	0.0001	0.0001	0.0001	0.0001	0.0004	0.0001
Mass fract total	1.0000	1.0000	1.0000	1.0000	1.0000	1.0000	1.0000	1.000
Total Flow lb/hr	3941530	5364.6	3936166	5364.6	3284.9	2079.7	273.7	1806.0
Temperature °F	302	302	302	201	201	201	69.98	69.98
Pressure psia	12.1	12.1	12.1	23.3	23.3	23.3	50	12.5

TO BE UPDATED

FILENAME: VISIODOCUMENT	AIR LIQUIDE ENGINEERING Lurgi	Arizona Public Service
	BP1 Scope	FLUE GAS PREPARATION AND CO_2 CAPTURE H_2SO_4 DESICCATION AND COOLING OF MEMBRANE FEED WITH LIQUID RING COMPRESSOR
	C. Romer	SIZE B; FSCM NO 32905; DWG NO 32905-BF-1001-ALT3; REV A; SCALE None; SHEET 5 OF 5

Figure 2-6. Process Flow Diagram and Material Balance of Air Liquide Alternative 3 for Flue Gas Preparation and CO_2 Capture

THIS PAGE INTENTIONALLY LEFT BLANK.

.

2.1.5 PRELIMINARY EQUIPMENT LIST

The preliminary equipment list in Table 2-2 provides a concept of the items required. Detailed review and engineering may affect the methods and modes required in completing the unit operations as originally conceived.

Table 2-2. Preliminary Equipment List for Flue Gas Preparation and CO_2 Capture Developed by Air Liquide

	Tag Number	Description	Construction Material	Comments	Process Flow Diagram (PFD)
1	01D01	Flue Gas Dehydrator/Cooler	Carbon Steel	Dilute 93% H_2S0_4 to 88% then reconcentrate	Alt 1 p.1
2	01ME01	Flue Gas Dehydrator/Cooler Internals	Ceramic / Carbon Steel Stainless	Ceramic Packing, Packing support, Distributor(s), Mist Eliminator, etc.	Alt 1 p.1
3	01D02	Desiccant Reconcentrator Vessel	Glass Lined Steel / Zirconium		Alt 1 p.1
4	01E01	Desiccant Cross exchanger	Hastelloy		Alt 1 p.1
5	01EO7	Desiccant Cooler	Duplex Stainless		Alt 1 p.1
6	01E02	U-bundle Reconcentrator Heater	Tantelum / Zirconium		Alt 1 p.1
7	01G01	Desiccant Pump	Hastelloy or Lined		Alt 1 p.1
8	01G08	Desiccant Regen Pump	Hastelloy or Lined		Alt 1 p.1
9	01003	Desiccant Filter	Lined Carbon Steel / Polypropylene		Alt 1 p.1
10	01E03	Reconcentrator Condenser	Duplex Stainless for Service water Chlorides		Alt 1 p.1
11	01G02	Vacuum Pump	Special Conditions Neutralizing acid vapors		Alt 1 p.1
12	01D04	Vacuum Pump Knock-out Pot	High Chromium Stainless Steel		Alt 1 p.1
13	01G03	Vacuum Seal water Pump	High Chromium Stainless Steel		Alt 1 p.1
14	01G04	Desiccant Make Up Pump	DI or Lined	Magdrive Pump	Alt 1 p.1
15	01D05	Desiccant Make Up Tank	Carbon Steel	Need a desiccant on tank vent to prevent dilution/corrosion	Alt 1 p.1
16	01G05A	Flue Gas Compressor	Stainless Steel / Carbon Steel		Alt 1 p.1
17	01E04	Flue Gas Cooler	Stainless Steel		Alt.1 p.2
18	01D06	Knock-out Pot	Stainless Steel		Alt 1 p.2
19	01G06	Membrane Feed Compressor	Stainless Steel		Alt 1 p.2

	Tag Number	Description	Construction Material	Comments	Process Flow Diagram (PFD)
20	01E05	M.P. Flue Gas Cooler	Stainless Steel		Alt 1 p.2
21	01007	Knock-out Pot	Stainless Steel		Alt 1 p.2
22	01PK01	Desiccation System	See items		Alt 1 p.2
23	01PK02	Vacuum Pump Package	Stainless Steel / Carbon Steel		Alt 1 p.1
24	01PK03	Flue Gas Low Pressure Compressor Package	See items		Alt 1 p.1
25	01PK04	Flue Gas High Pressure Compressor Package	See items		Alt 1 p.2
26	01PK05	Membrane Skid	See items		Alt 1 p.2
27	01008	Membrane CO_2 Filter	See items		Alt 1 p.2
28	01PK06	CO_2 Enriched Flue Gas Compressor Package	See items		Alt.1 p.2
29	01G07	CO_2 Enriched Flue Gas Compressor	Stainless Steel / Carbon Steel		Alt 1 p.2
30	01E06	CO_2 Enriched Flue Gas Cooler	Stainless Steel		Alt 1 p.2
31	01009	Knock-out Pot	Stainless Steel		Alt.1 p.2
32	01D10	CO_2 Enriched Flue Gas Supply Tank	Carbon Steel		Alt 1 p.2
33	01D11	Commercial CO_2 Supply Tank	Carbon Steel		Alt 1 p.2

2.2 ALGAE FARM

The phototrophic production of algae uses light input, CO_2, and nutrients within a liquid culture medium to create algae biomass. Two broad types of systems are used to cultivate algae: open cultivation systems and closed photobioreactors (PBRs). Open cultivation systems include natural or artificial ponds and raceways.

Raceway systems are oblong cultivators typically divided into two parallel lanes with a fluid propulsion means at one or more locations and a turn-around at the opposite end. Open raceways are susceptible to contamination and are thus generally limited to growing algae species that are a combination of fast-growing, naturally occurring, or extremophiles. Open raceways also have high rates of evaporation and often very low CO_2 capture rates due to their open nature. For over 15 years, the phycology field has recognized that raceway cultivators can

be built at substantial scale, but because they are open systems, they are limited to cultivating a few extremophile species, and the uncontrolled factors in raceways cannot be readily addressed.

On the other hand, closed PBRs greatly reduce the occurrence of contamination and control evaporative loss. The closed PBR allows much higher rates of capture for CO_2 introduced into the system. Closed and semi-closed PBRs consist of tubular systems such as that installed for production of clean inoculum, parallel glass plate PBRs, and plastic film cultivators such as those employed in the 6M radius cultivators at Redhawk. Closed PBRs typically provide higher aerial productivity rates than open raceway systems. They also come at substantial capital cost due to the system elements required to retain the algae, provide appropriate turbulence, modulate light exposure, regulate temperature, introduce CO_2, and remove oxygen. Operational costs also tend to be high due to the higher pumping energy. Many strategies have been pursued in the search for higher productivity levels (i.e., grams per square meter per day [$g/m^2/day$]) of PBRs while failing to recognize that the optimization function is not productivity in isolation but, rather, productivity per energy expenditure in such a CO_2 capture project. Raceways offer lower capital cost and energy usage per unit of cultivation area than do closed PBRs.

The approach for the design of the algae cultivation system intended for Cholla was to use many of the benefits of the raceway and its ability to be scaled to large culture volumes while using less energy than a closed PBR. Also, new design elements such as a covering of the raceway to control evaporative loss and increase the CO_2 capture rate, as well as provide a means of energy-efficient regulation of algae culture temperature could be incorporated.

The conceptual layout of the single cultivation system intended for use at Cholla, to be scaled up by employing many of the cultivation units described herein, consisted of two main raceway systems to facilitate algae growth. The algae culture would be mixed using dual paddlewheels from a single power drive train. The system would be covered with an inflated structure to enclose the raceway and isolate the ambient environment. The system covering limits evaporation and enables active thermal control, if needed, using evaporative cooling. There would also be a CO_2 supply system to blend CO_2 into the culture to efficiently meet the CO_2 capture rate within the project objectives. Each cultivator would have a fluid feed into the cultivator to provide freshwater makeup. All cultivators would have the required instrumentation

and controls (I&C) and would be connected to a web-based interface to monitor the culture conditions to ensure that the correct operational parameters are maintained.

In addition to the floating cultivator design, two cultivation systems were planned: an intermediate-scale raceway system and a production-scale raceway system. Table 2-3 summarizes the dimensions and volumes of these two systems. The intermediate-scale raceway would be used to scale-up culture from a 6M floating bioreactor (100 m^2 growth area and 12,000 L volume). The intermediate scale-cultivator would provide sufficient inoculum for production.

Table 2-3. Raceway Characteristics*

Parameters	Intermediate Scale	Production Scale
Lane Length, m	50	100
Lane Width, m	4	8
Raceway Area, m^2	450	1,800
Raceway Depth, cm	15	15
Raceway Volume, m^3	67.5	270
Liters (L)	67,500	270,000
Raceways per Cultivator	2	2
Cultivator Area, m^2	900	3,600
Cultivator Volume, m^3	135	540
L Total	135,000	540,000

* The intermediate scale is intended for culture scale-up. The production scale would be used for the bulk of algae production.

The intermediate scale cultivator consists of a pair of 50M cultivator raceways. The overall dimensions are 59 m long by 17 m wide. The maximum system height is approximately 2.5 m. Culture depth may vary from 10 to 20 centimeter (cm), with 15 cm being the target depth.

The production scale cultivators for Cholla would be the dual integral raceway design. The overall system dimensions are 118 m long by 33 m wide. The maximum system height is approximately 3.0 m. Culture depth may also vary from 10 to 20 cm, with 15 cm being the target depth.

Both the intermediate- and production-scale cultivators consist of the following patent-pending features:

- Raceway system to facilitate algae growth in modest layer culture
- Dual paddlewheels from a single power drive train

- Active thermal cooling using evaporative cooling via a combination of air-flow regulation through the cultivator and modulation of culture flow rate through nozzles
- Flow steering in the raceway turnarounds to avoid flow stagnation points and, thus, opportunity for biomass accumulation
- CO_2 supply system to blend carbon dioxide into culture
- Heat exchanger for culture heating
- Fluid feed into cultivator to provide a combination of makeup water and makeup nutrients
- Fluid withdrawal from cultivator to enable sampling and harvesting
- Automated instrumentation system to measure media pH, optical density, dissolved oxygen, and temperature
- All instrumentation and control installed in an Underwriters Laboratories Inc. (UL)-certified electrical panel
- Web-based interface to monitor culture status and system operation
- Trend monitoring for all monitored process variables

Figure 2-7, Figure 2-8, Figure 2-9, and Figure 2-10 show the schematic drawings of this dual integral raceway design.

Figure 2-7. Raceway Cultivator Top View

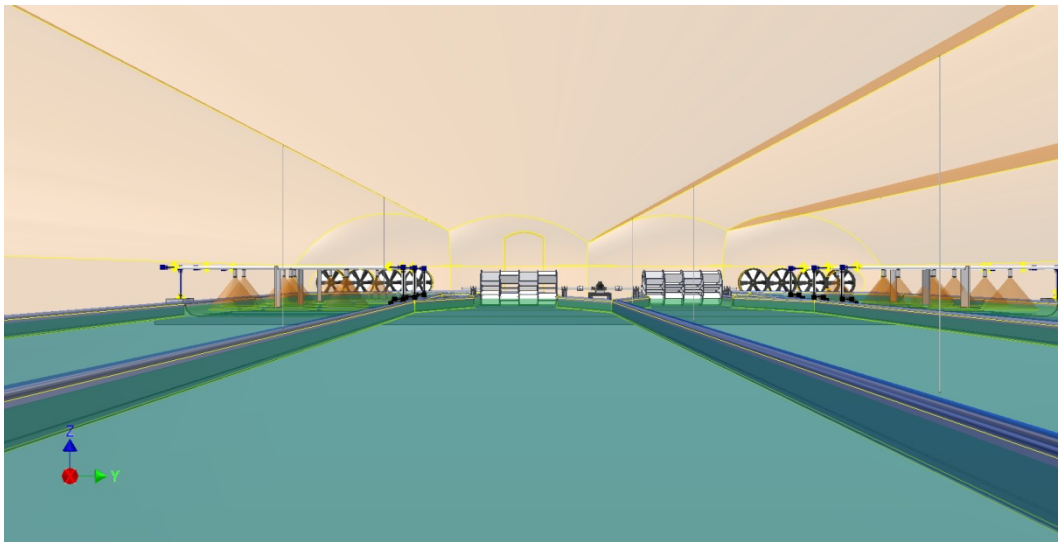

Figure 2-8. Raceway Cultivator Interior View*
*Culture spray enables direct evaporative cooling.

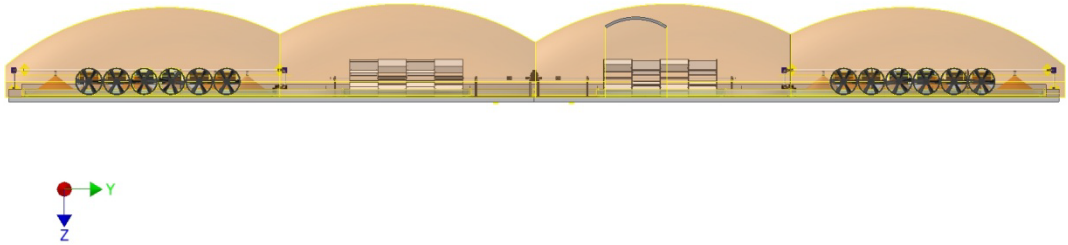

Figure 2-9. Raceway Cultivator Left End View*
*Fans are used to maintain structure inflation. Paddlewheel propels culture within raceway.

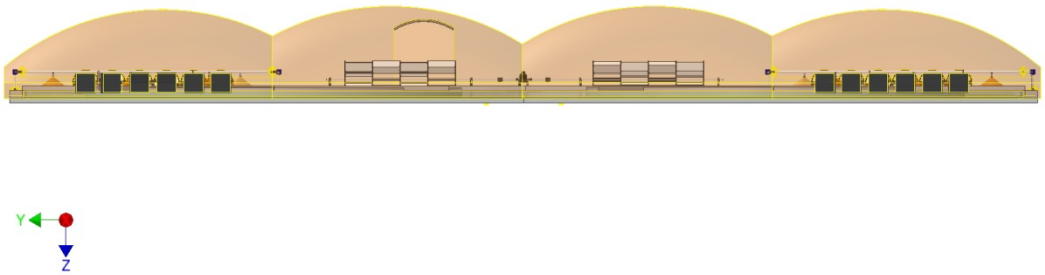

Figure 2-10. Raceway Cultivator Right-End View*
*Louvers are present to vent air from cultivator.

A few intermediate-scale cultivators were planned to be deployed at Cholla to scale-up inoculum to the large volume in a single production-scale cultivator. Such production-scale cultivators would then be arranged in the appropriate numbers to meet the active culture footprint of the final Cholla algae farm. Although this target footprint for active culture growth was not finalized, the modular nature of these cultivators easily accommodates various footprint sizes by deploying more or fewer of the single production cultivators as required. In this manner, a customizable size, large-scale algae production farm can be constructed using cultivators capable of controlling evaporative water loss and increasing CO_2 capture rate, as well as regulating the algae culture temperature in an energy-efficient manner.

When the culture density reached the appropriate point (about 1.1 grams per liter), a portion of the algae would be harvested. The harvesting would be done in two steps to minimize energy consumption. The first step would be settling, and the second would be through a Dynasep algae harvester. The harvester would produce an algae paste, and the permeate would be recycled for additional algae culturing. Figure 2-11 shows a conceptual process diagram for the dewatering system.

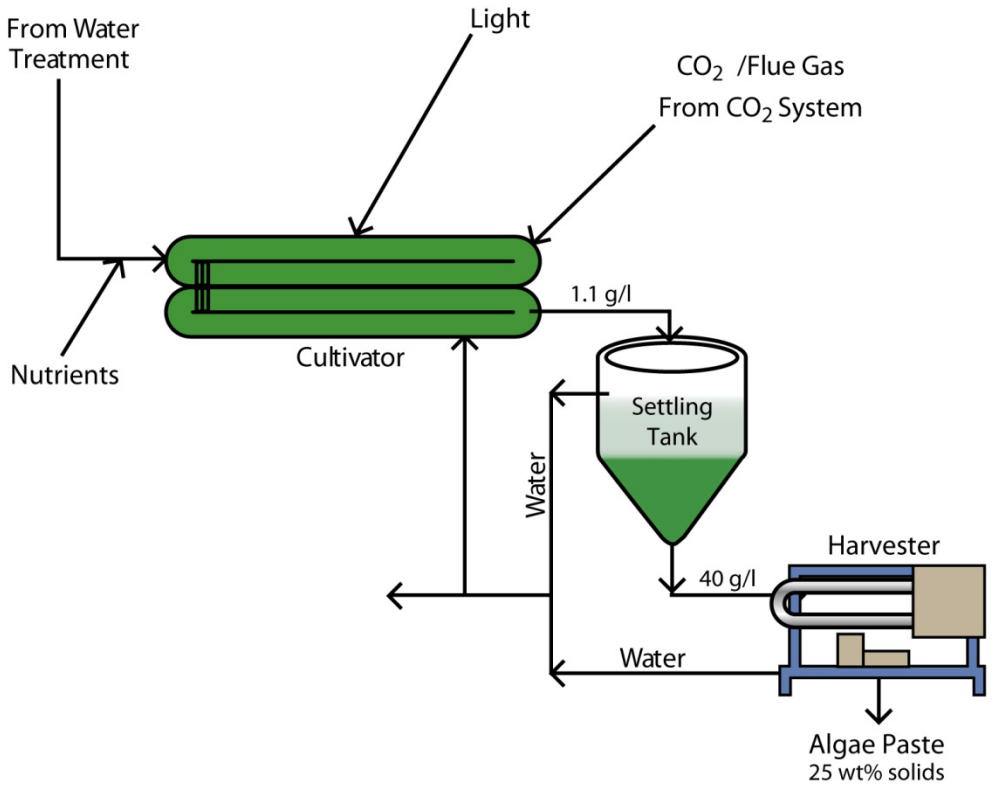

Figure 2-11. Conceptual Process Diagram for the Dewatering System

Algae inoculum and the inoculation strategy must be part of the normal operations for the 25-acre Cholla farm. The inoculation process is shown Figure 2-12. This step-type technique of inoculation can be used, because the culture density has minimum and maximum thresholds that allow for step change. The first two steps of preparing the inoculums were studied during the Coal to SNG Project. A hanging bag system would be used to cultivate a starter culture, which would then be used to inoculate a 6M closed-pond cultivator after the desired density was attained. A 50M cultivator was proposed as an intermediate-size inoculator at Cholla. The culture volume of a 50M cultivator is one-fourth that of a 100M cultivator. Once a 100M cultivator has reached proper algae culture density, it can provide the inoculum for other 100M cultivators.

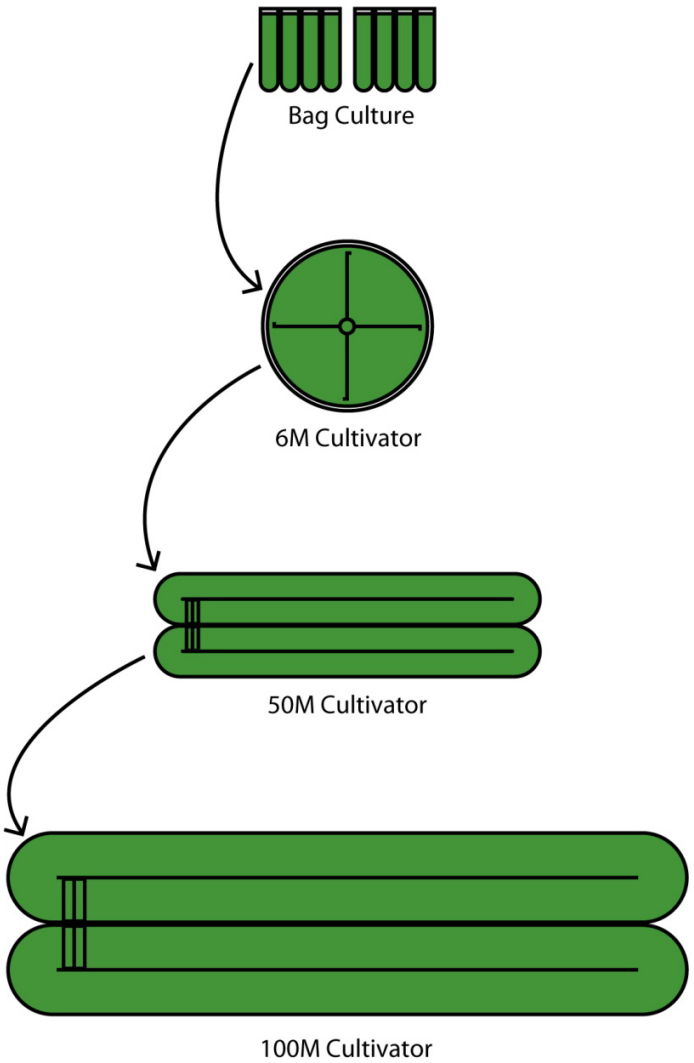

Figure 2-12. Conceptual Diagram of the Scaled-Up Inoculation Process

2.3 WATER MANAGEMENT

The project water was classified as to its intended use. Four primary water classifications are as follows: cultivation water, maintenance water, auxiliary water and potable water.

Cultivation water would undergo filtration and sterilization. The main sources for cultivation water would be permeate and saline aquifer water. Permeate water from the harvester would be recycled for cultivation and would undergo filtration and sterilization. Saline aquifer well water would enter a clarifier allowing suspended particulates to settle, and the particulates would then be properly disposed. Clarified saline aquifer water would then be chlorinated and placed in storage. Nutrients would be added to the water prior to introduction into the cultivators. If the salinity concentration of the permeate water (from the harvester) reaches a predetermined level, then the water would be diverted into maintenance water. Water contamination, salinity levels, and solids concentration would dictate either continual 'blow-down" or cycle replenishment. The wastewater (from maintenance, blow down, and other functions) would be directed to the power plant ash water system. Maintenance water would be used to clean the cultivators. Spent maintenance water would be filtered, chlorinated, and then recycled. Auxiliary water would be used for purposes such as chilling, compressors, etc. It is not yet known what systems would require auxiliary water. Potable water and its complimentary wastewater would be completely separated from these farm process water systems.

There are several water sources identified in the Cholla IES Project. The primary source of makeup water at Cholla is the site-located well 30A. A second source is Cholla Lake water. Cholla Lake is a 300-acre manmade impoundment adjacent to the farm, and it is used for Cholla Units 1 and 2 cooling. The makeup water for Cholla Lake is the third source; this is well water from the Coconino aquifer. A fourth source is natural precipitation, which could be retained on the project site. A final source is condensate from the flue gas slip stream. Water from the Cholla Units 1 and 2 steam condensers flows adjacent to the algae farm and is a year-round source of low-grade heat. Water that can no longer be used in farm operations becomes waste water and would be sent to the power plant ash water system.

2.3.1 WATER ANALYSIS FROM CHOLLA POWER PLANT

Cholla well 30A water has a salinity ranging between 1700 to 4000 parts per million (ppm) (depending on how close a well is to the lower boundary of the aquifer). As a comparison, the salinity of the seawater is generally around 35,000 ppm. Salinity in the aquifer (or more

accurately total dissolved solids [TDS]) may actually be from salts different than sodium chloride (NaCl), which makes up most of the TDS in seawater. Table 2-4 shows general water labeling characteristics.

Table 2-4. General Water Characteristics

Water Classifications	Classifications
Fresh	< 1,000 ppm TSD
Brackish	1,000–5,000 ppm TSD
Highly Brackish	5,000–15,000 ppm TSD
Saline:	15,000–30,000 ppm TSD
Seawater:	30,000–40,000 ppm TSD
Brine	40,000–300,000+ ppm TSD

More detailed water analysis on Cholla Lake and Well 30A is shown in Table 2-5.

Table 2-5. Water Analysis for the Cholla Power Plant Water Sources

Description (ppm)[a]	Cholla Lake	Well 30A
Manganese Total (ppm)	0.02	< 0.01
Nitrate (ppm)	<1	< 1
Phosphate Total (ppm)	< 0.4	< 0.4
Phosphate Total Inorganic (ppm)	< 0.2	< 0.2
Phosphate Ortho- (ppm)	U[b]	< 0.2
Phosphate Filtered Ortho (ppm)	< 0.2	–
Silica Total (ppm)	5.0	11.8
Fluoride (ppm)	0.6	0.4
Carbon Total Organic (ppm)	4.7	1.0
Turbidity (NTU)	1.2	1.6

[a] Parts per million (ppm) except as noted; Nephelometric Turbidity Unit (NTU)
[b] U is defined as undetectable; the number is too minute to be detected.

2.3.2 Preliminary Water Specification Based on Farm Biological Requirements

A preliminary water specification for the water management process was created based upon the farm biological requirements. These requirements are described below:

2.3.2.1 Treated Water Requirements

Microbial

- No organisms or biological particulates over 0.2 micrometer (µm). Note: American Society of Testing and Materials (ASTM) calls for 0.45 µm for reagent water use, but smaller particulates should lower operating costs. (R&D experiments would confirm proper size).
- Bacterial loads equivalent to drinking quality water (particularly as accumulated over time); that is, heterotrophic bacteria count (HBC) of 100/100 colony forming units per milliliter (cfu/ml).
- No cysts or encased stages of organisms (particularly as accumulated over time).
- Biological oxygen demand at or below original source water (aquifer); that is 3–5 mg O_2/L maximum, as a reasonable starting point.

Chemical

- No nitrites.
- < 2 ppm hypochlorite.
- Sodium ions 10 microgram per liter (µg/L) max; this may be relaxed in future.
- Chloride ions 10 µg/L max; this may be relaxed in future.
- No residual ozone or associated chemicals of the treatment process.
- No chemicals or compounds from the treatment system (particularly as accumulated over time).
- pH at or above 7.0 and at or below 7.5.
- Conductivity at or below original source water (aquifer); that is, 0.25 micro siemens per centimeter (µS/cm) max.
- Alkalinity at or below original source water (aquifer).
- Ammonia at or below original source water (aquifer).

- Chemical oxygen demand at or below original source water (aquifer).
- General metals analysis after treatment to be consistent with metals analysis of source water (no accumulation).
- Copper at or below original source water (aquifer). This may require sampling verification. Especially if cooling pond water is used, note that Cholla may add cupric agents specifically to hinder algae growth. (Even for the aquifer water, copper content needs to be periodically verified.)
- Endotoxin specifications may be extremely important. These toxins are generally released by lysed bacteria and may be of concern for employees as well as algae. (Laboratory R&D would finalize acceptable values).

Particulate

- No debris from any filtration, disinfection, and clarification processes.
- TDS at or below original source water (aquifer); that is, 500 mg/L TDS.
- If freshwater make-up is required, TDS should be below that of the aquifer.

2.3.2.2 Other Considerations

- Residuals should be kept to an absolute minimum or should be tested biologically prior to implementation. For example, coagulant or flocculent agents are used to clump and settle algae to make sure that these are removed from recycled water.
- Anticipated need for ozone and/or ultraviolet (UV) treatment or both to oxidize and break down active organic chemicals from algae culture unless alternate methods are proven to be effective.
- Development of methods for episodic and/or continuous cleaning/flushing procedures for distribution system to keep biofilms and other contaminants from building up and taking hold in pipes and components.

The water management process design was mainly contributed by Parsons. In Parsons' study, the water management system was divided into cold and hot water subsystems. The cold water system receives and treats returned water from the cultivators with makeup water from the well. It then supplies the treated cold water to various plant uses, including the cultivators. The hot

water system heats the cultivators and support structures during cold periods. The nutrient supply and several other small water-support systems are grouped together as support systems.

2.3.3 Cold Water Management

The Process Flow Diagram (PFD) and material balance of (conceptual) cold water management system are shown in Figure 2-13 and Figure 2-14 respectively. Water is largely received from the algae harvesters and to a much smaller extent from occasional wash down of the cultivators. The water is assumed to contain particulates, living organisms (algae and bacteria), dissolved proteins, nutrients and various salts, particularly NaCl. These solids separate in the clarifier with an approximate holding time of 4 hours with the clear water skimmed off and sent on for additional treatment. The settled solids (and some water) are sent by screw pump on to the ash pond stream.

After the clarifier is the clear water tank sized at approximately 10% of the clarifier; it is the surge tank for the UV treatment process for the elimination of most living organisms. In parallel is an ozone generator that is fed pure oxygen to create an ozone mixture. This is injected into the treatment stream to further treat the water, which then enters a contact tank (with recirculation). A small catalytic filter at the top of the tank ensures that the O_3 is converted back to O_2 prior to being released to the atmosphere. The treated water is further filtered for small particulates (in a cartridge filter) and odors (in a charcoal filter) before chlorination (by the chlorination skid) and transferred to the holding tanks (with recirculation). The two holding tanks serve as the chlorine contact tank, the buffered reserves for cultivator supply, and a 200,000 gallon (gal) fire reserve. Water from this tank is sent to the cultivators, utility stations, deionizer, and nutrient mixers.

Filtered well-water is added to the holding tanks to make up for process losses; on average this is expected to be about 360 gpm, the majority of which is due to evaporation. Filtered well water would also be sent to the chlorination skid to mix with calcium hypochlorite tablets.

This system is to be housed in a single building (size to be determined (TBD)), which would also house the water management support skids (see Section 2.3.5), except for the nutrient mixer, which location is TBD.

THIS PAGE INTENTIONALLY LEFT BLANK.

Figure 2-13. Process Flow Diagram of the Cold Water Management System by Parsons

THIS PAGE INTENTIONALLY LEFT BLANK.

STREAM	P1-001	P1-002	P1-003	P1-004	P1-005	P1-006	P1-007	P1-008	
DESCRIPTION	PERMEATE FROM HARVESTER	WASH DOWN WATER FROM CULTIVATORS	WATER	CLEAR WATER	10% WASH DOWN WATER TO ASH	WELL WATER	WATER	CHLORINE GAS	
TOTAL GPM	484	1057	1541	1435	106	1050	2485		
MASS FLOW RATE (LBS/DAY)								49.7	
Stream	P1-009	P1-010	P1-011	P1-012	P1-013	P1-014	P1-015	P1-016	P1-017
Description	WATER WITH CHLORINE GAS	WATER	RECIRC WATER*	WATER	WATER TO NUTRIENT MIXER	WATER	WASTE FROM FILTER TO ASH	AUXILIARY WATER SUPPLY	WASH DOWN PLUS WASTE
TOTAL GPM	2485	2485	2485	2485	2385	100	NEGLIGIBLE	100	106
Evaporation									
50	GAL/POND.MIN								
Chlorine Concentration									
5	PPM								

Figure 2-14. Material Balance of the Cold Water Management Process by Parsons

THIS PAGE INTENTIONALLY LEFT BLANK.

2.3.4 HOT WATER MANAGEMENT

The cultivators were intended to be operating year round and as such must be kept warm enough to keep the algae growing. It was planned that heating be provided to keep the cultivator environment at or above 50°F during the cold winter nights. A system to supply this heat from the hot channel return (from the condenser cooling return, expected to be at 105°F) would be provided.

The PFD and process balance of the conceptual hot water management system are shown in Figure 2-15 and Figure 2-16 respectively. Hot water at 105°F is drawn from the plant return channel by two separate loops, one for each of the 28 ponds section. In addition to the two pumps, a third redundant pump is supplied that can be used on either loop. The flow, under pressure is divided and delivered in pipes, below grade, to each cultivator where the flow to (TBD) heat exchangers is controlled by a temperature (pond or pond atmosphere - TBD) controlled via a flow control valve. A flow of about (150 TBD) gpm is available for each of the 56 ponds. The cool water return from the heat exchangers is collected into the respective channel return line. The western return channel returns upstream of the pump suction, but the relatively small amount of cool water insignificantly affects channel temperature.

The primary pumps would be (4200 TBD) gpm each and would be housed in a pump house near the return channel nominally midway between the four rows of cultivators.

THIS PAGE INTENTIONALLY LEFT BLANK.

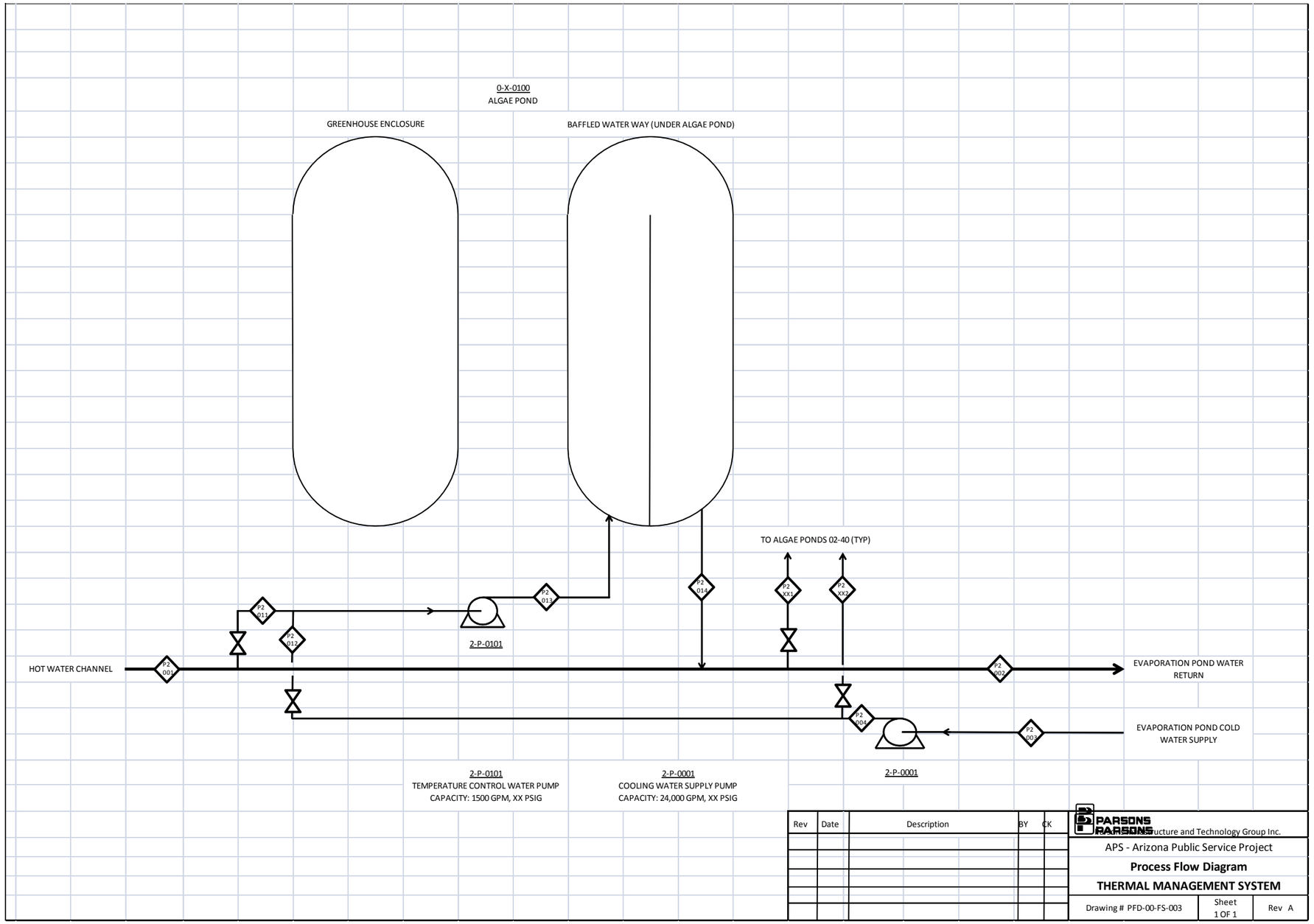

Figure 2-15. Process Flow Diagram of the Hot Water Management Process by Parsons

THIS PAGE INTENTIONALLY LEFT BLANK.

HEATING CYCLE

STREAM NO.	P2 001	P2 002	P2 003	P2 004			P2 011	P2 012	P2 013	P2 014
DESCRIPTION	HOT WATER SUPPLY CHANNEL	EVAPORATION POND WATER RETURN	EVAPORATION POND COOLING WATER SUPPLY	COOLING WATER SUPPLY PUMP DISCHARGE			POND HOT WATER SUCTION	POND COLD WATER SUPPLY	POND TEMPERATURE CONTROL PUMP DISCHARGE	POND TEMPERATURE CONTROL WATER RETURN
INSTANTANEOUS FLOW (LB_M/HR)	10480000	10480000	0	0			655000	0	655000	655000
INSTANTANEOUS FLOW (GPM)	21000	21000	0	0			1312	0	1312	1311
INSTANTANEOUS FLOW (ACFM)	-	-	N/A	N/A			-	N/A	-	-
TEMPERATURE (F)	80.0	80.0	N/A	N/A			80.0	N/A	80.0	72.0
PRESSURE (PSIA)	12.2	12.2	N/A	N/A				N/A		ATMS.
MOLECULAR WT.	18	18	N/A	N/A			18	N/A	18	18
DENSITY (LB_M/FT^3)	62.22	62.22	N/A	N/A			62.22	N/A	62.22	62.28
VISCOSITY (cP)	1.0	1.0	N/A	N/A			1.0	N/A	1.0	1.0
NOTES	1									

COOLING CYCLE

STREAM NO.	P2 001	P2 002	P2 003	P2 004			P2 011	P2 012	P2 013	P2 014
DESCRIPTION	HOT WATER SUPPLY CHANNEL	EVAPORATION POND WATER RETURN	EVAPORATION POND COOLING WATER SUPPLY	COOLING WATER SUPPLY PUMP DISCHARGE			POND HOT WATER SUCTION	POND COLD WATER SUPPLY	POND TEMPERATURE CONTROL PUMP DISCHARGE	POND TEMPERATURE CONTROL WATER RETURN
INSTANTANEOUS FLOW (LB_M/HR)	0	12012000	12012000	12012000			0	750750	750750	750750
INSTANTANEOUS FLOW (GPM)	0	24112	24078	24078			0	1505	1505	1507
INSTANTANEOUS FLOW (ACFM)	N/A	-	-	-			N/A	-	-	-
TEMPERATURE (F)	N/A	90.0	82.0	82.0			N/A	82.0	82.0	90.0
PRESSURE (PSIA)	N/A	12.2	12.2	12.2			N/A			ATMS.
MOLECULAR WT.	N/A	18	18	18			N/A	18	18	18
DENSITY (LB_M/FT^3)	N/A	62.11	62.20	62.20			N/A	62.20	62.20	62.11
VISCOSITY (cP)	N/A	1.0	1.0	1.0			N/A	1.0	1.0	1.0
NOTES										

NOTES:

1. HOT WATER CHANNEL FLOW RATE IN EXCESS OF TOTAL POND HOT WATER FLOW REQUIREMENTS, RETURN OF TEMPERATURE CONTROL WATER TO HOT WATER CHANNEL TO HAVE A MINIMAL IMPACT ON DOWN STREAM TEMPERATURE OF HOT WATER CHANNEL.

Rev	Date	Description	BY	CK

PARSONS
Parsons Infrastructure and Technology Group Inc.

APS - Arizona Public Service Project

Process Flow Diagram

THERMAL MANAGEMENT SYSTEM

Drawing # PFD-00-FS-XXX	Sheet 2 OF 1	Rev A

Figure 2-16. Hot Water Process Balance by Parsons

THIS PAGE INTENTIONALLY LEFT BLANK.

2.3.5 SUPPORT SYSTEMS/SKIDS

The water treatment system would use a number of packaged systems that are either packaged designs and/or equipment readily available. For cost effectiveness, these items were treated as unit systems that would be constructed, purchased or leased as cost trade-off studies indicate. They appeared in the Parsons-designed water treatment skid as unit systems. In addition, Parsons' scope included the nutrient mixer, which would be similar to the chlorine skid. All of these packaged units as well as their flow material balance are represented in Figure 2-17 and Figure 2-18 respectively. These skids are as follows:

Chlorination Skid

The chlorination skid was presumed to be a solids (calcium hypochlorite) feeder into a mixing/contact tank. Typically this is a complete packaged unit. Automatic control would be provided.

Nutrient Mixer Skid

The nutrient mixer skid was presumed to also be a solids (fertilizer) feeder into a mixing/contact tank. Average water flow would be (33 TBD) gpm. One screw feeder is shown; more would be supplied (TBD). Again, automatic control would be provided.

Ozone Generation Skid

Ozone is commonly generated using an O_2 supply and a packaged skid. The size of the unit would be determined.

De-ionized Water Skid

Deionized water skids are commonly purchased or leased. For this project, a reverse osmosis system of 50 gpm would be used to supply potable water and the electrolysis unit.

THIS PAGE INTENTIONALLY LEFT BLANK.

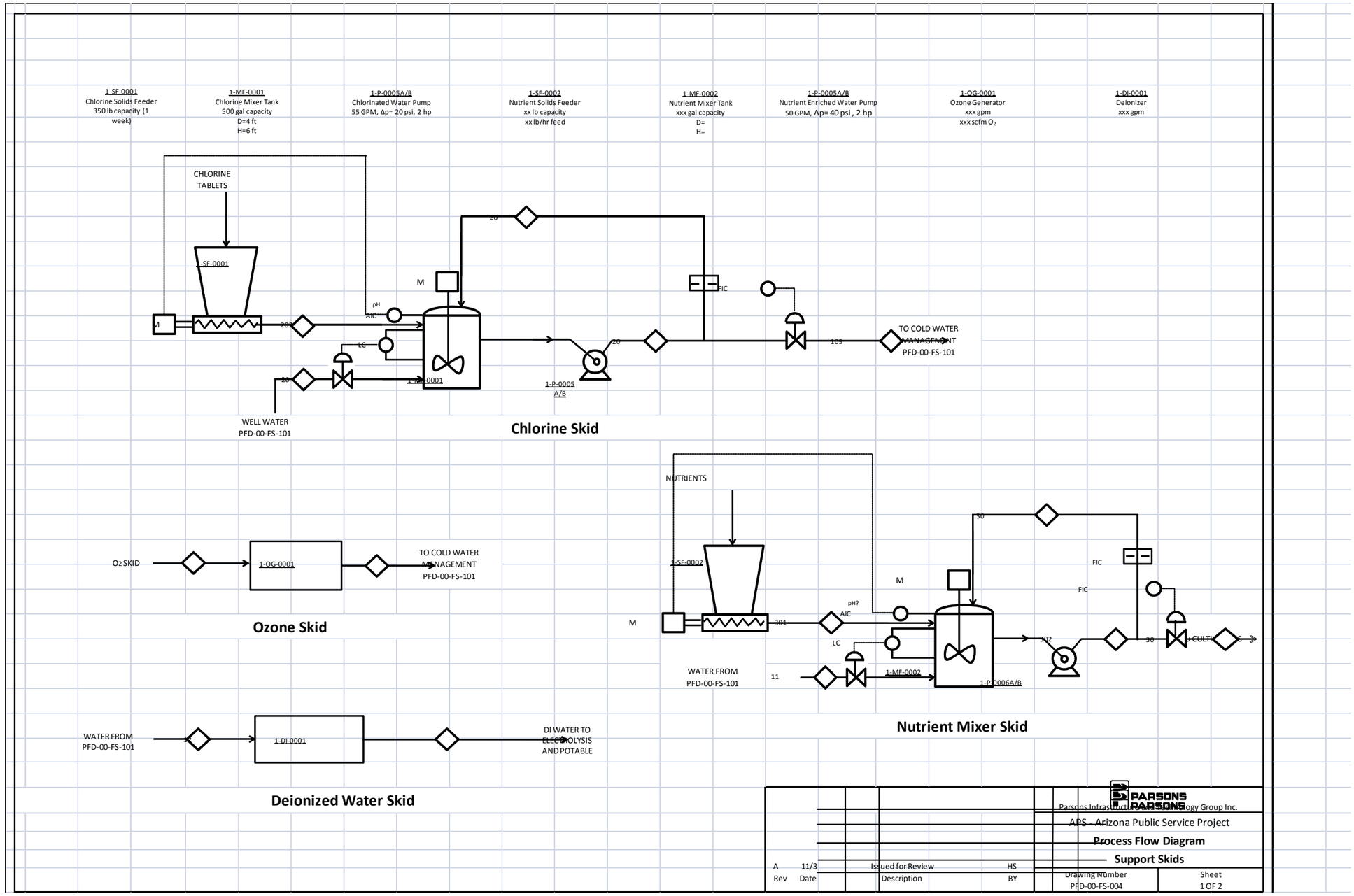

Figure 2-17. Process Flow Diagram of Water Treatment Skids by Parsons

THIS PAGE INTENTIONALLY LEFT BLANK.

Stream No	201	202	203	204	109	114	301	302	303	304	123
Flow	5 GPM	.013 lb/min	55 GPM	50 GPM	5 GPM	33 GPM	xx lb/min	33 GPM	0 GPM	33 GPM	50 GPM
Contents	Water	$Ca(ClO)_2$	Chlorinated Water	Chlorinated Water	Chlorinated Water	Water	Nutrients	Nutrient Enriched	Nutrient Enriched	Nutrient Enriched	Water

Rev	Date	Description	BY
A	11/3	Issued for Review	HS

PARSONS
Parsons Infrastructure & Technology Group Inc.
APS - Arizona Public Service Project
Process Flow Diagram
Support Skids
Drawing Number: PFD-00-FS-004
Sheet: 2 OF 2

Figure 2-18. Material Balance of Water Treatment Skid by Parsons

THIS PAGE INTENTIONALLY LEFT BLANK.

2.3.6 MAJOR EQUIPMENT LIST

The major equipment for the water treatment processes (based on the preliminary sizing) are shown in Table 2-6.

Table 2-6. Preliminary Equipment List for Water Treatment Process by Parsons

Water Management System	Quantity	Description	Sizing
1-Q-0001	1	Clarifier Tank	15,000 gal - inlet flow of 60 gpm, 14' ID X 14' H
1-Q-0002	1	Clear Water Tank	1,050 gal - inlet flow of 60 gpm, D = 6 ft, H = 5 ft
1-P-0001	1	Screw Pump	15 gpm, ΔP = 25 psi, Power = 2 hp
1-P-0002A/B	2	Pump	60 gpm, ΔP = 40 psi, Power = 2 hp
1-P-0003A/B	2	Pump	60 gpm, ΔP = 40 psi, Power = 2 hp
1-UV-0001	1	UV Machine	60 gpm , Power Req.= 0.20 kW
1-FILT-0001	1	Cartridge Filter	60 gpm, 100 microns
1-FILT-0002	1	Charcoal Bed	60 gpm
1-Q-0003	1	Ozone Contact Tank	900 gal, 60 gpm, contact time of 15 min, D = 6 ft, H = 5 ft
1-CAT-0001	1	Off-Gas Treatment Unit	Based on amount of O_3
1-Q-0004A/B	2	Buffer Tank	175,000 gal, D = 32 ft, H = 30 ft
1-P-0004A/B	2	Pump	2,000 gpm, ΔP = 50 psi, Power = 85 hp
1-FILT-0003	1	Cartridge Filter	100 gpm, 2 microns
1-FILT-0004	1	Cartridge Filter	1,750 gpm, 100 microns
Thermal Management System	**Quantity**	**Description**	**Sizing**
2-P-0001A/B/C	3	Horizontal Split-Case 1-Stage	4200 gpm, 85 hp
Temperature Control Valve	56	Temperature Control Valve	4"
2-X-01XX	336	Unit Water Heaters	25 gpm each, 420,000 Btu/hr each, 1/4 hp each (6 per pond)
Flue Gas System	**Quantity**	**Description**	**Sizing**
3-P-0001A/B	2	2 Stage High-Pressure blower	3500 scfm, 5 psi, 150 °F Flue Gas, 175 hp, Inlet Damper control.
Flue Gas Piping	4000 ft		24" sch 10 pipe minimum insulated duct elevated 1' on supports
3-KOP-0001	1	Knock-out pot	40" Deep x 200" Long
Flue Gas System	**Quantity**	**Description**	**Sizing**
Chlorination Skid	1	Chlorination Skid	5 gpm through it, 40 lbs/day solids feed for 20 ppm chlorine
Deionized Water Skid	1	Deionized Water Skid	50 gpm
Nutrient Mixer Skid	1	Nutrient Mixer Skid	33 gpm, TBD lbs/hr solids feed, TBD gal mixer
1-CAT-0001	1	Ozone Generator Skid	900 gal, 60 gpm, contact time of 15 minutes
Chlorination Skid	1	Chlorination Skid	5 gpm through it, 40 lbs/day solids feed for 20 ppm chlorine

2.4 BIOFUEL PRODUCTION

AL contributed to the process conceptual design for algae cell disruption, algae oil extraction, algae oil pretreatment and biodiesel production. The process conceptual design of cell disruption was incomplete. The AL study only included collection of information on currently available methods for cell disruption, a technical and economic comparison of these methods, and a preliminary evaluation of promising new techniques leading to laboratory or bench-scale tests. The determination of algae cell disruption techniques was planned to be done early in the project Budget Period 2 (BP2) as the outcome could direct and affect the selection of downstream technology for oil extraction and processing of the algae mass. Choosing the most efficient cell disruption technique would have a positive effect by lowering the overall production cost for algae oil and liquid biodiesel. Evaluation of the available and promising cell disruption techniques would require information about the nature of the algae species and strain or strains to be grown in the project and utilized for biodiesel production.

The evaluation of the best oil extraction method(s) to finalize the design basis of this process step was not completed either. The AL project team had been working closely with R&D personnel at APS who were experimenting with oil extraction in a small-scale environment. AL would need to select the most technically viable, economical and reliable process to be used for scale-up and implementation by the IES project. Also, the processing/disposition of "de-lipidated" biomass generated by the oil extraction process was planned to be included in the scope of engineering work. Several methods to induce algae cell wall breakage and extract oil were considered and evaluated.

Algae oil consists primarily of a mixture of triglycerides and free fatty acids with additional undesirable components in the form of phosphatide gums, proteins and other minor impurities. Chlorophyll is of particular concern as an impurity in algae oil: it is an undesirable component that must be reduced or substantially eliminated to make algae oil an acceptable feedstock for biodiesel production.

Obtaining analytic data specific to the oil that would be produced by APS is critical to properly determine the pretreatment methods and intensity required to produce a suitable feedstock for the biodiesel conversion process. At a minimum, the following attributes of the algae oil must be known:

- Free fatty acid content (and/or acid number)
- Total phosphorus/phospholipid content

- Chlorophyll content
- Moisture content
- Unsaponifiable content
- Impurity content
- Average molecular weight (AMW) and/or free fatty acid (FFA) content
- Iodine value
- Trace metals content
- Sulfur content

The crude algae oil would be pretreated so that it meets the feedstock requirements for the Lurgi transesterification process, which requires the attributes shown in Table 2-7 below:

Table 2-7. Pretreated Oil Quality

Attribute	Value	Units
FFA	0.1	% max.
Total Phosphorus	10	ppm max.
Moisture	0.1	% max.
Unsaponifiable	0.8	% max.
Impurities	0.2	% max.
Sulfur	12	ppm max.

AL proposed the following base pretreatment schemes:

- Fixed-bed purification (to remove phosphatides)
- Fixed-bed esterification (to convert FFA to methyl esters)

AL/Lurgi has been building biodiesel plants for more than 15 years, and it has been a market leader in designing plants to meet the industrial demand for higher capacities, improved economy and better-quality biodiesel. Lurgi's smallest continuous process for biodiesel production is a skid-mounted plant that produces 3 million gallons of ASTM D 6751-09 biodiesel per year (approximately 2560 pounds per hour (lb/hr) using a gravity of 0.86 and 350 operating days/year; based on today's estimation, a 25-acre farm could deliver crude algae oil at 35 lb/hr).

2.5 SNG PRODUCTION

2.5.1 PROCESS DESCRIPTION

The SNG production area would encompass a 2 tpd hydrogasifier, coal feeder, char removal system, electrolysis system, ASME gas storage vessels, safety system, control systems, and all the supporting equipment. Coal would be stored in an enclosed area, from which it would be supplied to the feed system. Western coal would be pulverized to 200 mesh and injected into an aerosol-type hydrogasifier, which would operate in the range of 1800°F and 1000 psia. This temperature is below that required for the formation of CO and CO_2, and above the temperatures at which tar forms. High temperature hydrogen would be injected into the dispersed coal stream, causing the formation of methane in the exothermic hydrogasification reaction. Un-reacted char would be removed from the hydrogasifier, and methane-rich product gas would be supplied to a gas flare or to the Cholla plant for combustion in the existing coal boilers.

Hydrogen in the cleaned syngas from the hydrogasifier would be removed and recycled back into the hydrogasifier using a membrane technology. A large-scale water electrolysis system would provide both hydrogen and oxygen for the process. An inert gas system would be selected using either CO_2 or nitrogen. Compressors for the hydrogen, oxygen, and inert gas would deliver gas into ASME storage vessels. Product gas from the 2 tpd hydrogasifier would be flared, unless operating permits at Cholla would allow its use in the existing coal-fired units. Char from the hydrogasifier would be supplied to the existing coal-fired units, where it would be mixed with coal and consumed by operations.

2.5.2 HYDROGASIFIER

A decision was pending regarding the design of the engineering-scale hydrogasifier reactor (ESHRx). Two designs were discussed: the Rockwell Advanced Flash Hydropyrolysis (AFHP) single throughput design or the Japanese ARCH internal recycling double-wall design. When analyzing the designs, three temperatures are considered:

- Inlet hydrogen gas temperature
- Reactor outlet temperature
- Superficial gas/coal mixing temperature at the top of the reactor

Setting the first two temperatures correctly would ensure that the reaction would be self-sustaining. By knowing the desired reactor outlet temperature (carbon conversion calculations are based on this temperature), the theoretical hydrogen injection temperature can be calculated for an adiabatic reactor. Both reactors were designed with four gas injection ports, which facilitated the mixing between gas and coal. Because the coal would be injected at ambient temperature, it would act as a heat sink to the hydrogen inlet gas. The temperature of this mixture at the point where coal mixes with gas is the superficial gas/coal mixing temperature. This temperature needs to be high enough to initiate the hydrogasification reactions. Prior estimates indicated that the superficial mixing temperature should be over 500 degrees Celsius (°C) (932°F).

Based on prior experience with rocket engines, the Rockwell design fed coal to a hot area where a portion of hydrogen combusts with oxygen to produce the additional heat. Other than the high-temperature feed area, the design is a simple drop-tube reactor. This simplicity in reactor design is advantageous when compared with the gas recirculation type. However, this design requires a relatively high hydrogen injection temperature to achieve the requisite gas and coal mixing temperature to maintain a steady state operation. As a result of the higher reactor outlet temperature, a quencher is required at the exit of the reactor.

The ARCH design overcomes the heat issues of the Rockwell design by suspending an inner tube in the center of the reactor to create an annular space. The gas/coal mixture flows in the core of the reactor and the hot product gas recycles in the outer annular space. This complicates the design, but the reactor reaches a self-sustaining steady state temperature with a relatively lower hydrogen injection temperature compared with that of the Rockwell design. One important aspect of the ARCH design is the gas recycle ratio (GRR), which is the amount of gas that is internally recycled in the annular space over the amount of hydrogen injected into the reactor. The GRR is controlled by the distance (Δz) between the top of the inner tube and the top of the outer tube, and by the diameter of the inner tube and the outer tube. For the ARCH design, a GRR of approximately 3 would provide enough heat from the product gas to ensure a superficial gas/coal mixing temperature high enough for the reaction. Figure 2-19 highlights the major differences between these two reactor types.

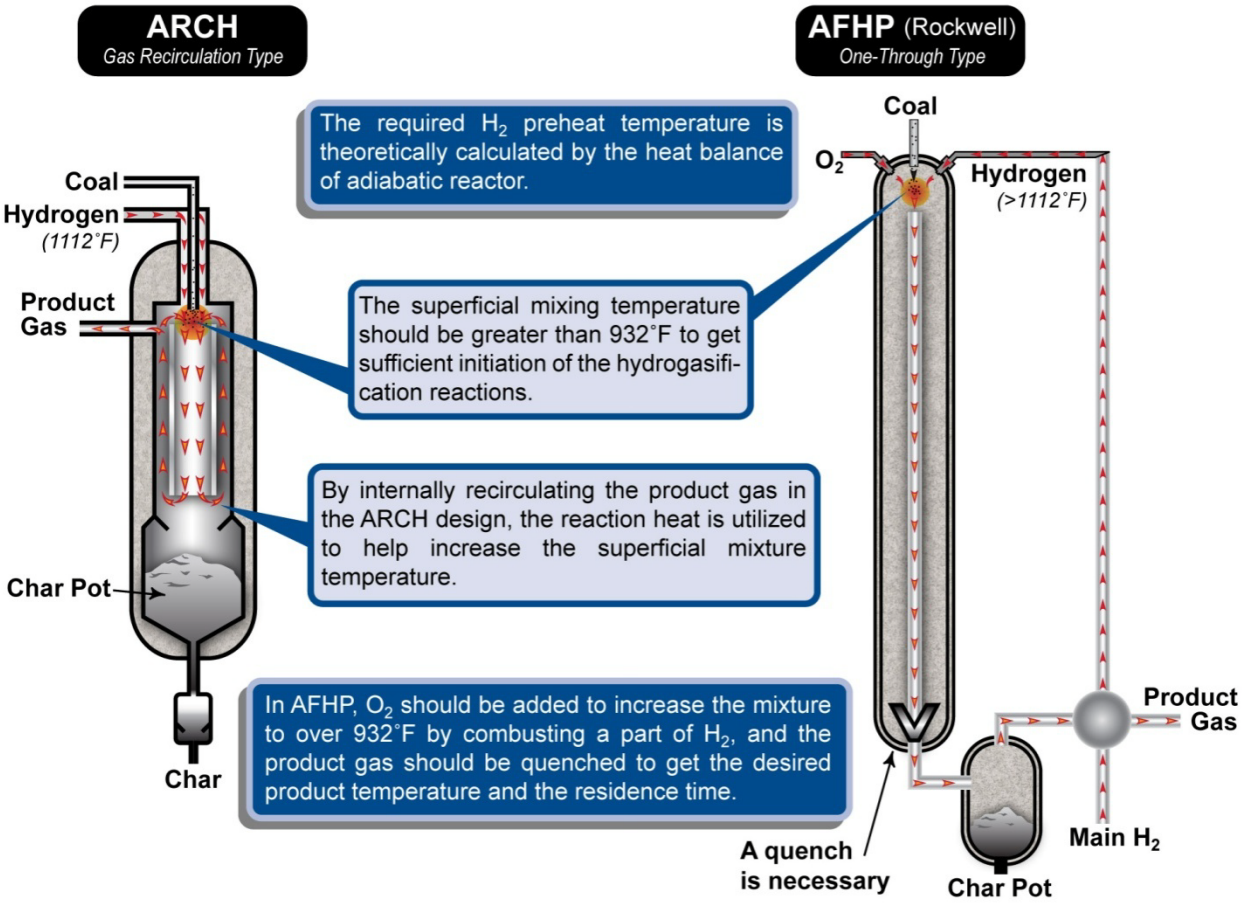

Figure 2-19. Comparison of Rockwell and ARCH Reactor Designs

In addition to APS input on the hydrogasifier design, APS was to provide further design input on coal feeding and char removal systems, but the project was terminated.

2.6 INFRASTRUCTURE

2.6.1 CIVIL

2.6.1.1 Site

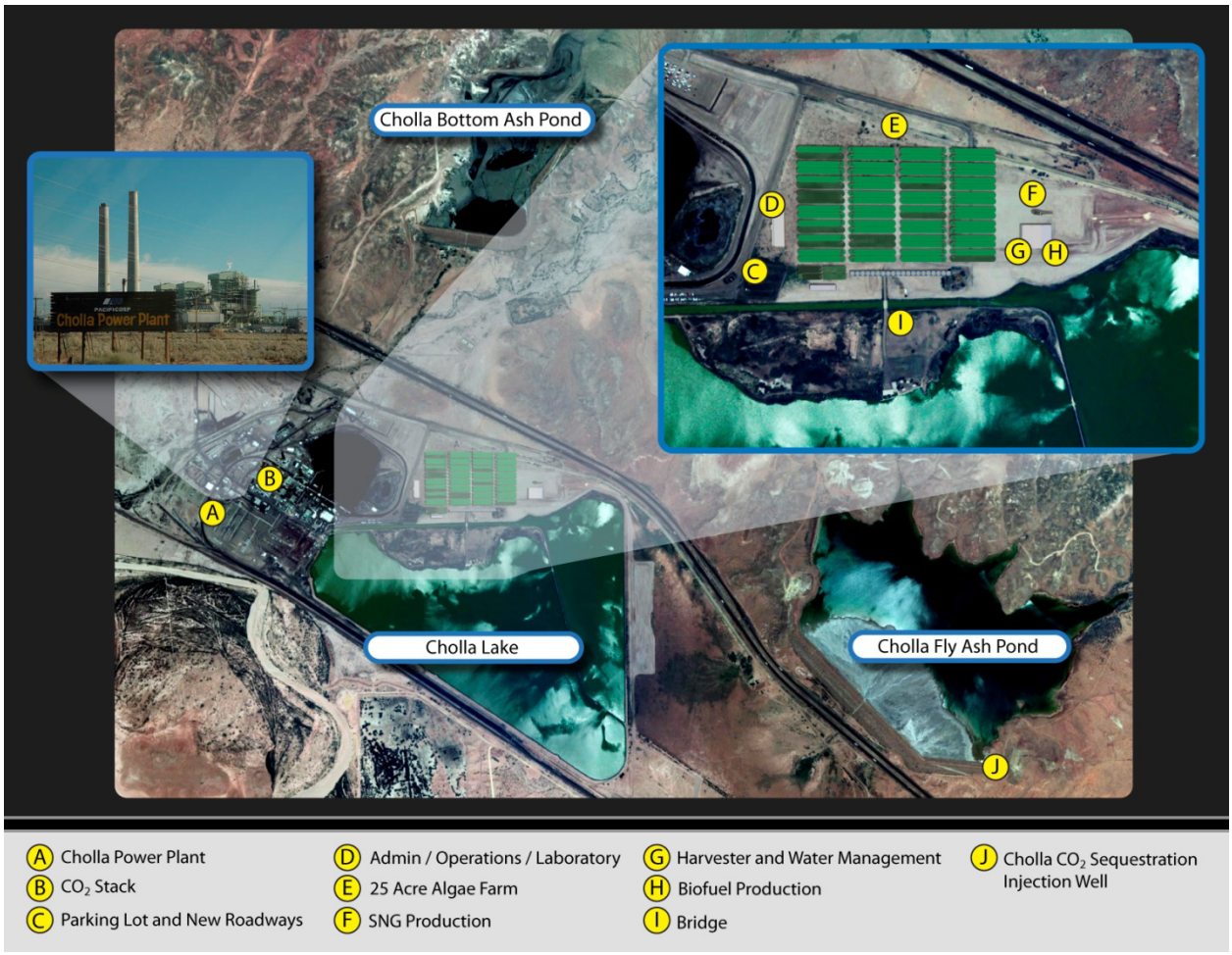

Figure 2-20. Schematic Cholla Site Design

The proposed site would consist of a combined area of about 80 acres. Figure 2-20 shows the planned Cholla site design. The algae farm was planned to be at the western side of site and encompassed approximately 29 acres of the site. The algae harvesting, dewatering, and hydrogasification pilot testing would be at the eastern site. Assuming 20 ft access roads of compacted gravel would be built around the perimeter of the algae farm and through the center of the farm to provide access to and around the buildings, it was estimated that 4000 to 6000 linear feet of roads would be required. The buildings were assumed to have an asphalt parking lot for approximately 30 cars at an estimated size of 10,000 square feet (ft^2). The site would be

enclosed within an 8000 ft perimeter fence with two security access gates. The site currently contains an existing rectangular storm-water detention basin that spans over the two lots for an area of approximately 24 acres. This basin would be filled in and a new basin would be constructed in the southeast property. The material from the new detention basin would be used to fill in the existing basin. Site demolition and reclamation was planned at the end of the project.

2.6.1.2 Grading

The existing site has a gentle slope from a north to south direction and has approximately a 5 ft fall over 1600 ft. Existing vegetation would require clearing and grubbing. It was assumed that the proposed algae farm would mostly follow the existing slope and drainage pattern. In absence of a current and updated survey, the grading and drainage concept and earthwork requirements were reevaluated. As a rough estimate, every foot of variation from the existing grade to the proposed grade over 80 acres would result in 129,000 cubic yards (yd^3) of grading. The actual variation and earthwork requirements would be determined in final design. Since the site should be level, Parson's initial assumption was that half of the earthwork would be cut, and half would be filled.

As mentioned above, there is an existing storm-water detention basin within the proposed site that would be filled in with material from the new detention basin to the southeast. The existing basin currently collects storm runoff from the existing facility to the west of the site. The cut and fill volume for this material was estimated to be between 15,000 to 25,000 yd^3 depending on the depth. The actual volume would be determined during final design. The storm-water collected by the detention basin would need to be diverted around the site via a drainage channel. Since this channel would also convey the water from approximately 225-acres of the existing facility, a hydrology study would be required to estimate the amount of runoff to the channel and the required channel size. The size and type of channel would be determined upon final design. Reclamation grading is assumed at the end of the project.

2.6.1.3 Utilities

All utilities would be provided on a temporary basis. Potable water tanks and water lines would be provided for the lab/administration building and the warehouse. Both water tanks would require pumps for adequate water pressure. Septic tanks and sewage pumps would be used for the lab/administration and warehouse buildings. Portable toilets may also be used depending on client requirements. Storm drain lines and culvert drains may be required

depending on site conditions and client requirements. Utility removal was assumed at the end of the project.

Below is a list of excluded utility work from a civil engineering standpoint.

- Process water line
- Algae farm irrigation water line
- Electrical duct banks
- Process water treatment

2.6.2 Architecture and Structure

Non-process structures and buildings would be temporary in nature and would include the buildings listed below. These structures can be purchased or leased for the duration of the project. Permanent foundations would be placed only where necessary. Structures would be climate controlled. The Administration building would include a shaded parking area for 30 spaces including handicapped spaces. All buildings would comply with Americans with Disabilities Act (ADA) requirements. Green building practices would be considered for all structures.

- Administration building – 8000 ft^2
- Laboratory building – 2000 ft^2
- Control building – 1200 ft^2
- Warehouse and storage building – 40,000 ft^2
- Shade structure for 30 parking spaces – 4500 ft^2
- Shade structures for equipment – as required
- Concrete pads for equipment – as required

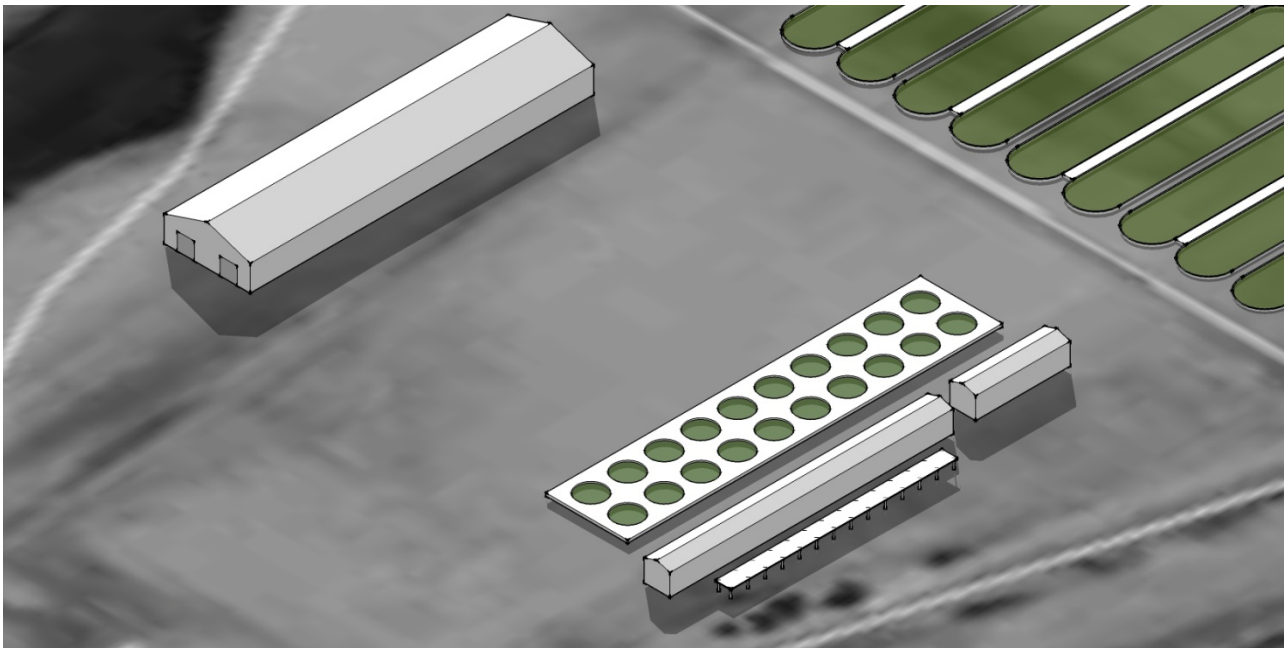

Figure 2-21. Schematic Diagram of Cholla Site Architecture and Structures

2.6.3 ELECTRICAL

2.6.3.1 Power System

The electrical utility service to the APS facility would require an overhead installation from the utility point of connection. The preliminary assessment indicated that a 20-kV, three-phase power line would be available to support the electrical requirements of the facility. The electrical substation, transformers, switchgear, and panels would be provided for the electrical equipment at various auxiliary loads and voltage levels.

A 20 kV, 3-phase, 3-wire substation would be provided to support one 20 kV/4.16 kV, three-phase auxiliary step-down transformer as well as water electrolysis loads.

From the 20-kV/4.16-kV,three-phase step-down transformer, a 4.16-kV three-phase switchgear would be provided to support various 4.16 kV auxiliary loads and an auxiliary 4.16 kV/480 V three-phase step-down transformer with an estimated load of 300 kW. Some of the anticipated 4.16 kV auxiliary loads are listed below.

- Flue gas blower
- CO_2 compressor
- SNG compressor

- H_2 recycle compressor

From the 4.16 kV/480 V three-phase step-down transformer, a 480 V three-phase switchboard would be provided to support 480 V auxiliary loads, power and lighting loads for the facility. All motors smaller than 250 horsepower (hp) such as cooling tower fan motors, coal and ash handling systems, etc. would be connected to a 480V three-phase switchboard. A 480 V/208 to 120 V three-phase step-down transformer would be provided to support 208 V and 120 V power loads in the administration and other support buildings.

The water electrolysis system had an estimated load of 2000 kW. The anticipated 20 kV auxiliary loads are listed below.

- Electrolysis water pump
- Electrolysis units
- H_2 to O_2 compressors feeding the hydrogasifier

All electrical wiring, conduit, and equipment installation were to meet all applicable codes, standards, and local regulation requirements.

2.6.3.2 Lighting System

Lighting would be provided in the administration building, laboratory building, control building, warehouse and storage building in compliance with applicable codes, standards and local regulation requirements. Pole-mounted exterior, site, and perimeter lighting would be provided as required. An emergency lighting system would be provided in all applicable buildings to meet code and local regulation requirements.

2.6.3.3 Telecommunication, Security, and Fire and Life Safety Systems

The telecommunication, security, and fire and life safety systems would be provided in the administration building, laboratory building, control building, warehouse and storage building in compliance with applicable codes, standards and local regulation requirements. The telephone service would be an overhead installation from utility point of connection.

2.6.3.4 General Installation Requirement

Electrical wiring and conduit installation shall be above ground and exposed.

3. HYDROGASIFICATION BENCH SCALE TESTING

As mentioned in Section 1, the project continued the R&D work performed under the Coal to SNG project, which was officially terminated by APS on March 31, 2010. In the Coal to SNG final scientific/technical report, the detailed hydrogasifier design, hydrogen injector design, process design, process operating procedures, results on several preliminary hydrogasification tests, initial exercise on 1-D modeling of hydrogasification and several major reactor repairs were summarized. As reflected in this report, the research intended to finish the hydrogasification testing proposed by test plan, the product analysis protocols (including gas, liquid and solid products), the analysis of experimental data as well as 1-D modeling to derive the kinetics of the hydrogasification of western coal to assist in the hydrogasifier scale-up design. Due to the project termination, not all of the efforts were completed. The following reports the work performed through March 31, 2010.

3.1 HYDROGASIFIER TEST PLAN

The experimental plan is presented in Table 3-1. The design of experiments utilized a three-factor central composite design. It was developed to maximize the amount of analysis that could be done in a budget-limited number of runs. Additionally, the experiments were grouped in blocks in case anything unforeseen happened, such as a critical reactor failure, so a meaningful analysis could still be completed. Runs that contributed to linear analysis of the response surfaces were grouped into the first block and runs that affected the curvature of the response are in the second block. All of the runs were randomized in the respective blocks to minimize any systematic error that may arise.

The experimental factors were chosen because previous experience indicated that these factors have a significant impact on the results and are repeatable. The three factors were reactor temperature, H_2:Coal, and reactor length. It is intuitive why the first two factors were chosen, but why reactor length was chosen is not. The reactor had six heated zones. By controlling the heater power output, the reaction zone length could be controlled and used as a coded variable for residence time, which is a function of the reactor length and hydrogen flow rate. The reaction zone length was defined as the length from the top of the reactor (this is where the coal and hydrogen were fed) to a point where the reactor temperature was insufficient to maintain the hydrogasification reactions (below 1300°F). There were three levels of reactor length that were attempted to be precisely controlled for every run (49 inches, 77 inches and 105 inches).

Table 3-1. Bench Scale Hydrogasification Experimental Plan

Run No.	H_2:Coal Ratio	Reactor Temperature (°F)	Reactor Length (inches)	Block
1	0.5	1500	105	1
2	0.4	1625	77	1
3	0.5	1750	105	1
4	0.3	1750	105	1
5	0.4	1625	77	1
6	0.5	1750	49	1
7	0.3	1750	49	1
8	0.3	1500	105	1
9	0.3	1500	49	1
10	0.5	1500	49	1
11	0.4	1500	77	2
12	0.4	1625	77	2
13	0.4	1625	105	2
14	0.4	1625	49	2
15	0.5	1625	77	2
16	0.3	1625	77	2
17	0.4	1750	77	2
18	0.4	1625	77	2

Temperature and H_2:Coal ratio are factors that are more identifiable with hydrogasification experimentation. The temperature setpoint was considered to be reached after there was a relatively flat temperature profile across the reactor length. Since coal feed rate has a single target of 8 lb/hr, the H_2:Coal was therefore set by varying the hydrogen flow rate. The coal feed rate was set to a single value to ensure:

- That approximately two hours of testing time with the designed coal hopper volume
- Hot hydrogen feed with an interested H_2:Coal ratio in the range of 0.3 - 0.5 would provide a high enough gas-solid mixing temperature to initiate hydrogasification reactions
- Error introduced by coal feeding system was minimized. It was determined that the precise hydrogen feed rate was much easier to achieve than coal feed rate

3.2 Gas, Liquid, and Solid Analysis

3.2.1 Gas Analysis

A SRI Multiple Gas Analyzer Two Gas Chromatograph (GC), configured to an 8610C chassis was used to determine product gas composition. The analyzer was equipped with a thermal conductivity detector (TCD) and was paired with a flame ionization detector (FID). Additionally, the FID was equipped with a methanizer for low-level CO and CO_2 detection. Ultra-high-purity helium was the carrier gas, and research-grade hydrogen and ultra-zero air were used for the FID flame. Finally, the GC was equipped with dual columns: Molecular Sieve 13X column for the separation of H_2, O_2, N_2, CH_4, CO and CO_2 and Hayesep-D column for all compounds in the C_1 – C_6 range. An event schedule was used as injections to the columns happened at different times. A fixed event schedule was used throughout a given experimental run:

Table 3-2. GC Event Schedule

Event #	Time of Event	Event
1	0.000	Zero
2	0.000	Carrier Gas # 2 On: sample injection into MS 13X
3	0.050	Inject Sample
4	3.550	Carrier Gas # 2 Off
5	3.600	Carrier Gas # 1 On: sample injection into Hayesep-D
6	5.000	Carrier Gas # 1 Off

There were two temperature programs used during testing: one with a temperature ramp and one without. Two temperature programs were chosen because of the length of time it takes the GC to cool from a high hold temperature. This method was chosen because a higher temperature aids in the detection of larger molecules (i.e., ethylene ($C_2H_{4)}$ and C_2H_6). Therefore to make data collection more efficient, the high-temperature ramp program was not initiated until it was determined that the hydrogasification process was at steady state. The temperature programs are shown below in Table 3-3 and Table 3-4.

Table 3-3. GC Temperature Program without Ramp

Temperature Event	Event	Event Length
1	Hold at 40°C	5 minutes

Table 3-4. GC Temperature Program with Ramp

Temperature Event	Event	Event Length
1	Hold at 40°C	5 minutes
2	Ramp at 20°C/min	3 minutes
3	Hold at 100°C	4 minutes

For calibration of the GC, two gas standards were purchased, and the GC was calibrated on every testing date. The components of the calibration gas, with molar concentrations, are given in Table 3-5 below.

Table 3-5. Calibration Gas Components and Concentrations

Component	Calibration Gas 1, %	Calibration Gas 2, %
Acetylene	1.01	0.00
Carbon Dioxide	3.04	2.01
Carbon Monoxide	5.08	1.99
Ethane	0.997	0.00
Ethylene	1.03	0.00
Methane	22.5	10.0
Nitrogen	9.89	5.04
Hydrogen	56.5	81.0

The concentration of a component in the product gas stream is calculated from the area under the intensity curve from the GC. For hydrogen, the concentration is taken from the TCD, which measures the difference between the thermal conductivity of hydrogen and the reference gas (helium). When measuring the concentration of hydrogen, there is more potential for error because (1) the thermal conductivity of hydrogen is higher than that of helium, so the intensity curve must be inverted; and (2) the slope of the concentration versus the peak area regression model is steep. For these reasons, along with the two calibration gases listed above, ultra-high-purity hydrogen was also used as a calibration gas.

Based on the regression of the calibration peak areas, it was determined that the GC software can estimate the concentration of the components in the product gas. The GC software can also be used to visually compare experimental peaks with calibrated peaks. Figure 3-1 and Figure 3-2 below show experimental and calibration gas peaks from the FID and TCD, respectively.

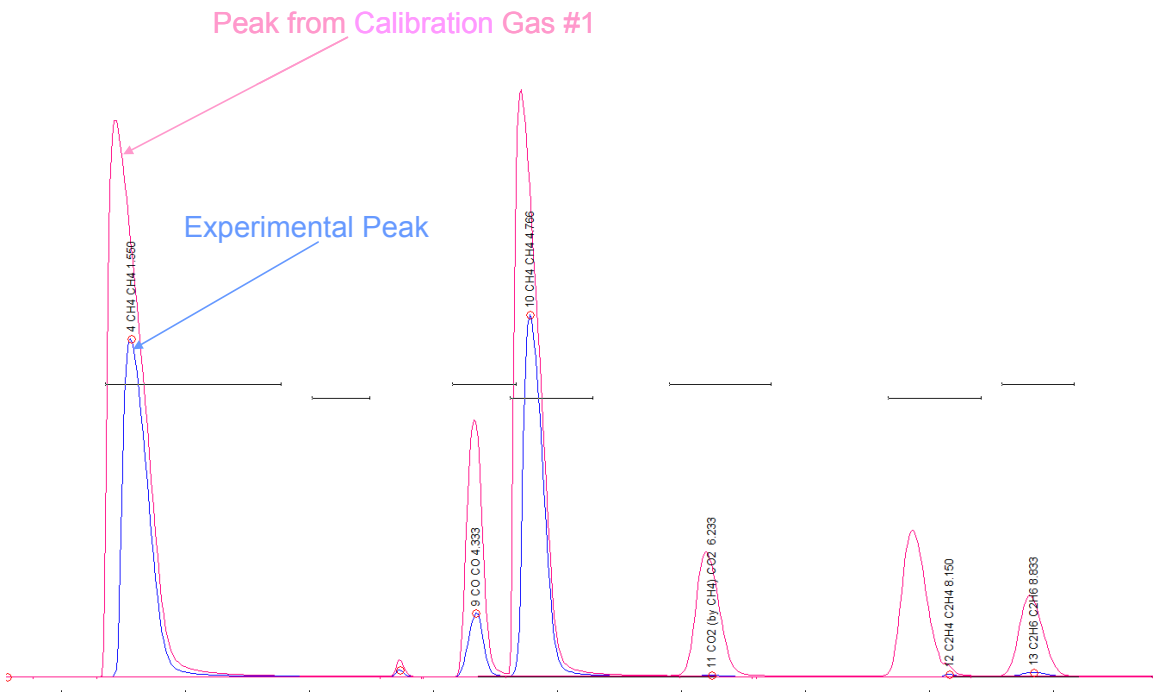

Figure 3-1. Experimental and Calibration Peaks from FID

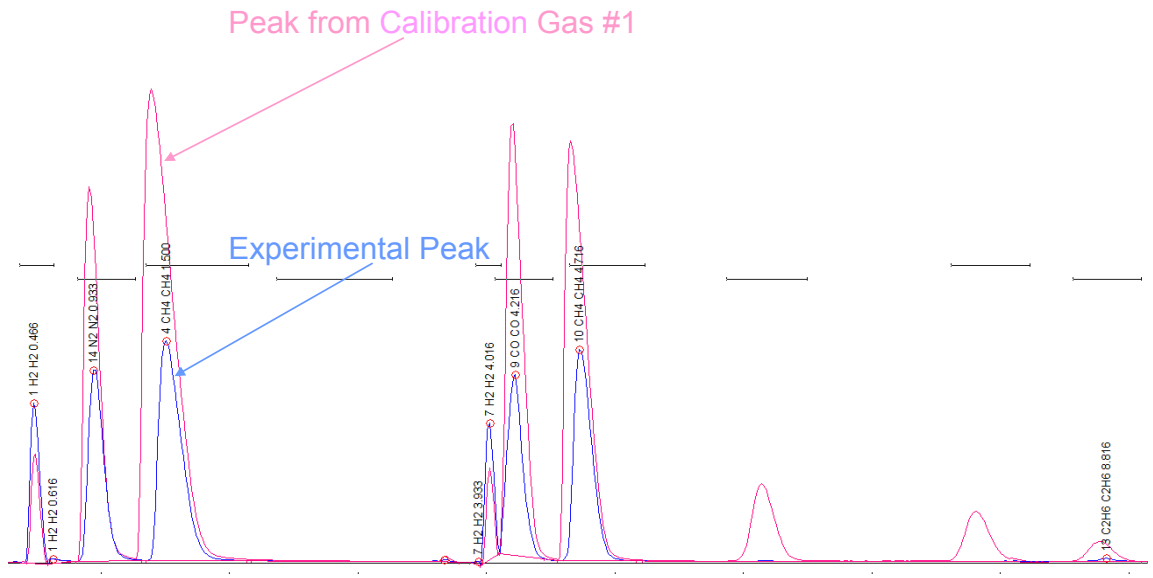

Figure 3-2. Experimental and Calibration Peaks from TCD

A comparison of the two figures shows that two peaks appear in the TCD spectrum before the experimental peak (the first in the FID). The first peak is hydrogen and the second is nitrogen in the TCD spectrum; these two components are undetectable with the FID. The nitrogen appearance in the product stream was suspected to be from a small leak across the reactor

bottom bellows. In addition, the peaks that were observed from the FID tended to be more intense and consistent than those from the TCD. For this reason, all of the product stream component concentrations were determined with the FID, except hydrogen and nitrogen.

Another piece of analytical equipment to analyze the product gas stream was a Mass Spectrometer (MS). The MS can measure component generation in real time, as opposed to the GC, which required periodic injections of the product gas. The MS was particularly important because it could measure sulfurous components in the product gas stream. A QMS 200 from Stanford Research Systems was used. This device had the capability to measure components with mass up to 200 atomic mass units (amu). For all tests, the MS was run in pressure-versus-time mode with a new scan triggered every 2 seconds. A Channel Electron Multiplier was used for sulfurous components to provide higher resolution during the scan.

The two sulfurous components that were being screened were H_2S and carbonyl sulfide (COS). To calibrate the instrument for sulfur, a gas mixture of 514 ppm COS and 4970 ppm H_2S balanced with H_2 was used. Due to the excess amount of H_2 used in the experimental run, sulfur tends to form H_2S, which explains why the concentration of H_2S was an order of magnitude higher than COS in the calibration gas. Figure 3-3 shows the MS signal of H_2S from the experimental run with average calibration signals.

When the MS was first turned on prior to coal feeding, the amount of H_2S in the system began to decline, which could be due to a number of factors. For example, H_2S has the propensity to adsorb on stainless steel, so the initial signal could be from H_2S adsorption. This is not seen as an issue, because after coal feeding commenced, H_2S in the system began to rise and after a while it became relatively steady, so that that this noise was centered around an average value. This type of noise level was expected due to the small amount of H_2S in the gas stream. Once the coal feeding ended, the amount of H_2S began to drop and approached the 0% gas calibration standard.

Using the average value of H_2S signal at steady state, a qualitative estimate of the amount of H_2S in the gas stream could be made with linear interpolation. For this case the concentration of H_2S was calculated to be about 620 ppm. A theoretical calculation indicated that if all of the reacted sulfur formed H_2S, the concentration of H_2S in the gas stream would be about 930 ppm. Considering the high level of uncertainty in measuring quantities this small, using the MS was a viable method to estimate and monitor the H_2S concentration in the product gas stream.

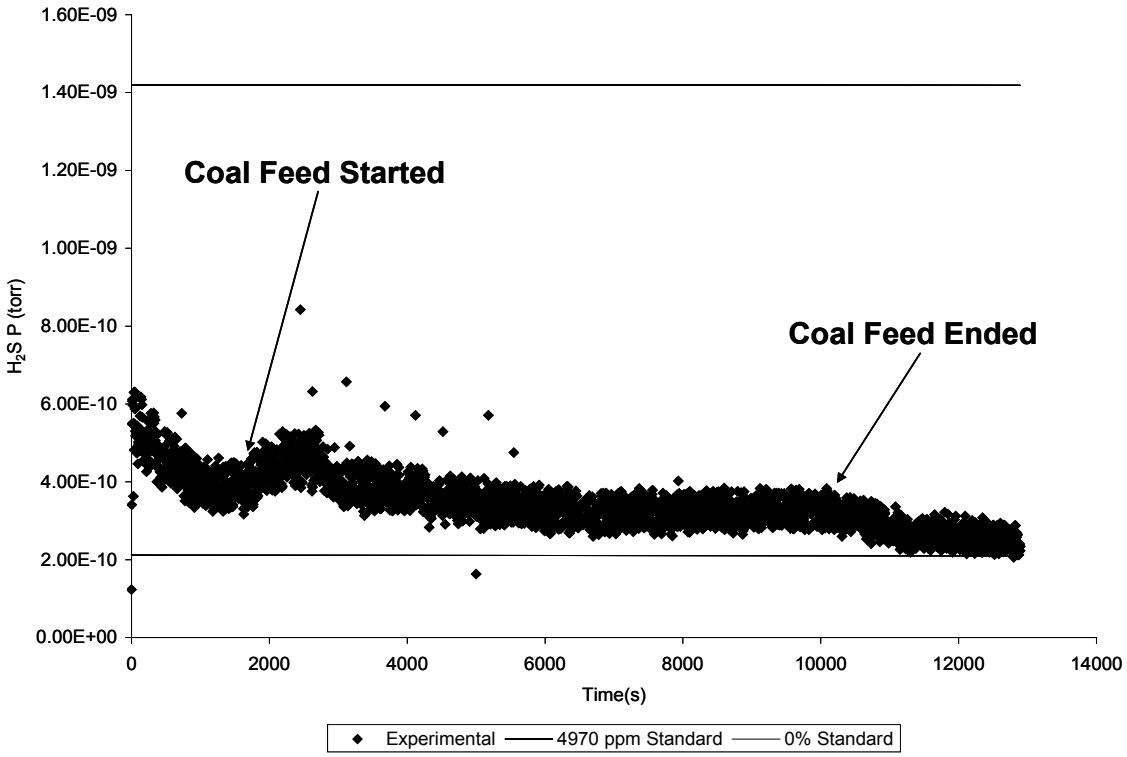

Figure 3-3. Mass Spectrometer Signal of H_2S from an Experimental Run

Experimental data from COS is shown in Figure 3-4. In this case, the noise of the data is clearly around the 0% standard. When feeding begins, there is no observable COS generation, which confirmed the hypothesis that most sulfur was converted to H_2S. Some COS may be formed in the system; however, the concentration will likely be in parts per billion.

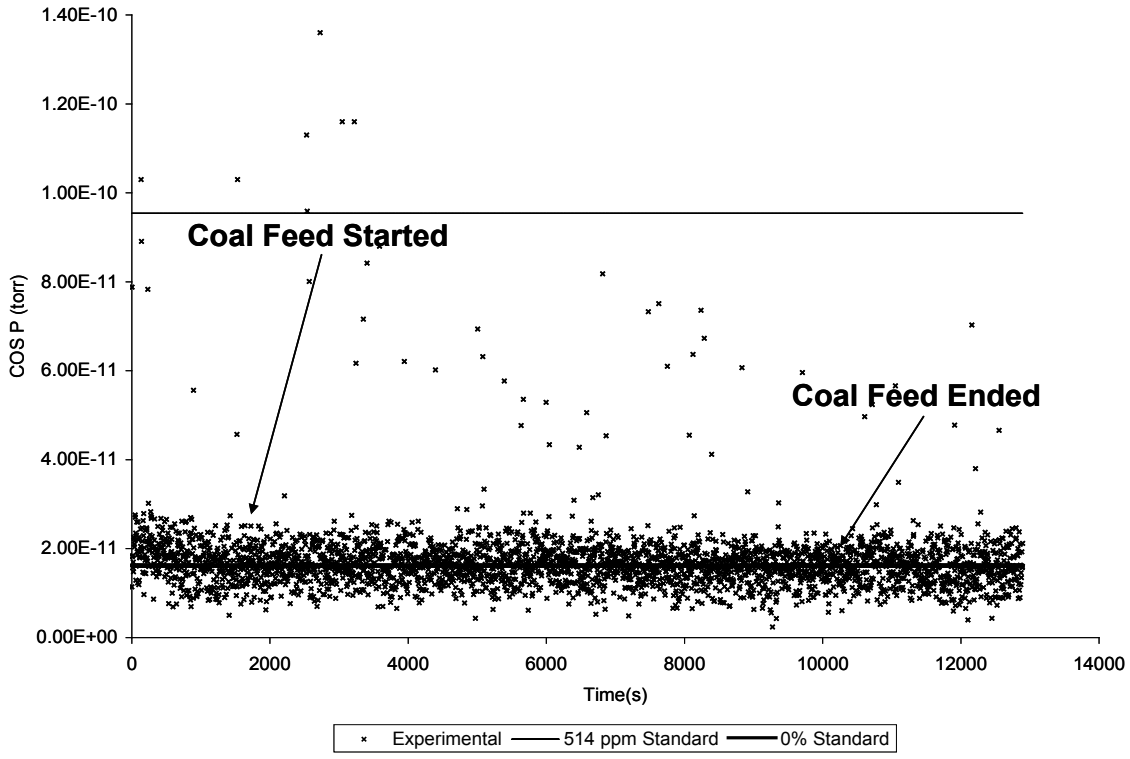

Figure 3-4. Mass Spectrometer Signal of COS from an Experimental Run

Extensive study of methane content in the product gas stream was performed using the MS. From Figure 3-5, it may be seen that as soon as coal feeding commenced, the methane content rapidly increased. During the run, there were also instances in which the methane signal decreased; at these points the coal feeder became clogged, so this decrease was expected. In addition, after the second clog, the reactor reached a relatively steady state. Finally at the end of the run when coal was no longer being fed, the methane concentration rapidly declined. With the ability to observe methane generation in real time, the steadiness of the reactor could be established. Most important, the MS could provide a way to determine the consistency of the feeding from the coal feeder.

Another interesting comparison is between H_2S and CH_4 generation shown in Figure 3-3 and Figure 3-5. The trends in these figures are consistent. This is especially evident at the beginning of coal feeding: an initial increase precedes an eventual decrease. These types of trends can also be observed in the subsets of data taken from the two pieces of analytical equipment to understand how consistent the data are.

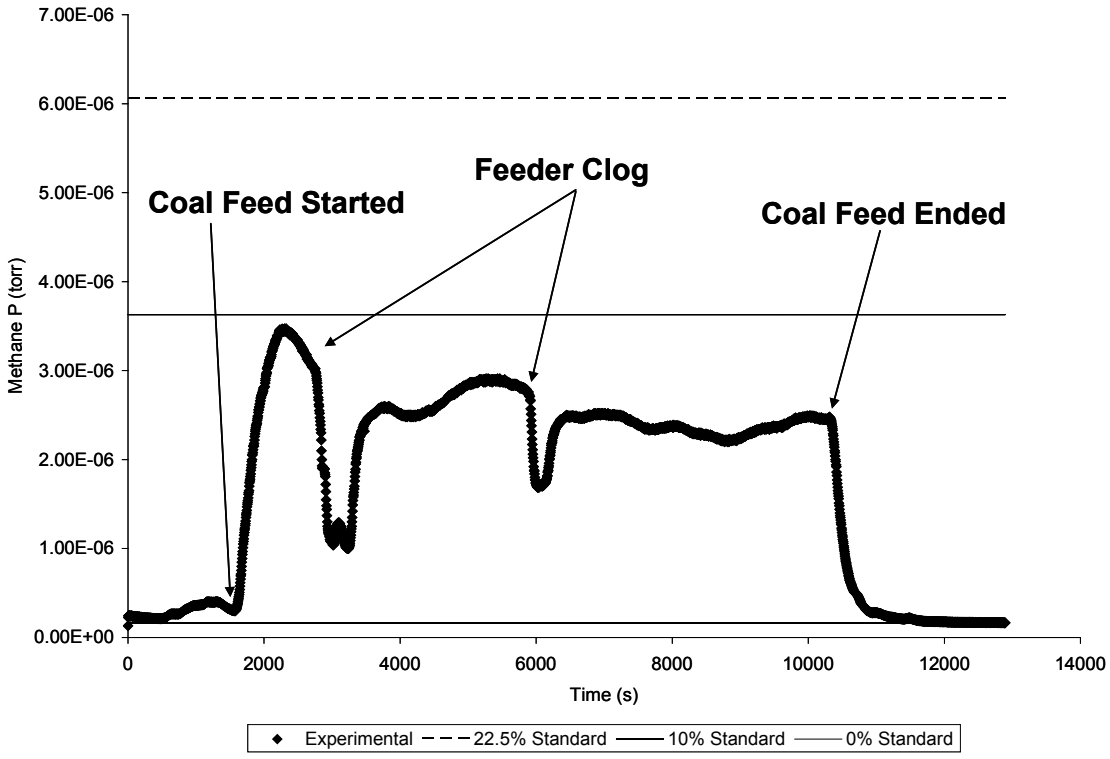

Figure 3-5. Mass Spectrometer Signal of CH_4 from an Experimental Run

Comparing the CH_4 concentration data from the MS and the GC demonstrates how well the data sets agree. Figure 3-6 shows the CH_4 generation curve from the MS along with the CH_4 concentration curve estimated from the GC. The overall trend of the data shows similar ebbs and rises over time. One point that clearly illustrates the agreement in data is the initial peak after feeding commenced. Looking at the MS results just after feeding began one can see that at this point the curve is just 10% below the concentration standard. By performing a linear interpolation, a CH_4 concentration of 9.5% was estimated for the product gas stream. At this point, the GC estimated a CH_4 gas stream concentration of 9.2%. Because both instruments gave approximately the same CH_4 product gas concentration and showed the same trend of overall concentration versus time, the analytical methods being used were determined to be sufficient for obtaining quality data sets for further analysis.

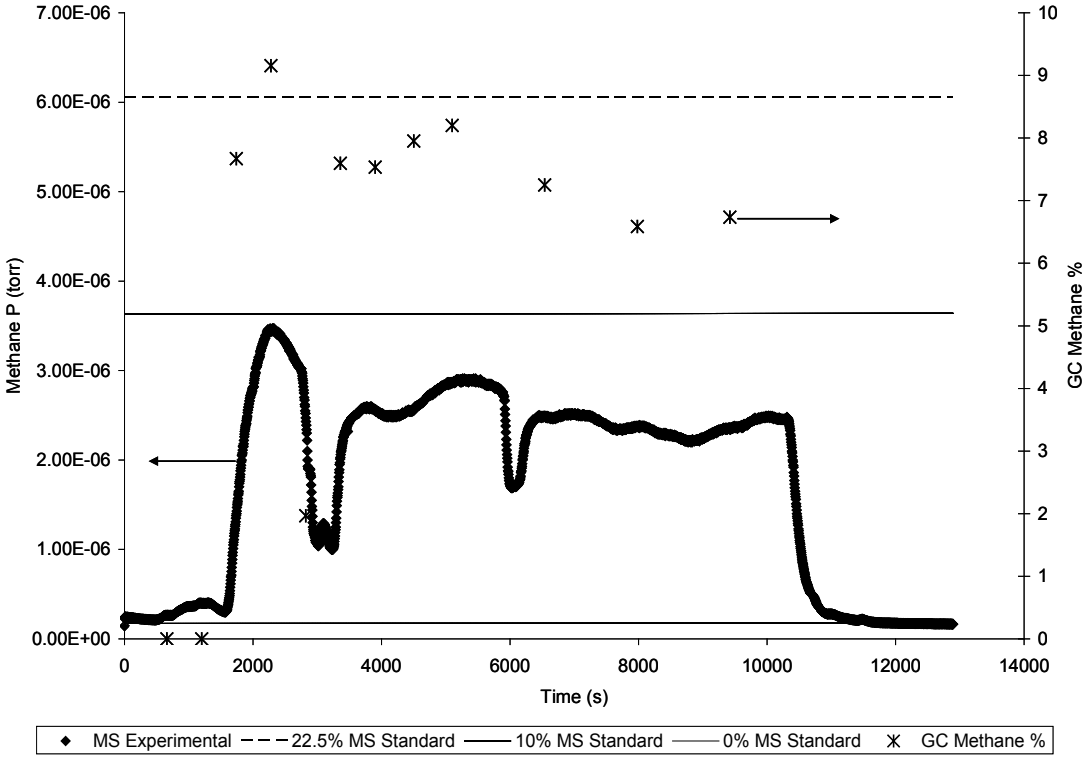

Figure 3-6. GC and MS Data Comparison

3.2.2 LIQUID ANALYSIS

The second aspect of the analytical work was condenser pot liquid analysis. Figure 3-7a shows liquid gathered from the upper condenser pot with water in the bottom phase and oil/BTX in the top phase. The reactor was designed with upper and lower condenser pots; the lower pot collects the condensed liquid during the transient state. When the reactor reached steady state, the lower pot was isolated from the upper pot. For this reason, two liquid samples were collected from each condenser pot for every run. Figure 3-7b shows the comparison of oil/BTX samples from the lower and upper pots. The reactor temperature was generally lower at the beginning of coal feeding, and it was adjusted to the desired temperature during the transient stage. The average lower reaction temperature caused less hydrocracking and thus produced more heavy oil. This is clearly shown in Figure 3-7b, as a dark color sample was obtained from the lower condenser pot.

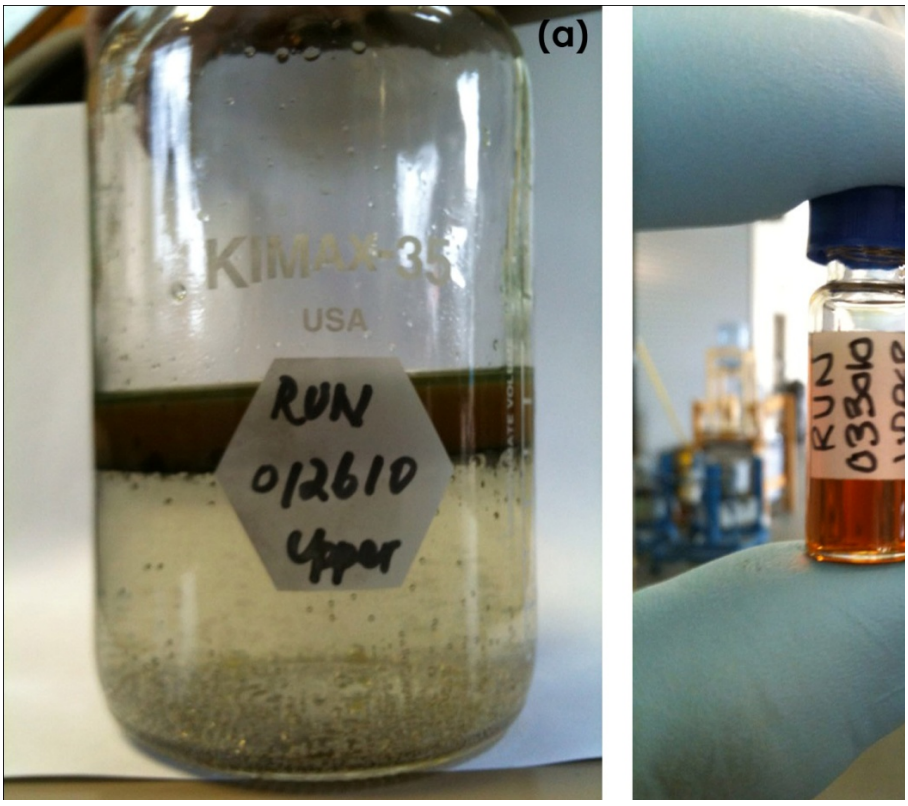

Figure 3-7. (a) Liquid from the Upper Condenser Pot; (b) Comparison of Oil/BTX Samples from Upper and Lower Condenser Pots

To analyze the samples, the liquid was first put into a separation funnel to separate the oil layer from the water layer. The oil samples were then dissolved in hexane and transferred into GC vials (Figure 3-7b). The samples were then analyzed on an HP 7890A GC equipped with an HP-INNOWAX column, and a 5975C MS. Generally, 0.2 microliter (μL) of the sample was injected into the column with a split ratio of 75/1. The oven temperature was programmed to increase from 50°C to 200°C at 25°C/min, then to 250°C at 5°C/min, and the temperature was held at 250°C for 8 min. The components in the oil samples were identified and quantitatively determined by MS. The spectra of oil layer samples from the upper and lower condenser pots from a test were compared as shown in Figure 3-8.

Table 3-6 compares the concentrations of the upper and lower condenser pot oil samples. Oil collected from lower condenser pot was confirmed to contain more heavier components.

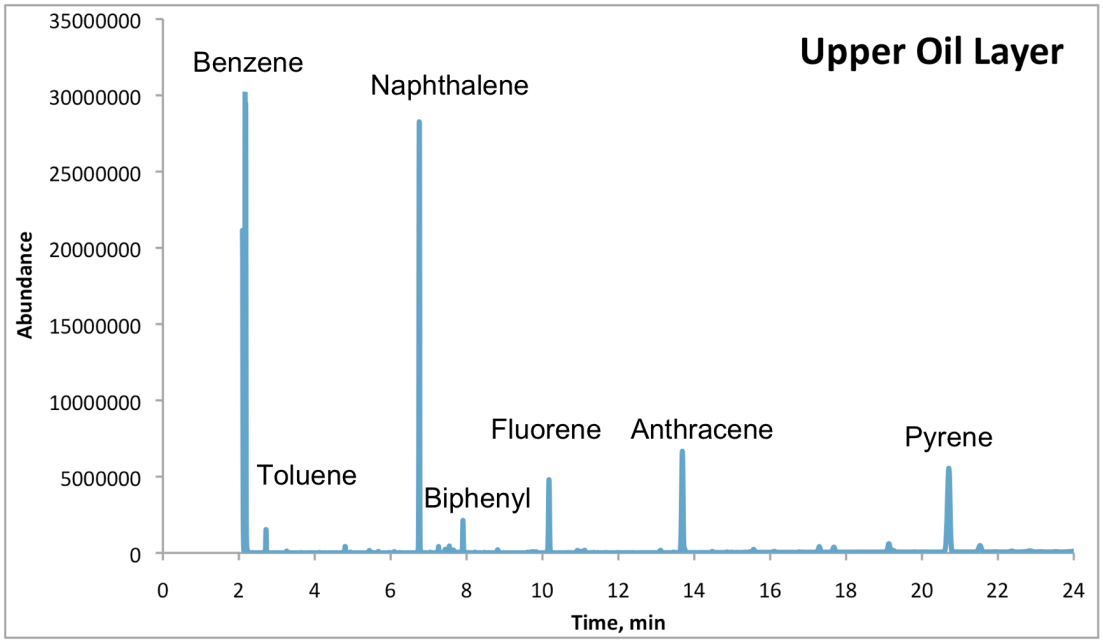

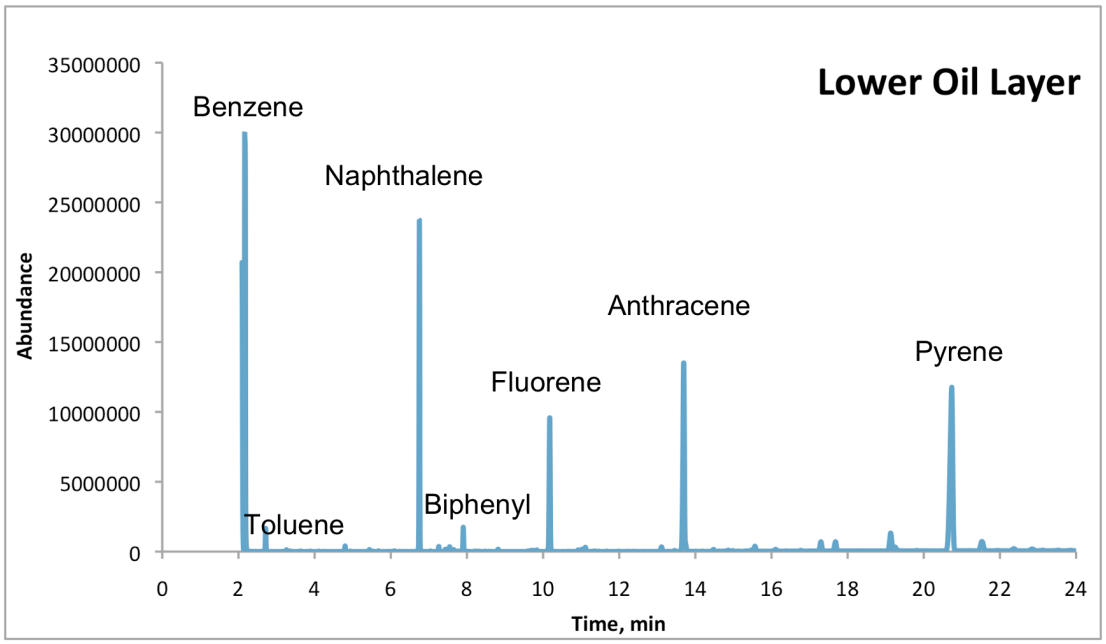

Figure 3-8. Gas Chromatographs of Upper and Lower Condenser Pot Oil Samples

Table 3-6. Components Concentration Comparison of Upper and Lower Condenser Pot Oil Samples

Component	Upper Liquid Pot (wt%)	Lower Liquid Pot (wt%)
Benzene (C_6H_6)	32.71	23.45
Toluene (C_7H_8)	0.98	0.86
Naphthalene ($C_{10}H_8$)	23.00	12.74
Biphenyl ($C_{12}H_{10}$)	1.62	0.97
Fluorene ($C_{13}H_{10}$)	5.56	8.16
Anthracene ($C_{14}H_{10}$)	11.25	16.92
Pyrene ($C_{16}H_{10}$)	16.13	26.15
Others	8.75	10.75

3.2.3 Coal and Char Analysis

The third and last aspect of the analysis of the hydrogasification tests was that of the coal and char. The coal and upper pot char samples from each test were sent to SGS Mineral Services in Denver, Colorado for proximate and ultimate analysis. Table 3-7 compares the proximate and ultimate analysis of coal and char sample from a hydrogasification test. Because the absolute ash content in coal and char does not change, coal feed rate was calculated through the ash balance between coal and char. The data in Table 3-7 also provides the basis data for the total carbon, hydrogen, nitrogen, oxygen and sulfur conversion calculations. To estimate the heavy metal contents in the product gas, SGS also analyzed the mercury and metal elements for one set of coal and char samples from a January 19th, 2010 test sample. Table 3-8 presents the comparison of metal element analysis of coal and char. The analysis on mercury indicated that mercury content in char was 0.03 micrograms per gram (μg/g) versus 0.07 μg/g in the fresh coal sample. Finally, SGS also provided Particle Size Distribution (PSD) data for the coal batches, which is shown in Figure 3-9 and further explained in the following section.

Table 3-7. Proximate and Ultimate Analysis of Coal and Char

Attribute	Coal	Char
% Moisture, Total	8.00	8.93
% Ash	27.90	44.48
% Volatile Matter	30.17	6.77
% Fixed Carbon	33.93	39.82
Total	100.00	100.00
Gross Calorific Value (Btu/lb)	8,812	7,052
% Sulfur	0.70	0.32
% Carbon	49.29	43.78
% Hydrogen	3.74	1.39
% Nitrogen	1.07	0.85
% Oxygen (Calculated)	9.30	0.25

Table 3-8. Comparison of Coal and Char Metal Element Analysis (01/19/2010 test sample)

	Metal Analysis	Coal	Char
Al	Aluminum	11.26%	11.36%
Ba	Barium	0.15%	0.14%
Ca	Calcium	1.70%	1.78%
Fe	Iron	2.57%	2.71%
Mg	Magnesium	0.43%	0.45%
Mn	Manganese	0.01%	0.02%
P	Phosphorus	0.07%	0.09%
K	Potassium	0.74%	1.05%
Si	Silicon	31.32%	30.99%
Na	Sodium	0.85%	0.84%
Sr	Strontium	0.03%	0.03%
Ti	Titaium	0.44%	0.44%

3.3 Experimental Data Analysis

3.3.1 Coal Properties and Feeding

It was difficult to feed coal consistently to the reactor throughout the tests. Calibration of the coal feeder was done many times to ensure that the auger rotation setpoint gave 8 lb/hr coal feed rate. Unfortunately, even with extensive calibrations, the coal feed rate during testing did not remain consistent from one run to another. Additionally, clogs in the coal feed tube occurred during testing and became more apparent when the first coal batch ran out and a new batch had to be used.

After experimental Run 7, the initial shipment of coal was exhausted and was replaced by a new batch. During the first test (experimental Run 8) with the new batch of coal, the coal feed tube clogged on a more frequent basis. In fact, clogging became so severe that experimental Run 9 was aborted due to an irremovable clog. The first hypothesis as to why the coal was clogging more frequently was that this batch of coal consisted of smaller particle sizes. As particle size becomes smaller, inter-particle forces become stronger than internal forces. The normalized PSDs of the coal batches were compared, as presented in .

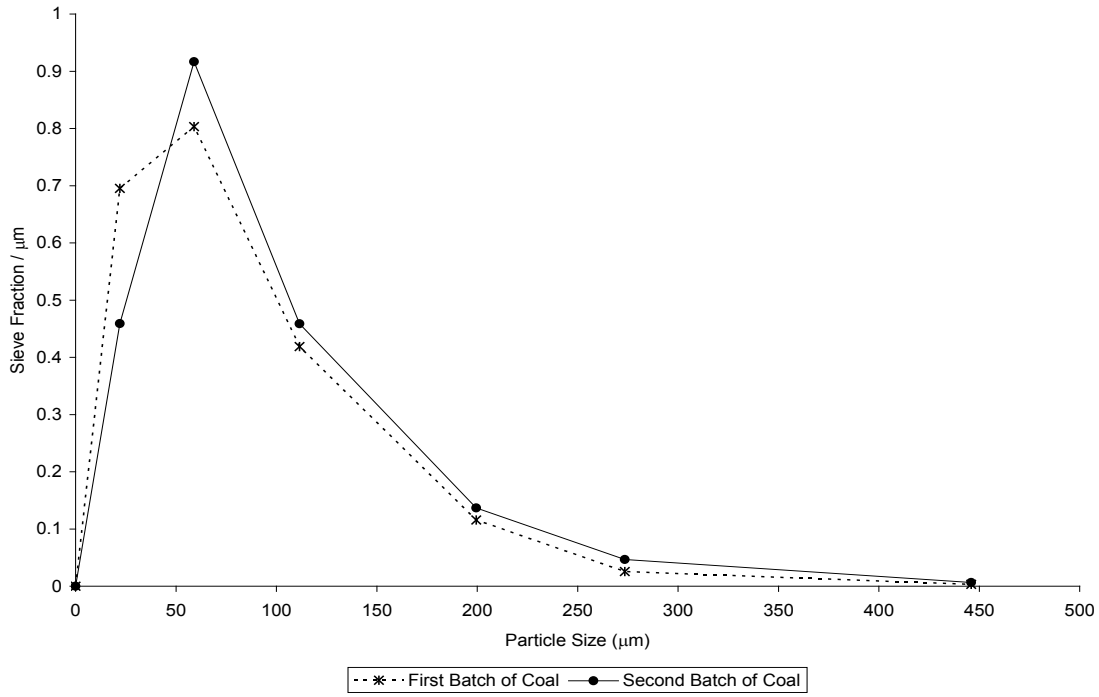

Figure 3-9. Particle Size Distributions from the Two Coal Batches

As seen in Figure 3-9, the coal from the second batch is slightly coarser than that of the first batch. The average particle size was calculated as 100 micrometers (μm) for the first batch and 90 μm for the second batch. However, this was not considered to be enough of a difference to cause increased clogging frequency. Further comparison of the proximate analysis of the two coal batches was studied. Table 3-9 has the proximate analysis used in every run, and values from the original batch are shaded and delineated by the experimental runs 1 through 7.

Table 3-9. Proximate Analysis of the Experimental Coal

Run #	Moisture Content (%)	Volatile Matter (%)	Fixed Carbon (%)	Ash (%)
1	5.70	31.9	34.7	27.7
2	5.53	32.1	34.6	27.8
3	5.63	32.4	34.3	27.7
4	5.69	32.2	34.4	27.7
5	5.67	32.7	34.1	27.6
6	5.72	32.0	34.7	27.6
7	5.70	31.5	35.1	27.8
8	8.00	30.2	33.9	27.9
9	*	*	*	*
10	8.18	31.1	33.1	27.7
11	8.03	30.6	34.2	27.2
12	8.03	30.6	34.2	27.2
13	8.15	29.4	35.4	27.1

* Due to the failed run, analysis of the coal was not done

A review of the data indicates that moisture content changed the most, increasing from about 5.5% to 8.0%. The increase in the moisture content will lead to an increase in capillary force, which will make the coal particles more cohesive. To overcome this additional cohesiveness, a larger viscous force is needed, which could be achieved by increasing the coal carrier gas flow rate. Using this way to alleviate the clogging was demonstrated during subsequent testing to a significant extent. Unfortunately, an increase in the coal carrier gas flow rate reduced the potential amount of heat brought in from the pre-heated hydrogen to the coal. An optimum hydrogen carrier gas flow rate was not defined, but is needed to ensure sufficient initial heat is provided to maintain the hydrogasification reactions and prevent coal clogging.

3.3.2 Temperature Profiles

Temperature profiles from the hydrogasification testing provide valuable insight into the operation of the reactor. For instance, as shown in Figure 3-10, steady state operation can be determined based on the temperature profile. The reaction conditions were a temperature setpoint equal to 1500°F, an H_2:Coal ratio set to 0.3, and an approximate residence time of 12.8 seconds.

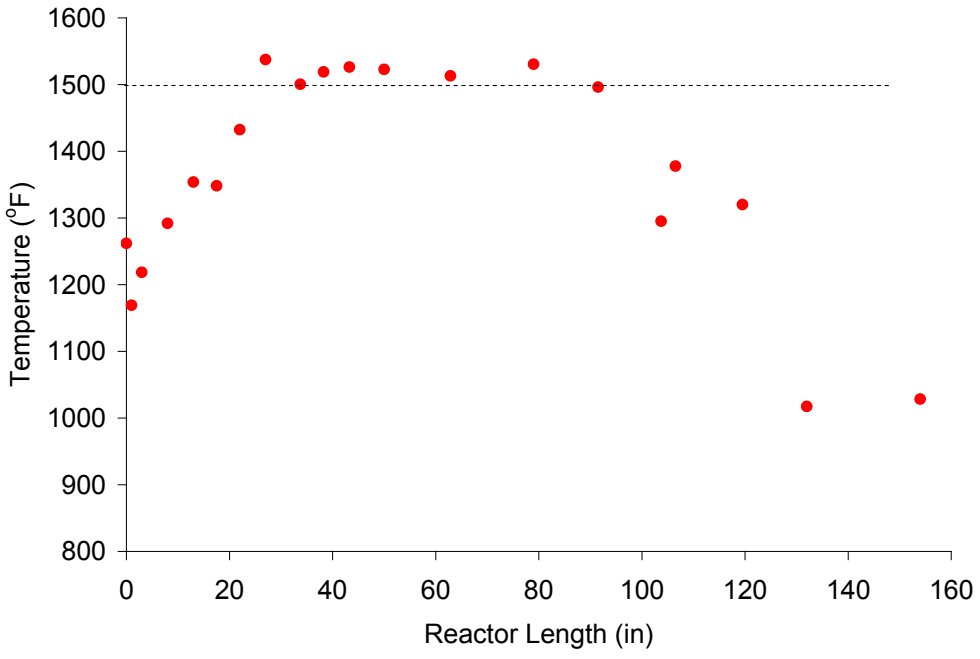

Figure 3-10. Reactor Temperature Profile from a Hydrogasification Test

The first point in Figure 3-10 is the hydrogen injection temperature, which is approximately 1250°F. This temperature is high enough to initiate the hydrogasification reactions, as may be seen by looking at the other temperature points. The superficial mixing temperature between the coal and gas had to be above 900°F to initiate the reactions. Finally, it may be seen at the middle of the reactor that a relatively constant temperature of 1500°F (which was the setpoint) was achieved.

The reactions initiating and occurring can also be observed from temperature-versus-time profiles at different locations of the reactor. Figure 3-11 shows temperature-versus-time profiles from three points in the reactor. Three thermocouples were located at the approximate top (length = 8 inches), middle (length = 63 inches), and bottom (length = 132 inches) of the reactor. It was evident that once coal feeding began the reactor temperature started to drop at the top of the reactor. This was due to the non-heated coal being introduced into the reactor with hot hydrogen. As the hydrogasification reactions proceeded, the reactor temperature rose due to the exothermic nature of the hydrogasification reactions. At approximately 45 minutes into the experimental run, steady state was achieved and the reactor temperature in the center of the reactor was at the 1500°F setpoint. When the coal feed was stopped at ~75 minutes, the temperature in the top of the reactor increased and in the middle/bottom of the reactor the temperature decreased. At this point fresh coal was no longer available to provide a temperature sink at the top of the reactor and energy was no longer being generated from the hydrogasification reactions, so this result was expected.

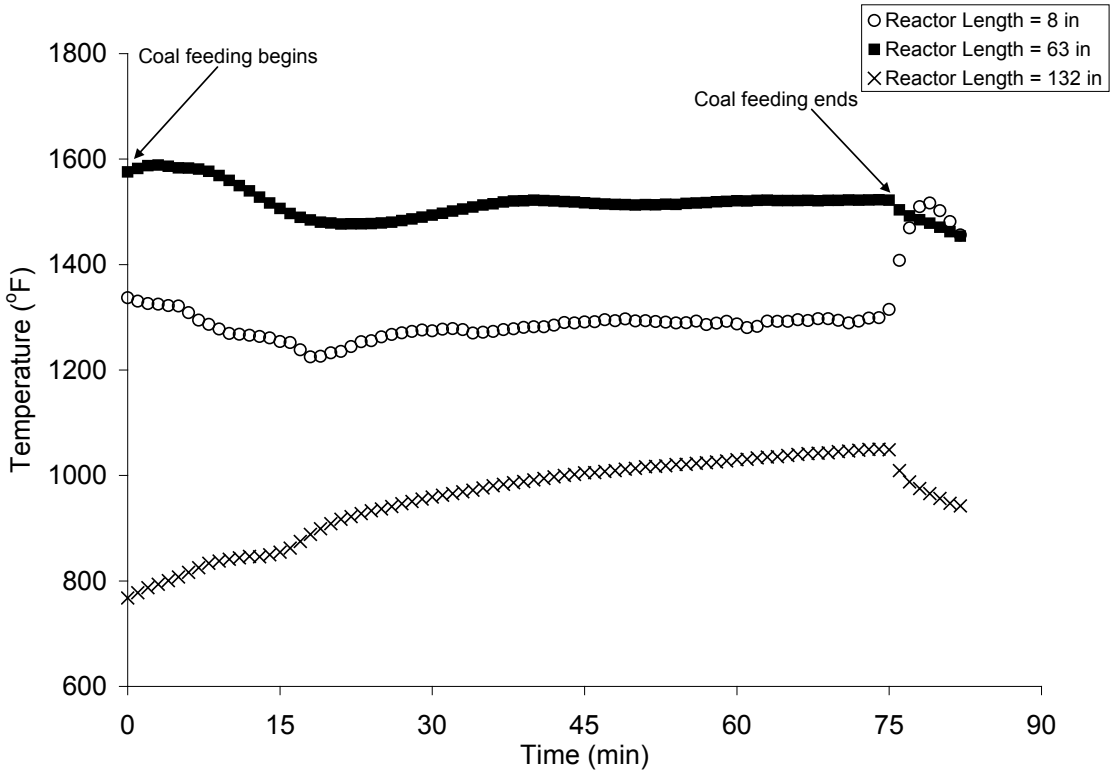

Figure 3-11. Temperature-versus-Time Profiles from a Hydrogasification Test

When coal clogging happened, a sudden temperature rise at the injection zone occurred due to the lack of heat sink resulting from the feeding of "cold" coal. When this happens, the operator should immediately pressure purge the coal feeding nozzle by building a 10-15 psig pressure difference between coal feeder and reactor to see if this pressure purge could "push" clear the clog, as indicated by a sudden temperature drop near the injection zone. If not, the reaction should be abandoned by first shutting down reactor heaters.

3.3.3 Data Analysis

The tests that had at least one hour of steady-state time were considered successful. Mass balances and conversion calculations were performed using the data from the gas GC, liquid Gas Chromatography and Mass Spectroscopy (GC/MS), and coal-char proximate and ultimate analyses.

To complete an overall mass balance of the system it is imperative to know the quality of coal that was fed. The ash content from the proximate analysis of coal and char was used along with the weight of char collected from the upper char pot for this calculation see Equation (1).

The reason ash content was chosen was because ash will not gasify and remain within the char.

(1)

With the known amount of coal and char, the overall conversions of the primary components in coal (C,H,O,S,N) can be completed using the ultimate analysis of coal and char. The calculation for total carbon conversion is shown in Equation (2). Conversion of the other components can be completed by replacing the requisite component ultimate analysis percentage.

$$\text{Carbon Conversion}(CC) = \frac{CW * UltC_{Coal}\% - ChW * UltC_{Char}\%}{CW * UltC_{Coal}\%} \quad (2)$$

The next part of the analysis is to complete the component mass balances and calculate carbon conversions to the species of interest in the system. By knowing the total solid mass of coal feed introduced into the system and ultimate analysis of the coal, the total amount of every individual component into the system as a solid phase is known. Additionally, the only other component entering the system is pure hydrogen in the gas phase. The components exit from the reactor in three phases: solid, gas, and liquid. Completing the component mass balance is the key to verify the quality of the experimental data.

The solid phase analysis is straightforward as char is the only solid component leaving the system. Given that, the calculation of each solid component leaving the system as char equals the amount of char times the ultimate analysis concentration of the component.

To determine the gas phase mass leaving system, the total volume of gas was measured with the exit flow meter throughout steady state along with the gas phase component concentration gathered with the GC. Flow through the meter was measured in standard volume, so this was converted into moles using the ideal gas law when calculating the amount of a component in the gas phase:

$$\text{Mass of Component in Gas} = \frac{\text{Component Fraction from GC} * MW_{compnet} * P * V_T}{R * T} \quad (3)$$

In Equation (3), $MW_{component}$ is the molecular weight of the component, P is the pressure, V_T is the total volume of gas exiting the reactor during steady state, R is the universal gas constant, and T is the temperature. With the mass of each component measured with the GC (CH_4, CO,

etc). in the gas phase known, the mass of the component's constituent components (i.e. the total mass of carbon in CH_4) can be calculated using stoichiometry.

For the liquid, there were two phases that had to be measured, a top phase that was BTX/oil and a bottom phase that was water. Once the phases were separated, they were individually weighed. Using data from the GC/MS the mass of the components in the BTX/oil phase were calculated using the component mass fractions and the total mass of that phase. The mass of the water collected was simply the weight of the measured water phase.

After the mass balance of the major components in coal (C, H, O, S, N) was complete, an analysis of the deviation between the incoming and outgoing components could be made. The deviation was calculated by finding the difference between the components in and out, then dividing by the amount of that component in. Overall, the mass balance of all components was very good for all of the runs. Carbon and hydrogen had the highest deviation with an absolute average deviation of about 3%. With this small error, the mass balance was considered satisfactory.

3.3.4 Preliminary Data Discussion

From the mass balance analysis, carbon conversions to major product components for all of the experimental runs are presented in Table 3-10. Additionally, the overall carbon conversion, along with the hydrogen conversions of the feed gas stream is presented. Finally, the actual H_2:Coal values and approximate residence times are given.

Table 3-10. Experimental Data Analysis

Run #	Actual H_2:Coal Ratio	Gas Resi-dence Time (s)	Carbon Conversion (%)	C to CH_4 (%)	C to CO (%)	C to C_2H_6 (%)	C to BTX (%)	C to Oil (%)	H_2 Conver-sion (%)
1	0.58	12.8	46.8	28.4	3.87	6.08	2.24	3.86	10.3
2	0.52	11.0	48.0	44.5	5.03	0.69	0.59	0.45	14.0
3	0.56	12.2	52.2	46.2	4.34	1.98	0.00	0.00	13.7
4	0.33	19.0	51.4	42.4	4.69	0.06	0.00	0.00	23.8
5	0.46	11.0	49.2	34.6	3.90	0.03	1.34	0.54	13.5
6	0.55	5.27	49.7	39.6	4.21	0.62	0.34	0.26	12.1
7	0.34	8.78	50.1	42.0	4.86	0.34	0.00	0.00	21.9
8	0.33	21.4	44.3	31.8	4.07	4.17	3.50	3.79	6.90
9	NA	NA	NA	NA	NA	NA	NA	NA	NA
10	0.56	5.94	44.0	20.2	3.16	9.82	2.43	5.22	12.1
11	0.40	11.7	43.2	23.1	3.45	6.81	3.32	4.06	7.98
12	0.40	11.0	49.4	37.8	4.28	0.59	0.71	0.72	9.32
13	0.40	15.1	49.0	45.1	5.06	0.49	0.09	0.16	18.5

Since the project was terminated on March 31, 2010, not all of the runs in the experimental plan were completed and a comprehensive data analysis was not achieved. The following section presents the preliminary analysis of the data that was obtained. From the data in Table 3-10, a few preliminary observations can be made. First, the highest overall carbon conversion and carbon conversion to CH_4 were 52% and 46% respectively. This was viewed as a significant achievement in the project. Another is the absence of carbon conversion to CO_2. Carbon conversion to CO_2 was minute, less than 0.5% for all experimental runs; hence it was not included. A small carbon conversion to CO_2 was not surprising, as the large excess of H_2 in the system pushed the equilibrium of the water-gas shift toward CO and water (H_2O). Finally, the overall trends in the table appear to agree with what was reported in the literature, and further preliminary analysis follows.

3.3.4.1 The Effect of Temperature

The literature has shown that temperature has the largest effect on hydrogasification reactions. Figure 3-12 shows the carbon conversion versus temperature data.

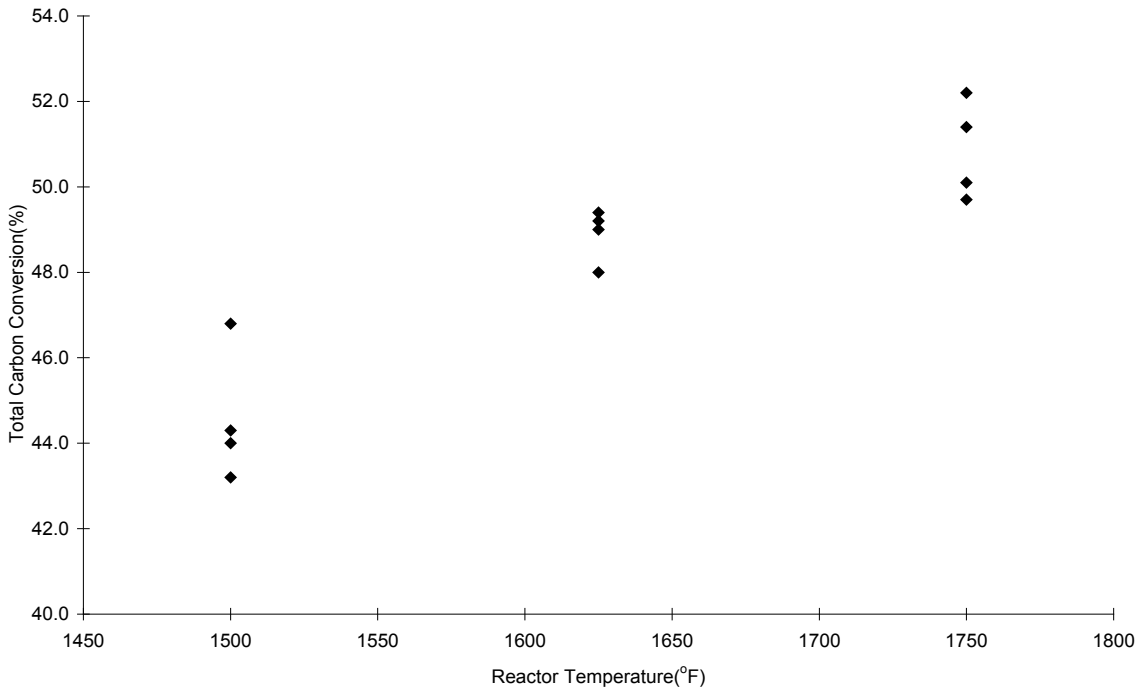

Figure 3-12. Total Carbon Conversion Versus Reactor Temperature

As seen from Figure 3-12, as the reactor temperature increased, the carbon conversion clearly increased as well.

However, analysis shows that carbon conversion into methane does not have a straightforward trend with temperature. A higher temperature will facilitate hydrocracking of BTX/oil into methane; however, if the temperature is too high, it may shift the main product from methane to carbon oxides. One key aspect of this testing is to find the optimum reaction temperature for methane formation within the experimental temperature range, as shown in Figure 3-13.

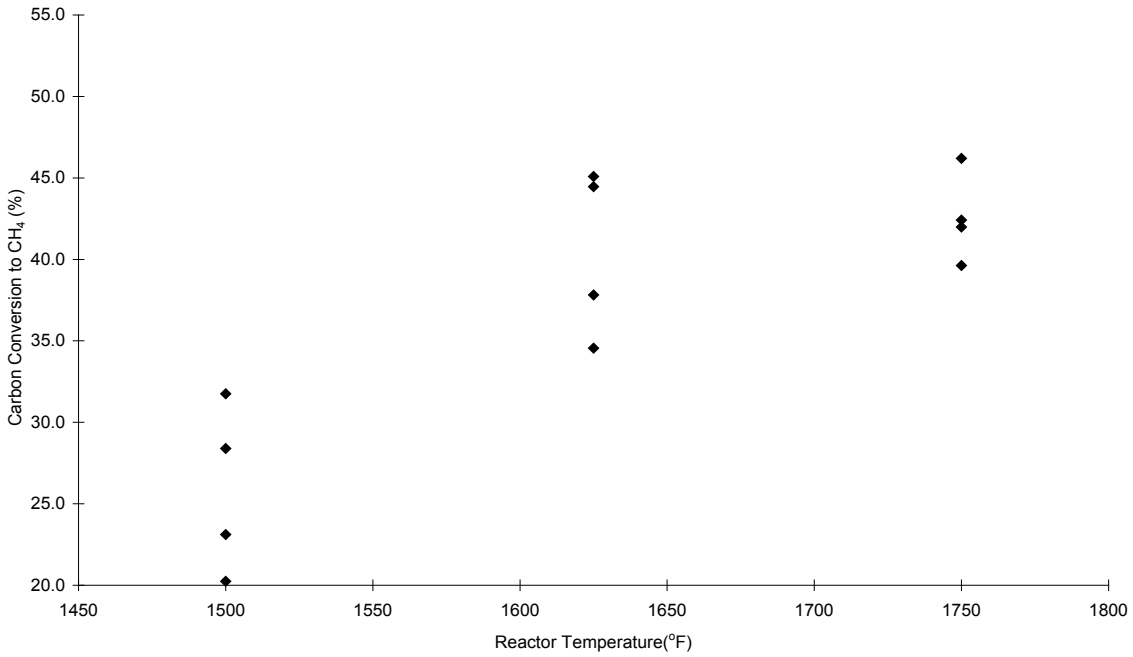

Figure 3-13. Carbon Conversion to CH_4 Versus Reactor Temperature

Although the overall trend shows that carbon conversion to CH_4 increases with increasing temperature, the trend is not as linear as was observed with the overall carbon conversion. Once the reactor temperature was at 1625°F, the slope of the points started to decline. By simple observation of the trend, there could be a potentially limiting value of how much carbon can be converted to CH_4 by simply increasing the reactor temperature.

Figure 3-14 shows the carbon conversion to BTX/oil versus temperature. In this case the amount of BTX/oil begins high and diminishes as the reactor temperature increases, eventually approaching approximately 0%. By approaching 0% there will be a very limited amount of

BTX/oil to hydrocrack; hence the amount of carbon conversion to CH_4 approaches an upper limit with increasing temperature.

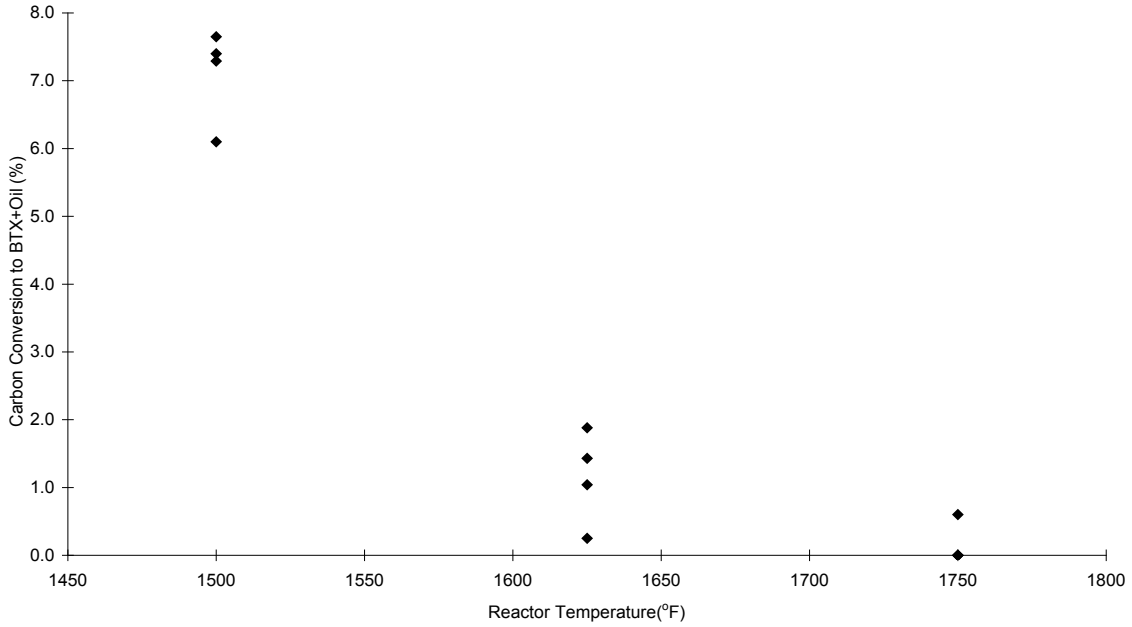

Figure 3-14. Carbon Conversion to BTX/Oil Versus Reactor Temperature

3.3.4.2 The Effect of Residence Time

The effect of residence time on conversion was explored as well. Figure 3-15 shows total carbon conversion versus temperature, grouped into two residence times. In this instance, the slopes of the trend lines are approximately the same. With the two trend lines essentially parallel to one another, carbon conversion occurs as a step change from one residence time to the next. This same type of step-change increase was also observed with carbon conversion to CH_4 and BTX/oil.

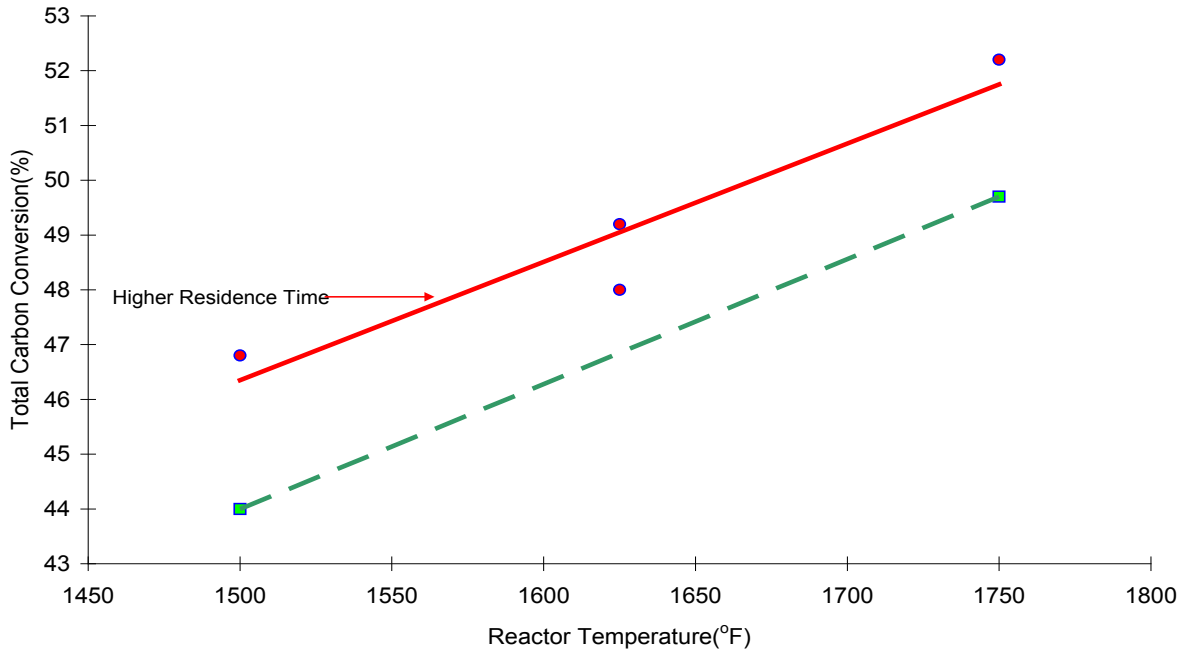

Figure 3-15. Effect of Residence Time on Carbon Conversion.

Figure 3-16 and Figure 3-17 show the effect of residence time on carbon conversion to CH_4 and BTX/oil, respectively.

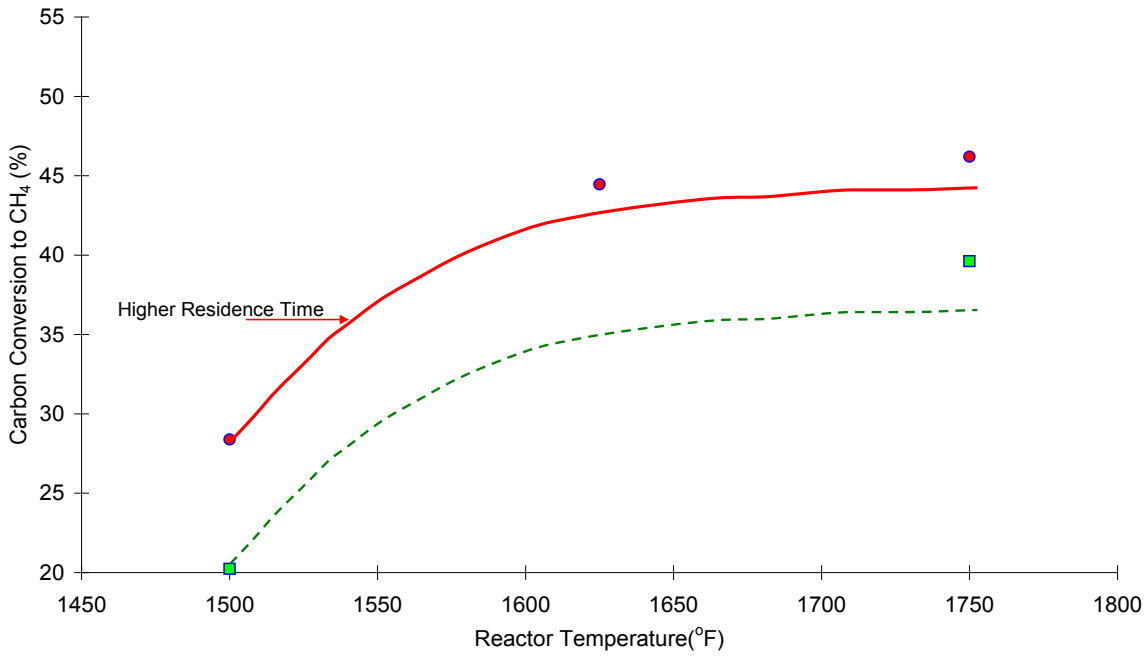

Figure 3-16. Effect of Residence Time on Carbon Conversion to CH_4

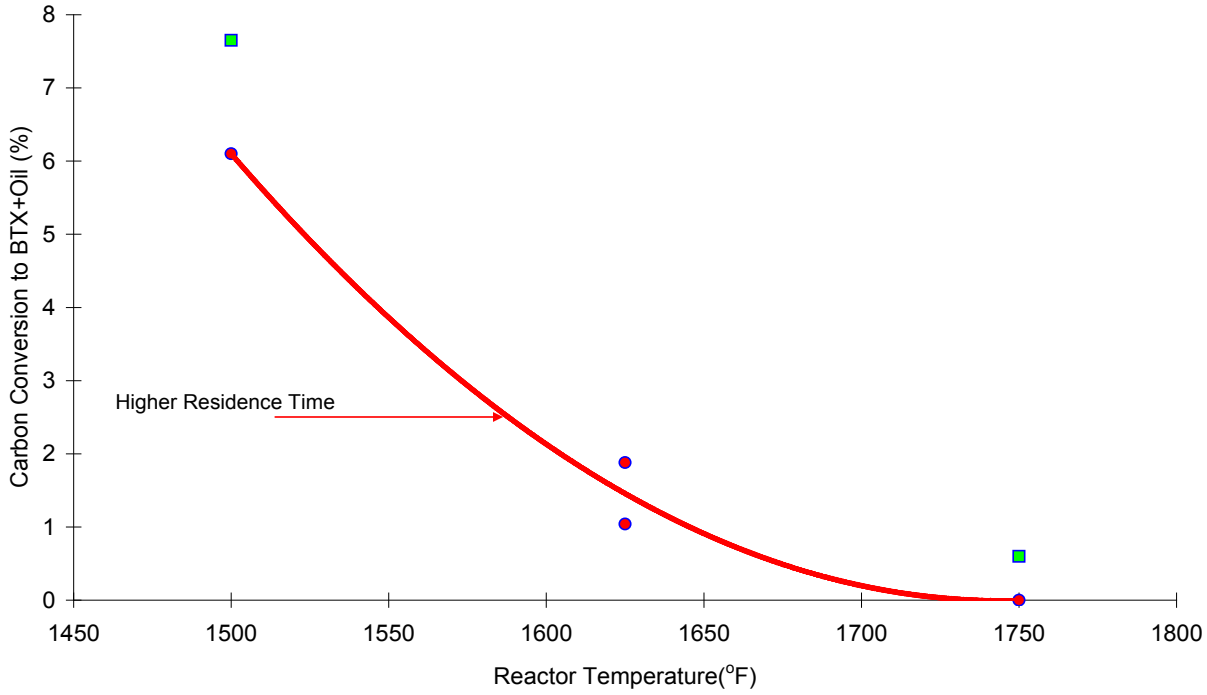

Figure 3-17. Effect of Residence Time on Carbon Conversion to BTX/Oil

Again, the slopes of the lines are approximately the same in the two figures. An increase in residence time is essentially a step change from one trend to the next. However, in the case of Figure 3-16 and Figure 3-17 the step changes are in opposite directions. Due to increased hydrocracking, it is not surprising that as residence time increased, carbon conversion to CH_4 increased and the carbon conversion to BTX/oil decreased. Both of the trends were expected.

3.3.4.3 The Effect of H_2:Coal Ratio

The last factor that was studied in this experimental plan was the H_2:Coal ratio. Figure 3-18 shows the total carbon conversion versus temperature, with two H_2:Coal data sets. The literature has shown that increasing H_2:Coal should increase the carbon conversion; however, this was not clear in the initial analysis. At the high and low temperatures, a higher ratio gave a higher conversion, as was expected. The lack of clarity comes at the medium temperature (1625°F), where the points are approximately grouped. This lack of clarity could be due to the uncertainty in the measurement of the H_2:Coal ratio.

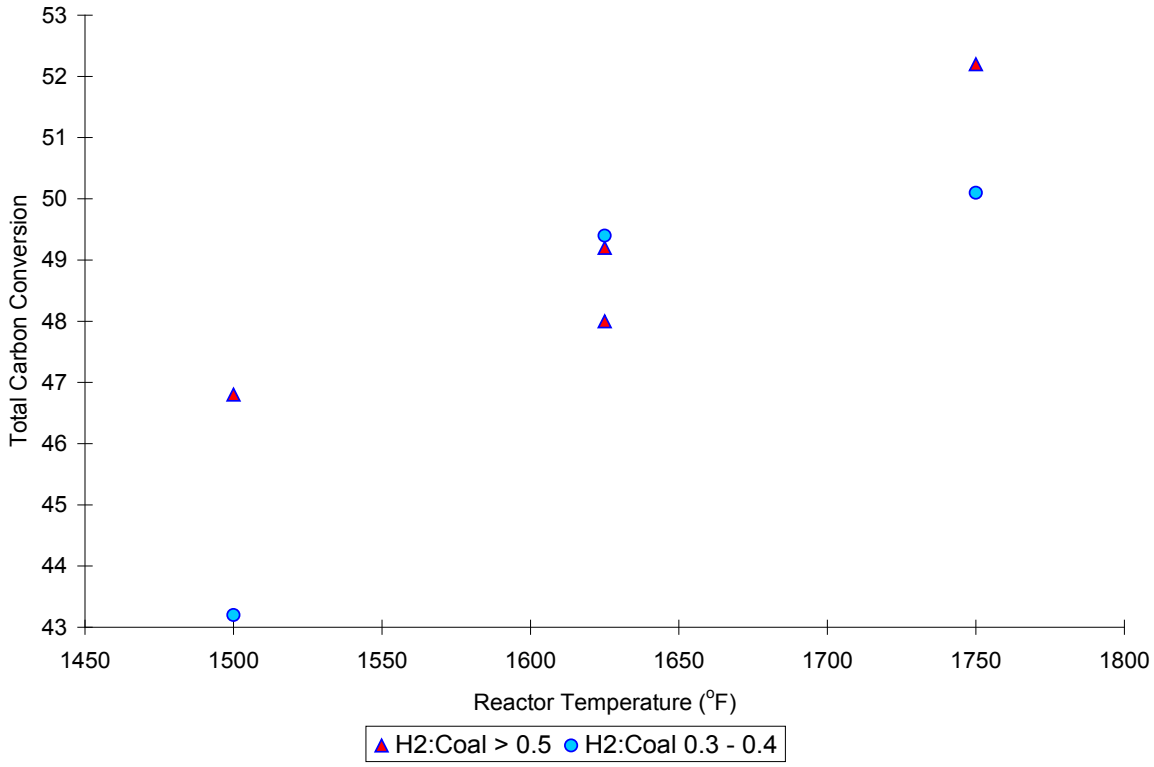

Figure 3-18. Effect of H_2:Coal on Carbon Conversion

3.3.4.4 Conversion of O, S, N and H from Coal

Results of the conversion of the other primary elements (O,S,N,H) of coal were investigated as well. Figure 3-19 shows the percentage of oxygen that was gasified from coal versus temperature. As the temperature was increased, there was no significant increase in the amount of oxygen gasified. This was likely due to the fact that nearly all of the oxygen was gasified out of the coal in every run. As such, the amount of sulfur gasified as the reactor temperature increased was similar to oxygen.

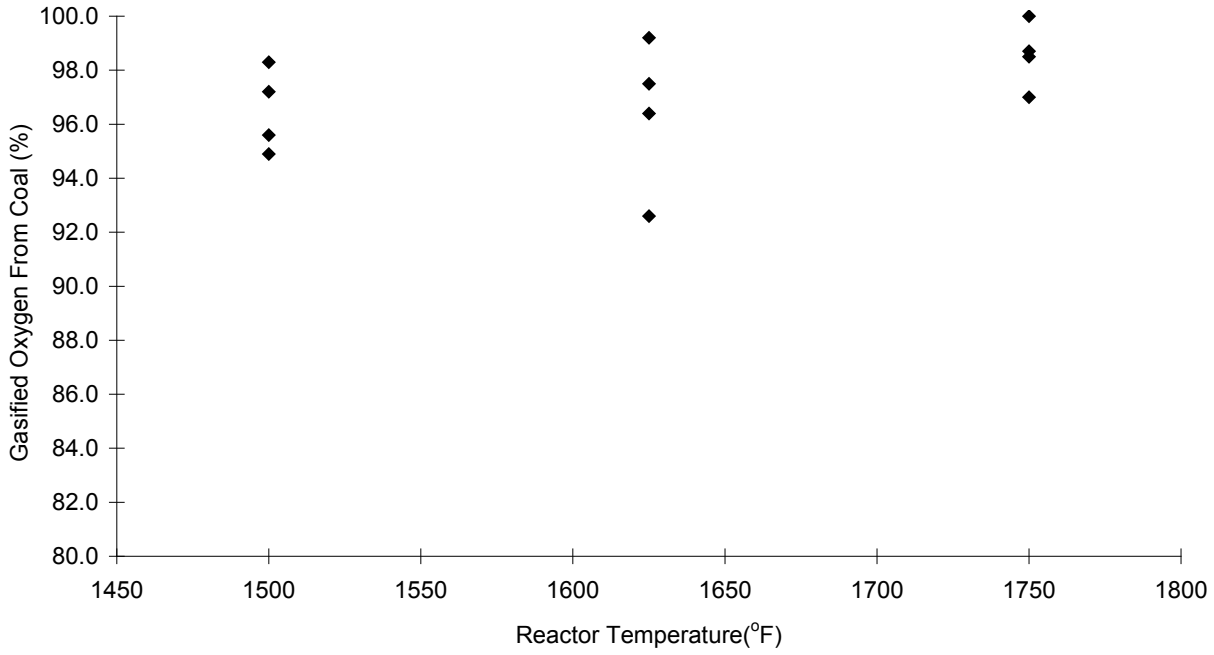

Figure 3-19. Percentage of Oxygen Gasified from Coal

Figure 3-20 shows the percentage of sulfur gasified from the coal versus temperature. There is no clear trend; however, approximately 70-80% of the sulfur was always gasified from the coal. This is a significant amount and in the event char is burned downstream of this process, having a reduced amount of sulfur will be beneficial.

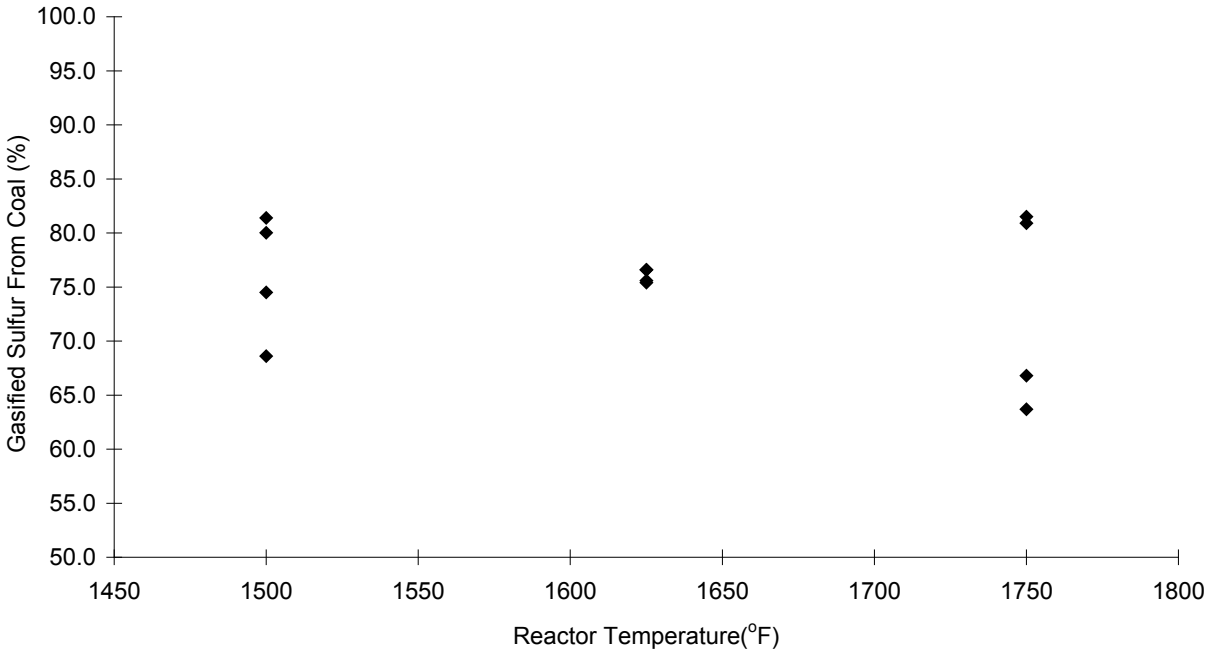

Figure 3-20. Percentage of Sulfur Gasified from Coal

Figure 3-21 shows the percentage of nitrogen gasified from the coal versus temperature, grouped based on H_2:Coal ratio. As may be seen from the figure, as temperature increased, the amount of nitrogen gasified increased. Additionally, the H_2:Coal ratio did not have an effect on the amount of nitrogen gasified from the coal.

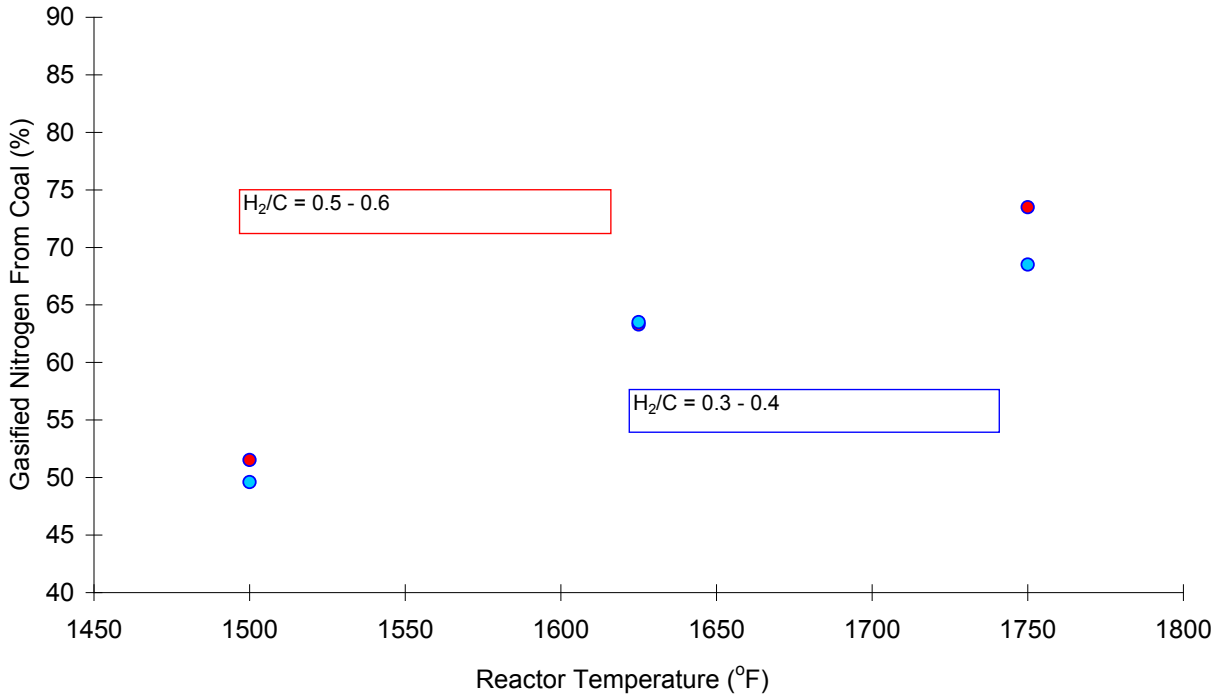

Figure 3-21. Percentage of Nitrogen Gasified from Coal

The final major component gasified from the coal was hydrogen. Figure 3-22 shows the percentage of hydrogen gasified from the coal versus temperature and is grouped based on H_2:Coal ratio. As was seen with nitrogen, as temperature increased, the amount of hydrogen gasified increased. Additionally, the H_2:Coal did not have an effect on the amount of hydrogen gasified from coal.

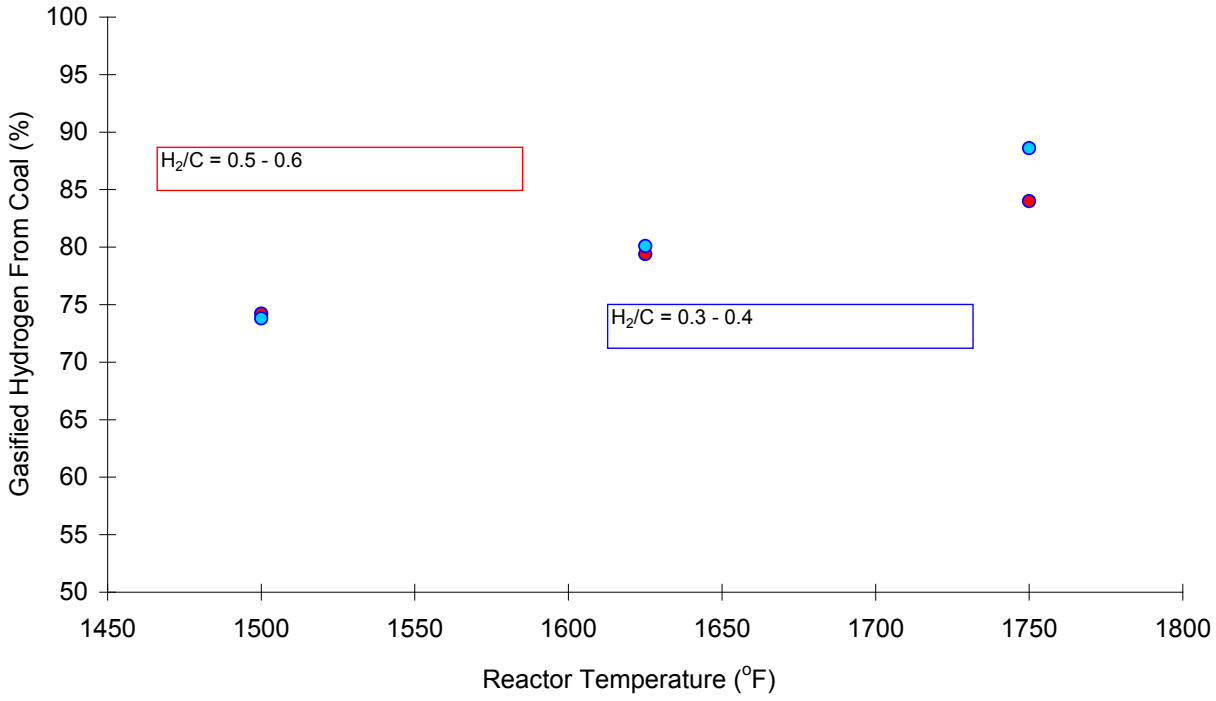

Figure 3-22. Percentage of Hydrogen Gasified from Coal

Appendix C presents the detailed test records for all the tests performed between January 2010 and March 2010.

3.4 KINETICS 1-D SIMULATION

3.4.1 EXPERIMENTAL DATA MODELING

To further evaluate the ARCH 1-D model that was described in APS Coal to SNG final scientific/technical report, experimental conditions from the hydrogasification tests were fed into the model and the results were compared with the experimental data. The model was a simple 1-D case, with kinetic parameters not necessarily tuned to this type of coal, however, the predictions from the model did an adequate job of representing the experimental data.

The simulated results are compared with the experimental results in Table 3-11 through Table 3-13. The key comparisons are the overall carbon conversion and the carbon conversion to CO, CO_2, CH_4, BTX and oil. For the experimental data, BTX includes benzene, toluene and xylene; and oil includes naphthalene and species heavier than naphthalene, i.e., biphenyl, fluorene, anthracene and pyrene. The tables also contain the comparison of the gas composition from the GC with the gas composition predicted by the model.

The overall carbon conversion was an experimental effort that was closely monitored; hence, experimental and modeling data were compared. On average the deviation between the experimental data and predicted value was approximately 25%. Considering the simplicity of the initial model, this average error is reasonable; however, the error may not be entirely attributed to the model. The gas compositions of the model and GC all compared fairly well, so these results will not be discussed further.

As was explained in the Coal to SNG final scientific/technical report, the initial reactions the model considers are pyrolytic reactions, which are represented by Equation (4).

$$u_s \frac{d(f_j)_p}{dz} = k_j\{f_j^* - (f_j)_p\} \qquad (4)$$

Where f_j = mass of component j / mass of coal; f^*_j represents the maximum fractional amount of a component that can be gasified from the coal particle; and subscript p represents gas products from the coal particle.

A likely source of error is from the estimation of f^*_j from these reactions, where the initial values of f^*_j were determined using Curie-point pyrolysis with a sub-bituminous coal. The issue is that a Curie-point pyrolyzer was not available to determine the f^*_j values for the coal used in this experimentation, so new f^*_j values were extrapolated from the original values using the coal

proximate and ultimate analysis. This was not the ideal method to determine the values of f^*_j because of the potential error associated with it; however, it did provide reasonable initial estimates of the values.

Further probing the results, the carbon conversion to specific components was analyzed. Carbon conversion to BTX is major source of deviation between simulated and experimental results. In all cases the model overestimates this value to a significant degree. This large overestimation is likely the cause of the prediction of the carbon conversion always being too large. In that regard, in many of the cases the carbon conversion to methane is under-predicted, so this may be causing a compensatory effect of a better overall conversion estimate. What this suggests is that the original parameters predicting these values are not entirely sufficient.

Table 3-11. Experimental-Versus-Model Results at 1500°F

01-08-10 Test		
Temperature (°F) =	1500	
Reactor Length (in) =	105	
H_2:Coal =	0.58	
H_2 Injection Temp(°F) =	1414	
Carbon Conversion (%)		
	Experiment	Model
CO	3.87	4.11
CO2	0	1.8
CH4	28.39	29.6
BTX	2.24	18.96
Oil	3.86	3.05
	44.44	57.52
Gas Product Stream Composition (%)		
	Experiment	Model
CO	0.56	0.88
CO2	0	0.40
CH4	4.11	6.36
H2	84.1	92.37

03-02-10 Test		
Temperature (°F) =	1500	
Reactor Length (in) =	105.25	
H_2:Coal =	0.33	
H_2 Injection Temp(°F) =	1351	
Carbon Conversion (%)		
	Experiment	Model
CO	4.07	3.70
CO2	0.10	1.70
CH4	31.75	29.50
BTX	3.50	15.80
Oil	3.79	5.00
Total	47.38	55.70
Gas Product Stream Composition (%)		
	Experiment	Model
CO	1.03	1.37
CO2	0.02	0.64
CH4	8.05	10.92
H2	90.37	87.06

03-11-10 Test		
Temperature (°F) =	1500	
Reactor Length (in) =	48.75	
H_2:Coal =	0.56	
H_2 Injection Temp(°F) =	1439	
Carbon Conversion (%)		
	Experiment	Model
CO	3.16	3.70
CO2	0.26	1.70
CH4	20.24	27.70
BTX	2.43	14.00
Oil	5.22	9.60
Total	41.12	56.70
Gas Product Stream Composition (%)		
	Experiment	Model
CO	0.53	0.85
CO2	0.04	0.39
CH4	3.39	6.28
H2	95.22	92.48

03-23-10 Test		
Temperature (°F) =	1500	
Reactor Length (in) =	77	
H_2:Coal =	0.4	
H_2 Injection Temp(°F) =	1392.53	
Carbon Conversion (%)		
	Experiment	Model
CO	3.45	4.00
CO2	0.16	1.90
CH4	23.11	29.20
BTX	3.32	15.20
Oil	4.08	6.60
Total	40.93	56.90
Gas Product Stream Composition (%)		
	Experiment	Model
CO	0.76	1.23
CO2	0.04	0.57
CH4	5.09	8.99
H2	93.36	89.21

Table 3-12. Experimental-Versus-Model Results at 1625°F

01-13-10 Test		
Temperature (°F) =	1625	
Reactor Length (in) =	77	
H_2:Coal =	0.52	
H_2 Injection Temp(°F) =	1534	
Carbon Conversion (%)		
	Experiment	Model
CO	5.03	4.49
CO2	0.01	1.44
CH4	44.46	32.2
BTX	0.59	19.41
Oil	0.45	0.14
	51.23	57.68
Gas Product Stream Composition (%)		
	Experiment	Model
CO	0.77	1.05
CO2	0.0022	0.34
CH4	6.81	7.56
H2	76.74	91.05

01-26-10 Test		
Temperature (°F) =	1625	
Reactor Length (in) =	77	
H_2:Coal =	0.46	
H_2 Injection Temp(°F) =	1519	
Carbon Conversion (%)		
	Experiment	Model
CO	3.9	4.37
CO2	0.03	1.49
CH4	34.55	32.3
BTX	1.34	19.7
Oil	0.54	0.21
Total	41.02	58.07
Gas Product Stream Composition (%)		
	Experiment	Model
CO	0.77	1.15
CO2	0.0066	0.39
CH4	6.83	8.52
H2	88.03	89.93

03-25-10 Test		
Temperature (°F) =	1625	
Reactor Length (in) =	77	
H_2:Coal =	0.4	
H_2 Injection Temp(°F) =	1441	
Carbon Conversion (%)		
	Experiment	Model
CO	4.28	4.1
CO2	0.30	1.7
CH4	37.82	35.6
BTX	0.71	14
Oil	0.72	1.4
Total	44.43	56.8
Gas Product Stream Composition (%)		
	Experiment	Model
CO	0.94	1.26
CO2	0.07	0.53
CH4	8.30	10.89
H2	90.62	87.33

03-30-10 Test		
Temperature (°F) =	1625	
Reactor Length (in) =	77	
H_2:Coal =	0.38	
H_2 Injection Temp(°F) =	1402	
Carbon Conversion (%)		
	Experiment	Model
CO	5.06	4.50
CO2	0.35	1.90
CH4	45.09	35.40
BTX	0.09	13.60
Oil	0.16	1.50
Total	51.25	56.90
Gas Product Stream Composition (%)		
	Experiment	Model
CO	1.24	1.46
CO2	0.09	0.62
CH4	11.06	11.40
H2	87.56	86.52

Table 3-13. Experimental-Versus-Model Results at 1750°F

01-19-10 Test		
Temperature (°F) =	1750	
Reactor Length (in) =	105.25	
H_2:Coal =	0.56	
H_2 Injection Temp(°F) =	1619	
Carbon Conversion (%)		
	Experiment	Model
CO	4.34	5.26
CO2	0	0.77
CH4	46.2	37.46
BTX	0	14.75
Oil	0	0
Total	52.52	58.24
Gas Product Stream Composition (%)		
	Experiment	Model
CO	0.7	1.16
CO2	0	0.17
CH4	7.46	8.27
H2	88.13	90.40

01-28-10 Test		
Temperature (°F) =	1750	
Reactor Length (in) =	48.75	
H_2:Coal =	0.55	
H_2 Injection Temp(°F) =	1673	
Carbon Conversion (%)		
	Experiment	Model
CO	4.21	4.7
CO2	0	0.9
CH4	39.62	33.6
BTX	0.34	17.4
Oil	0.26	0.06
Total	45.05	56.66
Gas Product Stream Composition (%)		
	Experiment	Model
CO	0.67	1.05
CO2	0	0.20
CH4	6.3	7.58
H2	85.2	91.17

02-03-10 Test		
Temperature (°F) =	1750	
Reactor Length (in) =	48.75	
H_2:Coal =	0.34	
H_2 Injection Temp(°F) =	1504	
Carbon Conversion (%)		
	Experiment	Model
CO	4.86	4.83
CO2	0.08	1.12
CH4	41.99	34.84
BTX	0	16.17
Oil	0	0.02
Total	47.26	56.98
Gas Product Stream Composition (%)		
	Experiment	Model
CO	1.24	1.73
CO2	0.02	0.40
CH4	10.72	12.47
H2	75.04	85.39

01-21-10 Test		
Temperature (°F) =	1750	
Reactor Length (in) =	105.25	
H_2:Coal =	0.33	
H_2 Injection Temp(°F) =	1526	
Carbon Conversion (%)		
	Experiment	Model
CO	4.69	4.89
CO2	0	0.96
CH4	42.41	38
BTX	0	13.75
Oil	0	0
Total	47.15	57.6
Gas Product Stream Composition (%)		
	Experiment	Model
CO	1.32	1.79
CO2	0	0.35
CH4	11.94	13.95
H2	78	83.90

It is evident from the results presented in Table 3-11 through Table 3-13 that the model is underestimating carbon conversion to CH_4 and significantly overestimating carbon conversion to BTX, so tuning the model will be necessary. The pyrolization reaction, represented by Equation

(4), is not the only path that CH_4 and BTX are formed in the gas phase, so simply tuning the f^*_j values and kinetic parameters will not necessarily make the model better. Both CH_4 and BTX (which in the case of this model is represented by benzene, (C_6H_6)) can also be formed from Rapid Carbon (RC), CH_mO_n as represented in Equations (5) and (6). The amount of CH_4 and BTX predicted from Equations (5) and (6) is not only dependent on the kinetic parameters, but also on the selectivity of the parallel reactions.

$$CH_mO_n + (2 + n - m/2)H_2 \rightarrow CH_4 + nH_2O \quad (5)$$

$$CH_mO_n + (0.5 + n - m/2)H_2 \rightarrow (1/6)C_6H_6 + nH_2O \quad (6)$$

In addition, both CH_4 and BTX can be formed by the hydrocracking of oil (which in the case of this model is represented by naphthalene ($C_{10}H_8$)) in another set of parallel reactions shown in Equations (7) and (8). Once again, the extent of conversion to CH_4 and BTX will not be solely dependent on the kinetic parameters, but also on the selectivity of the parallel reactions.

$$C_{10}H_8 + H_2 \rightarrow (5/3)C_6H_6 \quad (7)$$

$$C_{10}H_8 + 16H_2 \rightarrow 10CH_4 \quad (8)$$

Finally, the BTX may be further hydrocracked to form CH_4; see Equation (9).

$$C_6H_6 + 9H_2 \rightarrow 6CH_4 \quad (9)$$

As may be inferred from all of the reaction pathways to CH_4 and BTX, there are many parameters that can affect the carbon conversions to the respective constituents. In all there are 18 constant values that can be directly tuned to manipulate the carbon conversion to CH_4 and BTX. Some initial experimentation with manipulating one of the test-condition parameters was done to get a better understanding of how well the model could be tuned.

The model was tuned to the hydrogasification test on February 3, 2010, as the error for the overall carbon conversion, as well as the carbon conversion to CH_4 and BTX, was high for this case. Some of the f^*_j parameters that are likely to have the most effect on carbon conversion to CH_4 and BTX, along with a kinetic constant, were the first to be varied when tuning the model. This included halving the f^*_j values of BTX, RC, and oil. As may be seen in Table 3-14, halving the f^*_{BTX} value had little effect on all of the carbon conversions; however, halving the value of f^*_{RC} decreased carbon conversion to CH_4. Changing this pair of parameters did not provide the desired tuning effect, so the original values were retained. Halving f^*_{oil} did reduce the residuals for all of the carbon conversions, except conversion to CH_4, which increased. In spite of this, the

residual of carbon conversion to CH_4 did not increase much, so f^*_{oil} was concluded to be a good tuning parameter. Further looking at halving f^*_{oil}, halving it also approximately halved the carbon conversion to BTX. This, along with the previous result of halving f^*_{BTX}, indicates that a majority of the BTX may be coming from hydrocracking oil. Additionally, halving f^*_{oil} did not have as large of an effect on carbon conversion to CH_4, suggesting that the reaction may have a higher selectivity toward BTX.

Table 3-14. Carbon Conversions from Model Tuning

Comp.	Exp.	Org. Para.	0.5 f_{BTX}	0.5 f_{RC}	0.5 f_{oil}	High k_{BTX}	0.5 f_{oil} & High k_{BTX}
CH_4	41.99	34.84	35.26	26.56	29.17	40.13	35.40
BTX	0.00	16.17	15.12	15.16	8.62	9.93	2.36
Oil	0.00	0.02	0.01	0.01	0.00	0.96	0.03
Total	47.26	56.98	56.34	47.68	43.75	56.97	43.75

The next parameter that was adjusted was the Arrhenius pre-exponential constant (k_{BTX}), for the reaction rate of Equation (9). Because carbon conversion to BTX needed to be decreased and increased for CH_4, k_{BTX} was increased by an order of magnitude. Adjusting this value had a positive effect on the model predictions of BTX and CH_4; however, it did not help with the overall conversion. To get a better fit, the halved f^*_{oil} parameter was used along with the adjusted k_{BTX} value. As may be seen in Table 3-14, this gave the best overall model predictions of all of the tuned parameters.

A good fit was found by adjusting an f^*_j value along with a kinetic constant, adjusting the kinetic constants will likely be limited in the future. As was discussed initially, a major component of the model's error is likely coming from the extrapolated f^*_j values, as these values were originally experimentally determined from another sub-bituminous coal type. By simply adjusting the f^*_j for oil, the model fit was significantly improved, so the f^*_j value for CH_4 will be adjusted with that of oil.

3.4.2 ARCH Model Tuning

To tune the ARCH model, the f^*_{CH4}, f^*_{oil}, and k_{BTX} values were adjusted using three-factor full central composite designs. As was discussed in the previous section, three factors seemed to have the most significant affect on overall carbon conversion as well as carbon conversion to BTX and CH_4. Both f^*_{CH4} and f^*_{oil} were varied between 0.5 and 1.5 times the extrapolated value. As for k_{BTX}, this value was varied so that the natural log of the difference of the exponents varied between -10 and 10. By varying k_{BTX} this way, the model provided responses to k_{BTX} over a

range of magnitudes. Overall, the central composite design was executed for three test conditions. This was done to find optimized parameters at factor levels from the experimental plan. The three experiments that were chosen for tuning were the 01-26-10, 01-28-10 and 03-02-10 tests. Finally, the analyzed responses were the residuals for overall carbon conversion, carbon conversion to BTX, and carbon conversion to CH_4.

The responses from the model were analyzed and are shown in Figure 3-23 through Figure 3-25. These three figures are overlaid contour plots of f^*_{CH4} vs. $k_{BTX,}$ with the residuals as the responses. In making the plots, f^*_{oil} was kept at a minimum. This was done because the value of f^*_{oil} had a significant effect on the model, and having it at a minimum reduced the residual size considerably. In that situation, it was desirable to find values for the three factors that caused all three responses to be ±5% of the experimental conversion percent.

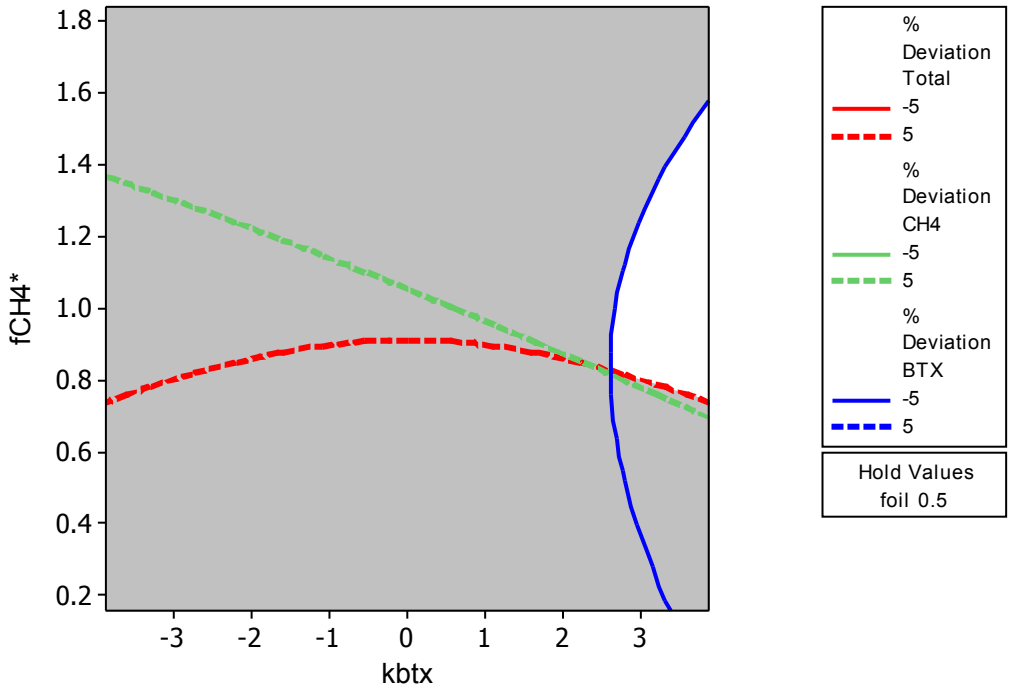

Figure 3-23. Overlaid Contour Plot of the Responses from the 03-02-10 Test

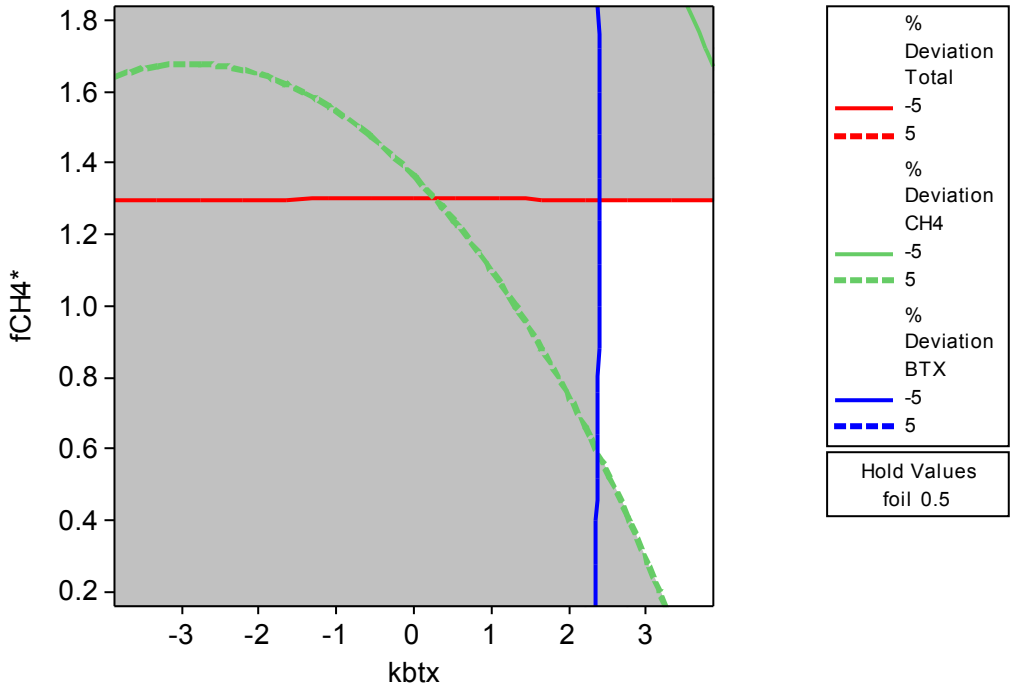

Figure 3-24. Overlaid Contour Plot of the Responses from the 01-26-10 Test

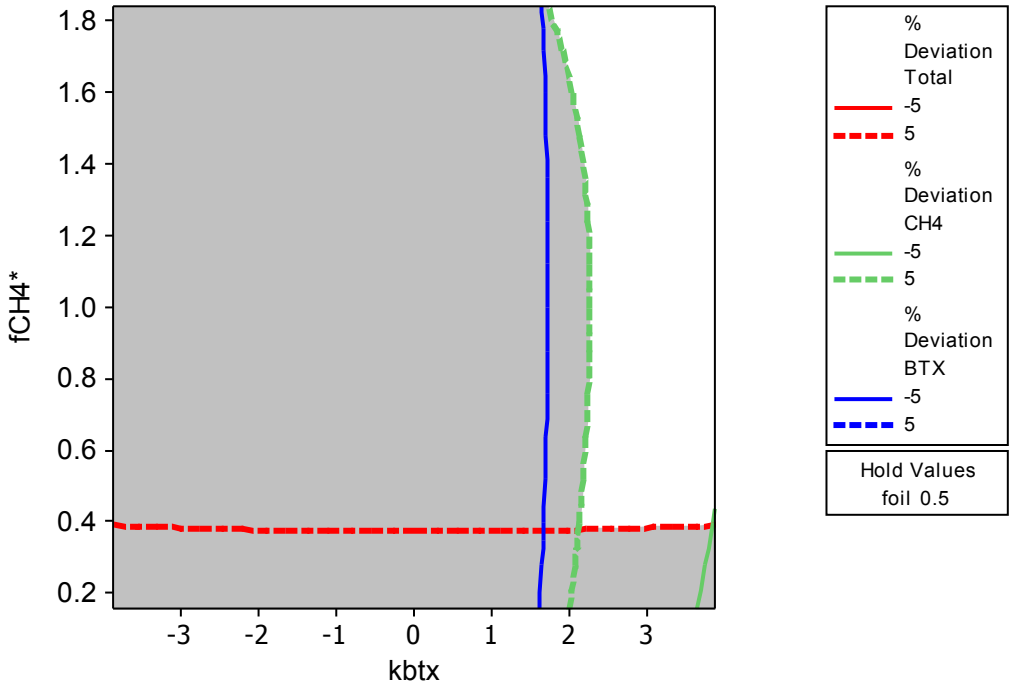

Figure 3-25. Overlaid Contour Plot of the responses from the 01-28-10 test

The non-shaded area of the contours is the region where all three residuals are within ±5% of the experimental value. By looking at all three model cases it may be seen that having the following approximate values for the three most important factors will have all responses within ±5% of the experimental value:

$$f^*_{CH4} = f^*_{CH4,o}$$

$$f^*_{Oil} = 0.5f^*_{Oil,o}$$

$$k_{BTX} = \ln(\exp(k_{BTX,o}) + \exp(3))$$

In the above values, the subscript o denotes the original value of the parameter. With the model tuned, the new values of the parameters were used to perform the model predictions again in Table 3-11 through Table 3-13.

3.4.3 Model Predictions

Using the parameter values from the previous section, the experimental conditions from the twelve experimental runs were simulated again. The results are presented in Table 3-15 through Table 3-17.

Table 3-15. Experimental-Versus-Model Results at 1500°F

01-08-10 Test		
Temperature (°F) =	1500	
Reactor Length (in) =	105	
H_2:Coal =	0.58	
H_2 Injection Temp(°F) =	1416	
Carbon Conversion (%)		
	Experiment	Model
CO	3.87	4.11
CO2	0	1.84
CH4	28.39	28.37
BTX	2.24	8.46
Oil	3.86	1.32
	44.44	44.093
Gas Product Stream Composition (%)		
	Experiment	Model
CO	0.56	0.91
CO2	0	0.41
CH4	4.11	6.25
H2	84.1	92.44

03-02-10 Test		
Temperature (°F) =	1500	
Reactor Length (in) =	105.25	
H_2:Coal =	0.33	
H_2 Injection Temp(°F) =	1348	
Carbon Conversion (%)		
	Experiment	Model
CO	4.07	3.73
CO2	0.10	1.71
CH4	31.75	28.23
BTX	3.50	8.08
Oil	3.79	0.94
Total	47.38	42.68
Gas Product Stream Composition (%)		
	Experiment	Model
CO	1.03	1.43
CO2	0.02	0.66
CH4	8.05	10.81
H2	90.37	87.11

03-11-10 Test		
Temperature (°F) =	1500	
Reactor Length (in) =	48.75	
H_2:Coal =	0.56	
H_2 Injection Temp(°F) =	1508	
Carbon Conversion (%)		
	Experiment	Model
CO	3.16	3.75
CO2	0.26	1.72
CH4	20.24	25.43
BTX	2.43	8.23
Oil	5.22	3.89
Total	41.12	43.02
Gas Product Stream Composition (%)		
	Experiment	Model
CO	0.53	0.86
CO2	0.04	0.40
CH4	3.39	5.86
H2	95.22	92.88

03-23-10 Test		
Temperature (°F) =	1500	
Reactor Length (in) =	77	
H_2:Coal =	0.4	
H_2 Injection Temp(°F) =	1403	
Carbon Conversion (%)		
	Experiment	Model
CO	3.45	4.00
CO2	0.16	1.84
CH4	23.11	27.35
BTX	3.32	8.42
Oil	4.08	2.00
Total	40.93	43.60
Gas Product Stream Composition (%)		
	Experiment	Model
CO	0.76	1.27
CO2	0.04	0.58
CH4	5.09	8.66
H2	93.36	89.49

Table 3-16. Experimental-Versus-Model Results at 1625°F

01-13-10 Test		
Temperature (°F) =	1625	
Reactor Length (in) =	77	
H_2:Coal =	0.52	
H_2 Injection Temp(°F) =	1484	
Carbon Conversion (%)		
	Experiment	Model
CO	5.03	4.32544
CO2	0.01	1.60733
CH4	44.46	34.0398
BTX	0.59	3.99126
Oil	0.45	0.2044
	51.23	44.1682
Gas Product Stream Composition (%)		
	Experiment	Model
CO	0.77	1.05
CO2	0.0022	0.39
CH4	6.81	8.29
H2	76.74	90.26

01-26-10 Test		
Temperature (°F) =	1625	
Reactor Length (in) =	77	
H_2:Coal =	0.46	
H_2 Injection Temp(°F) =	1468	
Carbon Conversion (%)		
	Experiment	Model
CO	3.9	4.22
CO2	0.03	1.64
CH4	34.55	33.69
BTX	1.34	4.51
Oil	0.54	0.29
Total	41.02	44.35
Gas Product Stream Composition (%)		
	Experiment	Model
CO	0.77	1.16066
CO2	0.0066	0.45154
CH4	6.83	9.27197
H2	88.03	89.1158

03-25-10 Test		
Temperature (°F) =	1625	
Reactor Length (in) =	77	
H_2:Coal =	0.4	
H_2 Injection Temp(°F) =	1466	
Carbon Conversion (%)		
	Experiment	Model
CO	4.28	4.17
CO2	0.30	1.67
CH4	37.82	32.86
BTX	0.71	4.55
Oil	0.72	0.35
Total	44.43	43.60
Gas Product Stream Composition (%)		
	Experiment	Model
CO	0.94	1.32
CO2	0.07	0.53
CH4	8.30	10.44
H2	90.62	87.71

03-30-10 Test		
Temperature (°F) =	1625	
Reactor Length (in) =	77	
H_2:Coal =	0.38	
H_2 Injection Temp(°F) =	1425	
Carbon Conversion (%)		
	Experiment	Model
CO	5.06	4.57
CO2	0.35	1.88
CH4	45.09	32.49
BTX	0.09	4.70
Oil	0.16	0.40
Total	51.25	44.04
Gas Product Stream Composition (%)		
	Experiment	Model
CO	1.24	1.53
CO2	0.09	0.63
CH4	11.06	10.86
H2	87.56	86.98

Table 3-17. Experimental-Versus-Model Results at 1750°F

01-19-10 Test		
Temperature (°F) =	1750	
Reactor Length (in) =	105.25	
H_2:Coal =	0.56	
H_2 Injection Temp(°F) =	1583	
Carbon Conversion (%)		
	Experiment	Model
CO	4.34	5.30
CO2	0	0.73
CH4	46.2	38.52
BTX	0	0.00
Oil	0	0.00
Total	52.52	44.552
Gas Product Stream Composition (%)		
	Experiment	Model
CO	0.7	1.21
CO2	0	0.17
CH4	7.46	8.81
H2	88.13	89.81

01-28-10 Test		
Temperature (°F) =	1750	
Reactor Length (in) =	48.75	
H_2:Coal =	0.55	
H_2 Injection Temp(°F) =	1607	
Carbon Conversion (%)		
	Experiment	Model
CO	4.21	4.49
CO2	0	1.04
CH4	39.62	36.78
BTX	0.34	0.88
Oil	0.26	0.09
Total	45.05	43.28
Gas Product Stream Composition (%)		
	Experiment	Model
CO	0.67	1.05
CO2	0	0.24
CH4	6.3	8.61
H2	85.2	90.09

02-03-10 Test		
Temperature (°F) =	1750	
Reactor Length (in) =	48.75	
H_2:Coal =	0.34	
H_2 Injection Temp(°F) =	1427	
Carbon Conversion (%)		
	Experiment	Model
CO	4.86	4.61208
CO2	0.08	1.33821
CH4	41.99	37.0855
BTX	0	0.65187
Oil	0	0.0578
Total	47.26	43.7454
Gas Product Stream Composition (%)		
	Experiment	Model
CO	1.24	1.75
CO2	0.02	0.51
CH4	10.72	14.06
H2	75.04	83.69

01-21-10 Test		
Temperature (°F) =	1750	
Reactor Length (in) =	105.25	
H_2:Coal =	0.33	
H_2 Injection Temp(°F) =	1479	
Carbon Conversion (%)		
	Experiment	Model
CO	4.69	4.97
CO2	0	0.88
CH4	42.41	38.23
BTX	0	0.00
Oil	0	0.00
Total	47.15	44.08
Gas Product Stream Composition (%)		
	Experiment	Model
CO	1.32	1.93
CO2	0	0.34
CH4	11.94	14.87
H2	78	82.85

As may be seen by looking at the tables, merely adjusting the k_{BTX} and f^*_{Oil} parameters enables the model to more accurately predict all of the values. What is most interesting about this result is that the value of k_{BTX} was predicted to be higher in this study than what was reported in the literature. This is not too surprising, as drop-tube-designed reactors generally have higher reaction rates. Favorably the result demonstrated that the basic 1-D model was able to model the experimental data really well. The next step in this process was to implement this model with the 3-dimensional (3-D) hydrodynamic model described in the Coal to SNG report. This implementation had begun and was assisted by the Computational Science Division, NETL. However it was not finished by the time the project ended.

3.5 Operational Issues

Several major repairs were conducted around the reactor under Coal to SNG project – mainly to improve hydrogen heating, reactor heating and steady coal feeding. These changes gave the relatively smooth operation that was delivered by this project during January 1 to March 31, 2010. Even with these changes, several small issues occurred during these 3 months, and they are reviewed below along with the reactor final status.

3.5.1 Gasket Replacement

A gas leak at the reactor top-hat region occurred in January 2010. Diagnosing the issue revealed that during the previous reactor repair in 2009, the original gasket between the top-hat and the reactor was not removed. Due to the high pressure and high temperature expected at the top flanges (700-1000°F and 1500 psig), a “Flat-Face to Recess” design was selected (as shown in Figure 3-26). The groove centers the gasket very accurately so that the load is distributed evenly. The groove also retains the gasket entirely and keeps it from pushing out under pressure and heat. Once the gasket is compressed per the Flexitallic specifications, it fills the groove, except that a portion of the gasket extends above the face of the flange to create a seal on the flat face of the top flange. The groove was installed on the reactor side of the flange so that when the reactor was in a vertical position, a replacement gasket could be set into the groove and held in place by gravity while the top-hat flat-face flange was installed. An onsite contractor, not sufficiently informed, did not notice this special design and placed the “new” second gasket on top of the original one during the reactor reassembly in 2009.

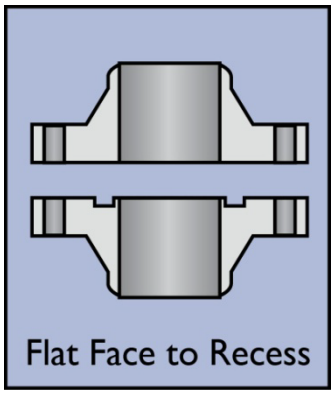

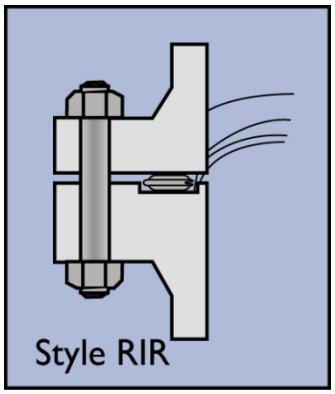

Figure **3-26**. Flat Face to Recess Flange Surface Design and Gasket Placement*
*:Special design for high pressure and high temperature

Having two consecutive gaskets did not allow the reactor to be completely sealed at this point and resulted in a gasket becoming a pressure-bearing component. Several solutions to this problem were discussed to mitigate reactor downtime; however, it was determined that de-telescoping the reactor, removing both gaskets and replacing them with a new gasket was the proper approach.

Figure **3-27**. Taking Out the Worn Gasket

Figure 3-28. Top Flange with New Gasket

A comprehensive plan was put into place to ensure the reactor repairs were timely and cost efficient. The reactor was de-telescoped, all gaskets were replaced, and the reactor was re-telescoped in a single day. The repair plan included time for identifying and securing the parts and tools, disconnecting all power wires and surrounding tubing, and reconnecting them at the completion of the repair work. All other major gaskets - coal hopper to reactor, upper and lower

bellows, reactor to upper char pot, and upper char pot to bottom char pot - were replaced at the time. In total, the reactor was down for two weeks, and repairs at the gasket were completed during this period of time and testing recommenced. The seal stayed tight through the remainder tests.

3.5.2 Repair of Product Gas Flow Meter

During the startup of an attempted hydrogasification test an incident occurred that caused the product gas flow meter to critically fail. During hydrogasification testing, nitrogen was used initially during startup for a system pressure test. Once the reactor passed the pressure test at the desired operating pressure, the reactor gas was switched from nitrogen to hydrogen. During the gas switchover during this test, an incorrect valve was opened, which caused approximately 5000 psig hydrogen to be vented directly to the exhaust line creating significant back pressure on the product gas flow meter. This back pressure resulted in the critical failure of the flow meter. A new meter was purchased and delivered within a week. Additionally, the valve that was mistakenly opened had further identification added to it to prevent this incident from occurring again in the future.

3.5.3 Repair of GC TCD Detector

During a hydrogasification test, it was observed that the TCD of the GC was not working properly, as the intensity of the peaks was diminishing. Contamination from testing was suspected. An attempt to clean the GC by baking was unsuccessful. So the resistivity of each of the four TCD filaments was measured. The resistivity of a filament on the sample side of the TCD was lower (~6 ohms) than the resistivity of the other three filaments (~32 ohms), which were within manufacturer specifications. A low resistivity is an indication that a filament is either contaminated or grounded. In this instance the filament was contaminated, so it was replaced. This action repaired the GC.

3.5.4 Remaining Issues

In addition to previously described issues, the dome of the Tescom back-pressure regulator (serial #26-1765) was constantly leaking. Attempts to end the leak by installing new domes were made, but no improvements were observed. This problem was so unusual that Tescom technical support planned a site visit to further diagnose the issue.

Finally, two Watlow heaters failed in the hydrogen preheater zone 2 and preheater zone 4. In spite of this, the overall capacity of the hydrogen preheater was still sufficient, and the hydrogen

injection operating temperature was capable of reaching the operation requirement. Because of this, a replacement was not scheduled to save testing time. Overall, Watlow heaters did not demonstrate to be robust products for this application. They contributed to a couple of incidents and tended to have a short operational life.

3.6 CONCLUSIONS ON HYDROGASIFICATION BENCH TESTING

Hydrogasification experimentation during this project was a continuation of the work initiated under the Coal to SNG project. For the details of the reactor design and other similar issues, please refer to the Coal to SNG final scientific/technical report. At the beginning of the IES project, much effort was put forth to ensure that the analytical methods being used were sufficient. This process began by using multiple calibration gases in the GC and MS. The calibration protocol required both pieces of analytical equipment to be calibrated every test day. Additionally, improved methods were developed to analyze the sulfurous species in the product gas stream. It was found that the methods to analyze the component concentrations in the product gas stream were good.

Along with ensuring the gas analysis was sufficient, methods to analyze both the liquids and solids collected from the hydrogasification tests were developed. For the liquids a method to separate the BTX/oil phase from the water phase was found. Once separated, the BTX/oil was then analyzed with a GC/MS. As for the solid phase, the coal and char from the upper char pot were sent offsite for proximate and ultimate analysis. Like the gas analysis, the analytical work for both the liquid and solid products from hydrogasification testing was considered satisfactory.

With the analytical methods considered satisfactory, hydrogasification testing began. A total of 13 runs were attempted with 12 being successful. Coal feeding continued to be a problem during testing and became more severe after a new coal batch had to be utilized. It was concluded that the coal clogging problem was due to higher moisture content in the new batch of coal. To overcome this problem, the coal carrier gas flow rate was increased.

As the runs from the experimental plan were being executed, mass balances of C, H, O, N and S of the coal were evaluated. Along with the mass balances, overall carbon conversion and carbon conversions to specific components were calculated. The mass balance, in conjunction with the analytical methods, was deemed satisfactory as the error from it was small.

Some data analysis was done with the obtained test data. Results show that increasing the temperature increased the carbon conversion to CH_4; however, an upper limit of the conversion

may have been reached. As the upper limit for carbon conversion to CH_4 was neared, the lower limit of carbon conversion to BTX/oil was approached. Given that result, increasing the residence time appeared to increase carbon conversion, which was expected. Finally, at this time, the effect from the H_2:Coal ratio was not clear.

Conversions of the other primary elements that were gasified from coal were also analyzed. It was found that essentially all oxygen gasified out of the coal regardless of the experimental conditions. Additionally, the amount of sulfur that gasified out of the coal appeared to be independent of the experimental conditions. Next, the conversion of nitrogen gasified from coal was concluded to depend on the reactor temperature only. Trends showed that as temperature increased, the amount of nitrogen that gasified from the coal increased. Finally, the amount of hydrogen that was gasified from the coal was analyzed. As was observed with nitrogen, the amount of hydrogen gasified from the coal increased with the increase of temperature.

Modeling work with the ARCH 1-D model progressed from the Coal to SNG project. To see the model development, please refer to the Coal to SNG final report. The model output compared well with the experimental results. The overall carbon conversions were off by about 25%, which was adequate for this initial model. Additionally, some of the error is likely coming from the estimation of the f^*_j values. With that hypothesis, some of the f^*_j values were varied and which improved the modeling fit substantially.

The model parameters from the ARCH 1-D model were tuned to find parameters that adjusted overall carbon conversion, carbon conversion to CH_4, and carbon conversion to BTX to be within ±5% of the experimental value. The results showed that f^*_{Oil} needed to be halved and that k_{BTX} had to be increased. With the new parameters, the model was run again for all of the experimental conditions and was able to more accurately predict all of the experimental conditions. With that, it was concluded that the model with the fitted parameters could be integrated into a comprehensive 1-D model of the reactor. This model would be an excellent tool for developing a commercial-scale hydrogasification reactor.

THIS PAGE INTENTIONALLY LEFT BLANK.

4. ALGAE TESTING

The algae testing in this project continued the R&D work performed under the Coal to SNG Project. Under the Coal to SNG project, an algae lab was built and a 6M cultivator testing system was designed, constructed and tested at the APS 3rd Avenue testing facility. During the course of IES, the research focused on the algae stressing to increase algae lipid content and reduce chlorophyll biologically, the development of methods for lipid analysis, oil extraction and biodiesel production from algae oil and algae biomass, and the demonstration of large-scale algae cultivation at APS's Redhawk algae testing facility.

4.1 ALGAE LABORATORY TESTING

4.1.1 DEVELOPMENT OF FATTY ACID ANALYSIS ON ALGAE BIOMASS

The conversion of algae oil (triglycerides) and FFA into methyl esters through esterification is a common method used to for algae-oil fatty acid analysis. Fatty Acid Methyl Esters (FAMEs) have a much lower boiling point compared to their corresponding oil and FFA molecules, which made it feasible to separate them through a GC method. The injection of an internal standard together with the sample reduces the error in the analysis and helps with determining the weight content of each fatty acid component. The esterification can be performed using an acid catalyst, a base catalyst, or a combination of both. Algae oil was found to contain relatively large amounts of FFA, which makes acid-catalyzed esterification a preferred method, since FFA cannot be converted into FAME using a base catalyst.

4.1.1.1 Fatty Acid Analysis Using Acid-Catalyzed FAME

4.1.1.1.1 Materials and Solutions:

- Reagent: Methanolic acid (10% v/v H_2SO_4 (sulfuric acid in methanol))
- Internal standard: 40 milligram per milliliter (mg/ml) methyl nonadecanoate in hexane (C19:0)
- Separation solvents: hexane containing 0.2% butylated hydroxytoluene (BHT) and saturated sodium bicarbonate ($NaHCO_3$) in a water solution
- 100 mg freeze-dried biomass for each analysis

4.1.1.1.2 Gas Chromatography and Mass Spectroscopy (GC/MS) Analysis

The FAME samples were analyzed on a HP-7890A GC equipped with an HP7673B injector and 5975C MS. A small amount (0.2 μl) of the sample was injected into the column with a split injection mode of 50/1. The GC injector temperature was 250°C, and the oven temperature was

programmed to increase from 150°C to 220°C at a rate of 5°C/min. High-purity helium gas was used as the carrier gas. FAMEs were identified by mass spectroscopy (MS) and quantified by comparing peak areas with the internal standard (C19:0) described above.

4.1.1.1.3 FAME Sample Preparation Procedure:

The following procedure was followed to prepare the FAME sample.

1. Tare and weigh 100 mg dry biomass into a 12 milliliter (ml) glass culture tube with screw cap.
2. Add 50-µl (40 mg/ml) internal standard (C19:0) into the tube.
3. Add 1-3 ml methanolic H_2SO_4 to the tube, vortex, then put it under ultrasonic for 5 minutes.
4. Heat to the desired temperature (60-100°C) in a heat block for 1-2 hours.
5. Remove from the heat block and cool to room temperature.
6. Add 1.0 ml saturated $NaHCO_3$ solution.
7. Add 2.0 ml hexane containing 0.2% BHT solution.
8. Vortex and then put it under ultrasonic for 5 minutes.
9. Centrifuge at 3550 rpm for 5 minutes.
10. Remove the top hexane layer, and fill it through a pipette with a glass fiber plug loaded with sodium sulfate into a GC vial.
11. FAME sample is now ready for GC analysis.

This method of preparing a sample proved to be a critical step for accurate lipid content analysis. This method ensured full conversion of all the oil and FFA contained in the tested biomass, which is affected by the breakage of the algae cell wall, esterification temperature, esterification time, reagent volume, etc. Table 4-1 presents a comparison of analytical results from GC/MS with the same algae sample (*Scenedesmus* obtained under stressed conditions in the outdoor cultivator at the 3rd Avenue facility harvested on November, 18th, 2009) but different sample preparation methods.

Table 4-1. Comparison of Different Esterification Conditions

Reaction Temperature	Reaction Time	Reagent Volume	FAP wt%
90 °C	1 h	1 ml	13.0
90 °C	1 h	2 ml	20.2
90 °C	1 h	3 ml	17.7
90 °C	2 h	2 ml	19.9
90 °C	2 h	3 ml	17.9
100 °C	1 h	1 ml	16.9
100 °C	1 h	2 ml	15.4
100 °C	1 h	3 ml	16.8
100 °C	2 h	2 ml	25.3
100 °C	2 h	3 ml	24.4

Analyzing the results in Table 4-1 shows that by increasing the esterification temperature, esterification time, and the reagent amount added, the fatty acid profile (FAP) increased from 13 wt% to 25 wt% of the dry biomass. Microscope observations of the biomass indicated that more cells were cracked with a higher fatty acid concentration. When the biomass reached 25-wt% FAP, most of the cells were cracked. This indicated that at more severe reaction conditions, the cells can be cracked almost completely and most of lipids inside the cells were converted to methyl ester. Therefore, for the subsequent FAME analysis, reaction conditions of 100°C for 2h with 2 ml of reagent were applied using the acid-catalyzed approach.

During the project, FAME analyses were performed to provide feedback on the lipid level of the biomass samples collected in the lab, at the 3rd Avenue facility and at Redhawk. This daily total lipid content monitor greatly assisted biologists in improving algae cultivation techniques and determining the right harvesting time. The FAME analysis was also used to study the effects of drying methods on oil extraction from the biomass, the effectiveness of various oil extraction methods, and the efficiency of biodiesel synthesis.

4.1.1.2 Fatty Acid Analysis Using Two-Stage Base-Acid Catalyzed FAME

A two-stage base-acid catalyzed FAME method was also developed and evaluated during the project. The newly developed two-stage method was conducted as follows:

1. Tare and weigh 100 mg of each algae sample into a 12 ml glass test tube.
2. Add 50 μl of 40 mg/ml internal standard (C19:0) to each test tube.
3. Add 1.0 ml of 0.5 N sodium methoxide reagent to each vial.

4. Vortex test tubes and ultrasonicate for 5 minutes.
5. Heat at 60°C on the heat block for 1 hour.
6. Remove test tubes from heat block and cool.
7. Add 1.0 ml of hexane to each test tube and vortex.
8. Centrifuge test tubes for 5 minutes.
9. Filter hexane layer (top layer) through a Pasteur pipette with a glass fiber plug loaded with sodium sulfate into a GC vial.
10. To the residue in test tubes, add 1.0 ml of 10% sulphuric acid-methanol reagent, and seal with screw top cap.
11. Heat at 100°C on the heat block for 1 hour.
12. Remove test tubes from heat block and cool.
13. Add 1.0 ml of saturated $NaHCO_3$ and 1 ml of hexane containing 0.2% BHT to each test tube and vortex.
14. Centrifuge test tubes for 5 minutes.
15. Filter hexane layer (top layer) through a Pasteur pipette with a glass fiber plug loaded with sodium sulfate and add into its corresponding GC vial.
16. Transfer GC vials to GC for analysis.

The two-stage method didn't improve the FAME analysis results when compared with the simple acid-catalyzed FAME approach, especially for the algae sample collected at the beginning of the stressing process. When algae grow under normal condition, the cell walls are too thick to break even under two-stage acid/base conditions. The thicker the cell wall, the harsher the condition(s) is needed to break the cell wall. Therefore the acid-catalyzed esterification was applied for all the FAME analysis for the project.

4.1.2 Algae Stress Study – Lab Scale

The technique of stressing algae by nutrient deprivation to increase its lipid and decrease its carbohydrate content is well known. The nutrient deprivation tests were initiated during the strain selection and screening process in late 2008 and early 2009 under the Coal to SNG project. Lipid accumulation experiments conducted during this project focused on cultivating the species *Scenedesmus* and stressing it by nitrate starvation. Through numerous lab experiments performed from October 2009 through March 2010, the process of using nutrient limitation to increase lipid content of *Scenedesmus* was investigated to increase the baseline

lipid level from 10 wt% total fatty acids in the unstressed biomass to a maximum level of 44 wt%. The stress process also greatly reduced chlorophyll content, which was observed by the green pigmentation fading to an increasingly yellow color. This biological method of reducing chlorophyll content in the algae crude oil would greatly help with downstream oil extraction and crude oil upgrading. Stress experiments were ongoing to maximize lipid content, minimize chlorophyll content, and minimize time required for the total stress process. The lipid level was measured by determining the fatty acid content of the biomass at regular intervals using the FAME method with GC/MS analysis. A full description of the oil extraction efforts on stressed biomass is following in section 4.3.2 of this report.

The first step of the stressing experiments was to determine the methods that increased lipid content. This was attempted in an initial experiment utilizing a thin-film culture with a light path of approximately 4 to 5 cm. Seed culture that had been growing in a nitrate-replete culture was used to inoculate two different 10 L thin-film cultures of media in which nitrate was not included. These cultures were allowed to grow for a number of days with all necessary conditions for growth except for nitrate, until stress became apparent due to the change in color of the culture. One of these experiments was set up indoors with artificial fluorescent light applied to both sides of the apparatus, while the second apparatus was set up outdoors, angled to the southern sky and therefore towards the sun. The color of both cultures began to turn yellow after around 10 days, and continued to appear increasingly stressed (less chlorophyll content) for another 10 days thereafter. After this time, both the indoor and outdoor cultures were harvested and the lipid content of the final cultures was analyzed and compared to samples taken at the beginning of the experiment. The results of the experiment for both the indoor and outdoor cultures can be seen in Figure 4-1.

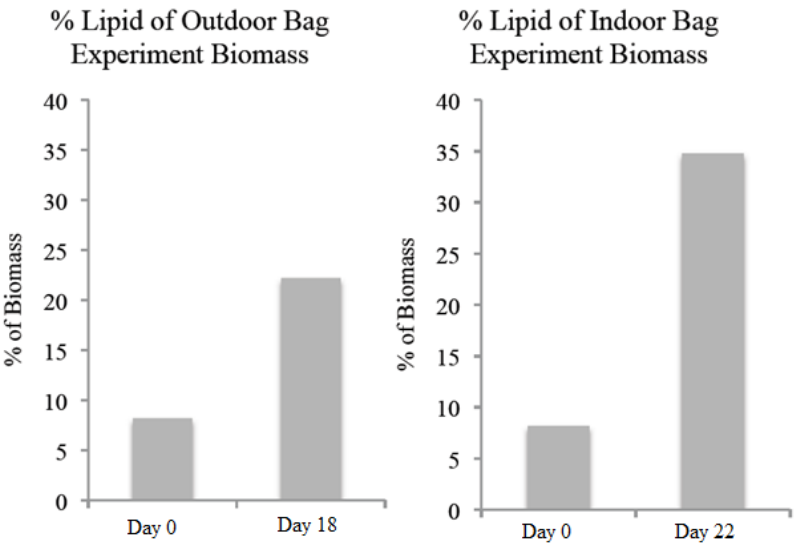

Figure 4-1. Comparison of Initial and Final Lipid Content in Macronutrient Stress Experiment Conducted on Outdoor (Left) and Indoor (Right) 10-L Cultures of Scenedesmus

The results of this first attempt to increase the neutral lipid content of this species were very promising. Both indoor and outdoor cultures turned a yellow color and showed a marked increase in lipid content, although the final lipid content of the outdoor culture at 22.2% was lower than that of the indoor culture at 34.8%.

A second validation of this initial observation of lipid increase was conducted to continue to improve the understanding of the timescale of this lipid accumulation process and the stressing effect by phosphate deprivation. For this second experiment, two indoor thin-film cultures were set up. One of these experimental cultures contained medium depleted of nitrate, while the second culture consisted of medium depleted of phosphate, which has also been shown in the literature to result in lipid accumulation by some species of algae. Both cultures were inoculated using a seed culture that had previously been growing in medium replete with all nutrients. Samples were taken from both experimental cultures as well as the inoculum source at the beginning of the experiment to determine lipid content. Although the first nitrate deprivation experiment resulted in an increase in lipid content, the 20 days required for this increase may not be practical for the application of this method, and therefore a shorter amount of time was examined in this second experiment. Samples were taken from both of the experimental cultures as well as the from the original inoculum culture five days into the experiment, and from both experimental cultures nine days into the experiment. The results of the lipid analysis of this experiment can be found in Figure 4-2.

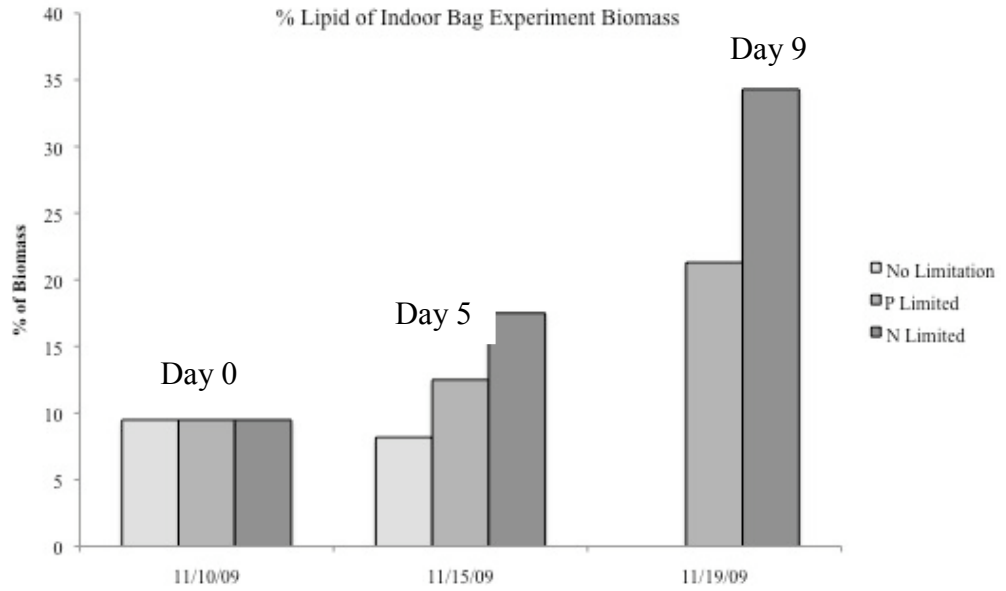

Figure 4-2. Comparison of Lipid Content over Time in Nutrient Stress Experiment Conducted in an Indoor 10-L Culture of Scenedesmus

After 5 days of this experiment, the lipid content of both nitrate- and phosphate-limited cultures had increased in relation to the nutrient-replete inoculum culture. By day nine of the experiment the nitrate-limited bag had turned yellow as shown in Figure 4-3, and the lipid content had increased to 34.3 wt% of the biomass.

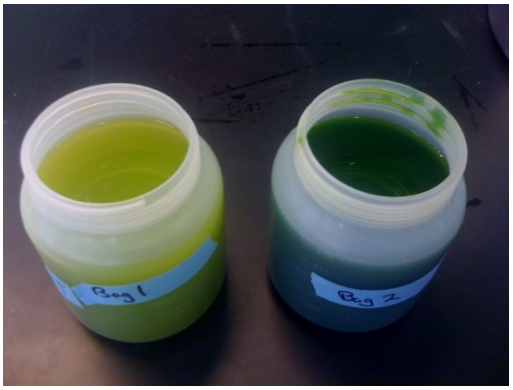

Figure 4-3. Picture of the Color Difference between the Nitrate-Stressed Sample (Left) and the Phosphate-Stressed Sample (Right)

The lipid accumulation occurred concurrently with loss of chlorophyll, causing the green culture color to become increasingly yellow. All cultures in this series of experiments had lost most of their chlorophyll content by day six - seven. Under normal growing conditions, chlorophyll can make up nearly 2% of the biomass; under nitrogen-limited conditions, this level can be reduced to approximately 0.03% of the biomass.

Although the phosphate-depleted culture did not change color or accumulate lipids to a level as high as observed in the nitrate-depleted culture, the lipid content did increase to 21.3% by day nine of the experiment. From this experiment it was clear that out of the two major nutrients

required for algae growth, the depletion of nitrate in combination with the continued presence of CO_2 and plenty of light, was the best method for increasing the lipid content of the algae biomass.

In order to begin to apply the methods described in these two experiments to larger cultures, a similar nutrient deprivation experiment was conducted in the large 3rd Avenue cultivator. Additionally, a third experiment was conducted on a partially dewatered culture. An algae culture of 4000 L was allowed to settle overnight. The settled biomass was then removed from the bottom of the tank and two 10 L subsamples were each placed in thin-film culturing devices as used in previous stress experiments. One of these cultures was placed under 24 hour fluorescent light in the lab, while the other was placed outdoors under natural sunlight. The final density of the settled culture was approximately 30 grams per liter (g/L) by ash-free dry weight. This density is concentrated by a factor of 20 as compared to the culture density prior to overnight settling. The aim of this experiment was to determine if a culture can be partially dewatered and transferred to a shorter light path (less depth, or a thin-film system) with little or no nitrate remaining in the medium, in order to induce the same stressing response observed in previous experiments, but in more biomass and with less volume. Both 10 L cultures were sampled periodically over the course of 15 days and were analyzed for lipid content. The results of this experiment can be found in Figure 4-4.

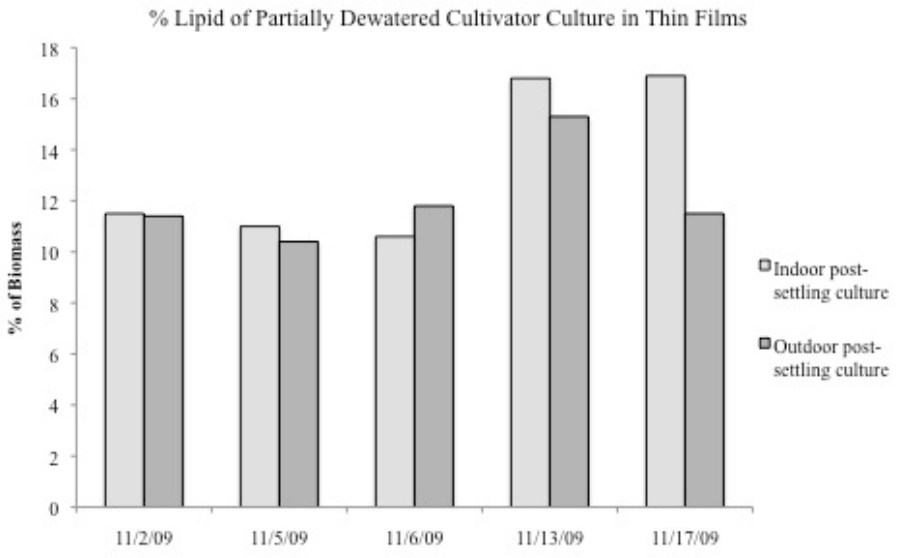

Figure 4-4. Comparison of Lipid Content over Time in Nutrient-Stressed Experiments Conducted on Partially Dewatered (Settled) Indoor and Outdoor 10-L Cultures of Scenedesmus

A slight increase in lipid content was seen in this very concentrated culture over the 15 day test period. This increase was far less than seen in previous stress experiments. It is likely that this 30 g/L culture, after settling in the 4-5 cm light path experimental apparatus, was still too dense to elicit the stress response in this species, possibly because not enough light was available to the culture as a whole. This may indicate that either a shorter light path apparatus or a more dilute culture may be necessary in a future stressing system.

The results of these experiments confirm the efficiency of this lipid accumulation method, and this process can be applied consistently to achieve predictable and repeatable lipid levels within a set period. This experimentation provided an understanding of the algae strain and its growth conditions, which resulted in a management tool that could allow for the production of stressed algae which contains extractable oil, in the large scale system.

4.1.3 Algae Stress Study – Large Scale

In order to apply the oil accumulation methods established in lab experiments, as well as test operational scenarios for increasing oil production from Redhawk cultures, an additional nutrient deprivation experiment was conducted in the 3rd Avenue 6M cultivator, where algae cultivation was previously initiated under the Coal to SNG project on August 17, 2009. The cultivation in this system was transitioned into an oil accumulation study on September 29, 2009. Figure 4-5 shows the continued growth curve for this culture and the post September 29 period related to this project.

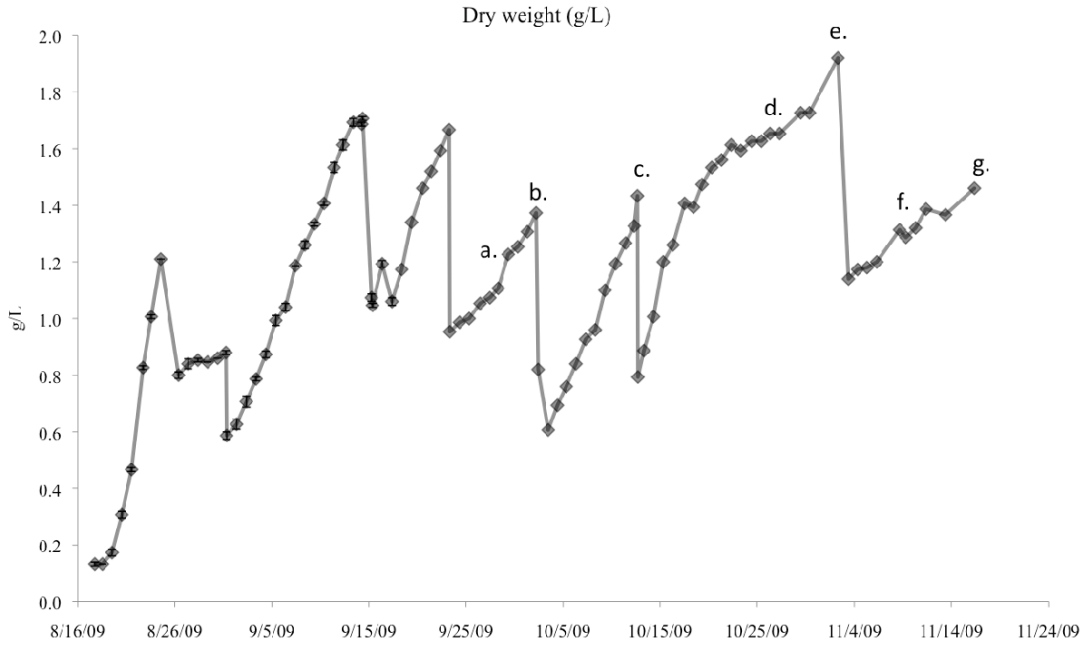

Figure 4-5. Scenedesmus Culture Density as Measured by Dry Weight (Grams of Dry Biomass per Liter of Culture)*

* a. First measurement related to the IES project. b. 8000 L harvest and refreshment with 4000 L fresh medium and 4000L recycled permeate. c. 4000 L harvest and the addition of nitrate deplete medium. d. removal of 1800L for use as Redhawk inoculum. e. 4000 L harvest and replacement of medium containing no nutrients. f. addition of all medium components required for growth except nitrate. g. final harvest of 8000 L after confirmation of lipid content of 25%.

The first two harvests during this period were conducted under normal conditions, while subsequent harvests were part of a nutrient deprivation experiment. An 8000 L harvest took place on October 3, 2009, and after this time the liquid medium that was returned consisted of 4000 L of fresh medium and 4000 L of recycled permeate. The addition of the recycled medium showed no negative effect on growth rate as compared to previous growth curves using fresh medium alone and also served as an initial attempt to begin to deplete nutrient levels in the medium. A second harvest was conducted on October 12, 2009.

After the October 12 harvest, a long-term nitrate deprivation experiment was initiated with the addition of nitrate-depleted medium after the harvest. This experiment served as a demonstration of techniques developed in lab experiments but on a larger scale and under natural sunlight conditions. Some nitrate still remained in the culture as well as in the algae cells even after this harvest and after refreshing with nitrate-depleted medium lacking. As a result the culture was still able to grow rapidly from October 10 to October 17, 2009. After this point, no further nitrate was measured in the medium, and the growth rate began to decrease.

On October 29, 2009, when 1800 L of culture was removed to inoculate the first cultivator at Redhawk without refreshing the volume, the growth rate increased again in the following days. This likely indicated that although there was no measurable nitrate left in the medium, individual cells might have still had internal stores of nitrate with which to grow. As a result of the decrease in volume in the cultivator, which increased the amount of light available, the culture was able to grow for two more days. This phenomenon indicated that another harvest was required to deplete nitrate even further, as well as to decrease the culture density to provide plenty of light to the culture under nitrate deprivation. As a result, another harvest was conducted on November 3, 2009. After the removal of 4000 L of culture, 4000 L of medium depleted of all nutrients was added. The resulting culture density was in the range shown to provide plenty of light for growth, and the lack of nutrients began to result in the observations of stress within the culture, namely enlargement of individual cells and a color change to yellow (reduction in chlorophyll).

During the operational period of this cultivator and the nitrate deprivation experiment, laboratory procedures were being developed in-house in order to extract, quantify, and analyze lipid content of the biomass being produced. The resulting analyses over the course of the nitrate deprivation experiment within the cultivator can be found in Figure 4-6.

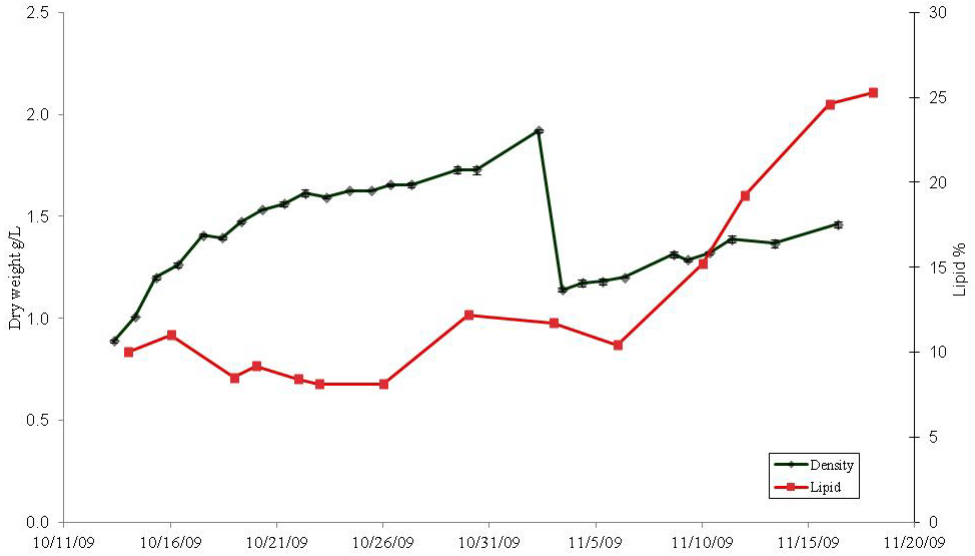

Figure 4-6. Lipid Content Estimates of 3rd Avenue 6M Biomass *

*All lipid analysis methods shown in this chart were under development at this time and as a result some data shown herein was attained through different methods. Therefore the values shown are only estimates.

Although Figure 4-6 employed various methods of analysis that were still under development, an increasing lipid content trend can be seen over the course of the culturing period. The final sample indicated the biomass to be 25% lipid after nutrient stressing. This observation, in addition to the yellowing color of the culture, led to the decision to harvest the entire culture, which provided about 10 kilogram (kg) of biomass at increased lipid content for lipid extraction work. The details of the oil extraction work can be found in section 4.3.2 later in this report. This final harvest was conducted on November 17, 2009, after 93 days of continuous culture. No culture-related factor other than the desire to recover the high lipid biomass was involved in the decision to end this operational period of the cultivator. A summary of productivity and harvests for all growth periods during this stressing demonstration can be found in Table 4-2. Although mean productivities in some cases were below the goal, many experimental manipulations took place to examine optimal operational culture densities as well as nutrient deprivation. When the culture was replete with nutrients and within the optimal culture density range, productivities reached and in some cases exceeded the targeted growth rate.

Table 4-2. Summary of Scenedesmus Productivity and Harvest Data from 6M Radius Cultivator at 3rd Avenue R&D Facility

Date	Aerial Productivity ($g/m^2/day$)				Harvest		
	Mean	SE	Max	Min	Volume (L)	Density (g/l)	Biomass (g)
9/24/09 - 10/3/09	4.96	1.12	12.27	1.41	8000	1.37	10960
10/4/09 - 10/12/09	11.46	2.56	33.68	7.13	4000	1.43	5720
10/13/09 - 10/17/09	13.68	2.30	20.28	6.32	--	--	--
10/18/09 - 11/3/09*	2.75	0.95	9.55	-2.10	4000	1.92	7680
11/4/09 -11/17/09*	1.79	0.90	5.36	-3.49	8000	1.46	11680

*under stressed conditions

The operation of this culture for over 90 days marked a significant step in this project, validating both the robustness of the cultivator and of the algae species currently used for this project. In addition, for the first time, in an *in situ* experiment on this project, a large outdoor culture was successfully manipulated in order to increase lipid content. For the growth period from November 4 to November 17, 2009, when the stressing was occurring, although the algae growth rate was significantly reduced to less than 2 $g/m^2/day$, oil production for this period was calculated as 0.45 $g/m^2/day$ or 661 gallon/acre/year. The next step was to apply this technique a number of times in the demonstration site at Redhawk.

4.1.4 SETTLING EXPERIMENTS

A series of observational laboratory experiments examined the feasibility of naturally settling *Scenedesmus* as a partial dewatering strategy. Previously examined species were found not to settle, even when not agitated. Results showed this species rapidly settles when left unmixed for a period of time. There was significant variability in the settling rate and final settled culture density. This variability could be result of many factors such as the growth phase, culture conditions, temperature, and pH; however, the key result was that some portion of the population in a given culture consistently settled to the bottom of the vessel in a matter of hours when left un-agitated.

Representative of this series of settling experiments, a 1.5 L of culture, at a density of 1.5 g/L (similar to the harvest density from an outdoor cultivation system), was placed in a covered 60° angled bottom funnel to simulate settling dynamics of a 60° cone bottom settling tank. The culture was left un-agitated for five hours to simulate a reasonable amount of settling time that could be accommodated after a harvest (night hours at Redhawk). The resulting culture can be seen in Figure 4-7.

Figure 4-7. Settled Scenedesmus Culture after 5 hours in a Conical Bottom Vessel

Although the culture on top is not completely clear, most of the biomass settled out after five hours. The settled biomass was found to be 47.7 g/L and the non-settled portion was 0.04 g/L. This five hour settling period, with no energy expenditure for dewatering, resulted in a nearly 32-fold increased concentration of the biomass.

Another observation of this settling was pertained to leaving a large amount of 3rd Avenue-harvested algae culture in typical dewatering tank overnight without stirring. This resulted in a settled culture density of approximately 30 g/L. The culture density before the settling period was 1.43 g/L; thus the concentration of the biomass increased by around 20 times without any energy input. As with any biological system, the culture dynamics affecting this settling vary; therefore, settling rates and final densities are likely to vary as well. As culture settling is tested on large-scale cultures, the dynamics and variability of this process will be better understood and utilized.

4.1.5 Cost Reduction of Media Components

4.1.5.1 Alternative Nitrogen and Phosphate Sources

At an industrial scale, the cost of nutrients - specifically the macronutrients of nitrogen (such as sodium nitrate) and phosphate (dipotassium phosphate) - represents a prohibitive cost in algae culturing or farming. To reduce the potential expense of nitrate and phosphate at a large scale, alternative forms of nitrogen and phosphate were investigated, and work was performed to identify bulk sources of these macronutrients. The fertilizer-based nutrients of urea and monopotassium phosphate (MKP) were identified as suitable replacements for these macronutrients, and a local supplier was located to provide these nutrients in bulk at greatly reduced cost.

These nutrient sources were tested initially in bottle cultures. Cultures previously growing in standard media were inoculated into bottles containing the new substituted medium. Culture growth and health were monitored over several cycles of growth and transfers into fresh urea/MKP media. No adverse effects of the urea/MKP medium were detected. The cultures remained healthy and appeared to grow normally. Several cultures of *Scenedesmus* were produced in the laboratory on this urea/MKP medium to further assess its effects on culture growth and health, and to compare this growth to cultures grown on the standard medium containing nitrate and phosphate. This included 2 L cultures grown in glass bottles and 10 L thin-film cultures. All cultures grown in the urea/MKP medium were healthy and grew normally as compared to those growing in the standard medium. Results have confirmed that urea and MKP are safe alternatives to sodium nitrate and dipotassium phosphate in the freshwater medium.

4.1.5.2 Reduction of Iron Solution in Redhawk Medium

Iron is another major components of the freshwater medium. The iron solution is comprised of ferrous sulfate and ethylenediaminetetraacetic acid (EDTA), a chelating complex of salts that help to solubilize the iron. After replacement of the most expensive media components of sodium nitrate and dipotassium phosphate with the much cheaper alternatives of urea and MKP, the iron solution constituents represented the remaining most expensive costs for media preparation and a significant opportunity for cost reduction at industrial scale. Because iron was measured at low levels in the Redhawk source water in previous analyses, it was proposed that the iron solution could be greatly reduced in the Redhawk culture medium.

To test this proposition, media makeup water was collected from the Redhawk site. This water

was used to prepare three sets of media: the first with standard amount of iron solution, the second with one-half the amount of iron solution, and a third with no iron solution added. The media were inoculated with *Scenedesmus* culture and allowed to grow for 14 days (Run 1). The run was then repeated to allow for consumption of residual nutrients that may have been present in the original culture used to inoculate the test cultures (Run 2). The cultures resulting from Run 1 were used to inoculate the cultures of the same media formulation in Run 2. The results of these runs are in Figure 4-8.

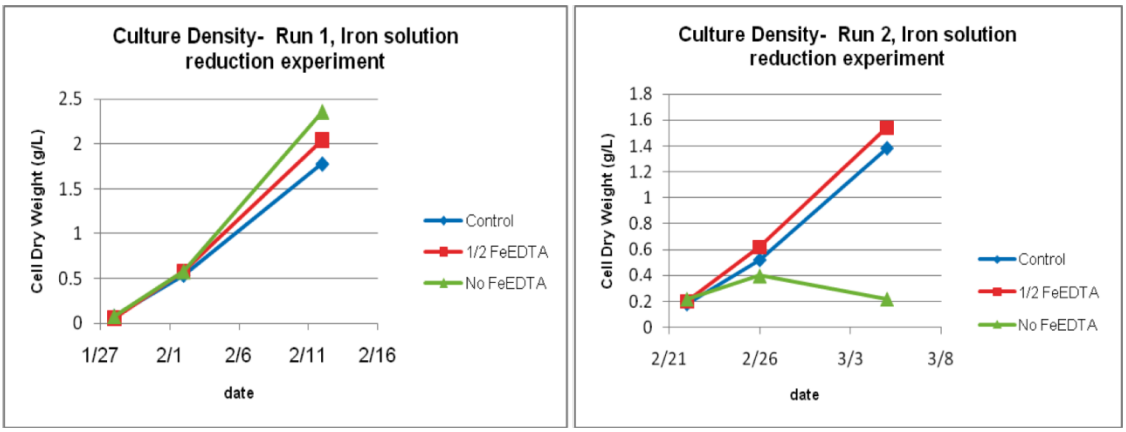

Figure 4-8. Scenedesmus Culture Densities in Run 1 and Run 2 of the Iron Solution Reduction Experiment Conducted in 1-L Volumes*

* Run 2 followed run 1 and repeated the experimental conditions of Run 1. Run 1 cultures were used to inoculate Run 2 cultures.

Because Run 2 was a repeat of Run 1 and used the same media formulations, the differing results of Runs 1 and 2 seemed to indicate that excess iron solution was present in Run 1 and in Redhawk source water generally. The death of the culture lacking iron solution in Run 2 demonstrated that excess iron solution was present in the seed culture (previously grown in standard freshwater medium) used to inoculate the test cultures. This residual iron source was consumed through Run 1 and Run 2, which sustained normal growth in Run 1 but led to eventual culture death in Run 2, where the culture seemingly became iron depleted. This also indicated that the iron solution cannot be eliminated from the medium recipe, but the results did suggest the quantity of iron solution could likely be reduced to one-half the standard amount. The cultures containing one-half the standard amount of iron solution grew slightly better than control in both Run 1 and Run 2. A third run was initiated to verify these results and to determine if the amount could be further reduced. In this run, ¾, ½, and ¼ the standard amount of iron solution were tested. The initial results are shown in Figure 4-9.

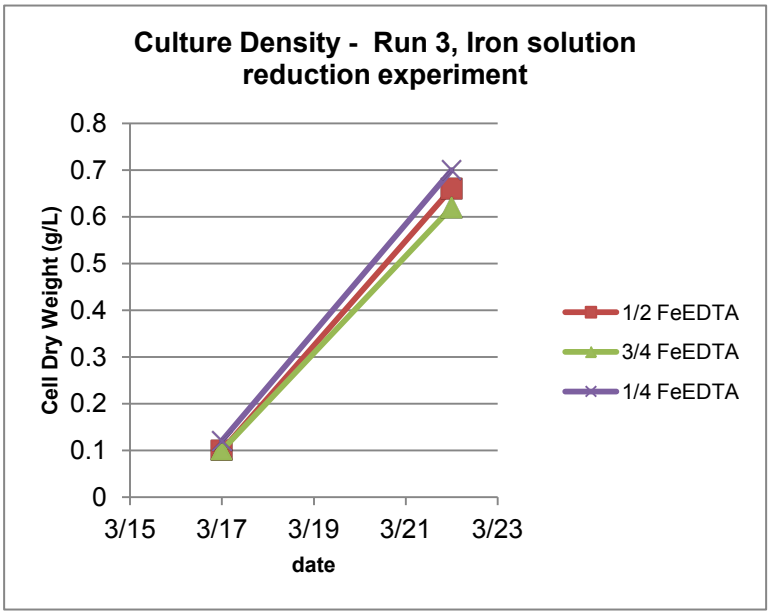

Figure 4-9. Scenedesmus Culture Densities in Run 3 of Iron Solution Reduction Experiment Conducted in 1 L Volumes

The data suggested that a one-half reduction of iron solution is safe and also demonstrated promise of possible further reduction to one-fourth the standard quantity as growth in all three test cultures was nearly equal. These results were preliminary and require further verification. Repetition of this run along with further experiments would be needed to clarify the exact amount of possible iron solution reduction. From these results it could be concluded that the iron solution in the Redhawk medium formulation could be reduced to one-half the standard amount.

4.1.6 Algae Growth in Cholla Aquifer Water

Initial tests were performed with Cholla aquifer water (pH 7.4, salinity 6.2 parts per thousand), which was proposed as a water source for culture growth at this site. These tests were designed to determine whether the Cholla aquifer water, at approximately 20% the salinity of seawater, would lead to reduced growth or death of *Scenedesmus*, a freshwater algae strain. This work was also performed to acclimate this freshwater algae strain to higher salinity and avoid the need for on-site acclimation at Cholla.

To test the culture's ability to acclimate to the aquifer water, a 2 L culture of *Scenedesmus* was inoculated using freshwater medium prepared in undiluted Cholla aquifer water. For comparison, a second culture was inoculated in the same manner with freshwater medium

made in distilled water. After several days of observation, the cultures did not show any noticeable differences in growth as demonstrated by similar culture color and densities. After the culture medium made with Cholla aquifer water reached significant density, it was reinoculated into fresh medium that was also prepared in Cholla aquifer water. This accomplished two goals: to continue to monitor effects of the Cholla water and to provide a source of *Scenedesmus* culture acclimated for growth in the Cholla water source. As of March 31, 2010 (69 days after first the inoculation into the Cholla aquifer water), the culture was healthy and continued to demonstrate normal growth. This initial test indicated the species was not adversely affected by the components of Cholla aquifer water.

Figure 4-10. Scenedesmus Culture in 5X Concentrated Cholla Aquifer Water

To simulate evaporation and subsequent accumulation of aquifer salts in the culture and culture medium expected at the Cholla site, Cholla aquifer water salts were concentrated to 5X the original levels. This represents an extreme case of evaporation and salt accumulation that is not likely to occur under expected culture conditions and was meant to gauge the culture's tolerance to these conditions. The salt concentration was reduced by gently boiling away the volume of an aquifer water sample to one-fifth of the starting volume. Freshwater medium was made using the concentrated 5X Cholla water and inoculated with a lab-maintained culture of *Scenedesmus*. Initial observations revealed an abnormal lighter green color to the culture and an overall cloudy appearance as shown in Figure 4-10, which was expected due to the high salt content. However, despite the culture's abnormal appearance, the culture did not lose biomass, and although the growth rate was severely depressed, the culture did eventually demonstrate an increase in density as shown in Figure 4-11.

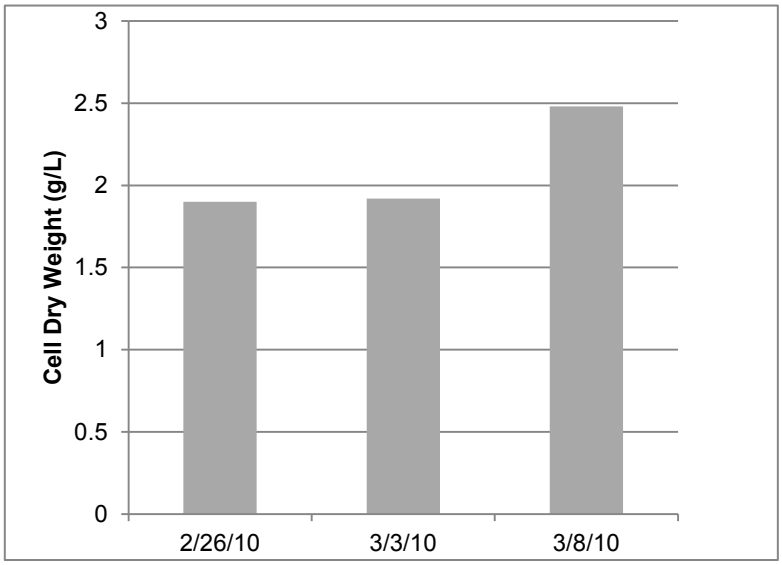

Figure 4-11. Growth of Scenedesmus in 5X Concentrated Cholla Aquifer Water

The salts may also have enhanced the algae lipid accumulation. A sample of the culture analyzed on day 20 of culture growth demonstrated a fatty acid content of 21.9% (baseline levels are approximately 7 to 8%). Other than the additional salts provided by the water source, the culture was grown with standard medium containing all nutrients. After 25 days, this culture was reinoculated into fresh medium made with 5X Cholla water. As of March 31, 2010 (38 days after original inoculation into 5X Cholla water), the culture still showed signs of depressed growth but did not show any signs of culture death. These initial results indicated that *Scenedesmus* tolerates at least some salt accumulation in Cholla aquifer water; if evaporation is reasonably controlled, the health and growth of *Scenedesmus* would not likely be negatively affected. However, to fully assess the effects of salt accumulation on this species, further testing should be conducted.

Scenedesmus was successfully acclimated to Cholla aquifer water and demonstrated tolerance to accumulation of salts in simulated severe evaporation. These tests indicated that Cholla aquifer water is suitable as a water source for this strain, provided that extended exposure to highly concentrated Cholla water due to evaporation is avoided. These experiments represent preliminary testing with Cholla water with cultures of *Scenedesmus*. Future experiments should continue to verify results and determine the detailed and long-term effects of the salts and other components of Cholla aquifer water on the growth, health, biomass composition, and quality of resulting products of *Scenedesmus*.

4.1.7 SUMMARY ON ALGAE LAB ACTIVITIES

During this project, different methods for analyzing fatty acid content of algae biomass utilizing GC/MS were examined, developed, and optimized. The procedure that arose from this work involved an esterification reaction that effectively cracked cells to accurately and consistently measure the fatty acid profile of tested biomass. Freshwater algae strain - *Scenedesmus* was selected for the study. Extensive study was conducted on algae stressing by manipulating the nitrate level in cultures to increase extractable non-polar lipid content. Indoor experimental cultures under nitrogen deprivation were found to accumulate lipids from less than 10 wt% to 40+ wt%. The lipid level of outdoor stressed-cultivator samples increased less than 10 wt% to 25+ wt%. When under stressed, it took anywhere from 7 to 22 days for the culture to greatly increase neutral lipid content. The cultivation methods developed in this section led to the larger scale demonstration in 6M radius cultivators at 3rd Avenue and at Redhawk.

The lipid accumulation process coincides with loss of chlorophyll, causing the green culture color to become increasingly yellow. All cultures in this series of experiments had lost most of their chlorophyll content by day six - seven. The high level of chlorophyll that can be extracted with neutral lipids has been known to be problematic in biofuels produced from algae oil. Under normal growing conditions, chlorophyll can make up nearly 2% of the biomass; under nitrogen-limited conditions, this level can be reduced to approximately 0.03% of the biomass. This technique allowed considerable progress in the area of oil extraction (section 4.3.2) utilizing biomass produced during this project.

Another line of laboratory research investigated during this project involved the utilization of nutrient sources in the algae culture medium, which are readily available at large scale in Arizona, and which are less expensive than the lab grade chemicals used for formulating the culture medium at a small scale. This experimentation first consisted of contacting local fertilizer vendors in the area and determining the most inexpensive, yet appropriate, sources of nitrogen and phosphorous that were available at the scale required to meet the needs of the intended culture size at Cholla. These nutrient source candidates were determined to be urea and monopotassium phosphate. Although monopotassium phosphate is a standard source of phosphorous for both algae and terrestrial agriculture, many trace elements and impurities in this bulk fertilizer that could reduce algae growth rate could be present, also leading to the necessity to carefully examine the effects of this fertilizer on algae growth in the laboratory before introducing it to large outdoor algae cultures. Both of the nutrient sources were incorporated into the liquid culture medium in order to compare the growth and health of a

culture using these nutrient sources to that of a culture using the standard sources nitrogen and phosphorous. The results of these tests indicated that both of these nutrient sources were able to sustain the growth of *Scenedesmus* without reducing growth rate or affecting lipid content. Subsequent experimentation also found that when the iron level in the culture medium was reduced to half that of the standard culture medium, growth rates were also unaffected. The combination of the many experiments that led to the changes in these three nutrient sources has a major effect on the cost of nutrients required for the large-scale cultures of algae at both Redhawk and Cholla. If the Redhawk system had been scaled up as originally designed, the cost of nutrients needed each day to support the target growth rate of 25 g/m^2/day of algae would have been approximately $12,000 using the sources of nutrients generally used in a laboratory environment. By integrating less expensive nutrient sources available in bulk, the daily cost of nutrients at Redhawk would have been $58.

Experimentation regarding the growth of the freshwater strain of algae *Scenedesmus* on the Cholla aquifer water - which has an elevated salinity level above that of freshwater (20% of the salinity of sea water) and 5X concentrated Cholla aquifer water, was also conducted during this project. *Scenedesmus* demonstrated a reasonable growth rate and health during these tests. The finding that this freshwater strain could grow well in the saline aquifer water was significant for the project. If the current algae species had not been able to grow in the unique Cholla water source, a search would have been conducted to find a strain that could successfully grow on this source. Furthermore, the study of using 5X more concentrated Cholla water indicates *Scenedesmus* could withstand the change of conditions and survive for some time until conditions could be returned to those of normal Cholla aquifer water.

4.2 Algae Cultivation at Redhawk

The APS Redhawk 1000 MW gas-fired plant is located 55 miles west of Phoenix and adjacent to the 4000 MW Palo Verde Nuclear Generating Station. A 25-acre algae testing site was built at APS Redhawk. The site has an independent 12.5 kV feeder, about half acre concrete thermal pond, two green houses (30 ft x 150 ft), and utility water. A 300 ft stack slip stream was installed to introduce the flue gas into the cultivation area. The site environmental, engineering, and biological parameters for the cultivators were monitored remotely. Alarms were sent via e-mail and phone to the appropriate personnel in the event of a parameter perturbation. Refer to Figure 4-12.

Figure 4-12. Redhawk Algae Testing Site in Summer 2009

4.2.1 REDHAWK ALGAE CULTIVATION SYSTEMS

4.2.1.1 Water Source and Treatment

The water filtration system for the Redhawk project includes several types of mechanical filtration technologies combined with chemical (Sodium Hypochlorite) and UV treatments. The system produces a clean water supply that is used for the cultivator pools as well as the cultivators themselves.

Cooling Pond

Treated effluent water from Phoenix is used as cooling water for the Palo Verde Nuclear Power Station, and this water is recycled to the cooling pond on the north end of the Redhawk facility. This water has received additional treatment at Palo Verde. A 150 gpm submersible pump is suspended from the main platform of the pump station on the south end of the pond. Water is then moved through a 3 inch Polyvinyl Chloride (PVC) pipeline to the first set of media filters.

Media Filters

There are two sets of media filters, primary and secondary. The purpose of these filters is to remove coarse materials from the incoming pond water. The line coming directly from the pond runs to three primary media filters that are plumbed in series and filter to approximately 20 μm. There is a 20 ppm concentration of chlorine injected just prior to the system for initial

disinfection. The two secondary media filters filter to approximately 10 μm in series. Flow is approximately 150 gpm exiting the second-stage media filters. Filtered water is then passed to the Filtered Water Storage Tank (T-01). Back flushing of the units occurs when there is a pressure differential between the intake and the discharge of 15 psi.

T-01 Filtered Water Storage Tank

T-01 has a 5000 gal capacity. This water is filtered to 10 μm and may have residual chlorine coming from the secondary media filters. Chlorine concentrations should be under 3 ppm at this point. There is a recirculating sand filter located adjacent to T-01 that continually removes any residual debris as well as an additional chlorine (sodium hypochlorite) injection system to increase chlorine levels if the liquid volume remains in storage for a period of time. There are high and low water sensors that self regulate the volume in the tank. Water from this tank can be directed to the cultivator pools, used as media filter back-flush water, or sent to the filtration skid for further filtration.

Filtration Skid

The components on the filtration skid are used as the final phase of filtration for any water that enters the cultivators. Water from T-01 is directed to the skid from pump T-03 at a rate of 8 gpm. There is an option for chlorine injection prior to going into the filtration skid. Refer to Figure 4-13.

Figure 4-13. Water Treatment Filtration Skid with Control Panels

The filtration skid consists of two sets of cartridge filters (2 filters-CF-A), which have a variable filtration capacity. Through the testing, 3.5 μm filters were installed. A UV unit is located between the first and second set of cartridge filters. This is the final disinfection process before water enters the cultivators. UV sterilizers kill organisms on contact, assuming proper water flow rate and UV bulb intensity. Acceptable flow for this unit is less than 10 gpm. The secondary cartridge filters also contain two sets of cartridge filters. They have the capability to filter to 0.03 μm (ultra-sterilization) if needed. This is the final stage of filtration before water enters the cultivators. Filtered water from here goes to media tanks T-02-A and T-02-B.

T-02-A and B-Media Tanks

Water from these tanks can be mixed with media chemicals and directed to the cultivators. These tanks can be filled and drained as needed based on harvest/refill schedules for the cultivators. Chlorine levels are monitored prior to directing water to cultivators. It is imperative

that hypochlorite levels are below two ppm before water enters the cultivators. If chlorine levels are too high, the tank water is circulated until all chlorine is degassed. Two carbon de-chlorination filters were installed in the media tanks to remove residual chlorine to a level below two ppm. These tanks require approximately 16 hours to fill based on an 8 gpm flow rate out of the filtration skid.

Water Source

Two main water sources were needed for the project at the Redhawk test site:

- Thermal pond water - water used in the cultivator pools on site that comes directly from T-01, having been run through the media filters and filtered to 10 μm. The flow rate out of T-01 is 100 gpm.
- Cultivator water - water used for the cultivators that comes from the media tanks T-02-A and T-02-B, having been run through the filtration skid and filtered to 3 μm. The flow rate out of T-02-A and T-02-B is 100 gpm.

Please refer to Appendix D for the Redhawk water treatment process Piping and Instrumentation Diagram (P&ID).

4.2.1.2 Gas Distribution

The algae testing facility at Redhawk was designed to use multiple sources of CO_2:

- Raw Flue Gas (RFG) containing 3-4% CO_2 from stack #1; the remaining RFG composition from the stack was: 68-69% nitrogen, 16% oxygen and 12% moisture. The high oxygen content came from the excess combustion air of the plant.
- Concentrated Flue Gas (CFG) containing 20-35% CO_2 produced by a Membrane Technology Research, Menlo Park, California (MTR) CO_2 membrane system.
- Simulated Flue Gas (SFG) containing 3-4% CO_2 made by blending compressed air with 100% pure CO_2.
- Pure 100% CO_2 delivered to the site.
- Enriched Flue Gas (EFG) containing more than 4% CO_2 made by blending RFG with 100% CO_2.

The test system(s) were designed to accommodate the gas streams presented above.

Raw Flue Gas (RFG)

RFG is extracted from the top of stack #1. The extraction point is located about 12 ft below the top of the stack. The gas is extracted by a Cincinnati blower (Model HP-12G, 30 hp with a 28-inch-diameter wheel). This blower generates a discharge pressure of about 12 inches Water Column (W.C.) at 2000 cubic feet per minute (cfm). A 12 inch steel duct extends from the extraction point on the stack, down along the side of the stack and then into the suction side of the Cincinnati blower. The duct then extends from the discharge of the blower and runs due north about 300 ft to the Redhawk algae testing facility. The duct has several elevation changes to allow for vehicle access under the duct. There are several sliding dampers installed in the duct system to allow the operator to control the flue gas flow rate or stop the flow. The blower does not have a variable speed motor, and so the damper valves provide a means to control the flue gas flow rate. There are also several condensate drain valves (ball valves) installed at the low points of the duct. These valves provide a way to drain the accumulated water that collects from moisture in the flue gas that condenses in the duct. Before starting the blower the drain valves should be opened and all condensate drained from the duct system. The drain valves should then be closed before starting the blower. Refer to Figure 4-14 for flue gas source.

Figure 4-14. Stack from which Flue Gas Is Directed towards MTR CO_2 Membrane Skid

The Flue Gas Blower (FGB) delivers 120,000 cubic feet per hour (cfh) to the algae testing facility. The facility operating at full capacity with a potential for 17 cultivators would require an estimated 12,000 cfh. Moreover, the flue gas compressor is sized for a maximum of 7500 cfh. Therefore the blower flow must be controlled to provide an adequate flow to the compressor inlet at a slightly (2-4 inch W.C.) positive pressure. The majority of the flow from the blower is discharged upward to the atmosphere just as it is from the outlet of the stack. Sliding damper valves V-211 and V-212 are used to adjust and control the flow of RFG.

A portion of the RFG stream is directed to the inlet of the gas compressor. This compressor is a Curtis Model Z-30 Oil Free Screw Compressor. This compressor was selected because it is oil free, thereby eliminating a potential contaminant (lubricating oil), which could compromise the algae growth. The compressor screw is stainless steel and is lubricated using water. The Reverse Osmosis (RO) system must be operating prior to starting the compressor. This is because the RO system generates the clean water that is required to fill the water receiver tank in the compressor enclosure.

The compressor is a 30 hp design and it will boost the inlet RFG from a few inches of W.C. to 100 psig maximum. The compressor capacity is 125 cfm. Normally the compressor is programmed (via the integral display on the compressor housing) to run until the outlet pressure reaches 100 psig. At this setpoint the compressor shuts off until the discharge pressure reaches 80 psig. At 80 psig the compressor re-starts and runs until the discharge pressure reaches 100 psig. This on-off cycle continues while the compressor is powered. The compressor requires 480 Volt Alternating Current (VAC), 60 amp, 3-phase supply (refer to Figure 4-15).

Figure 4-15. Oil Free Curtis Compressor

The RFG that is directed to the Curtis compressor is moist due to water vapor produced in the combustion process. The RFG flows through two inlet filters that are intended to remove particulates and some moisture, specifically any water droplets. The filters are oversized for the flow rate, but this allows more residence time and more separation of water from the gas stream. Since the pressure drop across the filters is low (1-2 in W.C.), it will not choke the RFG flow into the compressor. The first filter, F-201, is a particulate filter and the second, F-202, is a coalescing filter (Wilkerson M36). This sequence was recommended as "preferred" by the Wilkerson Tech Support Group. The filters are rated 1.0 micron and 150 psig, and include an auto-drain option. The auto-drain feature automatically opens a vent valve on the bottom of the filter to allow condensate to drain from the filter. The condensate flows into a sump pump, which pumps the water into a holding tank for re-use or disposal. The filter housings have an integral differential pressure indicator on the top to indicate the pressure drop through the filter. Normally the filter operates in the GREEN zone, which is a low-pressure drop. As the filter gets

loaded the pressure drop will increase. When the indicator reaches the RED zone then the filter should be inspected and cleaned or replaced. Generally, the RFG is clean and the filters should require very little maintenance.

The filtered RFG enters the gas compressor through a customized inlet connection. Because this compressor is normally used as an air compressor it was supplied with a conventional inlet air filter. This filter was removed and replaced with a flexible reinforced rubber connector. This connector provides vibration isolation between the compressor and the rigid pipe RFG inlet.

When the RFG discharges from the compressor it is warmer than at the inlet and has some moisture from the water-lubricated screw compressor. The RFG flows into another set of filters, F-203 (particulate, Wilkerson F36) and then into F-204, (coalescing, Wilkerson M36). These filters also have auto-drain systems. Valves LCV-203 and LCV-204 automatically drain any condensate from the filters. The condensate is drained into a sump pump and is pumped to the holding tank. More moisture may be extracted from these filters as the RFG is under pressure at this point and moisture will condense more readily. Also, as the ambient temperature gets cooler (in the winter), more moisture may be captured.

The compressed RFG is temporarily stored in a buffer storage tank, T-210, which is an ASME 120 gal carbon steel tank rated at 200 psig Maximum Allowable Working Pressure (MAWP). The tank has a manual drain valve, BV-205, on the bottom of the tank, and the outlet from this valve is connected to the sump pump. This drain valve should be opened daily to remove any moisture from the buffer tank. The buffer tank is intended to allow some accumulation or temporary storage of compressed RFG so that the compressor can cycle between 80 and 100 psig at a reasonable cycle rate. There is an ASME Safety Relief Valve (SRV) installed on the top of the tank. It is set at 200 psig and is sized to exceed the relief capacity required by the ASME “fire condition” and also to exceed the maximum output of the compressor. The storage tank has a pressure gauge, PI-210, that indicates the pressure in the tank. There are also isolation valves on the inlet (BV-213) and outlet (BV-215) of the tank and a sampling valve, BV-214, installed on the side of the tank.

The RFG flow exits from the tank T-201 through ball valve BV-215 and then flows through a flow indicator FI-201 (King Instruments, tube and float flow indicator). This flow indicator is used to measure the amount of RFG delivered to the cultivators or to the CO_2 membrane skid (purchased from MTR).

Downstream of FI-201, the flue gas piping splits into two flow legs. One leg, a 2 inch line feeds

the compressed RFG into the MTR membrane system. The second leg, a 1 inch line, delivers 80-100 psig RFG for direct use in the cultivators. A Tescom pressure regulator controls the pressure to the cultivator control panels.

The RFG pressure downstream of the regulator can be increased by turning the regulator knob clockwise until the desired downstream pressure is achieved. Flow indictor, FI-290, indicates the total RFG flow to the cultivators. The flow rate can be controlled using FCV-290. The RFG then flows into a two-inch yellow polyethylene pipeline (typically used for natural gas piping). This pipe is pressure rated to 75 psig. It is protected from overpressure by a TYCO safety relief valve set at 70 psig and sized to relieve at a higher rate than the compressor capacity.

The RFG containing 3-4% CO_2 can be distributed directly to the cultivator. The gas controls (flow valve, flow meters, and actuated control valves) are used to control the flow rate and flow duration of the RFG into the cultivator.

Concentrated Flue Gas (CFG)

CFG is RFG (3-4% CO_2) that is processed through the MTR CO_2 capture membrane skid (refer to Figure 4-16). The membrane separates the CO_2 from the RFG thereby enriching it to a higher CO_2 concentration. The actual CO_2 concentration is dependent on operating pressure, flow rates, initial RFG CO_2 content and temperature. The MTR system concentrates the CO_2 by using an array of membrane fibers that selectively allow CO_2 to pass through the membrane at a higher rate than other components in the RFG such as oxygen and nitrogen. The result is a gas product stream that has a higher CO_2 content. The “waste” stream from the membrane unit has a lower CO_2 content (2%), but the oxygen and nitrogen levels are higher than in the RFG that enters the MTR unit.

The MTR system requires about 40 psig at the inlet. The flow rate required was about 6000 scfh, which was approximately the flow capacity of the RFG compressor. Table 4-3 shows the test results conducted on site. The skid was able to capture about 50% of the CO_2 in the flue gas stream and enriched the CO_2 concentration from ~3.6% in the flue gas to ~18%. A picture of the skid is provided in Figure 4-16.

Table 4-3. Performance of MTR CO_2 Capture Membrane Skid

	Temp (°C)	Pressure (psia)		Flow Rate (scfm)			CO_2 Concentration (%)			Permeate Relative Humidity (%)	CO_2 Recov-ery (%)	CO_2 Mass Balance (%)
		Feed	Perm	Feed	Resi-due	Perm	Feed	Residue	Perm			
1	44	56	2.0	78.7	65.9	6.6	3.6	2.1	18.7	38	44	7.4
2	47	83	2.5	76.8	63.1	9.3	3.6	1.5	16.6	36	56	10.9

The MTR unit could operate over a wide range of flow rates and inlet pressures. Varying these would also vary the CO_2 concentration of the product stream. In general, a lower feed flow rate, higher O_2 feed concentration, lower CO_2 feed concentration and lower CO_2/N_2 (CO_2/O_2) selectivity of the Polaris membrane at higher temperature would reduce the CO_2 concentration in the permeate stream.

Figure 4-16. MTR CO_2 Capture Membrane Skid

Simulated Flue Gas (SFG)

SFG is a blend of compressed air and 100% CO_2. In general, the CO_2 content is about 4%, similar to the CO_2 content of the RFG. The CO_2 content can be adjusted to a higher level (11% CO_2) to simulate the RFG from a coal-fired plant. The remaining composition of the SFG is compressed air and contains about 76% nitrogen and 20% oxygen at a 4% CO_2 enrichment level. The compressed air is supplied by the Curtis compressor. In this mode the RFG blower is turned off. Fresh air is pulled into the compressor through damper valve V-211 and through the inlet filters F-201 and F-202. The compressor boosts the fresh air pressure to 80-100 psig at about 6000 cfh. The compressed air fills the buffer tank T-201 and the compressor cycles in the same manner it does with RFG.

Pure CO_2

Pure CO_2 is provided in liquid form by AL. The liquid CO_2 (LCO_2) is delivered in small cryogenic tanks (~250 liter) at about 300 psig. There is also a 6000 gal vertical storage tank installed at Redhawk that was to be used for either gas or liquid CO_2 storage. Regulator PCV-214 is used to reduce the CO_2 pressure as it exits the CO_2 liquid tank to the desired use pressure. Typically the regulator is adjusted so that the outlet pressure is about 40-50 psig as indicated on PI-214. SRV-224 provides overpressure protection for the CO_2 gas pipeline.

The 100% CO_2 pipeline splits into two legs. One side, which is ½ inch polypropylene tubing, provides 100% CO_2 directly to the inlet of the cultivator gas control panels. The second side tees into the flue gas line going to the cultivators. There are a flow control valve, FCV-202, and flow indicator, FI-202, in this leg of the 100% CO_2 system. These components can be used to direct the flow of pure CO_2 into the flue gas to produce enriched flue gas.

Enriched Flue Gas (EFG).

EFG can be made on site to closely simulate the RFG produced from a coal-fired plant (11% CO_2). EFG is made by blending RFG from the Curtis compressor with 100% CO_2.

Please refer to Appendix E for Redhawk gas distribution P&ID.

4.2.1.3 6M Cultivators

There were three 6M cultivators installed at the Redhawk Algae Testing Facility. The 6M cultivator design was developed, built and tested under the earlier APS Coal to SNG project. Please refer to its final scientific/technical final report for the cultivator design details. In summary, the 6M cultivator has a diameter of 12 m and a total surface area of 113 m^2, with an active culture footprint of 95 m^2. The cultivator is typically run at a total volume of between 10,000 and 15,000 L.

The cultivator top cover is inflated using a regenerative air blower. Air is directed through a yellow 2 inch gas pressure line from the blower to a regulating flow meter located on a gas distribution panel adjacent to the respective cultivator. Air is then metered into a 2 inch PVC gas line that runs from the gas panel out to a canopy air-injection opening near the center hub which finally discharges gas into the head space of the cultivator. Air exits via the canopy air exhaust line. Proper inflation of the dome is maintained by the flow meter located on the gas distribution panel.

The cultivators at the Redhawk facility are floating and anchored within thermal ponds. There are five thermal ponds on site. Thermal pond 1 houses one cultivator: C1. Thermal pond 2 houses two cultivators: C2 and C3. The cultivators for the remaining thermal ponds were never completed prior to the termination of the project. The primary purpose of the thermal pond is thermal regulation of the liquid volume within the cultivators. Given the extreme Arizona desert heat, temperatures can reach over 110°F in the spring and summer months. The thermal pond helps to offset these extreme temperatures because the large volumes of water create a temperature-buffering environment. Water for filling the thermal ponds is introduced from storage tank T-01. This water never comes in contact with the culture inside the cultivator. Adjacent to each thermal pond is a recirculating sand filter system for the pond. These filters keep the thermal pond clarified. Refer to Figure 4-17.

Figure 4-17. Thermal Pond Sand Filters

The pond is also kept disinfected through hypochlorite doses and conventional pool floats with disinfection tablets.

Each cultivator has associated sensors collecting and displaying data remotely via a labview network. Inline sensors include temperature, pH in, pH out, conductivity, liquid flow totalizer, CO_2 in, and CO_2 out. The pH sensors communicate to a solenoid valve that controls CO_2 flow into the cultivator. The pH high and low setpoints inform the communicating mechanism to either open or close the CO_2-controlling solenoid valve. Refer to Figure 4-18 for a photograph of one of the three cultivators at Redhawk.

Figure 4-18. 6M Redhawk Cultivators

In addition to air entering the head space of the cultivator, CO_2 is injected into the cultivator as well. There are several options for adding CO_2 to the cultivator (see gas distribution section for details). Gas is distributed in the chosen form to the gas distribution panel of the respective cultivator where it is regulated via flow meters and then discharged into the cultivator(s). Presently, the gas delivery system is configured to allow 100% liquid CO_2 delivery to all three cultivators. Flue gas from stack #1 was also piped into C2 and C3. Gas including air and CO_2 in C1 was delivered into the liquid volume loop via a ½ inch flexible line located before the intake of the centrifugal pump. CO_2 and flue gas were injected into the liquid volume loop via a ½-inch flexible line that has a specific injector mounted at the 90 elbow just after the discharge of the centrifugal pump on C2 and C3.

Water is introduced to the cultivator from one of two storage tanks, T-02-A and T-02-B. There are direct headers from these tanks to cultivators 1, 2 and 3. Water from the headers can be directed by valves to enter the respective cultivators. Typically water is introduced initially as part of a disinfection process prior to inoculation (refer to disinfection protocol). Volumes entering or exiting a cultivator are tracked via flow totalizers.

4.2.1.4 Culture Harvesting

The harvesting process involves transferring liquid volumes from the individual cultivators to the dewatering feed tanks. As described below, the harvesting procedure includes several steps.

Water/Media Preparation

Prior to harvesting material from a cultivator, the return water/media must be prepared in advance as soon as the harvest material is removed from the cultivator to insure that the culture continues mixing with as little interruption as possible. Generally a portion of material is harvested at a time versus a complete harvest unless there are circumstances that require a total harvest. Media components are calculated, added to the mixing tank and pumped into the harvested cultivator along with the proper volume of makeup water to bring the cultivator volume back to the intended working volume.

Harvest

The desired liquid volume from the cultivator is pumped via the 7.5 hp centrifugal pump out of the cultivator and valved into the overhead manifold that is directed to the dewatering feed tanks. Depending on the volume harvested, if the volume in the cultivator drops below the point

at which the pump is not able to function without cavitation, the pump should be shut down. If the pump is off, there is no circulation of culture.

Cultivator Refill

Once the harvested material is moved from the cultivator to the dewatering feed tanks, make-up water/media is added back to the cultivator from T-02-A or T-02-B. Once the total volume is returned to the cultivator, the cultivator main pump is restarted. Cultivator wands are checked for proper rotation, and inflation of the dome is regulated and stabilized.

4.2.1.5 Culture Dewatering

The DynaSep AlgaHarvest50 builds upon the previously installed alga harvester designed and constructed by DynaSep and placed in operation at APS in 2009. This new dewatering unit is designed to process a single harvest of a 600 m^2 bioreactor in an 8 hour processing period. The design goal is to produce algae paste of 8-12 wt %. By using a gear pump (pump 1) run on a Variable Frequency Drive (VFD), the system is able to draw material ("green water") from a feed tank and maintain a set pressure in the filter loops. Pump 1 discharges to the first stage filter loop, the largest loop in the system. This loop has a centrifugal pump (pump 2) that circulates the dilute algae repeatedly through the cross-flow filters at velocities that discourage the formation of an impermeable cake of solid algae biomass on the filter's inner surfaces. In this loop the equipment removes approximately 90% of the water as permeate, which is then discharged to a permeate tank. A slipstream of the algae concentrate moves from the first filter loop to the second. The second filter loop is smaller and uses a gear pump (pump 3) due to the increased viscosity of the material in this loop. Permeate can be routed directly to the tank or it can be run through the shell side of the second filter loop to provide cooling. The velocities are similar to those in the first loop to limit the algae solid from caking on the filter's interior surface. The second filter loop's discharge is the system's product - an algae paste concentrate greater than 8 wt%. Refer to Figure 4-19, Figure 4-20, Figure 4-21 and Figure 4-22.

Figure 4-19. Redhawk DynaSep Dewatering Unit

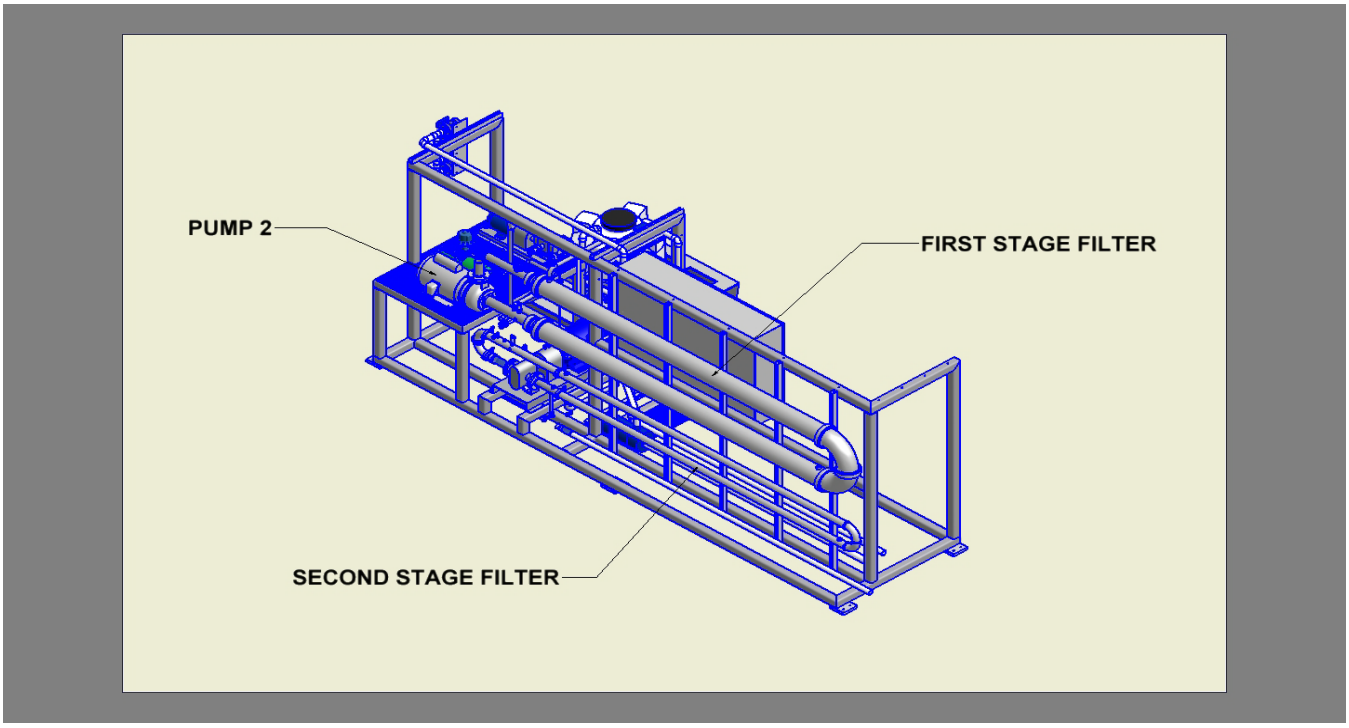

Figure 4-20. 1st and 2nd Stages of DynaSep Dewatering Unit

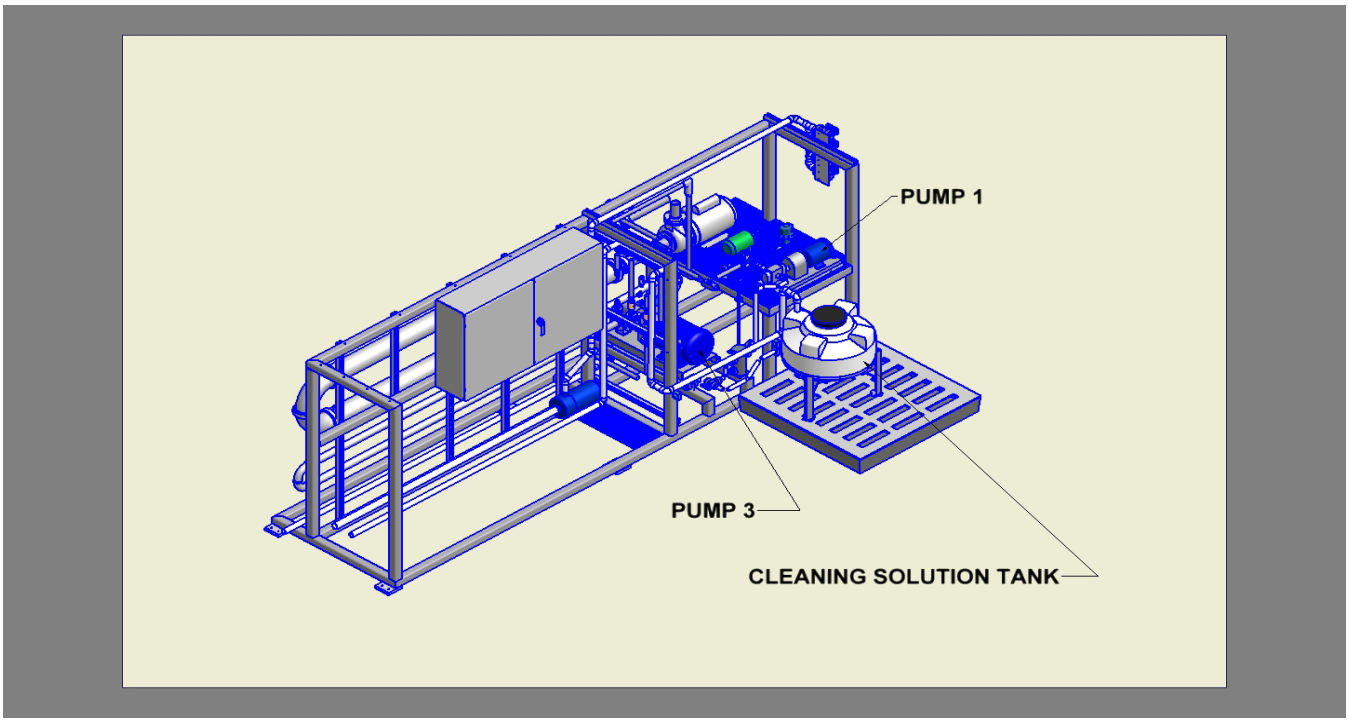

Figure 4-21. DynaSep Dewatering Unit with Pumps Indicated

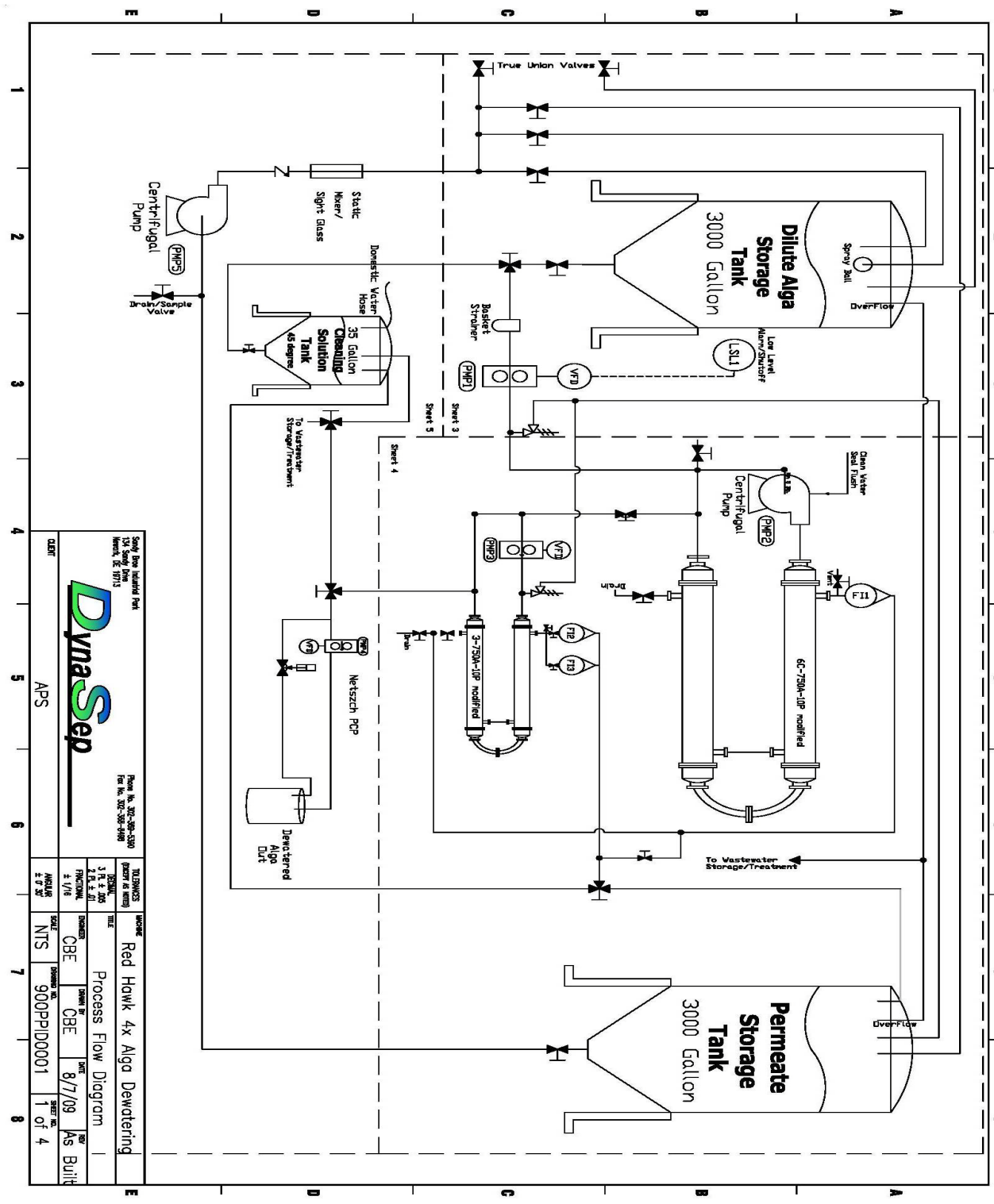

Figure 4-22. DynaSep AlgaHarvest50 Process Flow Diagram

This dewatering system was used for all harvests from which biomass was recovered during the operation of algae cultivators at Redhawk. Beginning on January 24, 2010, the dewatering system was used to process the first 10,000 L batch of algae culture from C1 at Redhawk. The system was then operated till the end of the project. During this period, approximately 72,000 L of algae culture were processed from the three cultivation systems at Redhawk, and approximately 22,500 L of stressed, elevated-lipid-content algae culture was also processed through the system and carefully collected and transferred to the laboratory. The biomass densities at the time of harvests ranged from 0.78 g/L up to 2.09 g/L. Clear permeate resulted as shown in Figure 4-23.

Figure 4-23. Water Recovered from Dewatering System

In a number of cases, the recovered medium was recycled directly back to the cultures in order to recycle the water and any nutrients remaining in the medium. The recovered medium - the water and any salts or nutrients in solution recovered from this dewatering system - is clear and free of cellular debris and bacteria. This enables media reuse with much lower risk than most other current algae dewatering technologies. The resulting biomass paste from the dewatering system ranged from 7% solids when the system is first engaged or when the culture volume being processed is not large enough for the dewatering system, up to 20% solids when the system is running optimally and the batch of culture being processed is large enough for the high-throughput design of the system. An example of the 20% solids paste exiting the dewatering system can be seen in Figure 4-24.

Figure 4-24. Concentrated Algae Paste after Dewatering

All biomass paste of value, such as the high-lipid biomass from the lipid accumulation studies, was processed into buckets and frozen immediately. Elevated lipid content biomass was transferred to the lab for tray drying and oil extraction work, while low lipid level biomass was placed in buckets and frozen on site at Redhawk for any other potential study.

The robust operation of this dewatering system over the period of time during which algae was cultured at Redhawk marked a significant achievement in the demonstration of the integrated algae cultivation systems. One of the critical steps in the cultivating of algae is to be able to consistently harvest the algae biomass and recycle the recovered water. This dewatering system demonstrated these characteristics throughout the test period.

4.2.1.6 Culture Condition Controls and Automated Data Collection

Data on a number of biological, physical and chemical variables were automatically collected by the cultivator. Data were collected and stored continuously for the following parameters via inline sensors:

- Algae culture temperature
- pH in: located downstream of the cultivator pump
- pH out: located upstream of the cultivator pump; directed the CO_2 distribution solenoid to open or close as required
- CO_2 in: inline sensor indicating incoming CO_2 concentration
- CO_2 out: indicating concentration from the headspace of the cultivator
- Algae culture conductivity
- Pump flow: reflection of culture circulation through cultivation loop.

This data was collected and registered on a Labview system that was monitored in the control room. Control panels, which communicated information from the sensors to the Labview system was located adjacent to the individual cultivators. In addition to the remote data collection, CO_2 regulation into the cultivators was regulated by solenoid valves located on the

gas distribution panels for each cultivator. Distribution of CO_2 was dictated by preset high- and low-pH setpoints. If a pH excursion occurred, the solenoid opened or closed, starting or stopping CO_2 flow to the cultivator.

4.2.2 REDHAWK CULTIVATION TEST DETAILS

4.2.2.1 Redhawk Cultivator 1

Cultivation began at Redhawk by inoculating C1 on October 28, 2009. Three algae cultivators were eventually operated, coming on-line one at a time. Initial growth curves of the algae were measured, and depending on the intended use of a particular cultivator (growing the inoculum, maintenance of optimal conditions, or lipid accumulation), regular harvests were conducted. Harvesting was decided based on culture density and/or the lipid content of the culture. A calculated volume was then pumped from the cultivator to one of two destinations. Harvest material was either transferred to another cultivator as a source of inoculum or directed to the dewatering feed tanks. If a harvested cultivator was completely harvested, the cultivator was either disinfected or re-inoculated at a later date, or it was turned around immediately. For a partial harvest, a calculated volume of fresh media was added to the existing culture, while for a complete harvest, a complete volume of fresh media and fresh inoculum was added. All algae processed through the dewatering unit was collected, labeled, and stored in the freezer at Redhawk.

The algae cultivation process at Redhawk began when a total of approximately 1733 L of inoculum from the 3rd Avenue cultivator was added along with 90 L of dense, pure culture from the laboratory inoculum system. In addition to the inoculum, 8000 L of media was added to the cultivator giving a total initial culture volume of just under 10,000 L with a starting density 0.227 g/L by ash-free dry weight. The culture was initially covered with a shade cloth to protect the dilute culture from the high irradiance of sunlight. Once the culture was acclimated, and an increase in density (growth) began, the shade cloth was removed. On November 13, 2009, 2000 L of fresh media was added to the cultivator to bring the volume up to 12,000 L. During this time, the health of the culture remained high as indicated by fluorescence measurement, and the density of the culture gradually increased after inoculation to a high of 1.9 g/L on December 7, 2009, as shown in Figure 4-25.

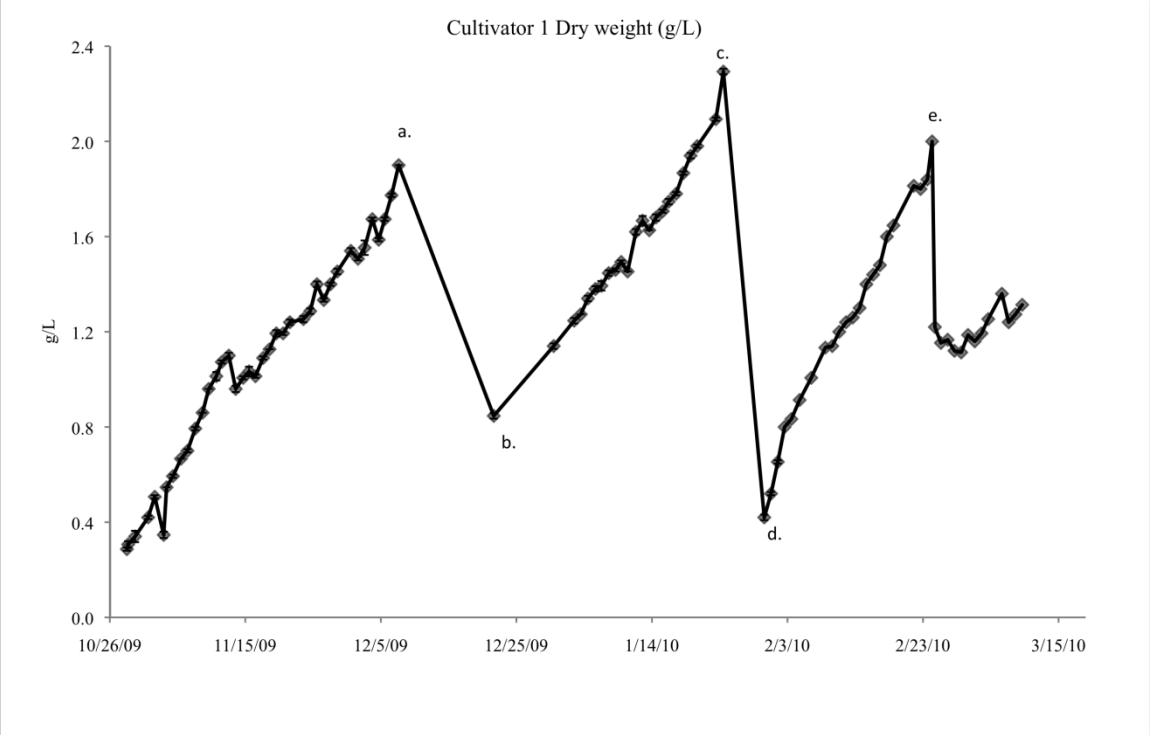

Figure 4-25. Cultivator 1 Culture Density as Measured by Dry Weight *

* Dry Weight: grams of dry biomass per liter of culture
a. Harvest 6000 L as inoculum for C2 (12/7). b. Harvest 4500 L as inoculum for C3 (12/21). c. Harvest 10,000 L (1/24). d. Re-inoculation (1/30). e. Harvest 4400L as inoculum for C2 and C3 (2/24). f. Pump cavitation, some culture may have settled. g. Pump cavitation, some culture may have settled.

Although the general growth trend of the culture has been very stable, some fluctuations in culture density measurements can be seen in the initial days of growth. The decrease in density on November 13, 2009, as mentioned, was a result of the addition of 2000 L of media to the culture. However, some of these fluctuations may also be related to working through the new challenges involved in the start-up of the cultivator. A troubleshooting period was required to stabilize the cultivator operationally.

One example of an operational challenge resulted in a pump cavitation due to inadvertent over-inflation of a dome resulting in cultivator ring rising from the water, creating a higher profile and exposing the center console intake port. This caused air to enter the intake lines of the pump, causing cavitation of the liquid distribution pump. When cavitation occurred, the wands ceased to spin and mixing of the culture decreased. This problem was generally corrected immediately; however, drops in density, such as that seen on November 2, 2009, were likely due to a sample being collected too soon after a pump cavitation event prior to the culture being fully mixed. A refinement period was required to optimize mixing, depth profiles, and operational robustness.

After the initial growth and operational period, this initial cultivator C1 was then used as inoculum culture for the propagation of algae culture in the subsequent two cultivators as they came online in December 2009. On December 7, 2009, 6000 L of C1 was used to inoculate the newly assembled C2. This event is reflected in the culture density data for C1 shown in Figure 4-25. After using 6000 L of C1 to inoculate C2, C1 was allowed to grow, and the culture was kept replete with nutrients; in C2 and C3, nutrient-limitation stress was studied, as will be discussed subsequently. For the next growth period, C1 increased in biomass density from 0.8 g/L up to 2.3 g/L. Generally, cultures have been harvested below this density in order to maintain optimal light penetration and growth, but due to the logistics of operations and the assembly of other cultivators, and commissioning of the dewatering system during this period, the harvest of C1 was delayed. However, a few days of high productivity still occurred even at this high culture density.

On January 24, 2010, all of the C1 culture was harvested to test the dewatering system and to reduce the density of the culture to within standard operational densities that had been established in previous experiments. The biomass harvested during this period was collected and stored frozen in a number of buckets in the form of paste consisting of approximately 20% to 25% solids paste. On January 30, 2010, a total of 3000 L of culture from C2, which had previously been inoculated from the C1 culture, was used to reinoculate C1 after a two-day period during which the top liner and center liquid distribution hub of C1 could be repaired from damage sustained in a storm exhibiting 90 miles per hour (mph) gusts of wind. After the mechanical systems were repaired, C1 was re-inoculated with the 3000 L of culture from C2 (which originated from C1) and 9000 L of fresh growth medium. The first 3 days of growth after the refreshing of C1, in combination with the lower culture density allowing for better light penetration to the entire culture, resulted in biomass productivities of 12.63, 16.84, and 18.53 $g/m^2/day$, respectively. These relatively high productivities occurred despite the short days at this time year, but they did occur when skies were clear. This illustrates the importance of carefully maintaining the culture within the optimal density range to achieve high productivity, when possible.

This growth period was continued until February 24, 2010; after stressed biomasses were harvested from C2 and C3, culture from C1 was used to re-inoculate each of these cultivators. As a result, the density of C1 at this time was reduced to 1.14 g/L. The subsequent growth period of C1 resulted in less than optimal productivities, likely due to settling of culture on the bottom liner from a few events leading to reduced mixing. A complete harvest of C1 was

planned in order to reduce this possible buildup of settled culture in the cultivator. On March 10, 2010, C1 was completely harvested. In the following days the cultivator was completely disinfected and the system was re-inoculated on March 17, 2010 with inoculum supplied by C2. Two days later, C1 experienced a complete failure of a welded section at the bottom of the sump chamber of the center column. This failure forced the entire contents of C1 to be drained from the cultivator directly into the thermal pond. This required relatively major repair, and the cultivator had to be removed from the thermal pond for these repairs to be conducted. Prior to closeout, C1 was operational for 130 out of 153 days (84%) consisting of three cycles, the longest of which was 87 days.

4.2.2.2 Redhawk Cultivator 2

The second operational cultivator at Redhawk, C2, was inoculated on December 7, 2009, and the first sample was taken on December 9, 2009, initiating the growth curve shown in Figure 4-26. C2 was inoculated with 3000 L of culture from C1 and with full nutrient medium at a volume of 9000 L. The resulting growth period continued from this date until January 28, 2010, when the culture reached a density of 1.94 g/L. At this time, 3000 L of culture was used to re-inoculate C1, as explained previously, and the rest of the C2 culture was harvested and processed to test the dewatering system for the second time. This harvest marked the end of the active growth test in C2, and the subsequent re-inoculation of C2 consisted of nutrient-depleted medium, along with already partially stressed biomass from C3. In order to achieve this, 6000 L of culture from C3 was combined with 6000 L of nutrient-depleted medium to re-inoculate C2. The marked decrease in growth during this period as a result of the lack of available nutrients can be seen in Figure 4-26.

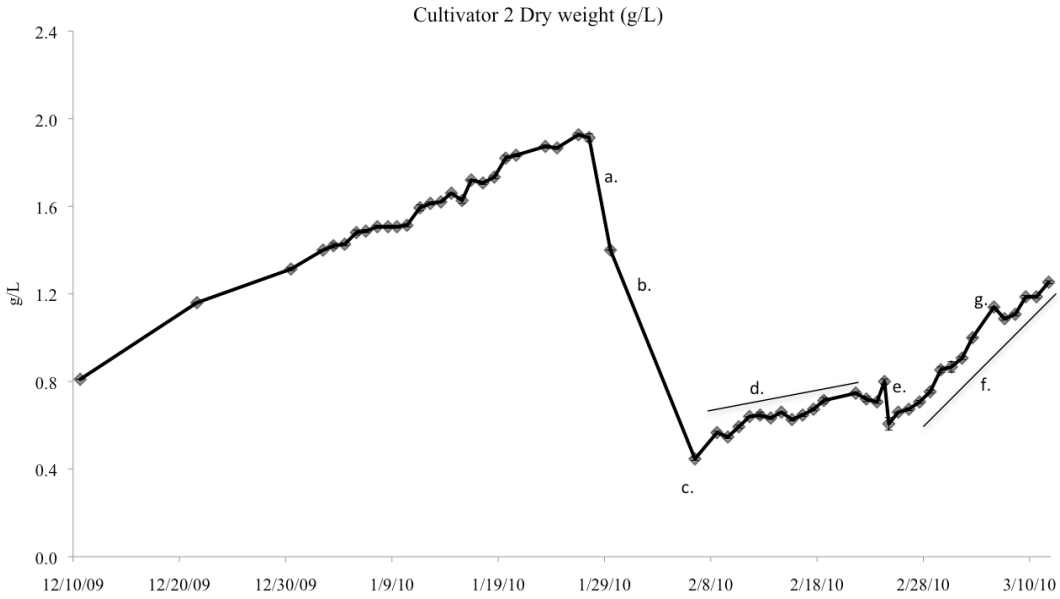

Figure 4-26. Cultivator 2 Culture Density as Measured by Dry Weight*

* Dry Weight: grams of dry biomass per liter of culture
a. Harvested 3000 L as inoculum for C1 (1/28). b. Harvested remaining 9000 L (2/1). c. Inoculation with 6000 L culture from C3 (2/5). d. Period of relatively level growth due to nutrient limitation. e. Harvest 12,000 L. Re-inoculation with 2200 L from C1 (2/24). f. Growth during this period possibly due to excess nitrate in culture. g. Possibly poor mixing due to pump cavitation and wand breakage issues (3/7).

This period of stress induction ended on February 24, 2010, when the lipid content of the biomass was deemed high enough to harvest. The entire culture was dewatered to recover the biomass for oil production in the laboratory. Oil production results can be found in section 4.3.2 later in this report.

Regular samples were taken to monitor lipid accumulation and adjust parameters as necessary. Lipid content was measured as total fatty acid content using FAME with GC/MS analysis. The growth and lipid content data for this period of stress in C2 can be seen in Figure 4-26 and Figure 4-27.

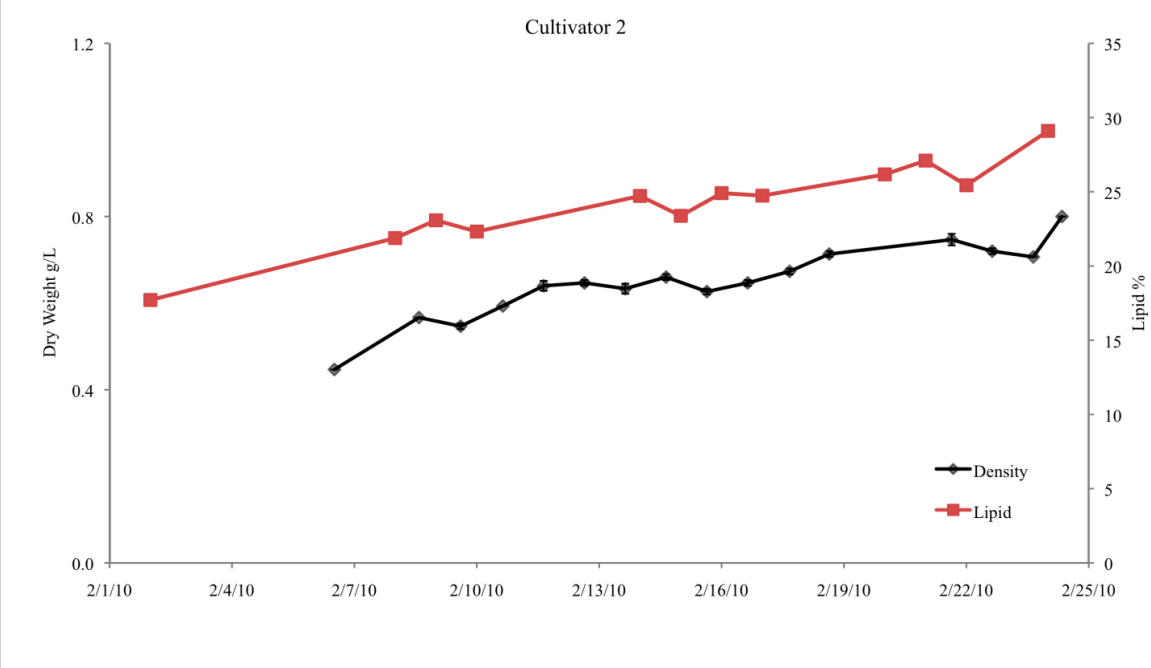

Figure 4-27. Cultivator 2 Culture Density and Lipid Content during First Nitrate Deprivation Attempt

On February 5, 2010, the biomass in C3, which had just begun to show an increased lipid level, was split into C2 along with an addition of nitrate-depleted medium. Because of the immediate nitrate deprivation and the fact the inoculum source was already from a nitrate-depleted culture, this culture immediately showed signs of nitrate limitation (as shown in Figure 4-27) indicated by the very minimal growth rate during this entire period with increasing lipid content.

During this period of growth inhibition due to nitrate deprivation, the lipid content of the biomass in C2 increased from an already elevated level of 17% to over 25% of the biomass as shown in Figure 4-27. This period of lipid accumulation was ended when C2 was harvested on February 24, 2010, to capture this large amount of high-lipid, low-chlorophyll biomass. All of the biomass harvested from C2 on February 24, 2010 was dewatered to approximately 25% solids and quickly frozen and stored for subsequent drying and oil extraction research. See section 4.3.2 for description of oil extraction efforts on this biomass.

Lipid productivity is an important metric for evaluating the system performance. These initial lipid accumulation tests were performed to determine if it was possible to accumulate neutral lipids in the biomass of this strain of algae in large outdoor cultures. A subsequent step would be to determine the exact conditions that result in optimal lipid productivity and maintain the culture within those conditions to maximize lipid productivity. Although these tests were not yet attempting to maximize lipid productivity, the possibility of doing so in the future can be seen in

Table 4-4, which shows the potential for increasing the mass of lipid produced per liter of culture per day. Table 4-4 shows the lipid productivities achieved in the culture in C2 during the first nitrate deprivation attempt. Very different lipid productivities are achieved, ranging from just over 6 milligrams per liter per day (mg/L/day) of lipid production up to nearly 25 mg/L/day, which was equivalent to 346 to 1312 gal per acre year (assuming one year with 365 operational days). (As a comparison, soybean oil production is between 50 to 100 gal per acre year.)

Table 4-4. Lipid Productivity of C2 Culture across 3 Time Periods during the Initial Lipid Accumulation Test

	mg/l/day	$mg/m^2/day$	gallon/acre/year*
2/8/10-2/14/10	6.5	692.4	346
2/15/10-2/21/10	9.3	988.7	495
2/22/10-2/24/10	24.7	2621.9	1312
* 1 year has 365 days			

The actual oil production rate would be lower than this calculated number due to processing losses during oil extraction. Although the growth rate of the algae culture ceases under nutrient limitation, the usable neutral lipid content begins to increase. Therefore, the key to optimizing oil production will be to determine the shortest period of time when the most lipid accumulates without a reduction in standing culture density, and to harvest immediately after this period of time.

Immediately following the harvest of February 24, 2010 C2 was re-inoculated with biomass from C1 in order to begin the stressing process again. The resulting growth curve and lipid content for this second test can be seen in Figure 4-28. Given a residual level of nitrate in the inoculum, the density of the culture began to rise over the next 21 days. The average lipid productivity over this time was ~8.5 mg/L/day. As a result, the density was reduced again by harvesting algae from C2 to be used as inoculum for C1. This volume was replaced again by nutrient-depleted medium, which did appear to increase the lipid content subsequently.

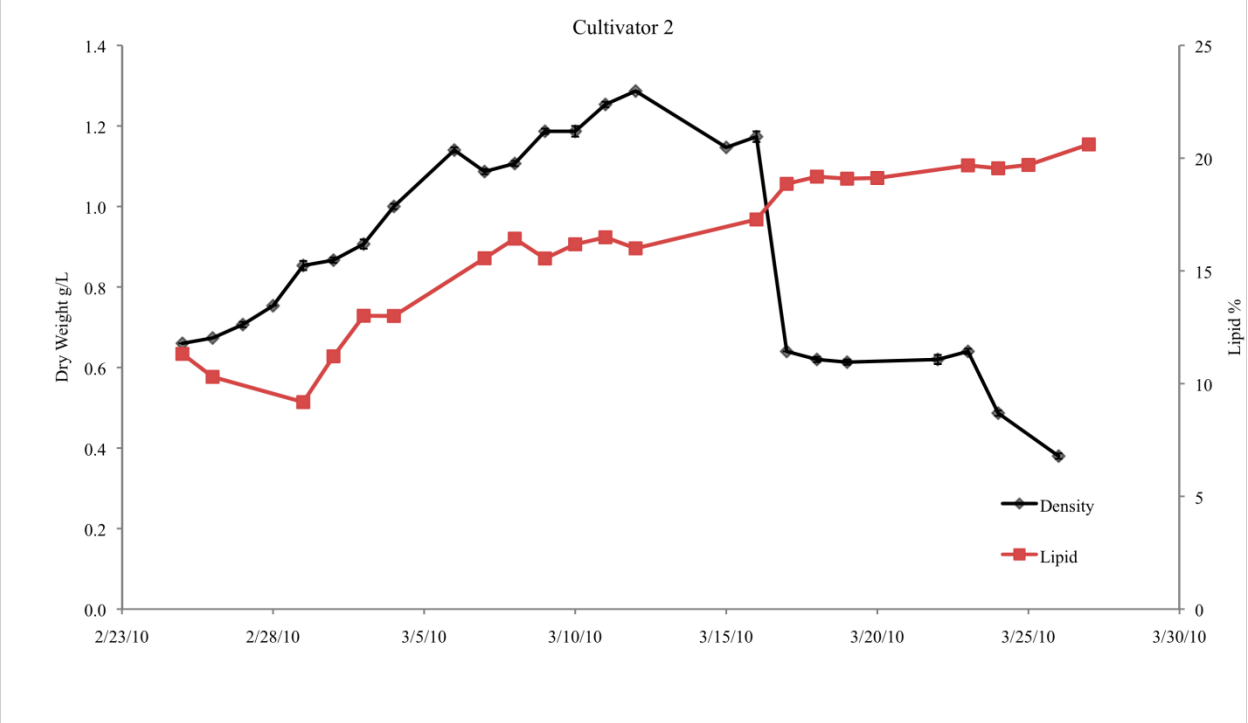

Figure 4-28. Cultivator 2 Culture Density and Lipid Content during Second Nitrate Deprivation Attempt.

During the 12 days from March 17 to March 29, 2010, the density of the culture dropped slightly and lipid levels remained fairly constant. Periodic interruptions to mixing due to cavitation of the recirculation pump may have allowed for the culture to create a settled layer that eventually formed a biofilm on the bottom liner. Given the stabilization of lipid levels over time (March 17–27, 2010) in C2, a decision was made to harvest the culture, disinfect the cultivator, and re-inoculate with fresh culture. A harvest occurred on March 29, 2010. A subsequent decision was made not to restart the cultivator. Cultivator 2 was operational for 105 out of 112 days (94%) prior to closeout, consisting of three cycles, the longest of which was 53 days.

4.2.2.3 Redhawk Cultivator 3

On December 21, 2009, the third and final operational cultivator at Redhawk, C3, was inoculated with 4500 L of inoculum from C1 and 7500 L of nutrient-depleted media. This initial growth and oil accumulation period can be seen in Figure 4-29. During this period, the proper maintenance of the culture was affected by equipment issues when the circuit board failed to signal the CO_2 solenoid properly, which led to periods when CO_2 was not delivered to the culture. In addition, a notable windstorm affected Redhawk systems on January 21, 2010. Regardless of these operational excursions, the culture remained healthy.

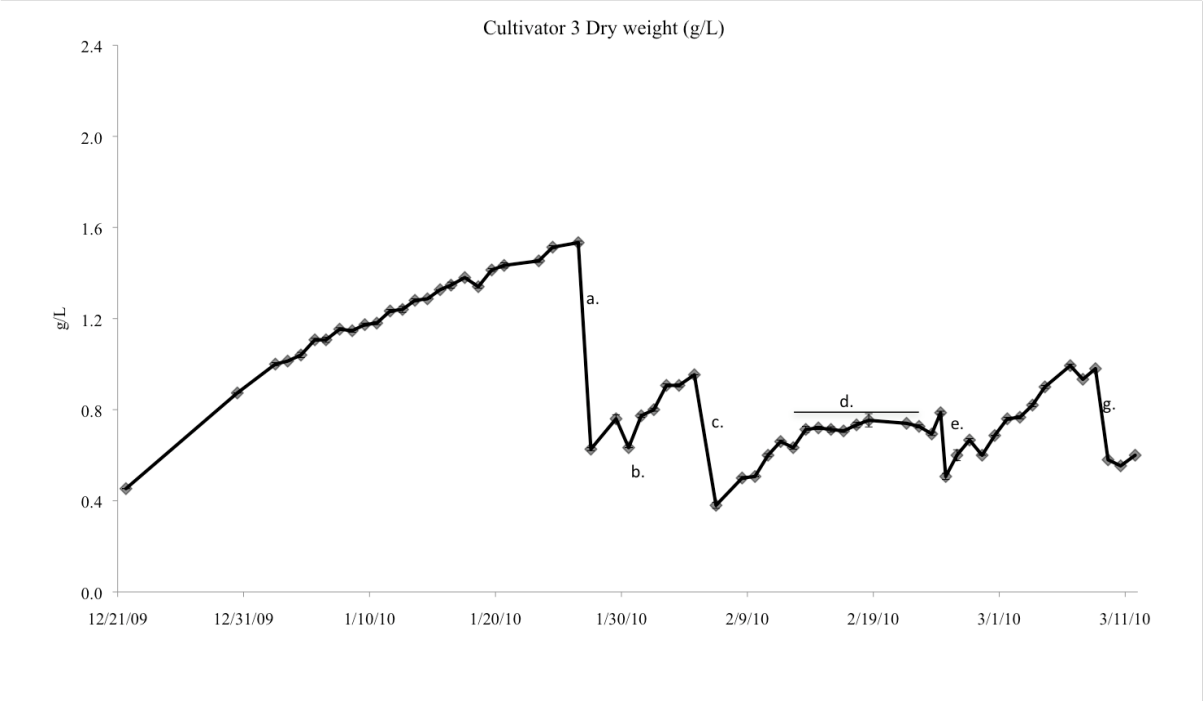

Figure 4-29. Cultivator 3 Culture Density as Measured by Dry Weight*

* Dry Weight: grams of dry biomass per liter of culture
a. Harvested 9000 L (1/27). b. Possibly poor mixing due to dislodged wand.
c. Harvested 6000 L (2/4). d. Period of level growth due to emphasis on stressing culture (no nitrate). e. Harvested 10,500 L. Re-inoculate with culture from C1 (2/24). g. Harvested 6000 L (3/8).

On January 27, 2010, 9000 L was harvested to reduce the density of C3. The cultivator was refilled with 9000 L of permeate originally from C1. Permeate was used because continuing issues with the water treatment system compromised the availability of fresh water to be used as the return media source. In addition, given the ultimate intention to reuse water (permeate) as makeup water/media (as was previously deemed acceptable following laboratory tests), the use of permeate was planned knowing that residual nutrients might remain in the permeate.

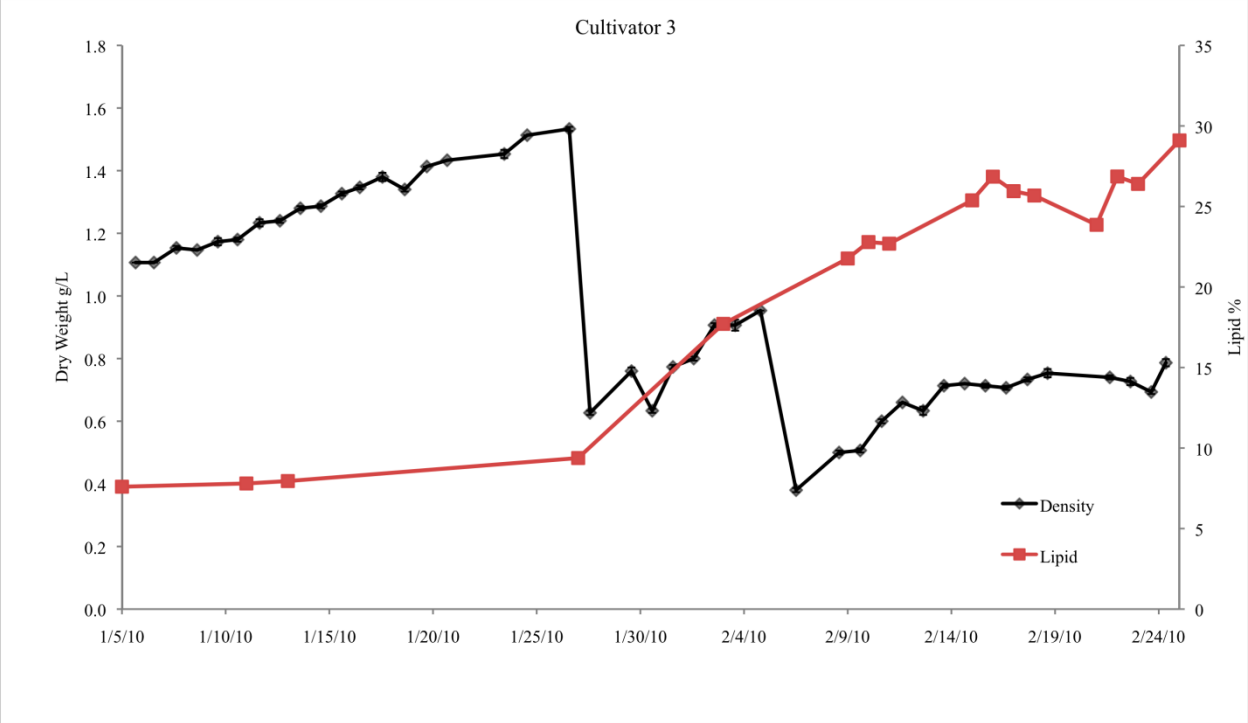

Figure 4-30. Cultivator 3 Culture Density and Lipid Content during First Nitrate Deprivation Attempt

After the January 27, 2010 harvest, the culture continued to increase in density, indicating growth continued although at a reduced rate. Nitrate deprivation did begin to take effect during this period, however, as indicated in the February 3, 2010, lipid data, showing an increase in lipid as compared with previous samples. This intermediate nitrate-deprivation phase, continued growth, and increasing lipid content indicated that full nitrate deprivation would occur soon. To speed this process, a second harvest was conducted on February 4, 2010, to reduce nitrate even further by diluting the culture with nitrate-depleted medium. After this harvest, the growth curve indicated a further increase in culture density, but during this time the lipid level also increased to nearly 30% of the biomass.

By the time the culture growth ceased as a result of full nitrate deprivation, the lipid level appeared to reach equilibrium at a level near 30% of the biomass until the final sample during harvest, when both culture density and total lipid content appeared to increase. During this time, the culture also turned yellow, indicating a reduction in chlorophyll content. With the cessation of increasing culture density, the lipid content at its peak, and the low chlorophyll content, a full harvest was conducted on February 24, 2010, to recover all of the biomass for drying and oil extraction. Oil extraction results can be found in section 4.3.2 later in this report.

Figure 4-31. Concentrated, Low-Chlorophyll Algae Paste after Dewatering

The lipid productivities during this lipid accumulation test in C3 can be seen in Table 4-5. The initial period of the test, when the culture was too dense to receive ample light, little growth and little lipid accumulation was occurring, as was made clear by the very low productivity during this time. The two subsequent periods, however, when harvests were conducted to further deplete nutrients and reduce the culture density, resulted in much higher lipid productivities mostly due to the rapid content increase in the algae By the end of the test, lipid levels stopped increasing, and the culture density remained stable (the culture stopped growing), and as a result the lipid productivity was lower for the final period before the complete harvest.

Table 4-5. Lipid Productivity of C3 Culture across Four Time Periods during the Initial Lipid Accumulation Test

	mg/l/day	$mg/m^2/day$	gal/acre/year*
1/5/10-1/27/10	2.7	286.7	143
1/27/10-2/4/10	13.75	1460.2	730
2/6/10-2/11/10	16.49	1751.2	876
2/11/10-2/24/10	6.1	647.8	324
* 1 year has 365 days			

Although the lipid productivity was low for the final period before the harvest, the level of lipids in the biomass was highest at this time. As a result, a great deal of biomass with extractable neutral lipids was yielded by this experiment.

After the complete harvesting of stressed biomass on February 24, 2010, the cultivator was immediately re-inoculated on the same day with 2200 L of culture from C1 and 9800 L of nutrient-depleted media. The lipid content and culture density for this second lipid accumulation test in C3 can be found in Figure 4-32.

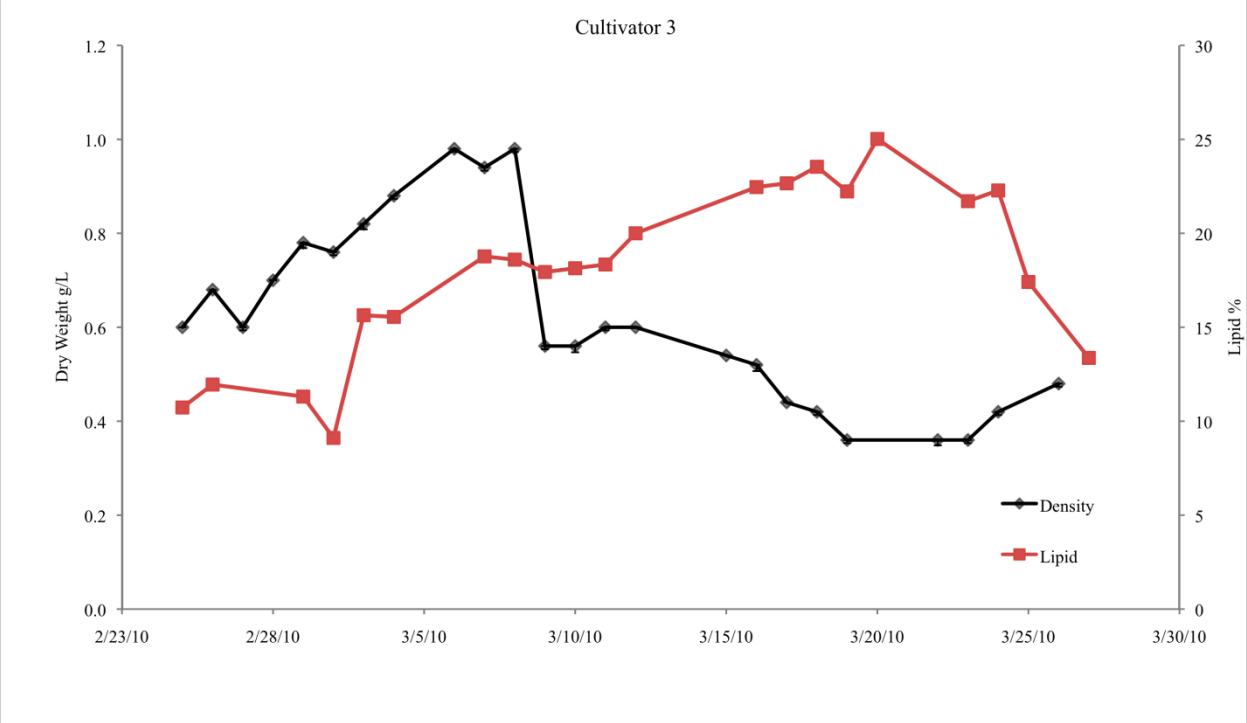

Figure 4-32. Cultivator 3 Culture Density and Lipid Content during Second Nitrate Deprivation Attempt

As the nitrate-depleted and the growth in C3 began to decrease, the lipid levels gradually increased. A partial harvest was conducted on March 7, 2010, to reduce nitrate levels even further. The harvest was apparently effective in that no growth occurred after this period. The lipid content in C3 continued to rise for 11 days after this partial harvest, but in this attempt, the health and status of the culture began to decline shortly thereafter and the lipid content also began to decrease.

As opposed to the result of the first nitrate deprivation attempt in C3, the cultures during this run were allowed to persist in this deprived state for a longer period, and eventually the lipid content began to decrease. For a number of logistical reasons, harvests could not be conducted at the time of peak lipid content. Also during this time, a malfunctioning control panel periodically interrupted the culture mixing and affected pH control. These interruptions were likely responsible for the decreases in culture density near the end of the growth curves because the culture settled onto the bottom liner, and for the decrease in lipid content because the pH range was not optimal and the CO_2 supply may have been limited, which degraded the culture and the lipids within. By the time the cultures were harvested completely, the lipid content and the total amount of biomass was reduced. Nevertheless, all biomass was processed and dewatered to paste form, frozen, and stored for possible future research in drying and oil extraction. During

the entire period of testing at Redhawk C3 was operational for 97 out of 97 days (100% operational) prior to shutdown, consisting of two cycles, the longest of which was 64 days.

The results of these experiments confirm the efficiency of this lipid accumulation method at a much larger scale than previously conducted in the lab, and this process can be applied consistently to achieve predictable and repeatable lipid levels within a set period. This experimentation provided an understanding of the algae strain and its growth conditions, which resulted in a management tool that could allow for the production of more usable oil from the biomass produced in the large-scale systems. Further experimentation should be used to reduce the amount of time required to induce this nutrient stress and the resulting lipid accumulation in the algae biomass. In so doing, lipid productivity of these algae cultures could likely be maximized to a level greater than that occurring in these initial tests, which had the aim of simply determining whether or not the application of the lab-determined technique was achievable at larger scale in outdoor cultures.

4.2.3 Summary of Algae Cultivation at Redhawk

Over the course of this project, great progress was made in the construction, commissioning and integration of multiple systems into a functional algae farm with clear implications for development at large scale, although the complete original buildout plan for the Redhawk site was not entirely realized. Each system was essentially developed from the ground up - in most cases involving new technologies or utilizing existing technologies in a new application. Original operational systems or applications developed include:

- Unique algae cultivator design
- Enhanced method of harvest
- Unique method for dewatering algae at large scale
- Enhanced design for gas separation, concentration and distribution
- Enhanced method of thermal management for cultivators
- Enhanced methods for controlling environmental and physical parameters of cultivators remotely
- New protocols and methods for managing day-to-day operations of the farm

Within these categories a myriad of details were addressed to make these systems ultimately functional. Not only were the various systems constructed, but the commissioning process, which is always an arduous task even with known technologies and applications, was

completed and led to a viable production-based algae farm with all appropriate processes in place. The remaining tasks would have involved the continued refinement of the respective systems to bring each one into a predictable high-output production range. From what was learned at Redhawk, there are clear implications that the goal of developing a viable high-output algae farm at large scale would have been achieved. With only three cultivators in place, a full plan for build out would have been realized based on the modular system developed around these three cultivators.

The successful operation of C1 at Redhawk with actively growing algae culture, as well as the nitrate deprivation runs in C2 and C3, marked the culmination of laboratory support work, leading to the production of large amounts of biomass with a high level of extractable lipids and a lower level of chlorophyll. The demonstration of this technique in C2 and C3 showed that these stressing techniques could be applied to the culture in situ in the same growth systems. Another important milestone in the demonstration of beneficial use of CO_2 at Redhawk was the long-running operation of associated and integrated systems. During the operational period at Redhawk, 11 major harvests were conducted, allowing for the gain of a great deal of operational experience and testing of the equipment. The total volumes and biomass for these harvests after the initial scale-up using C1 are shown in Table 4-6.

Table 4-6. Redhawk Cultivators (C1, C2, C3) Harvest Summary

Cultivator 1 Summary			
	Harvest		
Date	Volume (L)	Density (g/L)	Biomass (g)
10/28/20 – 12/1/10	*Initial culture scale-up using C1*		
12/1/09 – 12/7/09	6000	1.9	11,400
12/30/09 – 1/24/10	10,000	2.29	22,900
1/31/10 – 2/24/10	4,400*	1.96	8,624
2/25/10 – 3/9/10	12,000	1.22	14,640
Cultivator 2 Summary			
	Harvest		
Date	Volume (L)	Density (g/L)	Biomass (g)
12/9/09 – 1/28/10	12,000	1.94	23,280
2/5/10 – 2/24/10	12,000	0.84	10,080**
2/25/10 – 3/11/10	12,000	0.36	4,320
Cultivator 3 Summary			
	Harvest		
Date	Volume (L)	Density (g/L)	Biomass (g)
12/21/09 – 1/27/10	9,000	1.56	14,040
1/28/10 – 2/4/10	6,000	0.96	5,760
2/5/09 – 2/24/10	10,500	0.78	8,190**
2/25/10 – 3/11/10	18,000	0.63	11,400
		*used as inoculum	**high fat

Over the course of this project, a combined total of 332 days of culture growth within C1, C2 and C3 of three 6M cultivators at Redhawk was demonstrated. For C1, there were six harvest events between December 9, 2009, and March 19, 2010. A total of 38,900 L was harvested, of which 14,900 L was used as inoculum and 24,000 L was harvested directly or used to test the dewatering unit. No stress product came from C1.

For C2, there were six harvest events between December 10, 2009 and March 29, 2010. A total of 42,000 L was harvested, of which 9000 L was used as inoculum, 12,000 L of stressed algae was harvested and processed, and 21,000 L of non-stressed algae was harvested and processed or used to test the dewatering unit.

For C3 there were five harvest events between December 21, 2009 and March 29, 2010. A total of 43,500 L was harvested, of which 6000 L was used as inoculum, 10,500 L of stressed

algae was harvested and processed, and 27,000 L of non-stressed algae was harvested and processed.

Any discrepancies in total harvest volumes versus biomass processed indicate that not all harvested algae were utilized as final products for processing. Material was used for inoculation, test purposes, and start-up, in addition to actual processed. The slight losses at various stages of the initial integration and operation of these systems indicate the research and development nature of the project, and with operational experience these losses were and would continue to be reduced greatly. The two major batches of stressed algae from C2 and C3 processed on February 24, 2010 were frozen as dewatered algae paste and transferred to the lab for drying and oil extraction work to be conducted on this material.

During this time, optimal growth conditions were investigated as well as conditions resulting in increased lipid content in the algae biomass. This project led to greatly increased understanding of both how to keep cultures healthy and growing optimally through operational management and how to induce lipid accumulation in a large batch of algae before a harvest. No contamination events negatively affecting growth rate occurred during this period, although optimal productivity of the cultures was not always maintained as a result of logistical and operational limitations, as well as from deliberate nitrogen limitation.

When optimal conditions and plentiful nutrients were provided, algae productivities in C1, C2, and C3 reached 28.67, 16.73, and 17.68 g/m^2/day respectively as shown in Table 4-7. Also apparent are the relatively low mean productivity levels exhibited during this period. A number of factors led to these results. For instance, in C2 and C3, this low productivity was expected as a result of the intentional nutrient limitation to increase lipid production and reduce chlorophyll content. However, the low productivity exhibited by C1 is not due to nutrient limitation because that technique was not applied to the culture. On many occasions, as a result of logistical and equipment limitations, harvests of the culture could not be carried out as scheduled to maintain optimal growth conditions. As a result, C1 during this period often operated at a culture density higher than that which is likely optimal, thus reducing productivity. In addition, mixing in the systems was periodically discontinued due to a malfunction of the control system and cavitation of the recirculation pumps as a result of the pumps being mounted above the cultivators. As a result, the pH fluctuated periodically, and settling occurred when mixing was interrupted, which prevented much of the biomass in the cultivator from being sampled through liquid culture sampling.

Table 4-7. Redhawk Cultivators (C1, C2, C3) Aerial Productivity Summary

Cultivator 1 Summary				
Date	Aerial productivity ($g/m^2/day$)			
	Mean	SE	Max	Min
10/28/20 – 12/1/10	*Initial culture scale-up using C1*			
12/1/09 – 12/7/09	11.89	1.55	15.21	6.02
12/30/09 – 1/24/10	5.64	1.28	22.88	-5.35
1/31/10 – 2/24/10	8.50	1.50	28.67	-1.70
2/25/10 – 3/9/10	2.87	1.56	9.26	-5.89
Cultivator 2 Summary				
Date	Aerial productivity ($g/m^2/day$)			
	Mean	SE	Max	`Min
12/9/09 – 1/28/10	2.70	0.87	13.64	-4.17
2/5/10 – 2/24/10	2.59	1.38	16.73	-4.21
2/25/10 – 3/11/10	5.45	1.55	12.63	-6.74
Cultivator 3 Summary				
Date	Aerial productivity ($g/m^2/day$)			
	Mean	SE	Max	Min
12/21/09 – 1/27/10	3.06	0.67	8.69	-4.71
1/28/10 – 2/4/10	7.87	3.31	17.68	0.00
2/5/09 – 2/24/10	3.28	1.56	16.73	-4.18
2/25/10 – 3/11/10	5.04	2.18	13.26	-8.42

During the complete harvesting of the culture and cleaning of the C1 liner, a great deal of biomass was observed to be in the system even after the liquid culture had been removed to the greatest extent possible. Thus a great deal of biomass accumulation was not represented in the volumetric samples leading to productivity estimates. Despite the overall low productivities as a result of the interruptions mentioned, peak productivities were very high during periods when all culture conditions were ideal. With more operational experience, it is likely that the mean productivities can be driven towards the peak productivities demonstrated.

An important result of this period of operating three 6M cultivators was the lack of contamination and the ability to avoid major culture losses as a result of the periodic interruptions to mixing and pH control. The ability to grow these cultures for so many continuous days indicates that the long periods of continuous culture likely required in an algae culture at the scale of the Cholla system are achievable.

A significant finding occurred as a result of applying laboratory developed techniques to the large outdoor cultures at Redhawk, and it allowed progress to be made in producing oil suitable for conversion to liquid biofuels, which was a major project objective. (See section 4.3.2 and section 4.3.3 for extraction and biofuel production efforts.) The method of nutrient limitation was applied at scale a number of times in situ in C2 and C3, resulting in large batches of material with increased levels of neutral lipid and reduced chlorophyll levels simply by eliminating a nitrogen source from the liquid culture medium. When this method of creating nitrogen-depleted medium was applied, over the period of 7 to 22 days the cultures were found to greatly increase neutral lipid content. During this time, the chlorophyll content of the cultures also decreased, resulting in less of the pigment being extracted with the oil during the subsequent extraction steps. The lipid productivities during the course of these experiments were relatively low, ranging from 2.7 mg of lipid/L of culture/day up to 24.9 mg/L/day, which is equivalent to ~350 gal/acre/year to ~1300 gal/acre/year oil production rate. However, no attempt was made during this period to optimize this lipid productivity, as the experiments were only initial experiments to determine if this laboratory-demonstrated method was possible in large outdoor cultures. These very promising initial results clearly show that this is the case. The technique could have likely also been applied to the large-scale cultivators planned for Cholla.

Further work is needed to investigate ways to reduce the amount of time required to induce this lipid accumulation, as reduced growth over a period of 7 to 22 days also tends to greatly reduce the amount of CO_2 captured during the period. Further work should also examine methods for inducing this response and maintaining increased lipid-content cultures in a continuous method rather than the batch method employed during this period. Regardless of the challenges in applying this technique at larger scale while minimizing loss of productivity, the demonstration of this technique in the cultivators and the production of large batches of biomass with increased oil content marked a major advance in the demonstration of the beneficial use of CO_2.

4.3 Algae Oil Extraction and Biodiesel Production

4.3.1 Algae Drying

After algae culture has been removed from the active growth system, and dewatered to the form a paste of about 25% solids, the next step towards production of oil or fuel is the drying step to obtain the dried algae biomass for the oil extraction process. The following section summarized the current commercial available drying methods as well as the study performed to determine the proper in-house drying methods for the project.

4.3.1.1 Current Commercial Drying Methods

There currently exist several methods of drying algae biomass at commercial scale. They are generally expensive, energy intensive, and inefficient. Table 4-8 compares currently utilized commercial drying methods.

Table 4-8. Comparison of Commercial Algae Drying Methods

Method	Cost	Energy input	Comments
Freeze Drying	High	High	Cell structure and contents preserved; gentle, slow
Vacuum-Shelf Drying	High	High	Cell structure and contents preserved; gentle, slow
Drum Drying	High	High	Fast, efficient; sterilizes product; breaks cell walls
Spray Drying	High	High	Fast, efficient; sterilizes product; can break cell walls
Rotary Drying	High	High	Can be less energy intensive if lower solids content is acceptable; fast, efficient
Natural Drying (sun, solar, wind)	Low	Low	Slow, large space and labor requirement, product quality/ preservation concerns
Cross-Flow Drying	Moderate	High	Electricity required, faster than natural drying, less costly than drum-drying or spray-drying

Currently, drying can account for up to 30% of production costs. Drum drying and other similar methods like rotary and spray drying are preferable methods as they are fast and generate a dried product that is of high quality and consistency; however they are relatively expensive. Freeze drying is another advantageous method as it is a gentle process that does not alter cell structures and components, but it is a slow process, difficult to implement at required scale and, like previous methods, requires excessive energy and costs. Natural drying is very economical with very low energy requirements and capital costs, but it is a very slow process that depends

on weather and can produce a highly variable and low-quality product. Additionally, natural drying generally requires a significant amount of space and land. All these currently utilized commercial methods are inadequate to dry algae biomass at a rate, energy and cost requirement and product quality that is desirable in commercial systems. Therefore, biomass drying represents a large area of development needed in the commercialization of the algae to biofuels process and a large opportunity for cost reduction if better methods are implemented.

4.3.1.2 Evaluation of In-House Drying Methods

During the course of the project, instead of trying to develop any new large-scale drying techniques, the effort mainly focused on evaluating several methods that were readily achievable using the existing lab facilities. The study examined the effects of these drying methods on the quality and oil extraction behavior of the dried algae biomass.

A chemical method of drying was investigated using acetone as drying agent based on the hypothesis that the existence of acetone would facilitate the algae cell wall breakage. Acetone was added into the wet bio-paste and then evaporated through natural drying in the venting hood along with water. After drying, FAME analysis was conducted on all samples to evaluate the effect of different drying conditions on the algae oil – that is, to determine if any degradation occurred during the process. The acetone-drying method was compared with natural drying of algae under ambient conditions in the venting hood and under elevated temperature using a tray-drying system (here referred as Harvester) with different drying times and drying temperatures. All treatments used the same batch biomass samples.. These results can be found in Table 4-9.

Table 4-9. Comparison of 5 Drying Methods on Resulting Lipid Level of Same Biomass

Drying method	Time, h	Temperature	FAP*, wt%
Acetone	12	Ambient	25
Hood	24	Ambient	24
Hood	96	Ambient	23
Harvester	2	93°C (200°F)	23
Harvester	24	21-38 °C (70-100°F)	20

*FAP: Fatty Acid Profile, indicating % lipids of the dry biomass.

Results indicate that there was little change in the resulting lipid content of the biomass across the 5 drying methods. Even with the high-temperature treatment applied in the tray dryer (Harvester), no degradation of lipids was found. Although the acetone-drying method, as well

as the various drying methods using the hood at room temperature all yielded similar results and had little effect on the resulting lipid content of the biomass, the fastest and most scalable method given resources and equipment currently available in the lab was the high-temperature-tray drying method. Based on this finding, this high-temperature-tray (93°C) drying method was used to dry large batches of biomass for this project. Acetone drying and freeze drying were used for the small quantity algae samples.

4.3.2 Oil Extraction from Algae

4.3.2.1 Oil Extraction Set-up and Processing

Soxhlet extraction was applied to the algae oil extraction started in October 2009, as shown in Figure 4-33a, by using a solvent mixture of dichloromethane and methanol with a molar ratio of 2 to 1 in 75-80°C water bath. Up to 20 g of dry biomass can be processed in every batch of extraction with 360 ml solvent mixture refluxing in the flask over the Soxhlet thimble. Figure 4-33b shows the acetone-dried biomass harvested from the 6M outdoor cultivator at 3rd Avenue before oil extraction. The dried biomass was ground in a mortar and pestle with methanol for ten minutes. Then the biomass with disrupted cells was transferred to the extraction thimble. The extraction was carried out until the solvents in the extraction thimble turned colorless, as shown in Figure 4-33c. Next, the extract, with the solvents, was centrifuged at 3550 rpm for 10 minutes and the upper layer was collected.

The bottom layer was combined with the pellets after extraction. The lipid-containing solvents were then recovered using rotary evaporation at 40°C (Figure 4-34a). Then the flowable lipid extracts were collected in a glass culture tube and weighed. The lipid extract was dissolved in hexane and analyzed using GC/MS to confirm there were no solvent residues in the lipids.

Figure 4-34b shows the lipids extracted from the dry biomass harvested from indoor thin-film stressed culture, which was highly flowable and yellowish. The biomass in the indoor thin-film was harvested when the lipid level reached 35 wt% and the biomass color turned yellowish, due to the degradation of chlorophyll. The oil extraction process indicated that as the culture under stressing condition became more yellow, the extraction process became easier and a higher amount of flowable extract was obtained.

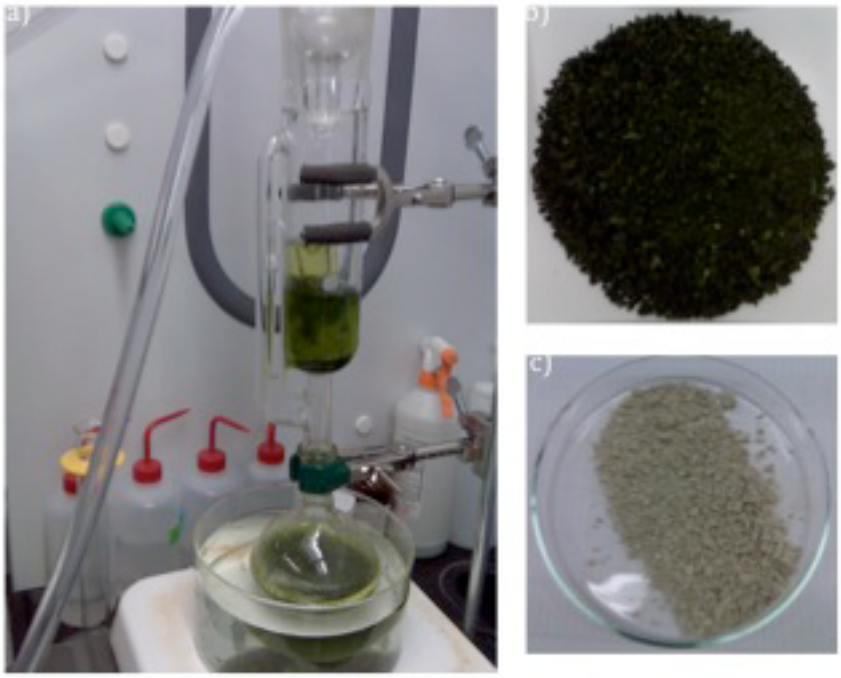

Figure 4-33. a) Soxhlet Extraction Set-up; b) Acetone-Dried Biomass before Oil Extraction; c) Biomass after Oil Extraction

Figure 4-34. a) Rotary Evaporation; b) Lipid Extracts; and c) Flowable Lipid Extracts

Thin-layer Chromatography (TLC) analysis was introduced to analyzed the components in the lipids after oil extraction. TLC was able to identify and quantify the composition of the extracted oil for neutral lipids like monoacylglycerol (MAG), diacylglycerol (DAG), triacylglycerol (TAG), polar lipids like phospholipids, and FFA. TLC-silica gel K6-Whatman with thickness of 0.25 mm

was used as a TLC plate. After activation at 110°C for 2 hr, the plate was cooled to room temperature. A solvent system of dichloromethane (CH_2Cl_2)-methonol (MeOH)-H_2O (65:25:4) was used as the developing solvent. A lipid standard of mono-, di- and triglyceride mix and lipid extracts from the dry biomass was dissolved in hexane and acetone (100:8 v/v) with concentration of 4 mg/ml.

The solvent was filled into the jar to a depth of just less than 0.5 cm. To aid in the saturation of the TLC chamber with solvent vapor, part of the inside of the beaker was lined with filter paper. The plate was spotted with the sample and then placed into the developing chamber with saturated developing solvents, as shown in Figure 4-35a. After the completion of TLC, the plate was dried for 5 minutes in a fume hood to let solvent evaporate and then exposed to an iodine vapor chamber to visualize the spots (Figure 4-35b). Lipids were identified by co-chromatography with neutral lipids standard, marked as S in the figure. The development of lipid extracts is marked as E. Then the plate was taken out and the spots were circled. The TLC was able to separate the lipids into different neutral and polar lipid components, as seen in Figure 4-35b. The two polar lipids need to be further identified by comparison with standard polar lipids. The results indicated that the lipids extracted from the biomass were mainly composed of neutral lipids of mono-, di- and triglyceride and two different polar lipids.

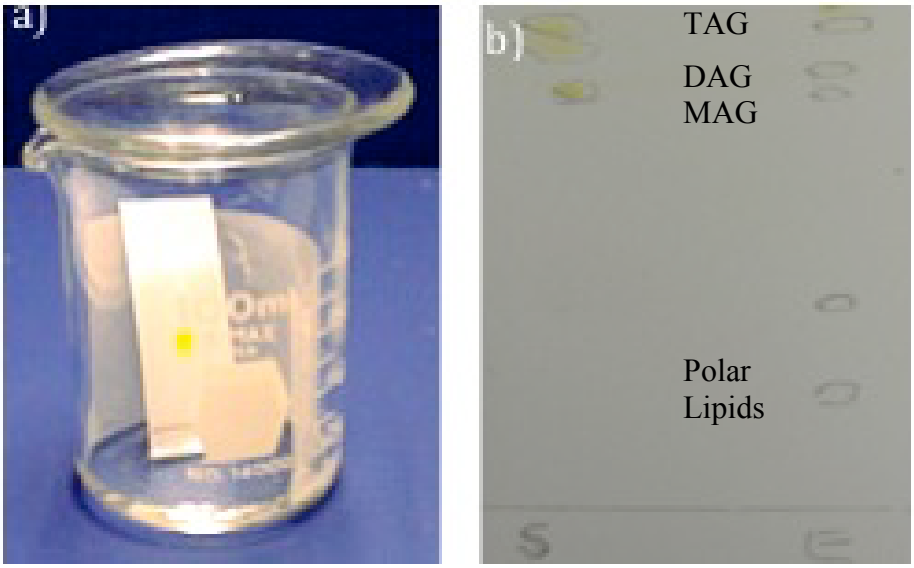

Figure 4-35. a) TLC Developing Chamber and b) Separation of Neutral Lipid and Phospholipid of Lipid Extracts (Right) Compared With the Neutral Lipid Standard (Left).

The FAME analyses on the lipid extracts and the corresponding biomass were performed with GC/MS. The spectrums of fatty acid profiles from both samples are shown in Figure 4-36. The fatty acid profiles of dry biomass and lipid extracts show similar GC spectrums with the dominant compositions of C16 and C18. The most abundant composition was oleic acid methyl ester with a content of 40 wt% and 39.5 wt% relative to the total fatty acid. The four 18-carbon acid methyl esters (oleic acid methyl ester, octadecanoic acid methyl ester, octadecadienoic acid methyl ester and oxtadecatrienoic acid methyl ester) combined made up 66 wt% and 66.5 wt% of the total fatty acids, which resulted in high-quality biodiesel.

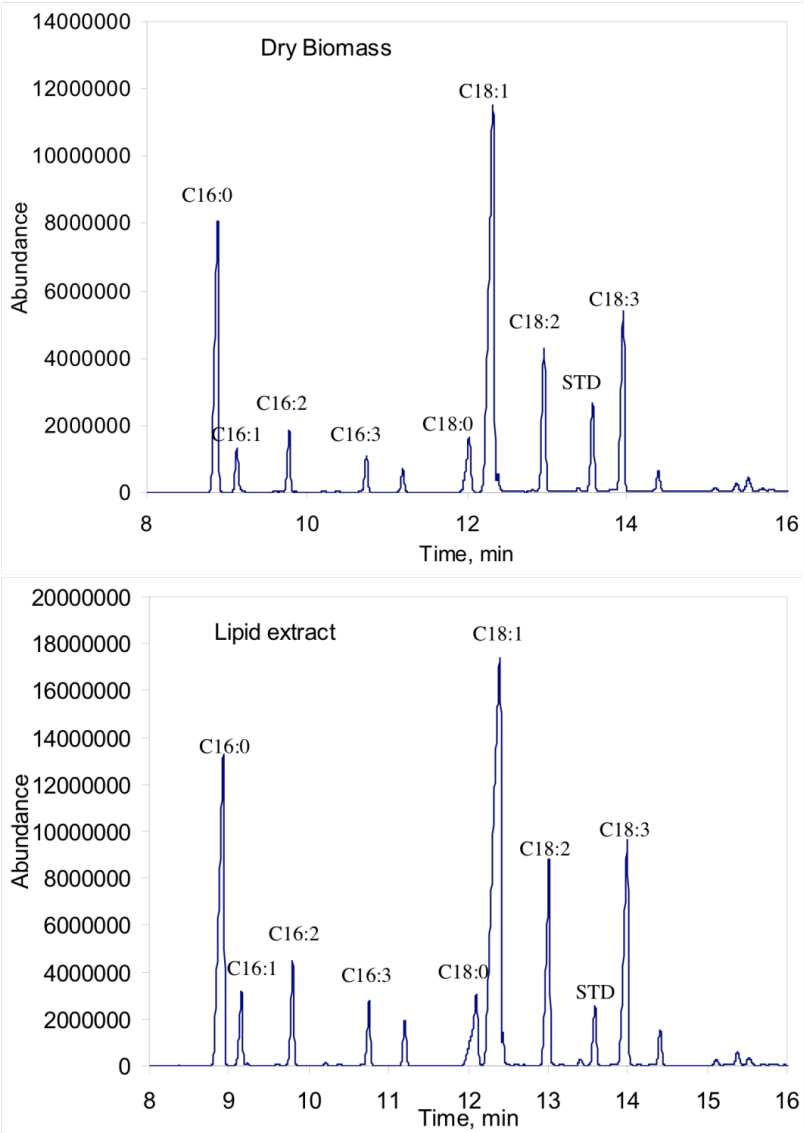

Figure 4-36. Gas Chromatographs of the Fatty Acid Methyl Esters in Dry Biomass and Lipid Extracts

4.3.2.2 Oil Extraction on Stressed Biomass

Table 4-10 presents the oil extraction results from three samples of biomass produced in indoor/outdoor thin-films under stressing conditions using Soxhlet oil extractions. In these treatments, biomass samples were dried using freeze-drying to investigate the relation between the oil extracts and the fatty acid contents of the biomass. The oil extraction treatments in this round were conducted using MeOH-CH_2Cl_2 as the solvents in a Soxhlet extractor. As shown in Table 4-10, the higher the fatty acid contents, the more lipid extracts were obtained. The amounts of total lipid extracts were always higher than the total fatty acid contents (FAP in Table 4-10) based on the dried biomass. This indicated that not all the lipid extracts were oil and could be esterified to the corresponding methyl ester, or biodiesel, which means that the algae oil to biodiesel conversion will not reach 100%. The indoor thin-film stressed sample delivered the highest fatty acid content of up to 43.5 wt% and the highest total lipid extract of 46.5 wt% based on dried biomass.

Table 4-10. Lipid Content and Oil Yield of the Stressed Biomass from Thin-films*

Samples	Drying method	FAP wt%	Extract solvent	Extracts wt%
Outdoor thin-film stressed	Freeze-dried	22.2	MeOH-CH_2Cl_2	28.5
Indoor thin-film stressed	Freeze-dried	34.8	MeOH-CH_2Cl_2	40
Indoor thin-film stressed	Freeze-dried	43.5	MeOH-CH_2Cl_2	46.5

* FAP indicates lipid content of biomass as determined by FAME method. Extracts wt% indicates the % of algae biomass that was extracted in the oil extraction treatment.

Table 4-11 presents the comparison of oil extraction results from stressed biomass obtained from the APS 3rd Ave. 6M testing facility. The test biomass used in this case was the biomass produced from October to December, 2009 in the cultivator at the 3rd Ave. site. The samples included an acetone-dried 20 g sample extracted with a solvent mixture of CH_2Cl_2 and MeOH; a hood-dried 20g sample extracted with a solvent mixture of CH_2Cl_2 and MeOH; and a hood-dried 20 g sample extracted with acetone. All treatments were carried out by grinding the dried biomass samples with mortar and pestle, transferring to a Soxhlet thimble, combining with 360 ml of solvent, and then transferring to a rotary evaporator at 40°C to recover lipid-containing solvents. The resulting lipids were then collected and weighed, the results of which are shown in Table 4-11.

Table 4-11. Lipid Content and Oil Yield Using Various Drying and Extraction Methods on 3rd Ave. 6M Stressed Samples*

Samples	Drying method	FAP wt%	Extract solvent	Extracts wt%
3rd Ave. 6M stressed	Acetone-dried	25.3	MeOH-CH_2Cl_2	35
3rd Ave. 6M stressed	Hood-dried	24.1	MeOH-CH_2Cl_2	25
3rd Ave. 6M stressed	Hood-dried	24.1	MeOH-CH_2Cl_2	22

* FAP indicates lipid content of biomass as determined by FAME method. Extracts wt% indicates the % of algae biomass that was extracted in the oil extraction treatments.

As can be seen from Table 4-11, the total lipid extract concentration from acetone-dried biomass is 10 wt% higher than the hood-dried samples, indicating that acetone drying did make the lipids from this biomass more easily extractable. Soxhlet oil extraction using acetone as solvent was tried, and it yielded a lower lipid extract concentration than MeOH-CH_2Cl_2 extraction, which was believed to be due to the high polarity of acetone. However, acetone can be recovered more easily than the MeOH-CH_2Cl_2 mixture, because CH_2Cl_2 can easily get lost during recovery due to the low boiling point, which then changes the ratio of MeOH to CH_2Cl_2, making its reuse more challenging. Therefore acetone could be considered as an alternative oil extraction solvent for large-scale oil extraction processing.

A standalone treatment was also examined investigating acetone extraction using the refluxing system instead of the Soxhlet system. This treatment was conducted on the same hood-dried biomass as used above. This biomass was loaded with acetone into a flask on the hot plate. During the extraction, the solvent was refluxed back into the flask and mixed with the biomass by stirring at a constant rate. This treatment yielded 16 wt% extract compared to the 22 wt% yielded from extraction using acetone with the Soxhlet system instead of the reflux system. More biomass can be used in the reflux system approach and the set-up is much simpler and less expensive compared to Soxhlet extraction set-up. Using the acetone-refluxing system has some benefits for larger-scale extraction.

Table 4-12 presents the Soxhlet oil extraction results from the Redhawk cultivators stressed biomass. These biomass samples were dried using acetone drying and 93°C tray drying in the harvester. These two treatments were to investigate if cell wall permeability is necessary for oil extraction. Acetone may increase permeability of the cell during the drying process as shown in Table 4-11 for 3rd Ave. 6M-harvested biomass. The oil extraction treatments in this round were also conducted using MeOH-CH_2Cl_2 as the solvent in a Soxhlet extraction, as shown in Table 4-12.

Table 4-12. Lipid Content and Oil Yield Using Various Drying Methods for Redhawk Stressed Samples

Samples	Drying method	FAP wt%	Extract solvent	Extracts wt%
Redhawk stressed	Acetone-dried	24.6	MeOH-CH_2Cl_2	32
Redhawk stressed	Harvester-dried	27.9	MeOH-CH_2Cl_2	33

* FAP indicates lipid content of biomass as determined by FAME method. Extracts wt% indicates the % of algae biomass that was extracted in the oil extraction treatments.

Acetone drying was found to have little effect on the total extract yield in the elevated lipid biomass produced from Redhawk. The oil extracted from the biomass with or without acetone drying resulted in a similar oil extract of 32-33 wt%. This was probably caused by the more fragile cell wall obtained from the Redhawk sample, which was harvested at the right time. The combination of high-temperature tray drying and Soxhlet extraction using MeOH-CH_2Cl_2 is the best option for the current biomass produced from Redhawk.

Continuous operation of oil extraction using the Soxhlet system was also attempted during this period using the optimal mixture of drying and oil extraction determined in the experiments above. During this time 240 g of biomass was extracted in 8 runs with 30 g being processed per run and two runs per day. A total of 100 ml of crude algae oil was produced through this process after solvent recovery using rotary evaporation.

4.3.3 Biodiesel Production from Algae

Recently, considerable attention has been given to biodiesel production, due to concern over the availability and environmental impact of fossil fuels. As an alternative to petroleum-derived diesel, biodiesel has several advantages: it comes from renewable plants, which are biodegradable and less toxic, and its combustion products have reduced levels of carbon dioxide, sulfur oxides and particulates. Biodiesel is normally made by transesterification of triglyceride from vegetable oil or animal fat. Transesterification is a chemical reaction between triglyceride and methanol with or without presence of a catalyst, which produces biodiesel (methyl esters) and glycerol (Figure 4-37). Because the reaction is reversible, excess methanol is used to shift the equilibrium to produce more biodiesel.

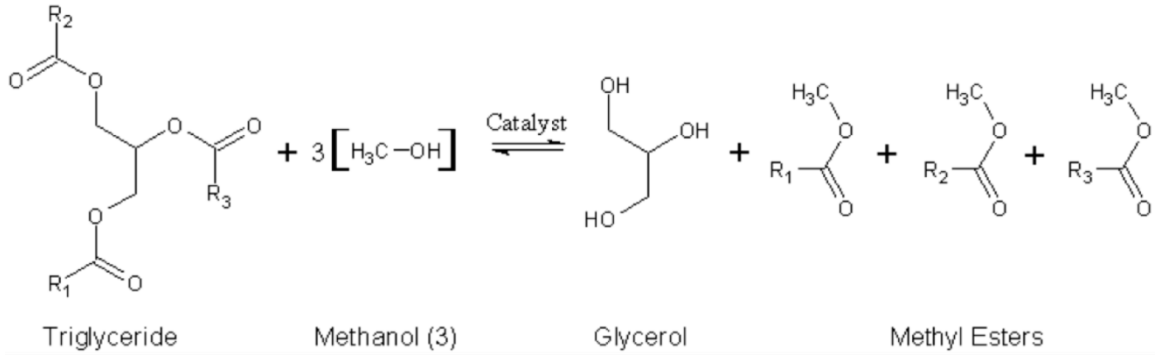

Figure 4-37. Transesterification of Triglyceride with Methanol

Transesterification can be carried out using homogeneous acid (sulfuric acid), base catalysts (sodium hydroxide and potassium hydroxide), heterogeneous catalysts (sulfated zirconium oxide, magnesium oxide, calcium oxide, etc.), enzymatic catalysts and also using a noncatalytic approach, such as supercritical alcohol. Using the transesterification reaction with alcohol, the first step is to convert the triglycerides to diglycerides and follow with subsequent conversion to monoglycerides and then to glycerol. Each step yields one methyl ester molecule from each glyceride.

Algae are a potential feedstock of triglycerides. Microalgae have a potential to produce 15-300 times more oil for biodiesel production than the traditional crops from the same amount of land but do not compete for arable space with food supplies. Biodiesel derived from algae is nontoxic and highly biodegradable with no sulfur. Not all algae oils are suited to make biodiesel. The *Scenedesmus obliquus* studied in this project mainly accumulates C16 and C18, which are suitable species for biodiesel production.

4.3.3.1 Algae Oil to Biodiesel through Acid Catalytic Transesterification

Homogenous acid-catalyzed transesterification is not as popular as the base-catalyzed process because the acid-catalyzed reaction is much slower than the base-catalyzed under the same conditions. However, the performance of the acid catalyst is not as strongly affected by the presence of FFAs in the feedstock. If the FFA content in the oil is about 3%, it has been found that the base-catalyzed transesterification process is not suitable to produce esters from unrefined oil. The acid catalyst, in fact, can simultaneously catalyze both transesterification and esterification. Due to the intrinsically high FFA in algae oil, the acid-catalyzed transesterification/esterification process was applied in this project. Esterification is a

subcategory of transesterification, including two reactants, fatty acids (carboxylic acids) and alcohols. Esterification reactions are acid-catalyzed reactions.

Acid-catalyzed transesterification reactions were conducted on the algae oils extracted from biomass with different lipid levels to produce biodiesel. The biomass was produced from indoor thin-film bags and from the outdoor cultivator at 3rd Ave. and Redhawk, respectively. The results are shown in Table 4-13. The oil extractions in these four typical treatments were conducted using MeOH-CH_2Cl_2 as the solvents in a Soxhlet extraction. The lipid extract yields from the varying biomass and drying methods are also listed in this table.

Table 4-13. Biodiesel Conversions through Acid-Catalyzed Transesterification on Different Algae Samples*

Samples	Drying Method	FAP wt%	Extract Solvent	Extracts wt%	Biodiesel/Oil %	Biodiesel/Biomass %
3rd Ave. 6M	Acetone-dried	25.3	MeOH-CH_2Cl_2	35	57.9	20.3
Redhawk	Harvester-dried	27.9	MeOH-CH_2Cl_2	33	58.3	19.2
Indoor thin-film	Freeze-dried	34.8	MeOH-CH_2Cl_2	40	79.7	31.9
Indoor thin-film	Freeze-dried	43.5	MeOH-CH_2Cl_2	46.5	52.9	24.6

* FAP indicates lipid content of biomass as determined by FAME method. Extracts wt% indicates the % of algae biomass that was extracted in the oil extraction treatment. Biodiesel/Oil % shows oil-to-biodiesel conversion through transesterification reactions, and Biodiesel/Biomass % is calculated using Extracts wt% * Biodiesel/Oil % / 100.

The biomass with different lipid contents produced from outdoor cultivators at the 3rd Ave. facility and Redhawk delivered almost the same oil-to biodiesel-conversion of 58 wt%, and similar biodiesel yields based on dried biomass of 19-20 wt%. The biomass with fat level of 34.8 wt% in the nitrate-limited indoor thin-film bag yielded 40 wt% oil extract based on dried biomass, and the highest oil-to-biodiesel conversion (79.7%). When the fat level reached 43.5 wt% for the nitrate-limited indoor thin-film bag biomass, it yielded the highest oil extract percentage of all treatments at 46.5 wt%; however, the oil-to-biodiesel conversion was only 52.9%, indicating that there may be an optimal total fat level in the algae biomass to yield the highest levels of biodiesel production.

4.3.3.2 Biomass Directly to Biodiesel

4.3.3.2.1 Biomass to Biodiesel through Acid-Catalyzed Transesterification

During the project, an attempt was made to directly convert the dried biomass to biodiesel in a single step through acid-catalyzed transesterification and excess methanol under supercritical conditions. This approach was an attempt to bypass the traditional oil extraction process.

4.3.3.2.2 Biomass to Biodiesel through Supercritical Methanol Transesterification

In biodiesel production, it is well known that the vegetable oils or fats used as raw materials for the transesterification under catalytic conditions should be water-free, since the presence of water has negative effects on the reaction. Water can consume the catalyst and reduce catalyst efficiency. The presence of water has a greater negative effect than that of FFA. The water content should be kept below 0.06%, much lower than the allowable free fatty acids content. Also, neutralization of the catalysts and recover of the catalyst is a necessary step for biodiesel production.

In the lab, a catalyst-free method employing supercritical methanol for biodiesel production from rapeseed oil was developed. The great advantage of this method is that free fatty acids present in the oil could be simultaneously esterified in supercritical condition, and water content up to 50% did not greatly affect the yield of methyl ester. In the supercritical condition, methanol is expected to be an acid catalyst itself. Also the dielectric constant of methanol dramatically changes to a number close to that of vegetable oil, which allows a homogeneous mixture in supercritical condition. It is assumed that a methanol molecule directly attacks the carbonyl atom of the triglyceride because of the high pressure. Under these conditions, hydrogen bonding in methanol would be significantly decreased, allowing methanol to be a free monomer. The transesterification is completed via methoxide transfer, whereby the fatty acid methyl ester and diglycerides are formed. Then, in a similar way, diglycerides are further transesterified into methyl ester and monoglycerides, which is converted further to methyl ester and glycerol in the last step.

The supercritical methanol transesterification process to convert biomass directly to biodiesel is shown in Figure 4-38. All the reactions were performed in 2 L high-pressure autoclave (Parr Instruments) made of 316 stainless steel and equipped with pressure and temperature monitors. The dried biomass and methanol were loaded into the autoclave. In a typical run, the autoclave was loaded with a given amount of biomass (100-200 g) and liquid methanol (400 ml). Then the reaction was run at 245°C, 1160 psig for 10-30 minutes, just above the critical condition of

methanol (240°C, 1140 psi). After each run, the gas was vented, and the autoclave content was poured into a collecting vessel. All the rest of the contents was removed from the autoclave by washing with methanol. The biodiesel and glycerol products were separated using the separation method discussed above for acid-catalyzed transesterification of biomass.

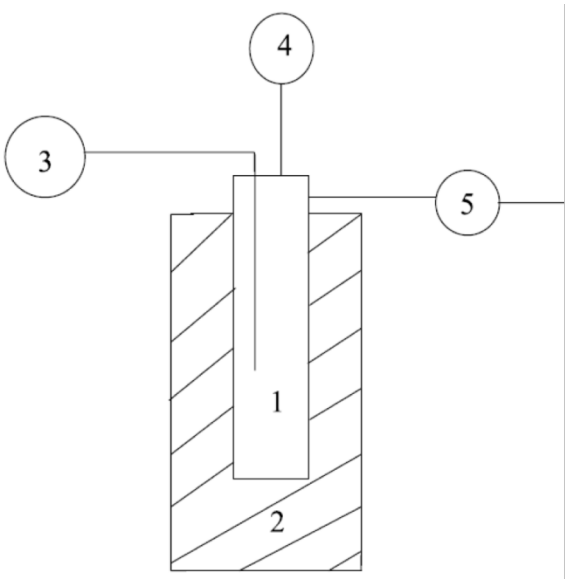

Figure 4-38. Supercritical Methanol Transesterification Set-Up*

* 1) autoclave, 2) electrical furnace, 3) temperature control meter, 4) pressure control meter, 5) gas venting valve

4.3.3.2.3 Biodiesel Quality Comparison Using Different Transesterifications

Two 3rd Ave. harvested biomass samples and one indoor thin-film bag biomass sample with different fat levels were tested for biodiesel production by both supercritical methanol and acid-catalyzed transesterification methods, and the results are shown in Table 4-14. The 3rd Ave. 6M biomass sample under the supercritical reaction condition only delivered 6.58 wt% biodiesel, and the biodiesel had a higher viscosity compared to the one obtained from the acid-catalyzed reaction. The acid-catalyzed reaction at lower temperature (100°C) and much lower pressure (40 psi) gave 18.8 wt% biodiesel. Also biodiesel from the acid-catalyzed reaction was more flowable and much less viscous. This indicated that the acid-catalyzed reaction for converting biomass to biodiesel was a better way to make high-quality biodiesel. The biomass harvested from the indoor thin-film bag with a fat level of 35 wt% was also tried using the acid-catalyzed approach. It delivered 35 wt% biodiesel as shown in Table 4-14, which was same as the fatty acid profile from the fatty acid methyl esterification analysis.

Table 4-14. Biodiesel Quality Comparisons Using Different Transesterification Methods

Samples	Methods	Reaction T, P	Biodiesel wt% (based on biomass)	Biodiesel Color	Viscosity	Biomass FAP wt%
3rd Ave. 6M	Super-critical	245°C, 1160 psig	6.58	Brownish	Higher	25
3rd Ave. 6M	Acid-catalyzed	100°C, 40 psig	18.5	Greenish	Lower	25
Indoor	Acid-catalyzed	100°C, 40 psig	35.0	Yellowish	Lower	35

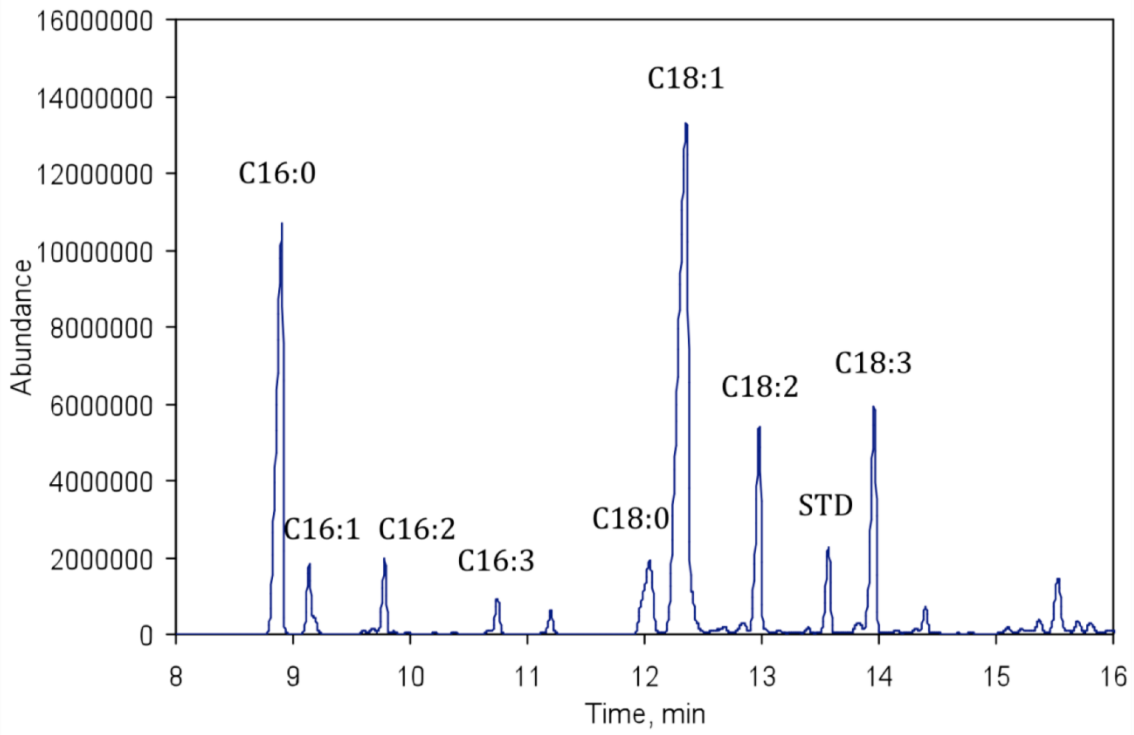

Figure 4-39. Gas Chromatograph of Biodiesel Produced from Indoor Biomass

The GC spectrum of biodiesel produced from indoor thin-film bag-harvested biomass is shown in Figure 4-39. The fatty acid profile of biodiesel shows similar GC spectrum to that of the biomass with the dominant molecules C16 and C18. The most abundant component is oleic acid methyl ester with a content of 40 wt% relative to the total fatty acid. The four 18-carbon acid methyl esters (oleic acid methyl ester, octadecanoic acid methyl ester, octadecadienoic acid methyl ester and oxtadecatrienoic acid methyl ester) constituted 64 wt%, which explains the high-quality biodiesel.

4.3.3.3 Biopaste Directly to Biodiesel

To try to lower the cost of biopaste drying, the project evaluated an attempt to bypass the drying process and convert wet biopaste directly to biodiesel using a supercritical methanol reaction in a high-pressure autoclave at 280°C, 1700 psi. The products were separated using hexane and water after sitting in the separation funnel overnight. In the supercritical condition, water acts as an acid catalyst more strongly than methanol itself. In this case, methyl ester was not detected in the hexane layer due to large amount of water in the paste (65 wt% in biomass), which means no biodiesel was generated during this process. The water layer was analyzed using GC, and the dominant component was glycerol.

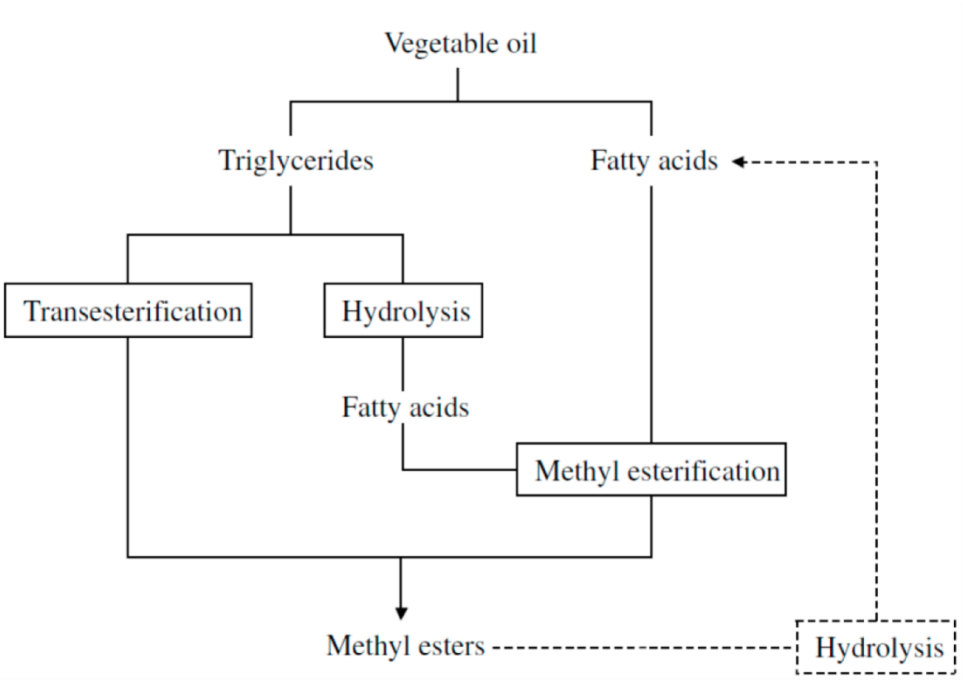

Figure 4-40. Reactions Involved in the Treatment of Biopaste by Supercritical Methanol in the Presence of Water

Three types of reactions were involved during this process: hydrolysis, transesterification and methyl esterification as shown in Figure 4-40.

Due to the large amount of water in the process (65 wt% of the biomass), the hydrolysis reaction went much faster than transesterification, free fatty acids produced can be further methyl esterified to methyl esters during supercritical treatment of methanol, which, however, was further hydrolyzed to fatty acids. Therefore, the main products in the process were fatty

acids and glycerol. Compared to transesterification of dried biomass to biodiesel, transesterification of wet biopaste to biodiesel appeared to be more challenging. Therefore, to ease the scale-up process in the future, biopaste to biodiesel will not be considered further. However, dried biomass directly to biodiesel should be continued and the potential scale-up could be performed.

4.3.4 Summary of Oil Extraction and Biodiesel Production

Throughout the IES reporting period, the project monitored the fat level of the algae biomass under nutrient-deprived conditions from both indoor and outdoor experimental culture at 3rd Ave. testing facility and from outdoor Redhawk algae testing facility. The fatty acids were quantified by GC/MS, which provided an immediate in-house feedback of data with which to understand the effects of manipulating the culture conditions on the lipid content of the biomass. By pairing this monitoring ability with biology, significant advances were made during this period by first learning how to produce biomass with increased lipid content and then applying these techniques to Redhawk cultures to produce large batches with increased lipid biomass.

Oil extractions of the final harvested algae biomass from the indoor thin-film bags and outdoor cultivators at the 3rd Ave. and Redhawk were performed with solvent extraction. Mixture of CH_2Cl_2 and MeOH (2:1 v/v) or acetone was used as solvents. The biomass with a fat level of 34.8 wt% obtained from the indoor thin-film delivered 40 wt% oil extract and the highest oil-to-biodiesel conversion (79.7 %). The biomass obtained from outdoor cultivators delivered up to 35 wt% total lipids and 20 wt% biodiesel. The optimal fat level in the biomass to generate the best quality of crude algae oil for biodiesel production need to be determined so that the biomass can be harvested at the right time once it is under stressing. Longer stressing does not always produce higher fat levels and a higher fat level doesn't always produce better quality oil (better conversion into biodiesel through transesterification).

Biodiesel production directly from biomass through an acid-catalyzed transesterification reaction and a supercritical methanol transesterification reaction were also evaluated during the project. The acid-catalyzed reaction delivered 35-wt% biodiesel, which matched the results from fatty acid analysis through the acid-catalyzed FAME approach. Biodiesel directly from biomass is an efficient and cost-effective way to produce biodiesel by skipping the oil extraction process, however, the reaction conditions and catalysts applied need to be further investigated. The demonstration of both oil extraction and direct conversion of biomass to biodiesel marks a significant advancement towards utilizing biomass produced in the Redhawk cultivators as a source of oil for liquid fuel production. These extraction and conversion processes serve as the

final steps in the integrated process for the demonstration of beneficial use of CO_2 by growing and manipulating algae biomass, followed by the dewatering, drying, extraction and conversion of algae oil to fuel, which were all successfully demonstrated during this IES reporting period.

The effects of different drying methods on the algae biopaste after dewatering were investigated. The fatty acid analyses on the dried biomass after different drying methods indicated that tray drying in the harvester at 93°C for 2 hours is best approach for current in-house algae drying method. Using batches of elevated lipid biomass produced at Redhawk, a total of 6.4 kg of dried biomass with a fat level of 28 wt% based on dried biomass was obtained from tray-drying in the harvester, indicating that this method of drying did not negatively affect lipid yield.

4.4 Conclusions of Algae Testing

APS Redhawk algae testing facility demonstrated an integrated system that included flue gas distribution; CO_2 capture; algae cultivation, harvesting, dewatering, storage; and site water management. Three 6M cultivators having a total of 339 m^2 foot print were operated for a total of 332 days of algae cultivation. The 6M floating cultivators achieved a 28 g/m^2/day algae growth rate, was able to be used as a stressor, proved to be robust and free of contamination and resulted in a good CO_2 capture rate. With the right stressing technology, the 6M cultivators produced algae with high 20s wt% biodiesel convertible lipid content. Cultivating high oil content algae is a critical step for algae to qualify as a potential biofuel feedstock especially via the regular oil extraction process instead of pyrolysis, gasification or fermentation. Unstressed green algae was found very tough to produce extractable oil due to the limited oil content (generally less than 10 wt%, could be 1 - 2 wt%). The stressing process simultaneously reduces the chlorophyll content in the algae which is suspect to interfere with phospholipids in the cell and make algae oil extraction hard to obtain. This stress process, on the other hand, also significantly reduced the algae growth rate. The demonstration at APS showed a close to ten times slow down on growth rate when algae is under stressed. Therefore, the maximum lipid production rate, which is the combination of algae biomass growth rate and lipid content should be evaluated given that the main interest is to produce the algae oil. The optimum cultivation conditions should be determined to maximize the yield of algae oil production.

Scenedesmus studied in this report proved to be a robust algae strain and can live up to 40°C. It demonstrated high growth rate and high lipid content when under stressed. Its lipid content

reached 44 wt% during the indoor study and 35 wt% during the outdoor study. Its lipid mainly contains 16 and 18 carbon chain length. Being a fresh water strain, *Scenedesmus* showed its growth in Cholla brackish saline aquifer which contains 1700 – 4000 ppm total solid dissolved (TSD) and adaptability in a five times more salt concentrated water source.

Energy consumption remains to be the big challenge for the project especially algae dewatering and drying. The project did not reach the point to maximize the energy efficiency for each process operation – flue gas distribution, CO_2 capture, cultivation, harvesting, dewatering, drying, oil extraction and biodiesel production. The efforts spent to approach this included: First, algae strain selection - Scenedesmus showed a capability of self-settling. By leaving in a 60° cone bottom settling tank, it could condense itself by 32-fold within five hours (biofocculation was not evaluated in the project due to the concern of introducing undesired chemicals); Second, evaluation of newly designed pilot scale dewatering system. This system could concentrate algae culture from 0.1 wt% to 20 wt% at a rate of 10 gal per minute; Third, investigation of different drying method to test the safety of using low grade heat to dry algae with relatively longer time (no biomass degrade and decomposing during the drying process); Fourth, evaluation of using low grade heat from coal power plant for algae drying and potentially whole algae farm's thermal management; Lastly and most importantly - evaluation of the possibility of directly producing biodiesel from dried biomass or even biopaste to eliminate the oil extraction step. Producing biodiesel from dried biomass has been proven in the APS lab scale study. The biodiesel yield obtained through this route was comparable comparing with what obtained through traditional oil extraction followed by oil to biodiesel conversion route. Due to the uncompleted project, the full characterization of the biodiesel generated from lab was not performed neither was the algae crude oil.

Water management is another big challenge of the project. Algae farming can use a significant amount of water. This would create a problem especially at Arizona to demonstrate any large size algae farming. The effort to overcome this challenge included: First, algae strain selection – the algae should grow and grow with a certain rate in the saline aquifer that is largely available in Arizona and is a non-arable water source. Even though *Scenedesmus* has already demonstrated its growth in Cholla brackish saline aquifer, more quantitative research is still required to determine its maximum growth rate and stressing performance in this saline aquifer water. Second, evaluation of water recycle – the water recovered from algae dewatering system contains unused nutrients, which could be rebalanced to the right level and recycled to save the total water and nutrient consumption. Cleaning the ecosystem in the recovered water,

water recycling, and water recovery still need to be further explored. Lastly, closed or half-closed cultivator design should be preferred to minimize the water loss through the evaporation.

Despite all the challenges, utilizing algae to capture CO_2 and convert it into organic carbon for biofuel production remains promising. This emerging industry is extremely interdisciplinary. At a minimum, it needs the contributions from farmers, biologists, mechanical engineers, chemical engineers, environmental engineers, and civil engineers etc. Successful large-scale implementation would require a collaborative sharing of expertise and integration of disciplines to make the possibility of an integrated energy system with beneficial carbon dioxide use a reality.

THIS PAGE INTENTIONALLY LEFT BLANK.

5. Acronyms and Abbreviations

Acronym	Description
°C	Degrees Celsius
°F	Degrees Fahrenheit
µg	Microgram
µg\g	Microgram per Gram
µg\L	Microgram per Liter
µL	Microliter
µm	Micrometer
µS	Micro Siemens
µS\cm	Micro Siemen per Centimeter
1-D	One-dimensional
3-D	Three-dimensional
5X	Five Times
6M	6 Meter Radius Cultivator
50M	50 Meter Radius Cultivator
100M	100 Meter Radius Cultivator
acfm	Average Cubic Feet per Meter
ADA	American Disability Access
AFHP	Advanced Flash Hydropyrolysis
AHP	Advanced Hydrogasification Process
AL	Air Liquide
AMW	Average Molecular Weight
amu	Atomic Mass Unit
APS	Arizona Public Service Company
ARCH	Advanced Rapid Carbon Hydrogasification
ASME	American Society of Mechanical Engineers
ASTM	American Society of Testing and Materials
BHT	Butylated Hydroxytoluene
Btu	British Thermal Unit
BP1	Budget Period 1
BP2	Budget Period 2
BTX	Benzene, Toluene, and Xylene
C1	Cultivator 1
C2	Cultivator 2
C3	Cultivator 3
CFA	Cartridge Filters A
CFD	Computational Fluid Dynamics
CFG	Concentrated Flue Gas
cfm	Cubic Feet per Minute
cfh	Cubic Feet per Hour

Acronym	Description
cfu	Colony Forming Unit
cfu/ml	Colony Forming Unit per Milliliter
CH_2Cl_2	Dichloromethane
CH_4	Methane
C_2H_4	Ethylene
C_2H_6	Ethane
C_6H_6	Benzene
C_7H_8	Toluene
$C_{10}H_8$	Naphthalene
$C_{12}H_{10}$	Biphenyl
$C_{13}H_{10}$	Fluorene
$C_{14}H_{10}$	Anthracene
$C_{16}H_{10}$	Pyrene
cm	Centimeter
cP	Centipoise
CO	Carbon Monoxide
CO_2	Carbon Dioxide
COS	Carbonyl Sulfide
Cr	Chromium
DAG	Diacylglycerol
DRTC	Delaware Research & Technology Center
EDTA	Ethylenediaminetetraacetic Acid
EFG	Enriched Flue Gas
ESHRx	Engineering-Scale Hydrogasifier Reactor
FAME	Fatty Acid Methyl Ester
FAP	Fatty Acid Profile
FFA	Free Fatty Acid
FGB	Flue Gas Blower
FID	Flame Ionization Detector
FM	Florescence Maximal
ft^2	Square Foot
ft^3/h	Cubic Foot per Hour
g	Gram
g/L	Grams per Liter
$g/m^2/day$	Grams per Square Meter per Day
gal	Gallon
GC/MS	Gas Chromatography and Mass Spectroscopy
gpm	Gallons per Minute
GRR	Gas Recycle Ratio
HBC	Heterotrophic Bacteria Count
H_2:Coal	Hydrogen-to-Coal Mass Ratio
H_2O	Water

Acronym	Description
H_2S	Hydrogen Sulfide
H_2SO_4	Sulfuric acid
hp	Horsepower
I&C	Instrumentation and Controls
IES	Integrated Energy System with CO_2 Use Project
K_{BTX}	The Arrhenius Pre-Exponential Constant
kg	Kilogram
kV	Kilovolt
kW	Kilowatt
L or l	Liter
lb	Pound
Lb/hr	Pound per Hour
LCO_2	Liquid Carbon Dioxide
LNG	Liquefied Natural Gas
m	Meter
m^2	Square Meter
MAG	Monoacylglycerol
MAWP	Maximum Allowable Working Pressure
MEDAL	Membrane Systems DuPont Air Liquide
mg	Milligram
mg/ml	Milligram per Milliliter
mg/L/day	Milligram per Liter per Day
MKP	Mono Potassium Phosphorus
ml	Milliliter
mph	Miles per Hour
MTR	Membrane Technology and Research, Inc., Menlo Park, CA
MW	Megawatt
NaCl	Sodium Chloride
$NaHCO_3$	Sodium Bicarbonate
NETL	National Energy Technology Laboratory
NTU	Nephelometric Turbidity Unit
P&ID	Piping and Instrumentation Diagram
PBR	Photobioreactor
PD	Positive Displacement
PFD	Process Flow Diagram
pH	Potential of Hydrogen
ppb	Parts per Billion
ppm	Parts per Million
PSD	Particle Size Distribution
psi	Pounds per Square Inch
psia	Pounds per Square Inch Absolute
psig	Pounds per Square Inch Gauge

Acronym	Description
PVC	Polyvinyl Chloride
R&D	Research and Development
RC	Rapid Carbon
RFG	Raw Flue Gas
RO	Reverse Osmosis
scfm	Standard Cubic Feet per Meter
SFG	Simulated Flue Gas
SNG	Substitute Natural Gas
SO_2	Sodium Dioxide
SRV	Safety Relief Valve
TAG	Triacylglycerol
TBD	To Be Determined
TCD	Thermal Conductivity Detector
TDS	Total Dissolved Solids
TLC	Thin Layer Chromatography
tpd	Tons per Day
TSD	Total Solid Dissolved
UL	Underwriters Laboratories
UV	Ultraviolet
V	Volt
v/v	Volume Concentration
VAC	Volts Alternating Current
VFD	Variable Frequency Drive
vol.	Volume
W.C.	Water Column
wt%	Weight Percent
yd^3	Cubic Yard